

Elementary Particle Physics  
Lecture Notes  
Spring 2002

Paolo Franzini  
University of Rome, *La Sapienza*

\ref in phyzzx is renamed \refo

*This notes are quite incomplete. Everything in the notes has been presented in class, but not all that was discussed is contained in the following.*

*The factor  $i = \sqrt{-1}$  and the sign for amplitudes is almost always ignored in the notes, an exception being when exchanging fermions and bosons lines.*

*There are some repetitions due to merging of files. That will fixed, sometimes.*

# Contents

<b>1</b>	<b>INTRODUCTION</b>	<b>1</b>
1.1	History . . . . .	1
1.2	Elementary particles . . . . .	1
1.2.1	Masses . . . . .	4
1.2.2	Conserved additive quantities . . . . .	5
1.3	Natural Units: $\hbar=c=1$ . . . . .	6
1.4	The Electromagnetic Interaction . . . . .	7
1.5	The many meanings of $\alpha$ . . . . .	8
1.6	The Gravitational Interaction . . . . .	9
1.7	Interactions and coupling constants . . . . .	10
<b>2</b>	<b>Order of Magnitude Calculations</b>	<b>13</b>
2.1	Introduction . . . . .	13
2.2	$e^+e^- \rightarrow \mu^+\mu^-$ . . . . .	13
2.3	$\nu + N \rightarrow \dots$ . . . . .	14
2.4	Compton scattering . . . . .	15
2.5	Muon decay . . . . .	16
2.6	Pair production and bremsstrahlung . . . . .	16
2.7	High energy hadronic total cross sections . . . . .	18
<b>3</b>	<b>Reaction rates and Cross Section</b>	<b>20</b>
3.1	$S$ -matrix, $T$ , $\mathfrak{M}$ , phase space and transition probability. . . . .	20
3.2	Decay rate, three bodies . . . . .	21
3.3	Integration Limits . . . . .	22
3.4	Decay rate, two bodies . . . . .	25
3.5	Scattering cross section . . . . .	26
3.6	Accounting for Spin . . . . .	27
<b>4</b>	<b>The Electromagnetic Interaction</b>	<b>29</b>
4.1	Introduction: Classical Rutherford Scattering . . . . .	29
4.1.1	Exact computation of $\Delta p$ . . . . .	30
4.1.2	Final remarks . . . . .	30
4.2	The Elementary EM Interaction . . . . .	30
4.3	The Rutherford cross section . . . . .	32
4.4	Electromagnetic Scattering of Spinless Particles . . . . .	34
4.5	Pion Compton Scattering . . . . .	36
4.6	Scattering from an Extended Charge Distribution, I . . . . .	39
4.7	Scattering from an Extended Charge Distribution, II . . . . .	40
4.8	Scattering with Spin . . . . .	43
4.9	Cross sections for $J=1/2$ particles . . . . .	46
4.10	$e^+e^- \rightarrow \pi^+\pi^-$ . . . . .	47
4.11	$e^+e^- \rightarrow \mu^+\mu^-$ . . . . .	49
4.12	Bhabha scattering: $e^+e^- \rightarrow e^+e^-$ . . . . .	51

<b>5</b>	$e^+e^- \rightarrow$ <b>Hadrons, R, Color etc</b>	<b>52</b>
5.1	$e^+e^- \rightarrow$ Hadrons . . . . .	52
5.1.1	Final remarks . . . . .	52
<b>6</b>	<b>The Weak Interaction. I</b>	<b>53</b>
6.1	Introduction . . . . .	53
6.2	Parity and Charge Conjugation . . . . .	54
6.3	Helicity and left-handed particles . . . . .	56
6.4	The V–A interaction . . . . .	57
6.5	Muon Decay . . . . .	58
6.6	Semileptonic weak decays . . . . .	62
6.7	Quarks and the weak current . . . . .	62
6.8	Pion Decay . . . . .	64
6.8.1	Pion decay to lepton plus neutrino . . . . .	64
6.8.2	$\pi^\pm$ decay to $\pi^0$ , electron and neutrino . . . . .	65
6.9	Inverse muon decay. . . . .	66
<b>7</b>	<b>STRANGENESS</b>	<b>68</b>
7.1	Discovery . . . . .	68
7.2	A New Quantum Number and Selection Rule . . . . .	68
7.3	Charge and $I_3$ . . . . .	69
7.4	Selection rules for hyperon decays . . . . .	70
7.5	Measuring the spin of the $\Lambda^0$ . . . . .	71
7.6	$\Sigma$ decays . . . . .	72
7.7	Computing the amplitudes . . . . .	73
7.8	$K$ decays . . . . .	74
<b>8</b>	<b>The Weak Interaction II. <math>CP</math></b>	<b>75</b>
8.1	Introduction . . . . .	75
8.2	Historical background . . . . .	75
8.3	$K$ mesons and strangeness . . . . .	75
8.3.1	The Strange Problem . . . . .	76
8.4	Parity Violation . . . . .	78
8.5	Mass and $CP$ eigenstates . . . . .	79
8.6	$K_1$ and $K_2$ lifetimes and mass difference . . . . .	80
8.7	Strangeness oscillations . . . . .	81
8.8	Regeneration . . . . .	82
8.9	$CP$ Violation in Two Pion Decay Modes . . . . .	83
8.9.1	Discovery . . . . .	83
8.9.2	$K^0$ Decays with $CP$ Violation . . . . .	84
8.9.3	Experimental Status . . . . .	87
8.10	$CP$ violation in two pion decay . . . . .	87
8.10.1	Outgoing Waves . . . . .	87
8.11	$CP$ Violation at a $\phi$ -factory . . . . .	89
8.11.1	$\phi$ ( $\Upsilon''$ ) production and decay in $e^+e^-$ annihilations . . . . .	89
8.11.2	Correlations in $K_S, K_L$ decays . . . . .	91
8.12	$CP$ Violation in Other Modes . . . . .	93

8.12.1	Semileptonic decays . . . . .	93
8.13	$CP$ violation in $K_S$ decays . . . . .	94
8.13.1	$K_S \rightarrow \pi^0 \pi^0 \pi^0$ . . . . .	94
8.13.2	$BR(K_S \rightarrow \pi^\pm \ell^\mp \nu)$ and $\mathcal{A}_\ell(K_S)$ . . . . .	94
8.14	$CP$ violation in charged $K$ decays . . . . .	95
8.15	Determinations of Neutral Kaon Properties . . . . .	95
8.16	CLEAR . . . . .	95
8.16.1	$K^0(\bar{K}^0) \rightarrow e^+(e^-)$ . . . . .	96
8.16.2	$\pi^+ \pi^-$ Final State . . . . .	97
8.17	E773 at FNAL . . . . .	98
8.17.1	Two Pion Final States . . . . .	98
8.17.2	$K^0 \rightarrow \pi^+ \pi^- \gamma$ . . . . .	99
8.18	Combining Results for $\Delta m$ and $\phi_{+-}$ from Different Experiments . . . . .	99
8.19	Tests of $CPT$ Invariance . . . . .	100
8.20	Three Precision $CP$ Violation Experiments . . . . .	100
8.21	KTEV . . . . .	100
8.22	NA48 . . . . .	102
8.23	KLOE . . . . .	102
<b>9</b>	<b>Quark Mixing</b> . . . . .	<b>103</b>
9.1	GIM and the $c$ -quark . . . . .	103
9.2	The $K_L$ - $K_S$ mass difference and the $c$ -quark mass . . . . .	104
9.3	6 quarks . . . . .	105
9.4	Direct determination of the CKM parameters, $V_{us}$ . . . . .	108
9.5	Wolfenstein parametrization . . . . .	110
9.6	Unitary triangles . . . . .	111
9.7	Rare $K$ Decays . . . . .	113
9.8	Search for $K^+ \rightarrow \pi^+ \nu \bar{\nu}$ . . . . .	114
9.9	$K_L \rightarrow \pi^0 \nu \bar{\nu}$ . . . . .	114
9.10	$B$ decays . . . . .	115
9.10.1	Introduction . . . . .	115
9.11	$B$ semileptonic decays . . . . .	116
9.12	$B\bar{B}$ Mixing . . . . .	117
9.12.1	discovery . . . . .	117
9.12.2	Formalism . . . . .	117
9.13	$CP$ Violation . . . . .	119
9.13.1	$\alpha$ , $\beta$ and $\gamma$ . . . . .	119
9.14	CDF and DØ . . . . .	121
9.15	$B$ -factories . . . . .	121
9.16	LHC . . . . .	122
9.17	$CP$ , kaons and $B$ -mesons: the future . . . . .	122
<b>10</b>	<b>The Weak Interaction. III</b> . . . . .	<b>125</b>
10.1	Beauty Decays . . . . .	125
10.2	Charm Decays . . . . .	127
10.3	Decay Rate . . . . .	128
10.4	Other Things . . . . .	128

10.5 Contracting two indexes. . . . .	128
10.6 Triple Product “Equivalent”. . . . .	128
<b>11 Quantum Chromodynamics</b>	<b>129</b>
<b>12 Hadron Spectroscopy</b>	<b>130</b>
<b>13 High Energy Scattering</b>	<b>134</b>
<b>14 The Electro-weak Interaction</b>	<b>134</b>
<b>15 Spontaneous Symmetry Breaking, the Higgs Scalar</b>	<b>135</b>
15.1 Introduction . . . . .	135
<b>16 Neutrino Oscillation</b>	<b>136</b>
16.1 Introduction . . . . .	136
16.2 Two neutrinos oscillation . . . . .	136
<b>17 Neutrino Experiments. A Seminar</b>	<b>139</b>
17.1 The invention of the neutrino . . . . .	139
17.2 Neutrino Discovery . . . . .	139
17.3 Something different, neutrinos from the sun . . . . .	141
17.4 Reactor and high energy $\nu$ 's . . . . .	154
17.5 The missing $\nu$ 's are found . . . . .	158
17.6 Future Experiments . . . . .	161
<b>18 The Muon Anomaly. A Seminar</b>	<b>163</b>
18.1 Introduction . . . . .	163
18.2 $g$ for Dirac particles . . . . .	164
18.3 Motion and precession in a B field . . . . .	164
18.4 The first muon $g - 2$ experiment . . . . .	166
18.5 The BNL $g-2$ experiment . . . . .	166
18.6 Computing $a = g/2 - 1$ . . . . .	171
18.7 $a_\mu$ . . . . .	171
18.8 HADRONS . . . . .	172
18.9 $\sigma(e^+e^- \rightarrow \pi^+\pi^-)$ . . . . .	173
<b>19 Higgs Bosons Today. A Seminar</b>	<b>177</b>
19.1 Why are Higgs so popular? . . . . .	177
19.2 Weak Interaction and Intermediate Boson . . . . .	178
19.3 Searching for Higgs. Where? . . . . .	180
19.4 Searching fo Higgs. How? . . . . .	184
<b>20 App. 1. Kinematics</b>	<b>195</b>
20.1 4-vectors . . . . .	195
20.2 Invariant Mass . . . . .	196
20.3 Other Concepts . . . . .	196
20.4 Trasformazione di uno spettro di impulsi . . . . .	197
20.5 Esempi . . . . .	200

20.5.1	Decadimenti a due corpi . . . . .	200
20.5.2	Decadimenti a tre corpi . . . . .	201
20.5.3	Decadimento $\pi \rightarrow \mu\nu$ . . . . .	202
20.5.4	Annichilazioni $e^+e^-$ . . . . .	202
20.5.5	Angolo minimo tra due fotoni da $\pi^0 \rightarrow \gamma\gamma$ . . . . .	203
20.5.6	Energia dei prodotti di decadimenti a tre corpi . . . . .	203
20.5.7	2 particelle $\rightarrow$ 2 particelle . . . . .	204
20.6	Limite di massa infinita e limite non relativistico . . . . .	204
20.6.1	Esercizio . . . . .	206
<b>21</b>	<b>App. 2. <math>L - J - S</math>, <math>SU(2,3)</math>, <math>g</math>, <math>a</math></b>	<b>207</b>
21.1	Orbital angular momentum . . . . .	207
21.2	$SU(2)$ and spin . . . . .	209
21.3	$SU(3)$ . . . . .	210
21.4	Magnetic moment . . . . .	214
<b>22</b>	<b>App. 3. Symmetries</b>	<b>216</b>
22.1	Constants of Motion . . . . .	216
22.2	Finding Conserved Quantities . . . . .	216
22.3	Discrete Symmetries . . . . .	217
22.4	Other conserved additive Q. N. . . . .	217
22.5	$J^{PC}$ for a fermion anti-fermion pair . . . . .	217
<b>23</b>	<b>App. 4. CKM Matrix</b>	<b>220</b>
23.1	Definition, representations, examples . . . . .	220
<b>24</b>	<b>App. 5. Accuracy Estimates</b>	<b>221</b>
24.1	Testing a theory or measuring one of its paramaters . . . . .	221
24.2	A priori estimates . . . . .	221
24.3	Examples . . . . .	222
24.4	Taking into account the experimental resolution . . . . .	223
<b>25</b>	<b>App. 6. <math>\chi</math>-squared</b>	<b>224</b>
25.1	Likelihood and $\chi^2$ . . . . .	224
25.2	The $\chi^2$ solution . . . . .	224
25.3	Matrix dimensions . . . . .	226
25.4	A Simple Example . . . . .	226
	<b>References</b>	<b>228</b>

this page is blank

# 1 INTRODUCTION

## 1.1 History

The history of elementary particle physics is only 100 years old. J. J. Thomson discovered the electron in 1897 and the electron remains the prototype of an elementary particle, while many other particles discovered between then and today have lost that status. Soon came the Rutherford atom and the nucleus and the Bohr quantization. Neutrons, neutrinos and positrons came in the 30's, some predicted and found shortly thereafter, though it took many years to prove the existence of the neutrinos<sup>1</sup> To understand the interaction of elementary particles, quantum mechanics and relativity are necessary. In fact more than the two as separate pieces are necessary. Quantum field theory, the complete merging of Lorentz invariance and quantum mechanics, properly allows the description of elementary particles and their interactions. Field theory explicitly accounts for creation and absorption of field quanta, corresponding to the experimental reality we observe in the laboratory.

## 1.2 Elementary particles

The discovery of the electron led to the first model of the atom, by Thomson himself. Soon after, the Rutherford experiment, executed by Geiger and Marsden, proved the untenability of the Thomson atom and the atom, or better the nucleus, becomes understood in its correct form. This rapidly leads to the understanding of the proton. Thanks to Thomson, Rutherford, Planck, Einstein, Chadwick and Mosley, early in the last century three elementary particles are known, the electron  $e$ , the photon  $\gamma$  and the proton  $p$ . The proton has lost this status today, or better some 40 years ago.

In a beautiful interplay between theory advances and experiments the list of particles grows rapidly, adding the neutron, the positron and the neutrino in 1932. Around 1930 the first glimpses of field theory are developing, culminating in 1950 with the Quantum Electrodynamics, QED, of Feynman and Schwinger, also Tomonaga, and the renormalization program. All the problems that had made Lorentz life miserable, the self-energy of the electron, the divergences of the classical electromagnetism, are understood. At the very least we know today how to get finite and even

---

<sup>1</sup>It turned out that there are three types on neutrinos, the first was found in 1953, the second was proved to exist in 1962 and the third became necessary in the 70's and has probably been observed in the year 2000.

very accurate answers for measurable quantities, which used to come out infinite in classical electromagnetism.

Fermi, inspired by the theory of electromagnetic radiation, introduces a four fermion effective theory of  $\beta$ -decay, which is violently divergent, if used next to lowest order. The agreement of experiments with lowest order calculations is however excellent and the theory makes the neutrino a reality, even though it will not be detected until 1953 ( $\bar{\nu}_e$ ). A four fermion interaction is non renormalizable. Yukawa also extends the em theory of radiation to the strong interactions, introducing a new field quantum, the pion. The pion corresponds to the photon of electromagnetism, but with zero spin and non zero mass. The Yukawa theory is renormalizable.

At the end of the World War II years, some new unexpected findings again pushed forward particle physics, mostly creating hard puzzles. First, after some confusion, a new fermion is discovered, the muon -  $\mu$ . The confusion is due to the fact that at first the muon was thought to be the pion of Yukawa, but Conversi *et al.* in Rome proved differently. The pion is soon later discovered. Then come strange particles, necessitating entirely new ideas about conservation laws and additive quantum numbers.

A period of rapid development, when new particles were discovered by the dozen, both created confusion and stimulated the birth of the new ideas which eventually led to today's understanding of elementary particles and their interactions<sup>(4)</sup>

**Table 1.1.** Elementary particles in 1960

$J$	Symbol	Generic name	Elementary?
0	$\pi^{\pm,0}, K^{\pm,0,\bar{0}}, ..$	(P)Scalar mesons	no
1/2	$e, \mu, e_{\mu}, \nu_{\mu}$	Leptons	yes
	$p, n, \Lambda, \Sigma...$	Baryons	no
1	$\gamma$	Photon	yes
	$\rho, \omega...$	Vector mesons	no
3/2	$\Delta^{++,+,0,-}, .. \Xi^{-,0}...$	Baryons	no

It is perhaps odd that today, particle physics is at an impasse: many new ideas have been put forward without experiment being able to confirm or refute. Particle physics has been dominated by experiments, theory building beautiful synthesis of ideas, which in turn would predict new observable consequences. It has not been so now for some time. But we strongly believe new vistas are just around the corner. A list of particles, around 1960 is given in the table below.

The vast majority of the elementary particles of a few decades ago do not survive

as such today. A table of what we believe are elementary particles is given below:

**Table 1.2.** Elementary particles in 2001

$J$	Symbol	Generic name	Observed
0	$H$	Higgs scalar	no
1/2	$e, \mu, \tau, \nu_e, \nu_\mu, \nu_\tau$	leptons	yes
	$u, d, c, s, t, b$	quarks	yes
1	$\gamma$	photon	yes
	$g_j^i$	gluon (8)	yes
	$W^\pm, Z^0$	vector bosons	yes
2		graviton	no

All spin 0, 1/2, 1, 3/2, 2... hadrons have become  $q\bar{q}$  or  $qqq$  bound states. We are left with  $1+12+1+8+3=25$  particles, plus, for fermions, their antiparticles, which in a fully relativistic theory need not be counted separately. Pushing a point we could count just  $1+12+1+1+2=17$  particles, blaming the existence of 8 different gluons on the possible values of an internal degree of freedom. Notice that we have included in the list the Higgs scalar, about which we know nothing experimentally. It is however needed as the most likely means to explain how the  $W$  and  $Z$  gauge boson acquire a non vanishing mass.

Almost in one day, 136 mesons and 118 baryons were just dropped from the list of particles, elementary that is. Still 17 or 25 elementary particles are a large number. Theories have been proposed, in which these 17 objects are themselves made up of a smaller number of constituents. These theories are not self-consistent at the moment. Other attempts to go beyond present knowledge invoke an entirely new kind of symmetry, called supersymmetry, which requires instead a doubling (or more) of the number of elementary particles. Again if such doubling were due to some internal degree of freedom, such that the new particles' properties were uniquely determined by those of the particles we know, we might be more willing to accept the doubling. It turns out that supersymmetry cannot be an exact, local symmetry. It can only be a global symmetry, broken in some way. Thus more parameters appear in the theory: the masses of the new particles and the coupling constants. There are other unanswered questions, we mention two in the following.

### 1.2.1 Masses

There are many puzzles about the masses of the elementary particles. Local gauge invariance, the field theory formulation of charge conservation, requires that the gauge vector fields mediating interactions are massless. This appears to be the case of the photon, to very high experimental accuracy. From the limits on the value of  $\epsilon$  in the Coulomb potential

$$V(r) \propto \frac{1}{r^{1+\epsilon}} \quad (1.1)$$

obtained in classical measurements, one finds  $m_\gamma < 6 \times 10^{-16}$  eV. Gluons do appear to be massless, although at low energy the theory is hard to use and verify.  $W$  and  $Z$  definitely are not massless. The Higgs meson is therefore introduced in the standard model to spontaneously break the electro-weak  $SU(2) \otimes U(1)$  gauge symmetry. The gauge bosons acquire a mass and miraculously the theory remains renormalizable.

To be more precise, many years of formal development have lead to the explicit construction of a “spontaneous” symmetry breaking mechanism which explains how the gauge bosons acquire mass. The corresponding “almost” gauge invariant theory was then proven to be renormalizable. The miracle is, perhaps, that this theory, incomplete and unsatisfactory, is confirmed by experiments, so far.

The mass of the Higgs itself is not determined, the appropriate energy scale being  $1/\sqrt{\sqrt{2} \times G_F} = 246$  GeV, where  $G_F = 1.166 \times 10^{-5}$  GeV<sup>-2</sup> is the Fermi coupling constant.

The values of the fermion masses seem even more peculiar. While the neutrino mass was originally assumed to be zero, there is no reason for it to be so, except in the construction of the standard model, the recently discovered top quark has a mass of 175 GeV. The spin 1/2 fermion masses, leptons and quarks, are generated in the standard model through Yukawa couplings to the Higgs field, with arbitrary constants  $\lambda$ , one for each fermion, each to be adjusted so as to give the observed mass. The theory offers no guide for the value of these coupling constants. The explanation of the standard model is therefore sterile, a confession of ignorance. The fermion masses’ spectrum is entirely a mystery at the moment. The zero mass of the neutrino, in fact, is not too well established. All measurements of  $m(\nu_e)$  are consistent with zero, typically giving  $m(\nu_e) < 10 - 15$  eV, although all recent experiments consistently find  $m^2(\nu_e) < 0$ . Recently observations on solar and atmospheric neutrino intensities have been taken to suggest that neutrinos oscillate between their possible flavors, leading to neutrino masses in the  $10^{-2}$ - $10^{-3}$  eV, although with some conflicts. It has been argued (Okun) that the natural values of the fermion mass

are either zero or 246 GeV, the value mentioned above. The observed values almost cover the whole range.

### 1.2.2 Conserved additive quantities

From the observed absence of expected process one is led to postulate the existence of additive quantum numbers corresponding to charge-like observables. Thus the stability of nuclear matter leads to assigning a baryon number to all hadrons and to the assumption that the baryon number  $B$  is conserved, maybe exactly. Again when the standard model became reasonably established, it became clear that it does not guarantee in any way the conservation of baryon number. Baryon conservation is just assumed, *i.e.* it is put in by hand. Minimal extension of the standard model predicted that the proton lifetime should be of  $\mathcal{O}(10^{28} \text{ or } 29)$  years but no decay has been detected, corresponding to lifetimes as large as  $10^{32}$  years. The interpretation of the results is somewhat ambiguous. Note that the lifetime of the universe is about  $5 \times 10^{10}$  years. From a practical point, one mole of protons is  $\sim 10^{24}$  protons and 1000 tons of matter,  $10 \times 10 \times 10 \text{ m}^3$  of water, contain  $10^{33}$  nucleons. Therefore a lifetime of  $10^{33}$  years means one decay per year! This limit might be reached in a few years by “Super Kamiokande”. SuperK recently suffered a terrible accident.

Another such quantity is the lepton number  $L$ . For that matter there are three conserved lepton numbers,  $L_e$ ,  $L_\mu$  and  $L_\tau$ . Reactions in which  $\mu \rightarrow e$  don't appear to go. Branching ratio limits are  $10^{-11}$ ,  $10^{-12}$ , many orders of magnitude lower than expected in naive models. Still exact conservation of  $L$  implies the existence of three new kinds of photon-like fields:  $\gamma_e$ ,  $\gamma_\mu$  and  $\gamma_\tau$ .

The problem with the conservation of such charges lies in the fact that, in field theory, conservation can be guaranteed by the existence of a local gauge invariance. A local gauge invariance requires however the existence of a massless gauge field, the equivalent of the photon field for the  $U(1)$  local gauge symmetry guaranteeing conservation of electric charge. There is no evidence whatsoever for such fields. Historically it was through attempts to understand conservation of baryon number that non-abelian gauge invariance and the corresponding Yang-Mills fields were introduced, leading later to the development of the correct theory of strong interactions, quantum chromo dynamics or QCD.

### 1.3 Natural Units: $\hbar=c=1$

Some physical constants are of universal importance and tend to appear in many relations. For both reasons it is convenient to choose units in which they become unity and dimensionless. Moreover there is no reason for having four or three or whatever dimensioned units other than convenience. When this is done physics appears more transparent, at the cost of having to convert to more common units at the end of a calculation. In the following we will use units, as is commonly done in particle physics, which follow from setting  $\hbar=c=1$ . Then  $[L] = [T]$ , from  $c=1$  and  $[E] = [L^{-1}]$ . Thus we are left with only one dimensionful quantity which can be taken either as energy, typically measured in eV, (or MeV or GeV) or length, usually measured in fermi,  $1 \text{ fm}=10^{-13} \text{ cm}$ , or time, for which we retain the second. Conversion from MeV to fermi to seconds follows from the value of  $c$  and  $\hbar$ . From  $\hbar \times c=197.327 \text{ 053 MeV} \times \text{fm}$ , we find

$$1 \text{ fm} \sim 1/197 \text{ MeV}^{-1}.$$

From  $c=2.99... \times 10^{10} \text{ cm/s} \sim 3 \times 10^{23} \text{ fm/s}$  we have  $1 \text{ fm} \sim 3.33 \times 10^{-24} \text{ s} = 1/197 \text{ MeV}^{-1}$ . Recalling that  $\tau = 1/\Gamma$ , we can rephrase this last statement as - a state which has a 197 MeV width decays with a lifetime of  $3.33 \times 10^{-24} \text{ s}$ . Other convenient relations are:  $1 \text{ mb}=2.57 \text{ GeV}^{-2}$  and  $1 \text{ GeV}^{-2}=389 \mu\text{b}$ . For convenience we list below some conversions between units of interest in particle physics.

**Table 1.3.** Unit conversion

To convert from	to	multiply by
1/MeV	s	$6.58 \times 10^{-22}$
1/MeV	fm	197
1/GeV <sup>2</sup>	mb	0.389

and the width-lifetime relations typical of strong and weak interactions

$$\begin{aligned} \Gamma=100 \text{ MeV} &\rightarrow \tau=6.58 \times 10^{-24} \text{ s} \\ \tau=10^{-10} \text{ s} &\rightarrow \Gamma=6.58 \times 10^{-6} \text{ eV} \\ \Delta m_K (\sim \Gamma_S/2) &=0.53 \times 10^{10} \text{ s}^{-1} \rightarrow \Delta m_K=3.49 \times 10^{-6} \text{ eV} \end{aligned}$$

## Physical Constants and Units

fermi	fm	$10^{-13}$ cm
barn	b	$10^{-24}$ cm <sup>2</sup>
angstrom	Å	$10^{-8}$ cm
Speed of light	$c$	$2.9979.. \times 10^{10}$ cm s <sup>-1</sup>
Electron charge	$e$	$1.602... \times 10^{-19}$ C
Planck's constant, reduced	$\hbar \equiv h/2\pi$	$6.582... \times 10^{-22}$ MeV s
Conversion constant	$\hbar c$	197.3... MeV fm
Electron mass	$m_e$	0.511... MeV
Proton mass	$m_p$	938.3... MeV
Fine structure constant	$\alpha$	1/137.035...
Fermi constant	$G_F$	$1.166 \times 10^{-5}$ GeV <sup>-2</sup>
Gravitational constant	$G_N$	$6.707 \times 10^{-39}$ GeV <sup>-2</sup>
Avogadro's number	$N_A$	$6.022 \times 10^{23}$ mole <sup>-1</sup>
Molar volume		22,414 cm <sup>3</sup> mole <sup>-1</sup>
$kT$ at 1 K		$8.617... \times 10^{-5}$ eV

## 1.4 The Electromagnetic Interaction

The (potential) energy of two charges of magnitude  $e$ , the electron charge, is

$$\begin{aligned}
 V &= \frac{e^2}{r} \quad \text{cgs units} \\
 &= \frac{e^2}{4\pi\epsilon_0 r} \quad \text{MKS units, rationalized}
 \end{aligned}$$

In natural units,  $\hbar=c=1$ ,  $[e^2] = [Vr]$  is dimensionless since  $[E] = [L^{-1}]$ .  $e^2$  is usually indicated with  $\alpha$  and is called the fine structure constant, since historically it was first measured in the study of the fine structure of the spectral lines. Putting back  $\hbar$  and  $c$ ,  $\alpha$  is given by:

$$\begin{aligned}
 \alpha &= \frac{e^2}{\hbar c} \quad \text{cgs units} \\
 &= \frac{e^2}{4\pi\epsilon_0 \hbar c} \quad \text{SI units}
 \end{aligned}$$

International System of Units (SI)

$\alpha$  as written above is dimensionless in both unit systems and its value is

$$\alpha = \frac{1}{137.03\dots} \quad (1.2)$$

Traditionally in electrodynamics two other systems are used. One is the Gauss system in which cgs-es, or esu, units are used for electric quantities and cgs-em units are used for magnetic quantities which results in powers of  $c$  appearing when both quantities enter in a formula. In Gauss units the Lorentz force is

$$\vec{F} = q(\vec{E} + \frac{1}{c}\vec{v} \times \vec{B}).$$

The other system of units is the Heaviside system which is like the Gauss one, except that the Coulomb law is *rationalized* by introducing a factor  $4\pi$  in the denominator. The value of  $\alpha$  remains the same, but the unit of charge is different. In the Heaviside system

$$\alpha \equiv \frac{e^2}{4\pi\hbar c} = \frac{e^2}{4\pi} \quad (1.3)$$

where the last expression is valid in natural units. Computations in quantum electrodynamics are usually performed in the Heaviside system.

## 1.5 The many meanings of $\alpha$

The constant  $\alpha$  gives us the strength of the electromagnetic interaction, one of the fundamental interactions of nature. Before discussing this we derive some simple expressions involving  $\alpha$ . The simplest system, which we can study in quantum mechanics, is the hydrogen atom. We can find the lowest energy state of the hydrogen atom, we set the proton mass to infinity for simplicity, by minimizing the total energy, expressed as a sum of the potential and kinetic terms. We begin with the classical expression for the energy

$$E = V + T = -\frac{\alpha}{r} + p^2/2m_e.$$

Quantizing the system means to use the so-called uncertainty principle which, in our natural units is simply  $p = 1/r$  ( $\hbar=c=1$ ). The meaning here is that if the electron is confined in a region of dimensions  $r$  its average momentum is  $\sim p$ . The minimum energy is found setting to zero the derivative of  $E$  with respect to  $p$

$$\frac{d}{dp}(-\alpha p + p^2/2m_e) = -\alpha + p/m_e = 0$$

giving  $p = m_e\alpha$  from which we find the Bohr radius  $a_\infty = 1/(m_e\alpha)$ , in natural units. Reintroducing  $\hbar$  and  $c$  we find a more familiar expression  $a_\infty = 4\pi\epsilon_0\hbar^2/m_e e^2$  in SI units ( $a_\infty = \hbar^2/m_e e^2$  in cgs units). In natural units the Rydberg constant is  $\alpha^2 m_e/2$  or  $R_\infty = 510\,999 \text{ eV}/(2 \times 137.036^2) = 13.605\dots \text{eV}$ . Since  $p/m_e = \alpha$ ,  $\alpha$  is the velocity of the electron in the lowest orbit. In the limit  $M_p/m_e =$

$\infty$ , all properties of the hydrogen atom are given in terms of the strength of the electromagnetic interaction  $\alpha$ , a number nobody has found a way to compute, it comes from experiment, and a second *mysterious* number, the electron mass.

## 1.6 The Gravitational Interaction

The gravitational or Newton constant, in SI units, is:

$$G_N = 6.67259 \times 10^{-11} \text{ m}^3 \text{ kg}^{-1} \text{ s}^{-2}$$

From  $V = GMm/r$  and in natural units with  $[L] = [T] = [M^{-1}] = [E^{-1}] =$ ,  $G_N$  has dimensions  $[M^{-2}] = [E^{-2}]$ . Conversion to natural units gives:

$$\begin{aligned} 1 \text{ m} &= 10^{15} \text{ fm} \\ \frac{1}{1 \text{ kg}} &= \frac{e}{c^2} \frac{1}{\text{eV}} \\ \frac{1}{1 \text{ s}^2} &= \frac{1}{c^2 \times 10^{30}} \frac{1}{\text{fm}^2} \end{aligned}$$

which together with

$$\begin{aligned} c &= 2.997\,924\,58 \times 10^8 \text{ m s}^{-1} \\ e &= 1.602\,177\,33 \text{ C} \\ 1 \text{ fm} &= \frac{1}{197.327\,053 \text{ MeV}} \end{aligned}$$

gives

$$G_N = 6.707\,112\,607 \times 10^{-39} \text{ GeV}^{-2}$$

We would like to try to characterize the gravitational interaction by a dimensionless parameter such as  $\alpha$  for the interaction between charges and electromagnetic fields. We can again write the potential energy for two equal masses:

$$V = G_N \frac{m^2}{r}.$$

We clearly run into a problem here,  $Vr$  is dimensionless,  $m^2$  certainly is not. In fact the gravitational constant has dimensions  $[G_N] = [E^{-2}]$ . The dimensionless interaction strength equivalent to  $\alpha$  is now  $G_N \times m^2$  and is not a constant at all, it grows with  $m^2$ . While the gravitational interaction is very small in particle physics, in an the atom or a nucleus for example, for large enough masses we run into problems. If we consider large enough masses, or small enough distances for that matter, we can get to an interaction strength of 1. At this point we run into problems

if we try to compute anything, since the perturbative expansion which takes into account repeated interactions diverges badly. The relation

$$G_N \times m^2 = 1$$

allows computing the mass at which the interaction strength becomes unity. This mass is called the Planck mass, given by:

$$M_{\text{Planck}} = 1.221\,046\,49 \times 10^{19} \text{ GeV}$$

and its inverse is the Planck length

$$L_{\text{Planck}} = 0.82 \times 10^{-19} \text{ GeV}^{-1} = 1.9 \times 10^{-20} \text{ fm}$$

We can note that in QED the charge is the source of the field and the charge is dimensionless. In gravity, the mass is the source of the field but mass is also energy.

## 1.7 Interactions and coupling constants

The elementary interactions are described by terms in the Lagrangian density,  $\mathcal{L}$ , linear in the field operators of the elementary objects involved. In general such terms appear multiplied by an arbitrary parameter, called the interaction coupling constant. The interaction Hamiltonian  $H_{\text{int}}$  is given by:

$$H_{\text{int}} = \int d^3x \mathcal{H}_{\text{int}} = - \int d^3x \mathcal{L}_{\text{int}}$$

where  $\mathcal{H}_{\text{int}} = -\mathcal{L}_{\text{int}}$  is a function of the interacting fields all at the same space-time point  $x$  and in general of their derivatives. Using  $\phi$  and  $\psi$  to generically describe a spin 0 and a spin 1/2 field, typical interaction terms are:  $\mu\phi\phi\phi$ ,  $\lambda\phi\phi\phi\phi$ ,  $g\phi\bar{\psi}\psi$ ,  $G\bar{\psi}\psi\bar{\psi}\psi$  and so on. The coupling constants appearing in different interactions have different dimensions, which we can easily determine. First we note that since  $\int \mathcal{L} d^3x$  has dimensions of energy we have  $[\mathcal{L}] = [\text{E}^4]$ . The mass terms in the Lagrangian, for spinless and spin 1/2 fields are respectively  $m^2\phi^2$  and  $m\psi^2$ . From which  $[\phi] = [\text{E}]$  and  $[\psi] = [\text{E}^{3/2}]$ , we shall simply say dimension 1, etc. The dimension of the coupling constants for the interactions above are therefore as listed below:

Interaction	Coupling Constant	Dimension
$\phi\phi\phi$	$\mu$	1
$\phi\phi\phi\phi$	$\lambda$	0
$\phi\psi\psi$	$g$	0
$\psi\psi\psi\psi$	$G$	-2

We now turn to the paradigm of an interacting field theory, quantum electrodynamics, whose Lagrangian is:

$$\begin{aligned}\mathcal{L}_{\text{QED}} &= \mathcal{L}_{\text{Dirac}} + \mathcal{L}_{\text{Maxwell}} + \mathcal{L}_{\text{int}} \\ &= \bar{\psi}(i\cancel{D} - m)\psi - \frac{1}{4}(F_{\mu\nu})^2 - e\bar{\psi}\gamma^\mu\psi A_\mu\end{aligned}$$

where  $A_\mu$  is the electromagnetic vector potential or better the photon operator, and the field strengths are  $F_{\mu\nu} = \partial_\mu A_\nu - \partial_\nu A_\mu$ . From the Maxwell term,  $A_\mu$  has dimensions 1, *i.e.*  $[A]=[E]$  and the interaction constant  $e$ , the electric charge of the electron, is dimensionless.

Yukawa analogy to QED, the so called Yukawa interaction, is

$$\mathcal{L}_{\text{Yukawa}} = \mathcal{L}_{\text{Dirac}} + \mathcal{L}_{\text{Klein-Gordon}} - g\bar{\psi}\psi\phi$$

where the photon is replaced with a scalar particle and  $g$ , as we saw, is dimensionless.

There are two kinds of considerations we can make here. Some coupling constants are dimensionless, which permits a meaningful comparisons of the relative strength of different interactions. This might just be a convenient point, and in fact today, with hopes of reaching a sort of *grand unification* in which three of the once different interactions, strong, em and weak, might all have the same strength, is not any more so important. More important is the fact that interactions with a coupling constant of negative energy dimensions are not renormalizable which means they do not give finite results beyond the first order. The argument can be made quite simple. In any theory, higher order terms involve integrals over the 4-momenta of intermediate particles, which have the form

$$\int^\infty d^4q \frac{1}{q^2}$$

and therefore are formally divergent. The standard procedure is to introduce a cut-off parameter  $\Lambda$  and perform the above integrations only up to  $\Lambda$ . At the end one takes the limit  $\Lambda \rightarrow \infty$ , hoping for a finite result, independent of  $\Lambda$ . This is not possible for couplings with negative dimensions. This goes as follows: the contribution of any term in the perturbative expansion to the scattering amplitude contains the coupling constant and must be dimensionless - at least all terms must have the same dimensions, which we reduce to zero. But the second requirement implies, for negative dimension couplings, that the diverging terms contain positive powers of  $\Lambda$ , thus we cannot hope anymore to remove divergences.

In addition to the interaction terms discussed above, we can have two more Lorentz-scalar terms with vector field and dimension zero coupling constants:

$$A^2\partial_\mu A^\mu \quad \text{and} \quad A^4.$$

The only Lorentz-scalar, renormalizable, interactions involving scalar, spinor and vector particles are therefore:  $\mu\phi\phi\phi$ ,  $\lambda\phi\phi\phi\phi$ ,  $g\phi\bar{\psi}\psi$ , the QED like interaction, often written as  $J^\mu A_\mu$  and the last two terms just above. All of these interactions appear in the present models of strong, em and weak interactions. In fig. 1.1 we illustrate the interactions by the corresponding lowest order amplitudes.

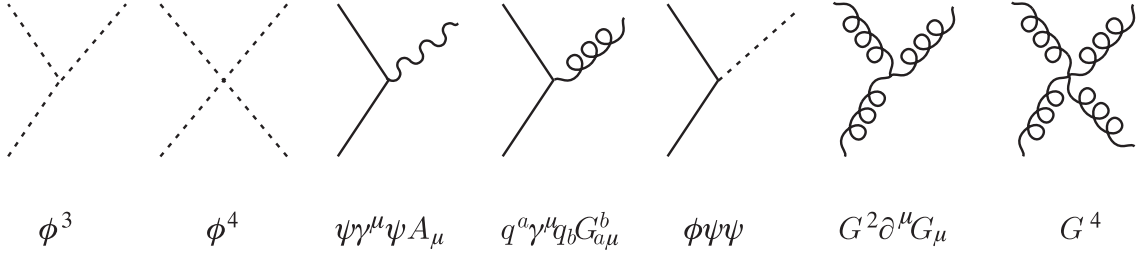


**Fig. 1.1.** Feynman graphs of the lowest order amplitudes for the renormalizable interactions observed in nature. Color indexes are indicated with a and b and all amplitudes are supposed to be color scalars.

In particular, it is a triumph of the standard model of having gone beyond the Fermi interaction, with coupling constant  $G_F=10^{-5} \text{ GeV}^{-2}$ , which at lowest order is an excellent description of the weak interactions. It is just the low energy limit of a vector-spinor-spinor interactions, current $\times$ vector field interaction, formally very similar to the electromagnetic interaction. Strong interactions have also become a current $\times$ vector field interaction, QCD, with the difference over QED, that gluons are ‘charged’ and therefore interact among themselves, requiring the trilinear and quadrilinear couplings last mentioned. The  $\phi\psi\psi$  interaction, originally introduced by Yukawa to explain the nuclear force, also appears in the standard model to explain fermion and intermediate vector boson masses.

Finally we can consider the QED Lagrangian for scalar particles. We find the terms  $eA^\mu\phi\partial_\mu\phi^*$  and  $e|\phi|^2A^2$  which correspond to a renormalizable interactions but do not appear to be realized in nature. There are no scalar charged point particles, unless we allow a proliferation of Higgs bosons.

## 2 Order of Magnitude Calculations

### 2.1 Introduction

Dimensional analysis, together with good physical intuition and some luck, allows simple and *relatively* accurate estimates of measurable parameters, cross sections and decay rate. At least we should get the right order of magnitude and functional dependence on the appropriate variables, when compared to experiment. The importance of the following examples lies in the fact that they help understanding of the mechanisms implied by the various theories of the elementary interactions. For these estimates we will use the values of various parameters as given below.

Fine structure constant	$\alpha$	1/137
Fermi constant	$G_F$	$10^{-5} \text{ GeV}^{-2}$
Electron mass	$m_e$	0.51 MeV
Nucleon radius	$r_p$	1 f
Strong interaction coupling constant	$g$	1

To the list of rules, we add that we must respect Lorentz invariance. Note that the calculation of the Bohr radius done previously does not belong to this class, it is the correct way of quantizing a classical system.

### 2.2 $e^+e^- \rightarrow \mu^+\mu^-$

We estimate the cross section for this process in the high energy limit. Both particles are charged leptons for which electromagnetism is the strongest interaction. The lowest order diagram for the process is shown in figure. In all the following calculations, we use Feynman graphs simply to count powers of the coupling constant which appear in the amplitude.

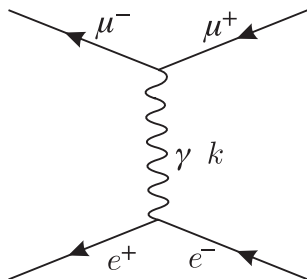


**Fig. 2.1.** Feynman graph for  $e^+e^- \rightarrow \mu^+\mu^-$ .  $k$  is the photon 4-momentum.

The process is described kinematically by just one variable:  $s = k^\mu k_\mu = E_{\text{CM}}^2$ . The amplitude is proportional to the electron charge squared *i.e.* to  $\alpha$ . The transition

probability is therefore proportional to  $\alpha^2$  Therefore in general:

$$\sigma(e^+e^- \rightarrow \mu^+\mu^-) = \alpha^2 \times f(s, m_e, m_\mu),$$

where  $f$  is a function of all independent Lorentz scalars. At high enough energy, the masses of both electrons and muons can be neglected. Dimensionally  $[\sigma] = [L^2] = [E^{-2}]$  and therefore:

$$\sigma(e^+e^- \rightarrow \mu^+\mu^-) = \frac{\alpha}{s}.$$

The complete calculation of the cross section from the amplitude of fig. 2.1 gives:

$$\sigma(e^+e^- \rightarrow \mu^+\mu^-) = \frac{4\pi}{3} \frac{\alpha}{s},$$

about 4.2 times bigger than our estimate. We will see why we get 2's and  $\pi$ 's in the complete calculations. Numerically:

$$\sigma(e^+e^- \rightarrow \mu^+\mu^-) \sim \frac{4 \times 10^{-32}}{s \text{ (GeV}^2\text{)}} \text{ cm}^2$$

which is agreement with experiment within the above factor of  $\sim 4^2$

### 2.3 $\nu + N \rightarrow \dots$

We want to estimate the total cross section for neutrinos on nucleons, summed over all possible final states. The amplitude of a weak process like this is proportional to  $G_F$  and at high energy, where all masses become irrelevant,

$$\sigma(\nu N) = G_F^2 f(s) = G_F^2 s,$$

where  $s$  is the CM energy and from the dimensions of  $\sigma$  and  $G_F$ ,  $f(s) = s$  follows. While the reaction we first examined is typically observed with colliding beams, in the present case one studies collisions of a beam of neutrinos of energy  $E$  against nucleons of mass  $m_N \sim 1$  GeV in a stationary target. In terms of these variables, we get  $s \sim 2m_N E_\nu$ , and the dimensional analysis result is:

$$\sigma(\nu N) \sim G_F^2 m_N E_\nu.$$

Inserting values for  $G_F$  and  $m_N$  and using  $1/\text{GeV}^{-2} \sim 0.4$  mb we find:

$$\sigma(\nu N) \sim 4 \times 10^{-38} \times E_\nu \text{ cm}^2, \text{ with } E_\nu \text{ in GeV},$$

to be compared with measurement:

$$\sigma(\nu N) = 0.6 \times 10^{-38} \times E_\nu \text{ cm}^2.$$

---

<sup>2</sup>1/s dependence is characteristic of point-like particles. FF modify  $s$  dependence.

As in the first case, within some factor, we obtain a reasonable estimate and the correct dependence on energy, even if the two cross sections differ by many orders of magnitude at 1 GeV. We also note the quite different energy behaviour. The muon pair cross section vanishes at high energy as  $1/s$  while the neutrino scattering cross section diverges as  $s$  ( $E_\nu$  in the laboratory). The diverging neutrino cross section is a signal of something wrong:<sup>3</sup>

## 2.4 Compton scattering

The lowest order amplitude for Compton scattering

$$e^\pm + \gamma \rightarrow e^\pm + \gamma$$

is shown in figure 2.2.



**Fig. 2.2.** Amplitude for  $e^\pm + \gamma \rightarrow e^\pm + \gamma$ .  $k$  is the photon 4-momentum and  $p$  that of the electron.

As before the cross section should have the form  $\sigma_{\text{Compton}} = \alpha^2 f(s, m_e)$ , the only variables involved in the process. In the non relativistic limit,  $s \rightarrow m_e$  and therefore:

$$\sigma_{\text{Compton}} = \frac{\alpha^2}{m_e^2}$$

while at high energy, the electron mass becomes negligible:

$$\sigma_{\text{Compton}} = \frac{\alpha^2}{s}.$$

A complete calculation, to lowest order, gives

$$\sigma_{\text{Compton}} = \begin{cases} \frac{8\pi}{3} \frac{\alpha}{m_e^2} & s \rightarrow m_e \\ 2\pi \frac{\alpha}{s} \ln \frac{s}{m_e^2} & s \rightarrow \infty. \end{cases} \quad (2.1)$$

While the low energy limit is off by a factor of  $8\pi/3$  as we have come to expect, we miss completely in finding the logarithmic  $s$  dependence at high energy as well as a factor  $2\pi$ . The appearance of the log term can in fact be explained on the bases of quite different considerations, see T.D. Lee.

<sup>3</sup> $S$ -wave unitarity requires, ignoring many numerical factors,  $pr < 1$  from which  $s^2 < 1/G^2$ . Unitarity is violated by the calculated cross section for CM energies  $\sim 1/\sqrt{G} \sim 300$  GeV.

## 2.5 Muon decay

Before continuing with other different cases, we consider the decay  $\mu^\pm \rightarrow e^\pm \nu \nu$  which gives us a first result which is quite wrong but about which we can do something and learn too. As always we begin with

$$\frac{1}{\tau} = \Gamma = G_F^2 \times f(m_\mu)$$

which is valid if we neglect the much smaller electron mass. Since  $[\Gamma] = [E]$  we are tempted to conclude:

$$\Gamma = G_F^2 m_\mu^5$$

a result which is wrong by a factor  $1/(192\pi^3)$  which is  $\sim 1/6000!$  What went wrong this time? Note that if we just compare decay rates of different parent particles the  $m^5$  dependence is in fact correct. The failure by a factor 6000 has to do with the number of particles in the final state and the sum over final states or simply the phase space available to the end products. A suppression factor of  $32\pi^2 \sim 320$  comes from going to three bodies in the final state rather than two as was the case so far. We were also always wrong by some factor of 4 to 8, which also comes from neglecting phase space and normalization. Still, after all this, the muon result is worse than the others by a factor of 4-8. Only an honest calculation can give the correct answer.

## 2.6 Pair production and bremsstrahlung

Pair production by a photon can only occur in the field of a nucleus with charge  $Ze$  which absorbs the recoil momentum necessary not to violate Lorentz-invariance as illustrated in fig. 2.3 A.

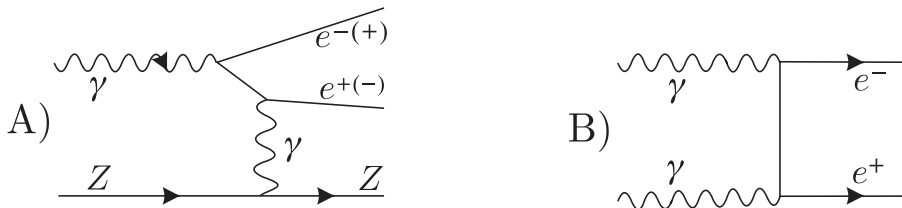


**Fig. 2.3.** A) Amplitude for pair production in the field of a nucleus of charge  $Ze$ . B) Amplitude for  $\gamma + \gamma \rightarrow e^+ + e^-$ .

Before dealing with pair production, we consider the two photon process  $\gamma\gamma \rightarrow e^+e^-$  whose amplitude is shown in fig. 2.3 B. By counting powers of  $e$  and dimensional

arguments we get the familiar result

$$\sigma(\gamma + \gamma \rightarrow e^+ + e^-) = \frac{\alpha^2}{s}$$

for high enough energies so that the electron mass can be neglected. The connection between this last process and the one we are interested in is clear: the Coulomb field of the nucleus, which we take to be of infinite mass, provides an almost real photon which, together with the initial photon, produces the  $e^+e^-$  pair. The electrostatic Coulomb potential is  $Ze/r$  whose Fourier transform,  $1/q^2$ , is the spectrum of the virtual photons corresponding to the potential. The 4-momentum of the virtual photon in fig. 2.3 A is  $p = (0, \vec{p})$ , *i.e.* the nucleus absorbs momentum but not energy because its mass is infinite. Because of this exchanged momentum the momenta of the two final electrons become independent in pair creation, contrary to the case of  $\gamma\gamma \rightarrow e^+e^-$ . Therefore, the final state of the pair production process contains an extra factor  $d^3p/E$  for the two electrons. Dimensionally this means that an extra factor  $p^2 \sim s$  must appear in the cross section, canceling the  $1/s$  factor in the  $\gamma\gamma$  result. Counting powers of  $e$  and  $Z$ , and taking into account the above, we finally write  $\sigma = Z^2\alpha^3 f(m_e)$  and therefore:

$$\sigma_{\text{Pair}} \sim \frac{Z^2\alpha^3}{m_e^2}.$$

The complete result is the Bethe-Heitler formula:

$$\sigma_{\text{Pair}} = \frac{28}{9} \frac{Z^2\alpha^3}{m_e^2} \ln \frac{E_\gamma}{m_e}$$

which is valid for a point nucleus, without screening. In fact, the Coulomb field does not extend to infinity because of the atomic electron screening. Taking this into account, the log term becomes a constant,  $\sim \ln(183 \times Z^{-1/3})$ .

Apart from the fact that we were reasonably able to guess the magnitude and energy behavior of the pair production cross section in matter for high energy photons, we want to comment on the implication of the result. At high energy, photons have a finite, non-zero, mean free path in matter which is essentially energy independent contrary to a naive expectation that absorption should disappear at high energy. Finally we remark that the same result applies to bremsstrahlung. The process by which a high energy electron, or positron, radiates crossing matter is identical to that of pair creation. Figure 2.4 B shows the relation of the bremsstrahlung amplitude to that of pair creation, fig. 2.4 A.

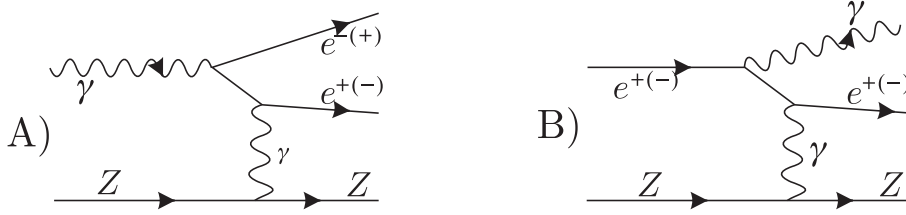


**Fig. 2.4.** A) Amplitude for pair production in the field of a nucleus of charge  $Ze$ . B) Amplitude for photon radiation by an electron in the field of a nucleus of charge  $Ze$ .

High energy electrons also have a finite, non-zero, mean free path in matter. At high energy the electron bremsstrahlung cross section is  $9/7$  times the pair production cross section. The property of matter when traversed by high energy electron or photons can be described in terms of a single parameter, the radiation length  $X_0$  which is closely related to the mean free path,  $\lambda \propto 1/\sigma$ . From the above discussion, the radiation length, expressed in  $\text{g cm}^{-2}$ , in the approximation that for all nuclei  $A/Z$  is a constant, is proportional to  $1/Z^2$ . The radiation length for air is 302 m, for water is 36 cm and for lead is 5.6 mm.

## 2.7 High energy hadronic total cross sections

Dimensional arguments lead naturally to a total cross section for scattering of any hadron pair at high energy of order  $\pi r^2$ , where  $r$  is the Compton wavelength of the pion, the lightest hadron. This is of course also the range of the strong or nuclear force and the radius of the proton. For proton-proton scattering we thus find:

$$\sigma_{pp} = \pi r_p^2 \sim 3 \times 10^{-26} \text{ cm} \sim 30 \text{ mb}$$

Hadrons, as we shall see are made up of quarks which at high energies can be treated as quasi free particles. Nucleons, also hyperons, are made up of three quarks. Mesons of two. We are thus led to expect:

$$\frac{\sigma_{\pi p}}{\sigma_{pp}} \sim \frac{\sigma_{Kp}}{\sigma_{pp}} \sim \frac{2}{3},$$

for any charge of pions and kaons. Together with the above result, dimensional arguments give:

$$\sigma_{np} \sim \sigma_{pp} \sim \sigma_{\bar{p}p} \sim \sigma_{\bar{p}n} \sim 30 \text{ mb.}$$

and

$$\sigma_{\pi^+p} \sim \sigma_{\pi^-p} \sim \sigma_{K^+p} \sim \sigma_{K^-p} \sim 20 \text{ mb}$$

The experimental values are:

$$\sigma_{np} \sim \sigma_{pp} \sim \sigma_{\bar{p}p} \sim \sigma_{\bar{p}n} \sim 45 \text{ mb}$$

$$\sigma_{\pi^{\pm}p} \sim 25 \text{ mb}, \quad \sigma_{K^{\pm}p} \sim 20 \text{ mb}$$

in *acceptable* agreement with the *guesses* above.

### 3 Reaction rates and Cross Section

#### 3.1 $S$ -matrix, $T$ , $\mathfrak{M}$ , phase space and transition probability.

The elements  $S_{fi}$  of the scattering matrix or  $S$ -matrix describe the transition from an initial state  $i$  to a final state  $f$ . Without interaction  $S=\mathbf{1}$ , where  $\mathbf{1}$  is an identity matrix. Transitions  $i \rightarrow f$ , with  $|i\rangle \neq |f\rangle$  are due to the transition matrix  $T$  defined by  $S = \mathbf{1} + iT^4$ . We also define the amplitude or matrix element  $\mathfrak{M}$  from

$$T_{fi} = (2\pi)^4 \delta^4(p_i - p_f) \mathfrak{M}.$$

$|T_{fi}|^2$  gives the transition probability density *i.e.* the probability for transitions  $i \rightarrow f$  into a unit volume of the  $f$  phase space:

$$\bar{w}_{fi} = (2\pi)^4 \delta^4(p_i - p_f) (2\pi)^4 \delta^4(0) |\mathfrak{M}|^2.$$

In the following we will always omit the factor  $i = \sqrt{-1}$  as well as the sign of  $T_{fi}$  or  $\mathfrak{M}$ , which do not affect first order calculations. We introduce a normalization 4-volume  $VT$  which will drop out in the end. For  $V \rightarrow \infty$  and  $T \rightarrow \infty$ ,  $(2\pi)^4 \delta^4(0) = VT$ . To obtain the transition probability to an element of the final state  $f$  phase space volume  $d\Phi_C$ , we must multiply  $\bar{w}$  by  $d\Phi_C$  and normalize. The phase space volume element is given by

$$d\Phi_C = \prod_{j=1}^n \frac{d^3 \mathbf{p}_j V}{(h)^3} = \prod_{j=1}^n \frac{d^3 \mathbf{p}_j V}{(2\pi)^3}$$

having used  $h^3 = (2\pi)^3 \hbar^3 = (2\pi)^3$ .  $n$  is the number of particles in  $f$ ,  $\mathbf{p}_j$  is the 3-momentum of particle  $j$  and the last expression is valid in the natural units which we use, as usual. We must take care of the proper normalization of the transition probability. We normalize the wave functions to  $2E$  particles per unit volume. The normalized transition probability is given by  $\bar{w}_{fi}$  above, divided by  $N$  below:

$$N = \prod_{j=1}^n 2E_j V \prod_{i=1}^m 2E_i V$$

where  $m$  is the number of particles in the initial state. The normalized transition probability per unit time therefore is:

$$dw_{fi} = \frac{\bar{w}_{fi}}{T} \frac{d\Phi_C}{N} = \frac{V |\mathfrak{M}|^2}{\prod_{i=1}^m 2E_i V} d\Phi$$

where

$$d\Phi = (2\pi)^4 \delta^4(p_i - p_f) \prod_{j=1}^n \frac{d^3 \mathbf{p}_j}{2E_j}$$

---

<sup>4</sup>Remember optics, Babinet's theorem and the optical theorem

The replacement of the proper phase space volume element  $d\Phi_C$  with  $d\Phi$  has the advantage that the latter is manifestly Lorentz-invariant<sup>5</sup> and is in fact called the Lorentz invariant phase space. For one particle in the initial state,  $m=1$ , there is no volume dependence left.

## 3.2 Decay rate, three bodies

Consider the decay

$$A \rightarrow 1 + 2 + 3 \dots$$

where a parent particle  $A$ , of mass  $M$  and 4-momentum  $P = (E, \mathbf{P})$  decays to particles 1, 2 *etc.*, each of mass  $m_i$  and 4-momentum  $p_i$ . The differential decay rate  $d\Gamma$  is given by:

$$d\Gamma = \frac{1}{2E} |\mathfrak{M}|^2 d\Phi$$

For three particles in the final state and in the CM of  $A$  the rate is

$$d\Gamma = \frac{1}{2M} |\mathfrak{M}|^2 \frac{d^3\mathbf{p}_1}{2E_1} \frac{d^3\mathbf{p}_2}{2E_2} \frac{d^3\mathbf{p}_3}{2E_3} \frac{(2\pi)^4}{(2\pi)^9} \delta^4(P - p_1 - p_2 - p_3)$$

Strictly speaking the result above is for  $A$ , 1, 2 and 3 being spinless particles. If spin are included but  $A$  is unpolarized and the final spins are not observed then substitute  $|\mathfrak{M}|^2 \rightarrow \sum_{\text{spins}} |\mathfrak{M}|^2$  and add a factor  $1/(2J_A + 1)$  for the average over the initial particle. Integrating over  $\mathbf{p}_3$  and collecting factors we have

$$\begin{aligned} d\Gamma &= \frac{1}{2M} \frac{1}{8(2\pi)^5} |\mathfrak{M}|^2 \frac{1}{E_3} \frac{d^3\mathbf{p}_1}{E_1} \frac{d^3\mathbf{p}_2}{E_2} \delta(M - E_1 - E_2 - E_3) \\ &= \frac{1}{2M} \frac{1}{8(2\pi)^5} |\mathfrak{M}|^2 \frac{1}{E_3} \frac{p_1^2 dp_1 d\Omega_1}{E_1} \frac{p_2^2 dp_2 d\Omega_2}{E_2} \delta(M - E_1 - E_2 - E_3) \end{aligned}$$

where we have to define how the angles  $\theta_1$ ,  $\phi_1$ ,  $\theta_2$  and  $\phi_2$  are measured. For unpolarized initial state we can chose any reference system. We then measure the polar angle of particle 2 with respect to the direction of particle 1 and we call this angle  $\theta_{12}$  to remind us of this. In the following  $p$  stands for the modulus of the 3-momentum  $\mathbf{p}$ . From  $\delta^3(0 - \mathbf{p}_1 - \mathbf{p}_2 - \mathbf{p}_3)$  we have  $-\mathbf{p}_3 = \mathbf{p}_1 + \mathbf{p}_2$ . Squaring  $p_3^2 = p_1^2 + p_2^2 + 2p_1 p_2 \cos \theta_{12}$  and differentiating, with  $p_1$  and  $p_2$  constant,  $p_1 p_2 d \cos \theta_{12} = p_3 dp_3$  or  $d \cos \theta_{12} = E_3 dE_3 / p_1 p_2$ . Substituting

$$d\Gamma = \frac{1}{16M(2\pi)^5 E_1 E_2 E_3} |\mathfrak{M}|^2 p_1 E_1 dE_1 d\Omega_1 p_2 E_2 dE_2 \frac{E_3 dE_3}{p_1 p_2} d\phi_2 \delta(E - E_1 - E_2 - E_3)$$

---

<sup>5</sup> $d^4p$  is invariant because the Lorentz transformation is an orthogonal transformation and  $d^3p/E$  is obtained from the former integrating out one dimension with the constraint that the  $p^2 = m^2$

and integrating

$$d\Gamma = \frac{1}{16M(2\pi)^5} |\mathfrak{M}|^2 dE_1 dE_2 d\Omega_1 d\phi_2$$

which is valid whether we observe the final spins or not. In the latter case integration over  $\phi_2$  gives  $2\pi$  and over  $\Omega_1$  gives  $4\pi$  resulting in

$$d\Gamma = \frac{1}{8M(2\pi)^3} |\mathfrak{M}|^2 dE_1 dE_2 \quad (3.1)$$

Integration over  $E_2$  gives the energy spectrum of particle 1 and over  $E_1$  the total decay rate. If  $|\mathfrak{M}|^2$  is not a function of the energies of the final particles the last two integrals acquire a simple geometrical meaning. The spectrum of particle 1 is proportional to  $E_{2,\text{Max}}(E_1) - E_{2,\text{Min}}(E_1)$  and the rate is proportional to the allowed area in the plane  $\{E_1, E_2\}$ , the so-called Dalitz plot. In all the above the choice 1, 2 out of 1, 2 and 3 is of course arbitrary, any of the two particles are equivalent:  $dE_1 dE_2 = dE_2 dE_3 = dE_3 dE_1$ .

### 3.3 Integration Limits

Ignoring the dependence on the particle energies of the matrix element we can obtain the energy spectrum of one particle, say  $i$ , integrating the second of eqs. (3.1) over the boundary of the allowed region in the plane  $\{E_i, E_j\}$ . The integration limits can be obtained in the following way. Consider the decay  $M \rightarrow 1+2+3$ , where  $M$ ,  $m_1$ ,  $m_2$  and  $m_3$  are the particle masses. We consider first the process  $M \rightarrow 1+\{2,3\}$ , in the rest frame of  $M$ , *i.e.* with  $\mathbf{p}_{2,3} = \mathbf{p}_2 + \mathbf{p}_3 = -\mathbf{p}_1$  and  $E_1 = E_2 + E_3 = M - E_1$ .  $M_{2,3}$  is the invariant mass of  $\{2,3\}$  given by  $M_{2,3} = \sqrt{E_{2,3}^2 - p_{2,3}^2}$ .  $M_{2,3}$  which can be expressed in terms of the variables of particle 1:

$$M_{2,3} = \sqrt{(M - E_1)^2 - p_1^2} = \sqrt{M^2 + m_1^2 - 2ME_1}$$

For  $E_1 = m_1$ , we have  $M_{2,3} = M - m_1$ , as expected since  $p_1 = 0$ . The minimum value of  $M_{2,3}$  is  $m_2 + m_3$  and, from a very useful relation  $E_1^{\text{Max}} = (M^2 + m_1^2 - (m_2 + m_3)^2)/(2M)$ .

Then we look at  $\{2,3\} \rightarrow 1+2$ . This is illustrated below.

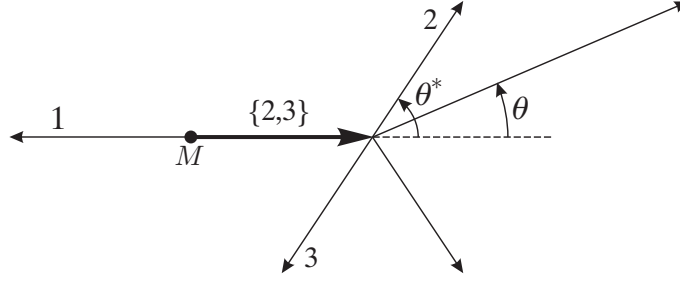


**Fig. 3.1.** Three body decay  $M \rightarrow 1+2+3$  as a two step process:  $M \rightarrow 1+\{2,3\}$ ,  $\{2,3\} \rightarrow 1+2$ . The parent particle has mass  $M$ , the three final particles have mass  $m_1$ ,  $m_2$  and  $m_3$ .  $\{2,3\}$  is the system made up of particles 2 and 3, with invariant mass  $M_{2,3}$ .

$\theta^*$  is the ‘decay’ angle in the  $\{2,3\}$  rest system. In the initial system,  $\{2,3\}$  moves with

$$\gamma = \frac{E_{2,3}}{M_{2,3}} = \frac{M - E_1}{\sqrt{M^2 + m_1^2 - 2ME_1}} (= 1 \text{ for } E_1 = m_1)$$

$$\gamma\beta = \frac{p_{2,3}}{M_{2,3}} = \frac{p_1}{\sqrt{M^2 + m_1^2 - 2ME_1}} (= 0 \text{ for } E_1 = m_1).$$

In the  $\{2,3\}$  system the energies and momenta of 2 and 3 are:

$$E_2^* = \frac{M_{2,3}^2 + m_2^2 - m_3^2}{2M_{2,3}}$$

$$E_3^* = \frac{M_{2,3}^2 + m_3^2 - m_2^2}{2M_{2,3}}$$

$$p_2^* = p_3^* = \sqrt{E_2^{*2} - m_2^2} = \sqrt{E_3^{*2} - m_3^2}$$

In terms of the above  $E_2$  and  $E_3$  are:

$$E_2 = \gamma E_2^* + \gamma\beta p_2^* \cos \theta^*$$

$$E_3 = \gamma E_3^* - \gamma\beta p_3^* \cos \theta^*$$

The integrations limits in  $E_2$  and  $E_3$  as function of  $E_1$  are:

$$E_2 = \gamma E_2^* - \gamma\beta p_2^* \text{ to } \gamma E_2^* + \gamma\beta p_2^*$$

$$E_3 = \gamma E_3^* - \gamma\beta p_3^* \text{ to } \gamma E_3^* + \gamma\beta p_3^*$$

From the above the spectrum in  $E_1$  is given by:

$$\frac{d\Gamma}{dE_1} \propto 2\gamma\beta p_2^* = \frac{p_1}{\sqrt{M^2 + m_1^2 - 2ME_1}}$$

An example of the boundary is given in fig. 3.2 for  $M=...$ , etc. and the corresponding spectrum in fig. 3.3.

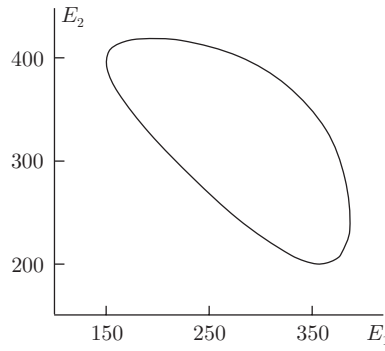


**Fig. 3.2.** boundary for  $M \rightarrow 1 + \{2,3\}$ ,  $\{2,3\} \rightarrow 2+3$ , for  $\mathfrak{M}=1$ .

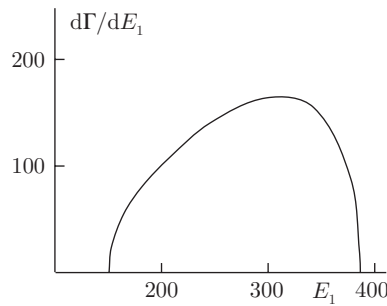


**Fig. 3.3.**  $E_1$  spectrum from  $M \rightarrow 1 + \{2,3\}$ ,  $\{2,3\} \rightarrow 2+3$ , with the boundary of fig. 3.2.

The procedure applies of course also to the case when  $\mathfrak{M}$  is (properly) included.

Even ignoring the energy dependence of the matrix element, the integration over the energy of the last of the three final state particles cannot be done generally in a closed form. If two of the masses are non-zero we find an elliptic integral. The integral can be performed if two of the masses vanish. If all masses vanish:  $\int dE_1 dE_2 = M^2/8$ . All this is obvious from fig. 3.4.

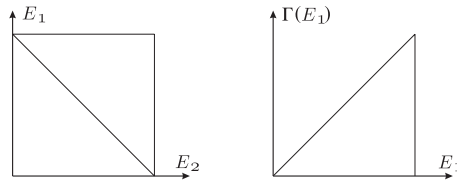


**Fig. 3.4.** Dalitz plot, left, for decay to three massless particles.  $E_1$  spectrum, right, for  $\mathfrak{M}=1$  and the boundary at left.

G. Wick has observed that:

1. For every massless particle, the kinematic boundary has a cusp.
2. For every pair of massless particles, the boundary contains a straight segment parallel to an axis.

Fig. 3.4 is in agreement with the above statements.

### 3.4 Decay rate, two bodies

Consider the decay of a particles of 4-momentum  $P$  and mass  $M$  into particles 1 and 2, with 4-momenta  $p_1, p_2$  and masses  $m_1, m_2$ , schematically  $M \rightarrow 1+2$ . In the center of mass of the parent particle:

$$\begin{aligned}\Gamma &= \int \frac{1}{2M} |\mathfrak{M}|^2 (2\pi)^4 \delta^4(P - p_1 - p_2) \frac{d^3 p_1}{(2\pi)^3 2E_1} \frac{d^3 p_2}{(2\pi)^3 2E_2} \\ &= \frac{1}{2M} \frac{1}{(2\pi)^2} \frac{1}{4E_1 E_2} |\mathfrak{M}|^2 p_1^2 dp_1 d\Omega_1 \delta(E - E_1 - E_2)\end{aligned}$$

In the CM,  $p_1 = p_2 = p$ . From  $E = E_1 + E_2 = \sqrt{m_1^2 + p^2} + \sqrt{m_2^2 + p^2}$  we get  $dE = (1/E_1 + 1/E_2)pdp$  or  $pdp = (E_1 E_2 / M)dE$ , substituting<sup>6</sup>

$$\Gamma = \frac{d\Omega}{8M \times 4\pi^2} \int |\mathfrak{M}|^2 \frac{p}{M} \delta(E - E_1 - E_2) dE = \frac{1}{32\pi^2} \frac{p}{M^2} |\mathfrak{M}|^2 d\Omega.$$

For a non-polarized initial state, apart from a possible factor  $1/(2J + 1)$

$$\Gamma = \frac{1}{8\pi} \frac{p}{M^2} |\mathfrak{M}|^2.$$

Comparison with a 3-body final state is not obvious because of dimensions:

$$\Gamma^{(3 \text{ body})} = \frac{1}{8M(2\pi)^3} \int |\mathfrak{M}|^2 dE_1 dE_2$$

unless the form of  $|\mathfrak{M}|^2$  is known.

We can get a feeling as follows. For two body decays, dimensional arguments require that  $|\mathfrak{M}|^2$  has dimension of an energy squared. We set  $|\mathfrak{M}|^2 \sim M^2 \times \text{“1”}$  and  $p/M=1/2$ , valid for massless final particles. For three body the dimensions are correct with  $|\mathfrak{M}|^2$  dimensionless. For massless particles  $\int dE_1 dE_2 = M^2/8$ . Then we can write  $\Gamma_{3 \text{ body}} = M/16/\pi \times (1/8/(2\pi)^2) \times \text{“1”}$  and  $\Gamma_{2 \text{ body}} = M/16/\pi \times \text{“1”}$  where “1” indicates a normalized interaction strenght. In this way we find  $\Gamma_{3 \text{ body}} = 1/8/(2\pi)^2 \times \Gamma_{\text{body}}$  or  $\Gamma_{3 \text{ body}} \sim \Gamma_{2 \text{ body}}/300$ . The factor  $1/32\pi^2$  obtained for massless particles becomes smaller for massive particles. In the limit  $m_1 + m_2 < M < m_1 + m_2 + m_3$ , the three body decay becomes kinematically forbidden! Still the argument is not rigorous.

---

<sup>6</sup>We can also get the correct answer from  $dE = dE_1 + dE_2 = p_1 dp_1 / E_1 + p_2 dp_2 / E_1$ . In the CM,  $p_1 = p_2$ ,  $dE = p_1 dp_1 E / (E_1 E_2)$  or  $p_1 dp_1 = (E_1 E_2 / E) dE$

### 3.5 Scattering cross section

The cross section for collision of two particles is defined through

$$d\bar{w}_{fi} = d\vec{\sigma} \cdot \mathbf{j},$$

where  $\mathbf{j}$  is the incident flux. Let a beam of particles  $a$ , with velocity  $\beta_a$ , collide with a stationary target of particles  $b$  according to the reaction  $a + b \rightarrow a + b$ . The incident flux is  $j = \beta_a/V$  and the cross section is given by

$$d\sigma = \frac{dw_{fi}}{j} = \frac{1}{2E_a\beta_a 2M_b} |\mathfrak{M}|^2 d\Phi.$$

The quantity  $E_a\beta_a M_b = M_b|\mathbf{p}_a|$  becomes in general, for collinear collisions,  $\mathbf{p}_a \parallel \mathbf{p}_b$  and of opposite sign:

$$|\mathbf{p}_a|E_b + |\mathbf{p}_b|E_a \text{ or, in the CM, } p_i E$$

where  $p_i = |\mathbf{p}_a| = |\mathbf{p}_b|$  and  $E = E_a + E_b$ . For collinear collisions we can also write the general expression above in an obviously invariant form:

$$|\mathbf{p}_a|E_b + |\mathbf{p}_b|E_a = \sqrt{(p_a p_b)^2 - m_a^2 m_b^2}.$$

In the CM we have:

$$d\sigma = \frac{1}{4p_i E} |\mathfrak{M}|^2 d\Phi$$

$d\Phi$  is calculated as in the two body decay:

$$\begin{aligned} d\Phi &= \int \frac{(2\pi)^4}{4(2\pi)^6} \delta^4(p_a + p_b - p_c - p_d) \frac{d^3 p_c}{E_c} \frac{d^3 p_d}{E_d} \\ &= \frac{1}{16\pi} \frac{p_f^2 dp_f d\Omega}{E_c E_d} \delta(W - E_c - E_d) \end{aligned}$$

where  $p_f = p_c = p_d$  is the center of mass 3-momentum and  $W$  is the total energy.

From  $dW = dp_f(p_f W)/(E_c E_d)$  we find:

$$\begin{aligned} d\Phi &= \frac{1}{16\pi^2} \frac{p_f}{W} d\Omega = \frac{1}{16\pi^2} \frac{p_f}{\sqrt{s}} d\Omega \quad \text{and} \\ d\sigma &= \frac{1}{4p_i \sqrt{s}} |\mathfrak{M}|^2 \frac{1}{16\pi^2} \frac{p_f}{\sqrt{s}} d\Omega = \frac{1}{64\pi^2} \frac{1}{s} \frac{p_i}{p_f} |\mathfrak{M}|^2 d\Omega. \end{aligned} \tag{3.2}$$

For  $|\mathfrak{M}|^2$  independent of  $\theta$ , integration of (3.2) over the entire solid angle gives:

$$\sigma = \frac{1}{16\pi} \frac{1}{s} \frac{p_i}{p_f} |\mathfrak{M}|^2$$

which is also valid in the laboratory, since  $\sigma$  is transverse to the transformation velocity, with  $p_i$  and  $p_f$  measured however in the CM.

Introducing the function

$$\lambda(x, y, z) = x^2 + y^2 + z^2 - 2xy - 2xz - 2yz$$

we can also write the differential cross section as the covariant expression

$$d\sigma = \frac{1}{2\lambda^{1/2}(s, m_a^2, m_b^2)} (2\pi)^4 \delta^4(p_a + p_b - \sum_{f=1}^n p_f) \times |\mathfrak{M}|^2 \prod_{f=1}^n \frac{dp_f}{(2\pi)^3 2E_f} \quad (3.3)$$

where  $s$  is the square of the CM energy,  $s = (p_a + p_b)^2$ . Finally introducing the variables

$$\begin{aligned} s &= (p_1 + p_2)^2 = (p_3 + p_4)^2 = m_1^2 + m_2^2 + 2(p_1 p_2) \\ t &= (p_1 - p_3)^2 = (p_2 - p_4)^2 = m_1^2 + m_3^2 - 2(p_1 p_3) \\ u &= (p_1 - p_4)^2 = (p_2 - p_3)^2 = \dots \end{aligned}$$

the cross section for the reaction  $1+2 \rightarrow 3+4$  can be written as:

$$\frac{d\sigma}{dt} = \frac{1}{64\pi s} \frac{1}{|\mathbf{p}_{1,\text{cm}}|^2} |\mathfrak{M}|^2 \quad (3.4)$$

where  $\mathbf{p}_{1,\text{cm}} = \mathbf{p}_{2,\text{cm}}$  is the initial state 3-momentum in the center of mass. In the center of mass:

$$t = (E_1 - E_3)^2 - (p_1 - p_3)^2 - 4p_1 p_3 \sin^2 \theta / 2 \Rightarrow -s \sin^2 \theta / 2$$

where  $E_i$  are energies,  $p_i$  3-momenta and  $\theta$  is the scattering angle between particles 1 and 3, where the limit correspond to  $E \gg m_1, m_2$ .

Note that only two variable are necessary to kinematically describe two body scattering. The variables  $s$ ,  $t$  and  $u$  satisfy

$$s + t + u = m_1^2 + m_2^2 + m_3^2 + m_4^2$$

see appendix A1.5.7.

### 3.6 Accounting for Spin

If initial and final particles have spins, we must pay some attention to properly count the additional degrees of freedom. We deal here only with the case of unpolarized initial particles and the case in which we do not observe the orientation of the spin of the final particles. In this case we must sum over the spin orientation in the final state and average over the initial spin orientation. The latter we also do by summing over the initial orientations and dividing by the weights  $2J + 1$ . In other words instead of  $|\mathfrak{M}|^2$  we must use

$$\frac{1}{2J_a + 1} \frac{1}{2J_b + 1} \sum_{\text{spins}} |\mathfrak{M}|^2$$

where  $J_a \dots$  are the intrinsic angular momenta of the initial particles and the sum extends to all spins, initial and final.

## 4 The Electromagnetic Interaction

### 4.1 Introduction: Classical Rutherford Scattering

Consider a particle of charge  $e$  approaching with an impact parameter  $b$  another massive particle of charge  $Ze$ , stationary, located at the origin  $O$ , fig. 4.1. The moving particle will be deflected under the action of the Coulomb force acting between the two particles,  $F = \alpha Z/r^2$ . The direction, away or toward  $O$ , of the force is unimportant. We make the simplifying assumption that the force acts on the moving particles with constant value, as obtained with  $r = b$ , *i.e.* at the point of closest approach, for the time it takes to move a distance  $2b$  over an undeflected path. The approximation is valid for  $b$  not too small, more precisely for a deflection angle  $\theta \ll 1$

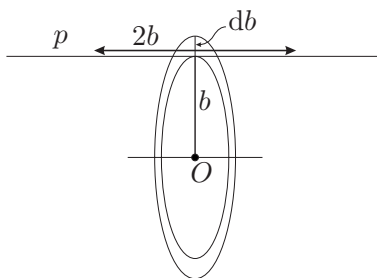


**Fig. 4.1.** Scattering of an “electron” by a massive charge.

The deflection angle is given by  $\Delta p/p$  where the momentum change equals the impulse of the force  $F$  acting for the time interval required to travel the distance  $2b$  at the speed of light.

$$\theta = \Delta p/p = F \times \Delta t/p = \alpha Z/b^2 \times 2b(\times c = 1)/p = \frac{2\alpha Z}{bp} \quad \text{or} \quad b = \frac{2\alpha Z}{\theta p}.$$

The scattering cross section is then:

$$\frac{d\sigma}{d\theta} = \frac{2\pi b db}{d\theta} = \frac{8\pi\alpha^2 Z^2}{p^2\theta} \frac{d}{d\theta} \frac{1}{\theta} = \frac{8\pi\alpha^2 Z^2}{p^2\theta^3}$$

which is the small angle limit of the Rutherford cross section:

$$\frac{d^2\sigma}{d\cos\theta} = \frac{\pi\alpha^2 Z^2}{2p^2\theta} \frac{1}{\sin^4\theta/2}$$

$$\frac{d\sigma}{d\theta} = \frac{8\pi\alpha^2 Z^2}{p^2\theta^3}$$

The reason why we find the correct answer is because the crude approximation used for  $\Delta p$  is in fact exact as we derive below.

### 4.1.1 Exact computation of $\Delta p$

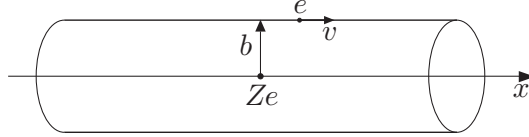


**Fig. 4.2.** Calculating  $\Delta p$  using Gauss theorem.

Referring to fig. 4.2, consider an infinite cylinder, of radius  $b$  around an axis  $z$  through the position of the heavy particle, parallel to the motion of the light particle of charge  $e$ . To compute  $\Delta p = \int_{-\infty}^{\infty} F_{\perp} dt$  we use Gauss theorem:

$$\int_{S_{\text{cyl}}} \vec{E} \cdot d\vec{\sigma} = Ze = \int_{-\infty}^{\infty} 2\pi b E_{\perp} dz \quad \text{or} \quad \int_{-\infty}^{\infty} E_{\perp} dz = \frac{eZ}{2\pi b}$$

from which

$$\int_{-\infty}^{\infty} F_{\perp} dz = \frac{e^2 Z}{2\pi b} = \frac{2\alpha Z}{b}$$

and

$$\Delta p = \int_{-\infty}^{\infty} F_{\perp} dt = \int_{-\infty}^{\infty} F_{\perp} dz / v = \frac{2\alpha Z}{\beta b}$$

where  $\beta = v$  is the velocity of the light particle.

### 4.1.2 Final remarks

Rutherford was very proud of his derivation of the classical formula for ‘‘Rutherford’’ scattering, especially when it turned out that his results remains unchanged in quantum mechanics. The importance of Rutherford’s idea of exploring the structure of a particles by scattering some probe against it remains fundamental today. Often we hear about Rutherford’s scattering when applied to quarks and gluons which we believe today to be the constituents of hadrons. This is meant figuratively of course, having to take into account relativity and spins for one, not to speak of the fact that no gluon or quark has been so far observed nor it’s likely to ever be observed.

Finally we wish remark that the spirit of the calculation above is the same as that of the so-called first Born approximation. Here we compute the transverse impulse imparted to the light particle, assumed to be travelling in an unperturbed orbit, in QM we use plane waves for the outgoing state to calculate the perturbation.

## 4.2 The Elementary EM Interaction

In field theory the coulomb interaction between two charges is described, to lowest order, in terms of the elementary process of the emission of a quantum of the

electromagnetic field, the photon, by one of the charges and the reabsorption of the same photon by the other charge. In fact the absorption and emission are the same process in field theory, described by the same amplitude, function of the variables describing the initial charge, the final charge and the initial or final photon. The most elementary process in quantum electrodynamics, QED, is the emission of a photon by a (moving) charge. The amplitude for this process is the matrix element of the interaction (energy) Hamiltonian density  $H$  between initial and final state. We represent this elementary process with the graph of fig. 4.3.

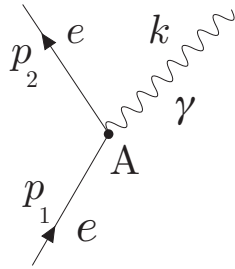


**Fig. 4.3.** The  $ee\gamma$  vertex.

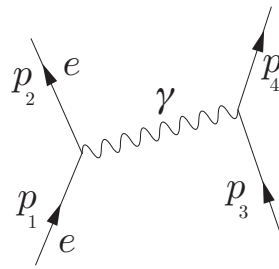


**Fig. 4.4.**  $ee$  interaction via  $\gamma$  exchange.

The graph is a representation of the physical process in space-time. Since we cannot sketch a 4-dimensional event on paper, *i.e.* in two dimensions, we use one axis, the y-axis, for time and the x-axis for space. The line with arrow going towards the point  $A=(x, t)$  is an incoming electron of 4-momentum  $p_1$ . At the space-time point  $A$ , a photon, the wavy line, is emitted and the electron continues to propagate as indicated. The electron's 4-momentum after photon emission is  $p_2$  and the photon's 4-momentum  $k$  is given by  $p_1 - p_2$ . If  $k \neq 0$  and  $|k|^2=0$ , as we know to be the case for a real photon, then energy and momentum are not conserved. This can be seen taking the modulus squared of the initial and final 4-momenta,  $p_1$  and  $p_2 + k$ :  $|p_1|^2 = m_e^2$ ,  $|p_2+k|^2 = |p_2|^2 + |k|^2 + 2E_e E_\gamma - 2\vec{p}_2 \cdot \vec{k} = m_e^2 + 0 + 2E_\gamma(E_e - \vec{p}_2 \cdot \vec{k}/|\vec{k}|) > m_e^2$ , since the quantity in parenthesis is always positive. Physically, this means that an electron cannot become an electron plus a photon, except for  $|k|=0$ , which is no photon at all. This however changes when we put together the emission of a photon by one electron with the absorption of the same photon by another electron. We represent this process with the graph of fig. 4.4.

For both processes in fig. 4.3 and 4.4,  $k^2 < 0$ . When this is the case the photon is not a free photon in vacuum. We describe this situation with the word *virtual*, *i.e.* the photon is said to be virtual or that the photon is off its mass shell.

We can interpret this situation with the help of the uncertainty principle. Let us consider the reaction in its CM and assume for simplicity that  $m_1=m_2=m_3=m_4$ . Then  $E_1 = E_2 = E_3 = E_4$ . For the process in fig. 4.4 we can distinguish three

intervals in time. Before the photon is emitted, we have particles 1 and 3, with total energy  $2E$ . After the photon is emitted but not absorbed, the energy is changed by an amount  $E_\gamma$ , violating energy conservation. After the photon is reabsorbed everything is fine again. The question is now whether we can observe this energy violation. The answer is of course no, if the virtual photon is present for a time  $T$ , satisfying  $T < 1/E_\gamma$ , in our units with  $\hbar=1$ . If a photon lives for a time  $T$ , during that time it travels a distance ( $c=1$ )  $L = T = 1/E_\gamma$ . Since a photon can have arbitrarily small energy it can travel arbitrarily large distances. We discover thus that the electromagnetic interaction has an infinite range of action, as Coulomb's law tells us.

It is interesting to compare this situation to an interaction due to the exchange of a particle of finite mass  $m$ . In this case the energy of the virtual particle is always greater than  $m$ . Thus, requiring that energy be conserved, within the limits of the uncertainty principle, we find that this kind of interaction is limited in its range to  $r < 1/m$ . For a particle of 197 MeV mass, the interaction range is limited to the order of 1 fm. This is in fact the case of the nuclear interaction which is due to the exchange of  $\pi$  mesons or pions of 140 MeV mass. Its range is  $\sim 1$  fm. The argument was historically used in the reverse way, deducing from observation of the finite range of the nuclear forces, that they must be due to the exchange of a massive particle.

It should be noted that the above picture is not the way Feynman diagram are meant to be understood. Energy and momentum are conserved at every vertex and any space-time point. Internal lines correspond to particles which are off their mass shell.

### 4.3 The Rutherford cross section

First we recall the formula for the scattering cross section in terms of matrix element and phase space factor as obtained in perturbation theory, using however relativistic covariant formalism. We consider the scattering reaction  $1+3 \rightarrow 2+4$ , see fig. 4.4, where all particles are spinless. The infinitesimal cross section for scattering into a six-dimensional element of the phase space of the outgoing particles 3 and 4 is given by:

$$d^6\sigma = \frac{1}{|\mathbf{v}_1 - \mathbf{v}_3|} \frac{1}{2E_1} \frac{1}{2E_3} |\mathfrak{M}|^2 \frac{d^3\mathbf{p}_2}{2E_2(2\pi)^3} \frac{d^3\mathbf{p}_4}{2E_4(2\pi)^3} (2\pi)^4 \delta^4(p_1 + p_3 - p_2 - p_4)$$

where  $p_i = \{\mathbf{p}_i, E_i\}$  are the four momenta of the particles,  $\mathfrak{M}$  is the matrix element  $\langle 2, 4 | \mathcal{H} | 1, 3 \rangle$  and  $|\mathbf{v}_1 - \mathbf{v}_3|$  is the relative velocity of the two particles, essentially

the flux factor. If particle 3 is at rest,  $\mathbf{v}_3=0$  and we set  $|\mathbf{v}_1| = \beta$ . Integrating over  $\mathbf{p}_4$  and cancelling some  $2\pi$  factors gives:

$$\begin{aligned} d^3\sigma &= \frac{d^3\mathbf{p}_2}{\beta} \frac{\delta(E_{in} - E_{out})}{(2\pi)^2 4E_1 E_3 4E_2 E_4} |\mathfrak{M}|^2 \\ &= \frac{p_2 E_2 dE_2 d\Omega}{\beta} \frac{\delta(E_{in} - E_{out})}{(2\pi)^2 4E_1 E_3 4E_2 E_4} |\mathfrak{M}|^2. \end{aligned}$$

To first order, the matrix element is obtained from the term  $J_\mu A^\mu$  in the em interaction Hamiltonian density:

$$\mathfrak{M} = \langle 2, 4 | e J_\mu^{(1, 2)} A^\mu \frac{1}{k^2} e A_\nu J^\nu{}^{(3, 4)} | 1, 3 \rangle = e^2 \frac{v_\rho u^\rho}{k^2}$$

where  $v$  and  $u$  are four vectors, functions of the coordinates respectively of particles 1, 2 and 3, 4. The factor  $1/k^2$  is the amplitude for the virtual photon propagation from emission to absorption, the propagator, and we have summed over polarization states. The vectors  $v$ ,  $u$  can only be linear combinations of the relevant momenta in the problem. The matrix element  $\langle 2 | J_\mu^{(1, 2)} | 1 \rangle \propto v$  is therefore a linear combination of the 4-vectors  $p_1$  and  $p_2$ ,  $ap_1 + bp_2$ . In fact there is no freedom in the choice of the coefficients  $a$  and  $b$ . Gauge invariance requires that the em current be conserve, *i.e.*:

$$\frac{\partial}{\partial x_\mu} \langle 2 | J^\mu | 1 \rangle = 0.$$

The matrix element in the eq. above contains the wave functions of the initial particle 1 and of the final particle 2, therefore it contains the factor  $\exp i(x_\mu p_1^\mu - x_\mu p_2^\mu)$ . The operator  $\partial_\mu$  acting on  $\langle J^\mu \rangle$  gives therefore a factor  $(p_1 - p_2)_\mu = k_\mu$  and the current is conserved only if  $v = p_1 + p_2$ . Then current conservation is guaranteed,  $(p_1 - p_2)(p_1 + p_2) = 0$ , since  $m_1 = m_2$ .

The matrix element of the current for spinless particles at the 1, 2,  $\gamma$  vertex is thus  $e(p_1 + p_2)_\mu$  and at the 3, 4,  $\gamma$  vertex we have  $e(p_3 + p_4)_\mu$ . The complete matrix element for scattering of a particle of charge  $e$  by another of charge  $Ze$  is therefore  $|M| = e^2 Z \times (p_1 + p_2)_\mu (p_3 + p_4)^\mu / k^2$ , in units such that  $e^2/4\pi \equiv \alpha = 1/137$ , with  $k = p_1 - p_2$ . Rutherford scattering is the scattering of a light particle 1 by a heavy particle 3, at rest. We therefore use the kinematics limit

$$\begin{aligned} E_1 &= E_2 = E, & |\vec{p}_1| &= |\vec{p}_2| = p \\ E_3 &= E_4 = M, & \vec{p}_3 &= 0, \vec{p}_4 = \vec{p}_1 - \vec{p}_2 \end{aligned}$$

for which the matrix element becomes:

$$|\mathfrak{M}| = e^2 Z \frac{4EM}{k^2}.$$

Substituting above and integrating over  $E$  we have:

$$\frac{d^2\sigma}{d\phi d\cos\theta} = \frac{e^4 Z^2}{(2\pi)^2} \frac{pE}{\beta} \frac{(4EM)^2}{4EM 4EM (k^2)^2} = 4\alpha^2 Z^2 E^2 \frac{1}{(p_1 - p_2)^4}$$

Finally, since in our limit  $p_1 - p_2 = \{0, \vec{p}_1 - \vec{p}_2\}$ ,  $(p_1 - p_2)^2 = 2p^2(1 - \cos\theta) = 4p^2 \sin^2\theta/2$

$$\frac{d^2\sigma}{d\phi d\cos\theta} = \frac{\alpha^2 Z^2}{4} \frac{E^2}{p^4} \frac{1}{\sin^4\theta/2} = \frac{\alpha^2 Z^2}{4} \frac{1}{\beta^2 p^2} \frac{1}{\sin^4\theta/2}. \quad (4.1)$$

The cross section in equation (4.1) was first derived by Rutherford using classical electrodynamics. It remains today a fundamental tool in the investigation of elementary particles and their interactions. Notice that this result contains only one quantity with dimensions, the  $p^2$  factor in the denominator. The result is therefore in units of an inverse energy squared if we measure  $p$  in energy units. We might need to convert to  $\text{cm}^2$  or b for practical reasons, using the conversion factors given in chapter 1, table 1.3. Pay attention to the units with which you measure  $p$ . The scattering cross section as computed is valid for scattering of point charges. This is correct for electrons but not generally so for other particles.

#### 4.4 Electromagnetic Scattering of Spinless Particles

We generalize in the following the result obtained above to the electromagnetic scattering of two charged, spinless, point particles of identical mass which we call for convenience pions. We also choose the case of  $\pi^+ + \pi^- \rightarrow \pi^+ + \pi^-$  to which the annihilation amplitude also contributes. The amplitudes are shown in fig. 4.5. The electromagnetic current of the pion at the lower vertex in the exchange graph at right in the figure) follows from gauge invariance and is the same as derived earlier for ‘‘Rutherford scattering’’

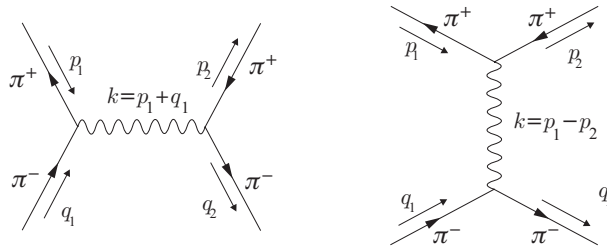


**Fig. 4.5.** Feynman diagrams for electromagnetic  $\pi^+ + \pi^- \rightarrow \pi^+ + \pi^-$  scattering. The diagram at left is often called the annihilation diagram and the one at right the photon exchange amplitude. The direction of the external momenta is indicated as well as the charge flow, in the convention that positive current corresponds to negative charge motion.

$J_\mu = e(p_1 + p_2)_\mu$  and the amplitude for photon exchange is given by:

$$\mathfrak{M} = e^2(p_1 + p_2)_\mu \frac{1}{k^2}(q_1 + q_2)^\mu$$

where  $k = p_1 - p_2$  is the photon 4-momentum. Using

$$\begin{aligned} s &= (p_1 + q_1)^2 = 2(p_1 q_1) + 2m_\pi^2 = 2(p_2 q_2) + 2m_\pi^2 \\ t &= (p_1 - p_2)^2 = -2(p_1 p_2) + 2m_\pi^2 = -2(q_1 q_2) + 2m_\pi^2 \\ u &= (p_1 - q_2)^2 = -2(p_1 q_2) + 2m_\pi^2 = -2(q_1 p_2) + 2m_\pi^2 \end{aligned}$$

one gets

$$\mathfrak{M} = e^2 \frac{s - u}{t} \quad (4.2)$$

for the photon exchange diagram. Note that the amplitude (4.2) diverges for zero momentum transfer, the pole of the photon propagator. This is a reflection of the nature of the Coulomb potential which has an infinite range. We have already encountered this infinity in eq. (4.1), which diverges as  $\theta \rightarrow 0$ . A complete calculation in QED removes the infinity.

By gauge invariance the current at the vertex on the in fig. 4.5, left, is  $J_\mu = (q_1 - p_1)_\mu$  and similarly at the upper vertex. The amplitude for the annihilation diagram therefore is

$$\mathfrak{M} = e^2(q_1 - p_1)_\mu \frac{1}{k^2}(q_2 - p_2)^\mu = e^2 \frac{t - u}{s}. \quad (4.3)$$

which formally corresponds to exchanging the variables  $s$  and  $t$ . The annihilation amplitudes has no divergence since the timelike photon has mass squared  $s > 4m^2$ .

The complete amplitude finally is:

$$\mathfrak{M} = e^2 \left( \frac{s - u}{t} + \frac{t - u}{s} \right). \quad (4.4)$$

Another way to see the connection is to note that the “mass” of the virtual photon is  $\sqrt{s}$  in the annihilation case and  $\sqrt{t}$  in the exchange case. Also the current in the former case is  $e(p_1 + p_2)_\mu$  and in the latter  $e(q_1 - p_1)_\mu$ . The expression derived contains two terms which reflect the two diagrams in fig. 4.5. If we consider  $\pi\pi \rightarrow \pi\pi$  scattering with all pions having the same charge, there is no annihilation term. Likewise for  $\pi^+\pi^- \rightarrow \Pi^+\Pi^-$  with  $m(\Pi) > m(\pi)$  there is no exchange contribution.

The cross section for  $\pi^+\pi^- \rightarrow \pi^+\pi^-$ , in the CM, is obtained combining eq. (4.4) and eq. (3.2):

$$\begin{aligned} \frac{d\sigma}{d\Omega} &= \frac{\alpha^2}{4s^3} \frac{1}{\sin^4 \theta/2} \left\{ \frac{s^2}{s - 4m^2} + s(1 - \sin^2 \theta/2 + 2 \sin^4 \theta/2) \right. \\ &\quad \left. + 4m^2 \sin^2 \theta/2(1 - 2 \sin^2 \theta/2) \right\}^2. \end{aligned} \quad (4.5)$$

The complicated results reflects the presence of two amplitudes. At high energy (4.5) reduces to

$$\frac{d\sigma}{d\Omega} = \frac{\alpha^2}{s} \frac{(1 - \sin^2 \theta/2 + \sin^4 \theta/2)^2}{\sin^4 \theta/2}$$

For  $\pi^+\pi^-$  annihilation into a pair of particles of mass  $M$  the cross section is

$$\frac{d\sigma}{d\Omega} = \frac{\alpha^2}{4s} \left(\frac{s - 4m^2}{s}\right)^{1/2} \left(\frac{s - 4M^2}{s}\right)^{3/2} \cos^2 \theta/2$$

which for  $s \gg m^2$ ,  $M^2$  simplifies to

$$\frac{d\sigma}{d\Omega} = \frac{\alpha^2}{4s} \cos^2 \theta$$

The scattering of a negative, singly charged spinless particle by a positive spinless particle of charge  $Ze$  and mass  $M$  is given by (4.2) modified as

$$\mathfrak{M} = Ze^2 \frac{s - u}{t} \quad (4.6)$$

from which, with the help of (3.3), one obtains the Rutherford cross section (4.1). Let  $E$  and  $E'$  be the incoming and outgoing pion energies,  $\theta$  the pion scattering angle and  $E_r$  the recoil energy of the target. Neglecting the pion mass  $m$ , but keeping  $M$  finite, we find  $t = -(2EE'(1 - \cos \theta) = 2M(M - E_r) = 2m(E' - E)$  and

$$\begin{aligned} E' &= \frac{E}{1 + 2E/M \sin^2 \theta/2} \\ t &= \frac{-4E^2 \sin^2 \theta/2}{1 + 2E/M \sin^2 \theta/2} \\ s &= M^2 + 2ME \\ u &= M^2 - 2ME - t \end{aligned}$$

and finally

$$\frac{d\sigma}{d\Omega_{\text{lab}}} = \frac{Z^2 \alpha^2}{4E^2 \sin^4 \theta/2} \left( \frac{1 + E/M \sin^2 \theta/2}{1 + 2E/M \sin^2 \theta/2} \right)^2. \quad (4.7)$$

The last factor in (4.7) accounts for the recoil of the target and vanishes for  $M \rightarrow \infty$  giving the result (4.1) for  $\beta = 1$  and  $p = E$ , *i.e.* for  $m=0$ , and a  $Ze$  charge for the target particle.

## 4.5 Pion Compton Scattering

By pion-Compton scattering we mean scattering of a photon on a unit charge spin zero particle of mass  $m$ . The processes is sketched in fig. 4.6.

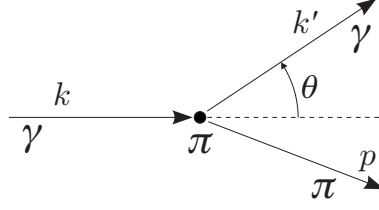


**Fig. 4.6.** Compton scattering of photons on an pion  $\pi$  initially at rest.  $k$ ,  $p'$  and  $k'$  are 4-momenta.

Let  $\theta$  be the scattering angle of the photon in the laboratory, where the pion is at rest. From fig. 4.6 the components of the four momenta,  $E$ ,  $p_x$ ,  $p_y$ ,  $p_z$  in the laboratory are

$$\begin{aligned}
 p &= m(1, 0, 0, 0) \\
 k &= \omega(1, 0, 0, 1) \\
 k' &= \omega'(1, \sin \theta, 0, \cos \theta) \\
 p' &= (m + \omega - \omega', -\omega' \sin \theta, 0, \omega - \omega' \cos \theta).
 \end{aligned} \tag{4.8}$$

$\omega$  is the photon energy,  $\theta$  the angle between incident photon, along the  $z$ -axis, and recoil photon. The last of equations (4.8) is obtained from  $p' = k + p - k'$  in order to satisfy Lorentz invariance. In addition  $(p + k)^2 = (p' + k')^2$  or  $p \cdot k = p' \cdot k'$ , from which the famous relation (in natural units  $\lambda = 2\pi/\omega$ ):

$$\omega' = \frac{\omega}{1 + \omega/m(1 - \cos \theta)} \quad \text{or} \quad \frac{1}{\omega'} - \frac{1}{\omega} = \frac{1}{m}(1 - \cos \theta). \tag{4.9}$$

For convenience we also give the variables  $s$  and  $t$ :

$$\begin{aligned}
 s &= (p + k)^2 = m^2 = 2m\omega \\
 t &= (k - k')^2 = -2\omega\omega'(1 - \cos \theta)
 \end{aligned}$$

The Lagrangian for spinless particles interacting with the electromagnetic field is:

$$\begin{aligned}
 \mathcal{L} &= \mathcal{L}_{\text{Klein-Gordon}} + \mathcal{L}_{\text{Maxwell}} + \mathcal{L}_{\text{Interaction}} \\
 &= \partial_\mu \phi^* \partial^\mu \phi - m^2 \phi^* \phi + \frac{1}{4} F_{\mu\nu} F^{\mu\nu} \\
 &\quad + ie A_\mu [\phi^* \partial_\mu \phi - (\partial^\mu \phi^*) \phi] + e^2 A_\mu^2 \phi^* \phi
 \end{aligned} \tag{4.10}$$

where the last term is required by gauge invariance. Correspondingly the amplitude for pion Compton scattering contains the three terms of fig. 4.5. The third diagram requires a combinatorial factor of two, corresponding to the two ways of labelling the photon lines.

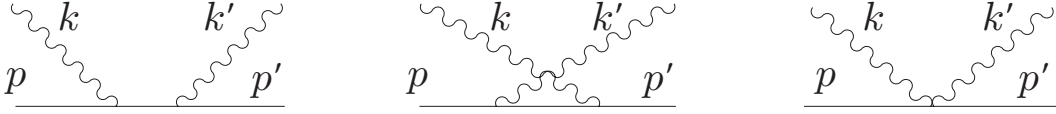


**Fig. 4.7.** Feynman diagrams for pion ‘Compton’ scattering.  $p$  and  $k$  are the initial pion and photon 4-momenta, becoming  $p'$  and  $k'$  after scattering.

The complete amplitude, contracted with the photon polarization vectors, is:

$$\mathfrak{M} = e^2 \epsilon'_\mu(\mathbf{k}') \mathbf{T}^{\mu,\nu} \epsilon_\nu(\mathbf{k})$$

with

$$T^{\mu,\nu} = \frac{(2p' + k')^\mu (2p + k)^\nu}{(p + k)^2 + m^2} + \frac{(2p - k')^\mu (2p' - k)^\nu}{(p - k')^2 + m^2} - 2\delta^{\mu,\nu}.$$

Here we recognize a current  $\times$  field term contracted with a second current  $\times$  field term and the pion propagator

$$\frac{1}{(p + k)^2 + m^2}$$

which has a pole at  $(p + k)^2 = -m^2$  and therefore there is no divergence in the cross section for Compton scattering.

$T^{\mu,\nu}$  is transverse for pions on the mass shell:

$$k_\nu T^{\mu,\nu} = k'_\nu T^{\mu,\nu} = 0$$

Taking the absolute value squared, summing over the final photon polarization and averaging over the initial one we get:

$$\begin{aligned} \frac{1}{2} \sum_{\text{pol}} |\mathfrak{M}|^2 &= \frac{1}{2} e^4 \sum_{\text{pol}} [\epsilon'_\mu(\mathbf{k}') \mathbf{T}^{\mu,\nu} \epsilon_\nu(\mathbf{k})] [\epsilon'_\rho(\mathbf{k}') \mathbf{T}^{\rho,\sigma} \epsilon_\sigma(\mathbf{k})]^* \\ &= \frac{1}{2} e^4 T^{\mu\nu} \delta_\mu^\rho T^{\rho\sigma} \delta_\nu^\sigma = \frac{1}{2} e^4 T^{\mu\nu} T_{\mu\nu} \\ &= 2e^4 \left\{ m^4 \left( \frac{1}{pk} - \frac{1}{pk'} \right)^2 - 2m^2 \left( \frac{1}{pk} - \frac{1}{pk'} \right) + 2 \right\}. \end{aligned} \quad (4.11)$$

The result (4.11) appears to diverge for  $\omega, \omega' \rightarrow 0$ . In fact from (4.8) we have  $pk = m\omega$ ,  $pk' = m\omega'$  and

$$\frac{1}{pk} - \frac{1}{pk'} = \frac{1}{m} \left( \frac{1}{\omega} - \frac{1}{\omega'} \right)$$

which together with (4.9) gives

$$\frac{1}{2} \sum_{\text{pol}} |\mathfrak{M}|^2 = 2e^4 [(1 - \cos \theta)^2 - 2(1 - \cos \theta) + 2] = 2e^4 (1 + \cos^2 \theta) \quad (4.12)$$

Now that we laboriously arrived to (4.12) we wish to remark that the labor was in fact unnecessary. Let’s work in the lab and, remembering (4.8), we choose the

following set of independent real polarization vectors:

$$\begin{aligned}
\epsilon_\mu(\mathbf{k}, 1) &= 0, 1, 0, 0 \\
\epsilon_\mu(\mathbf{k}, 2) &= 0, 0, 1, 0 \\
\epsilon'_\mu(\mathbf{k}', 1) &= 0, -\cos\theta, 0, \sin\theta \\
\epsilon'_\mu(\mathbf{k}', 2) &= 0, 0, 1, 0 \quad .
\end{aligned}
\tag{4.13}$$

Since they satisfy  $k\epsilon = k'\epsilon' = p\epsilon = p'\epsilon' = 0$  the only gauge invariant, non vanishing amplitude is  $\mathfrak{M} = -2e^2(\epsilon(\mathbf{k})\epsilon(\mathbf{k}'))$ . Summing over the photon polarizations:

$$\begin{aligned}
\frac{1}{2} \sum_{\text{pol}} |\mathfrak{M}|^2 &= 2e^4 \sum_{\lambda, \lambda'=1,2} \epsilon_\mu(\mathbf{k}, \lambda) \epsilon'^\mu(\mathbf{k}', \lambda') \epsilon_\rho(\mathbf{k}, \lambda) \epsilon'^\rho(\mathbf{k}', \lambda') \\
&= 2e^4(1 + \cos^2\theta)
\end{aligned}
\tag{4.14}$$

which is identical to (4.12). Finally we find the cross section in the laboratory

$$\frac{d\sigma}{d\Omega} = \frac{\alpha^2}{2m^2} \frac{1 + \cos^2\theta}{(1 + \omega/m(1 - \cos\theta))^2} ,$$

which in the low energy limit,  $\omega \rightarrow 0$ , corresponding to classical scattering of electromagnetic radiation from a charge, simplifies to

$$\frac{d\sigma}{d\Omega} = \frac{\alpha^2}{2m^2} (1 + \cos^2\theta).$$

The total cross section, in the same limit,

$$\sigma = \frac{8\pi\alpha^2}{3m^2}
\tag{4.15}$$

is called the Thomson cross section and provides a means to compute the charge to mass ratio of a particle. If the mass of the particle is known, we can use the measured cross section to define the value of  $\alpha$  at zero momentum transfer. The result (4.15) was already mentioned in chapter 2, eq. (4.9).

At zero energy, the photon scattering cross section on a pion of mass 139.57... is 8.8  $\mu\text{b}$ . Although we have derived the Thomson cross section for particles of spin zero, in the low energy limit spin interactions, which are relativistic effects, does not affect the result. It therefore also applies to the Compton effect on free (atomic) electrons. Since the mass squared of the electron is  $\sim 75,000$  times smaller than that of the pion, the corresponding cross section is much larger,  $\sigma \sim 0.66 \text{ b}$ .

## 4.6 Scattering from an Extended Charge Distribution, I

The cross section (4.1) computed in section 4.3 describes scattering of point charges, because we have used  $Ze^2/r$ , whose Fourier transform is  $1/k^2$  *i.e.* the photon propagator, as the potential energy for  $r > 0$ . For scattering from an extended distribution of

charge we have to go back to the explicit form of the potential, introducing a charge distribution function of  $\mathbf{r}$ , which we assume here to be spherically symmetric. The calculation which we will outline in the following section procedure is similar to the classical formulation of scattering by a Coulomb potential due to a point charge, except that a double integration will be necessary. Without entering, for the moment, in details it is common to introduce the so called form factor, the 3-dimensional Fourier transform of the charge distribution, a function of the 3-momentum transfer from the probe particle to the target particle. In general for a finite charge distribution  $\rho(x)$ , we can find the corresponding form factor  $F(\mathbf{q}^2)$ . The scattering cross section is then given by:

$$\frac{d\sigma}{d\Omega} = \frac{d\sigma}{d\Omega}\Big|_{\text{point}} \times |F(q^2)|^2$$

where the subscript point refers to scattering of point charges. The effect of a diffuse charge distribution can be correctly understood by classical arguments. For the Coulomb force, as well as any other long range one, small angle scattering corresponds to large impact parameter collisions. If the charge distribution of a particle has a finite size, small angle scattering from a point charge or a diffuse charge will be equal, essentially because of the Gauss theorem. The average scattering angle increases with decreasing impact parameter for a point charge. However for a finite charge distribution, the effective charge is smaller, resulting in a smaller probability of observing large scattering angle events. In general, we therefore find that for a diffuse charge we have:

$$\begin{aligned} \frac{d\sigma(\theta)}{d\Omega} &= \frac{d\sigma_{\text{point}}(\theta)}{d\Omega} \quad \text{for } \theta = 0 \\ \frac{d\sigma(\theta)}{d\Omega} &< \frac{d\sigma_{\text{point}}(\theta)}{d\Omega} \quad \text{for } \theta > 0 . \end{aligned}$$

## 4.7 Scattering from an Extended Charge Distribution, II

We introduce the problem using non relativistic quantum mechanics. The Rutherford cross section is given by

$$\frac{d\sigma}{d\Omega} = |f(\mathbf{q}^2)|$$

where  $f(\mathbf{q}^2)$  is the scattering amplitude and  $\mathbf{q}$  is the 3-momentum transfer

$$\mathbf{q} = \mathbf{p}_{\text{in}} - \mathbf{p}_{\text{out}}.$$

The scattering amplitude is the matrix element of the potential:

$$f(\mathbf{q}^2) = \frac{m}{2\pi} \int \Psi_{\text{out}}^* V(\mathbf{x}) \Psi_{\text{in}} d^3x.$$

To lowest order we compute the scattering amplitude using the so called first Born approximation, *i.e.* we use plane wave for both incident and outgoing particle,  $\Psi_{in} = \exp(-i\mathbf{p} \cdot \mathbf{x})$  *etc.* Then

$$f(\mathbf{q}^2) = \frac{m}{2\pi} \int V(\mathbf{x}) e^{-i\mathbf{q} \cdot \mathbf{x}} d^3x.$$

and, for the Coulomb potential  $Ze^2/x$

$$f(\mathbf{q}^2) = \frac{2mZe^2}{q^2}$$

from which

$$\frac{d\sigma}{d\Omega} = \frac{4m^2Z^2e^4}{q^4}. \quad (4.16)$$

Eq. (4.16) is the same as eq. (4.1) with the same approximation that  $M = \infty$ , the scattered particles has the same energy and momentum as the incident one,  $p_{in} = p_{out}$ . From the latter

$$q = 2p \sin \frac{\theta}{2}.$$

In the low energy limit,  $E = m$  and  $\beta = p/m$ .

We consider now a scattering center, centered at the origin, of charge  $Ze$  distributed over a finite region of space, with a charge density distribution  $\rho(r)$ , normalized as

$$\int \rho(r) d^3r = 1.$$

We must compute the scattering amplitude for the potential energy contribution from a volume element  $d^3r$  and integrate over  $\mathbf{r}$ :

$$V = \frac{Ze^2}{4\pi|\mathbf{x}|} \Rightarrow dV = \frac{Ze^2}{4\pi|\mathbf{z}|} \rho(r) d^3r.$$

This is shown in fig. 4.8.

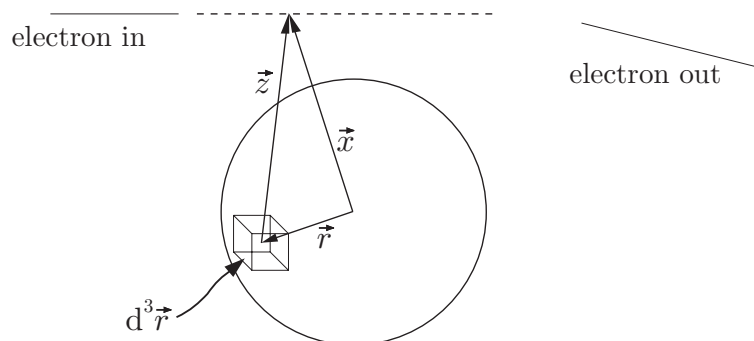


**Fig. 4.8.** Vectors  $\vec{r}$ ,  $\vec{x}$ ,  $\vec{z}$  and the volume element  $d^3r$ .

The integral for a point charge

$$\int e^{-i\mathbf{q}\cdot\mathbf{x}} \frac{d^3x}{|\mathbf{x}|} \propto \frac{1}{|\mathbf{q}|^2},$$

where we recognize the appearance of the propagator in the standard Feynman approach, becomes

$$\int \rho(r) e^{-i\mathbf{q}\cdot\mathbf{r}} d^3r \int e^{-i\mathbf{q}\cdot\mathbf{z}} \frac{d^3z}{4\pi|\mathbf{z}|}$$

where  $\mathbf{q}=\mathbf{p}_{\text{in}}-\mathbf{q}_{\text{out}}$  and the relation between the vectors  $\mathbf{x}$ ,  $\mathbf{z}$  and  $\mathbf{r}$ ,  $\mathbf{x}=\mathbf{r}+\mathbf{z}$ , is shown in fig. 4.8. In the second integral  $\mathbf{r}$  is constant and therefore we can set  $d^3x = d^3z$ . The last integral is therefore the same as the corresponding one for the point charge case, while the first is the Fourier transform of  $\rho(r)$ ,  $|F(q^2)|$ . By construction  $F(q^2 > 0) < 1$  and the scattering cross section is indeed:

$$\left. \frac{d^2\sigma}{d\Omega} \right|_{\text{ExtendedCharge}} = \left. \frac{d^2\sigma}{d\Omega} \right|_{\text{Rutherford}} \times |F(q^2)|^2.$$

In the above  $F(q^2 = 0) = 1$  and  $F(q^2 > 1) < 1$ . We recall that for Rutherford scattering  $q^2 = 4p^2 \sin^2 \theta/2$ , thus  $F(q^2) < 1$  for  $\theta > 0$  confirming the classical guess above.

We can appreciate better scattering by an extended charge distribution by introducing the mean square radius of the distribution and expanding the form factor in power series. By definition:

$$\langle r^2 \rangle = \int r^2 \rho(r) d^3r.$$

Expanding the form factor gives:

$$F(q^2) = 1 - \frac{q^2 \langle r^2 \rangle}{6} \dots$$

Neglecting higher order term, for  $q^2 \sim 1/\langle r^2 \rangle$ ,  $F(q^2) \sim 1 - 1/6$  and  $|F(q^2)|^2 \sim 1 - 1/3$  or  $1 - 0.33$ . Thus in a scattering experiments against an object with an rms radius of 1 fm and a momentum transfer of order 197 Mev/c we would find a cross section which is reduced by  $\sim 33\%$  with respect to the Rutherford cross section. Note that in all the above  $q$  is a 3-momentum. We give below some example of the functional form of  $F(q^2)$  for various charge distributions.

Charge distribution $\rho(r)$	Form factor $F(q^2)$
$\delta(r)$	1
$\rho_0 \exp(-r/a)$	$1/(1 + q^2 a^2)^2$
$\rho_0 \exp(-r^2/b^2)$	$\exp(-q^2 b^2)$
$\rho_0, r \leq R; 0, r > R$	$(3 \sin qr - qr \cos qr)/q^2 r^2$

Clearly for  $r$  of  $\mathcal{O}(a)$ , we begin to see an effect of the finite size of the charge distribution for  $q^2$  values of  $\mathcal{O}(1/a^2)$  as we expect because of the uncertainty relation.

We will introduce later a fully relativistic generalization of this concept, substituting  $|\mathbf{q}|^2$  with  $q_\mu q^\mu = t$ . By its definition, in scattering processes,  $t < 0$  and the form factor  $F(q^2)$  is not anymore the Fourier transform of the charge distribution, except in the brick-wall or Breit frame of reference. It is however obviously Lorentz invariant. Thinking in terms of 3-momenta and  $|\mathbf{q}|^2$  (usually  $t \approx -|\mathbf{q}|^2$ ) keeps the meaning apparently simple but loses Lorentz covariance.

## 4.8 Scattering with Spin

The extension to scattering processes involving one or more particles with spin is very simple, although we will rarely do complete calculations. The case of extended charge distribution can be treated in a very similar way. We give in the following the results for two basic cases. The first is scattering of electrons from an object of spin zero and charge  $Ze$ . This process is called Mott scattering and the corresponding cross section is given by:

$$\left. \frac{d\sigma}{d\Omega} \right|_{\text{Mott}} = \frac{\alpha^2 Z^2}{4\beta^2 \mathbf{p}^2 \sin^4 \theta/2} \left(1 - \beta^2 \sin^2 \frac{\theta}{2}\right) = \left. \frac{d\sigma}{d\Omega} \right|_{\text{Rutherford}} \times \left(1 - \beta \sin^2 \frac{\theta}{2}\right).$$

This result remains valid also for scattering from an extended charge  $Ze$ :

$$\left. \frac{d\sigma}{d\Omega} \right|_{\text{Mott,extended}} = \left. \frac{d\sigma}{d\Omega} \right|_{\text{Rutherford,extended}} \times \left(1 - \beta \sin^2 \frac{\theta}{2}\right).$$

The form factor is understood here to be included in the Rutherford cross section, since it belongs to the spin zero object. The form of the additional terms is such that for small  $\beta$  Mott and Rutherford scattering are identical as we would expect, spin interactions being relativistic effects.

The case of spin 1/2 against spin 1/2 is more complicated because spin 1/2 particles have a dipole magnetic moment. This means that we have two form factors: electric and magnetic. The second can be understood as being due to a magnetic dipole density of our extended object whose Fourier transform is the magnetic form factor. For a Dirac proton the invariant amplitude is

$$\mathfrak{M} = e J_\mu(p_e, p'_e) J^\mu(p_p, p'_p) \frac{1}{k^2}, \quad k_\mu = (p_e - p'_e)_\mu = (p_p - p'_p)_\mu$$

with  $p_e$  and  $p_p$  the electron and proton 4-momenta. The cross section in the lab system is:

$$\left. \frac{d\sigma}{d\Omega} \right|_{\text{Lab}} = \frac{\alpha^2}{4E^2} \frac{\cos^2(\theta/2) - (q^2/2M^2) \sin^2(\theta/2)}{[1 + (2E/M) \sin^2(\theta/2)] \sin^4(\theta/2)}$$

in the limit  $m/E \ll 1$ , where  $q = p_e - p'_e$ . The factor in square brackets in the denominator is due to the proton recoil, which we no longer ignore. (Show that inclusion of recoil results in a factor  $E/E' = 1/[...]$ ). For spin 1/2 particles of finite radius and with a magnetic moment different from the Dirac value we must generalize the form of the current density. From Lorentz invariance the current must be a function of all the coordinates, we work in momentum space, of the in and out particles, transforming as a 4-vector. The spin coordinates appear via the appropriate spinor- $\gamma$ -matrices factors. In addition we have terms in  $p_\mu, p'_\mu$  all multiplied by *arbitrary* functions of any Lorentz invariant we can construct, in this case just  $q^2 = q_\mu q^\mu$  with  $q = p - p'$ . Then the current is:

$$J_\mu = e\bar{u}(p')[p_\mu\Gamma_1(q^2) + p'_\mu\Gamma_2(q^2) + \gamma_\mu\Gamma_3(q^2)]u(p)$$

which, by requiring that it be conserved, reduces to:

$$J_\mu = e\bar{u}(p')[(p + p')_\mu\Gamma_1(q^2) + \gamma_\mu\Gamma_3(q^2)]u(p)$$

where  $\Gamma_i(q^2)$  are form factors related to charge and magnetic moment density distributions. The term  $(p + p')_\mu$  can be transformed into a magnetic-like interaction  $\sigma_{\mu\nu}q^\nu$  by use of the Dirac equation for the proton, or the neutron,  $(\not{p} - M)u = 0$ . Then the current can be written as:

$$J_\mu = e\bar{u}(p')[\gamma_\mu F_1(q^2) + i\sigma_{\mu\nu}q^\nu \frac{\kappa}{2M}F_2(q^2)]u(p)$$

where the form factors  $F_1(q^2)$  and  $F_2(q^2)$  are normalized in such a way that at infinity we see the charge of the proton as  $1(\times e)$  and of the neutron as zero:

$$F_1(q^2 = 0) = \text{charge} = \begin{cases} 1 & \text{for proton} \\ 0 & \text{for neutron,} \end{cases}$$

while  $\kappa$  is the experimental value of the anomalous magnetic moment,  $\mu - \mu_{\text{Dirac}}$  in units of the nuclear magneton,  $\mu_N = e/2M_N$ , and therefore:

$$F_2(q^2 = 0) = \begin{cases} 1 & \text{for proton} \\ 1 & \text{for neutron,} \end{cases}$$

$$\kappa = \frac{\mu - \mu_{\text{Dirac}}}{\mu_N} = \begin{cases} 2.79 - 1 = 1.79 \\ -1.91 - 0 = -1.91. \end{cases}$$

Note that the Dirac part of the dipole magnetic moment does not contribute to the magnetic form factor. Rather, the Dirac part of the dipole magnetic moment is already accounted for in  $J_\mu = \bar{\psi}\gamma_\mu\psi$ . From the current above we find:

$$\frac{d\sigma}{d\Omega}\Big|_{\text{Lab}} = \frac{\alpha^2}{4E^2} \frac{\left(F_1^2 - \frac{\kappa^2 q^2}{4M^2}F_2^2\right) \cos^2 \frac{\theta}{2} - \frac{q^2}{2M^2}(F_1 + \kappa F_2)^2 \sin^2 \frac{\theta}{2}}{[1 + (2E/M) \sin^2(\theta/2)] \sin^4(\theta/2)}$$

the so called Rosenbluth formula. One can *remove* or hide the “interference” term between  $F_1$  and  $F_2$  by introducing the form factors

$$G_E = F_1 + \frac{\kappa q^2}{4M^2} F_2$$

$$G_M = F_1 + \kappa F_2$$

in terms of which:

$$\begin{aligned} \frac{d\sigma}{d\Omega}\Big|_{\text{Lab}} &= \frac{\alpha^2}{4E^2 \sin^4(\theta/2)} \frac{E}{E'} \left[ \frac{G_E^2 + bG_M^2}{1+b} \cos^2(\theta/2) + 2bG_M^2 \sin^2 \frac{\theta}{2} \right] \\ &= \frac{\alpha^2 \cos^2(\theta/2)}{4E^2 \sin^4(\theta/2)} \frac{E}{E'} \left[ \frac{G_E^2 + bG_M^2}{1+b} + 2bG_M^2 \tan^2 \frac{\theta}{2} \right], \quad b = -q^2/4M^2. \end{aligned}$$

$G_E$  and  $G_M$  are called the electric and magnetic form factors normalized as

$$G_E(q^2 = 0) = \frac{Q}{e} \quad G_M(q^2 = 0) = \frac{\mu}{\mu_N}$$

where  $Q$  is the particle charge,  $e$  the electron charge,  $\mu$  the magnetic moment and  $\mu_N$  the nuclear magneton, *i.e.*  $e/2m_N$ , with  $m_N$  the proton mass ( $\sim$ neutron mass). The form factors  $G_E(q^2)$  and  $G_M(q^2)$  do not have a simple physical connection to charge and magnetic moment density distributions, except in the Breit or brick-wall frame, H-M, p. 177-8. Still the rms charge radius is connected to the form factors, eg

$$\langle r^2 \rangle = 6 \left( \frac{dG_E(q^2)}{dq^2} \right)_{q^2=0}.$$

Experimentally:

$$G_E(q^2) = \left( 1 - \frac{q^2}{0.71} \right)^{-2} \quad \text{in GeV}.$$

The extra power of two in the denominator is an embarrassment. Still we derive several conclusions from all this. First of all, we find that the mean square proton charge radius is:

$$\langle r^2 \rangle = (0.8 \text{ fm})^2$$

in reasonable agreement with other determinations of the size of the proton. The same result applies to the anomalous magnetic moment radius for proton and neutron. Second, the shape of  $G_E$  is the Fourier transform of a charge distribution of the form  $e^{-mr}$ :

$$F(|\mathbf{q}|) = \left( 1 - \frac{q^2}{m^2} \right)^{-2}, \quad q^2 = -|\mathbf{q}|^2$$

That means that somehow masses larger than that of the pion appear to be involved. Finally the form factor above has a pole at  $q^2 \sim 0.7 \text{ GeV}^2$ , a value that is not reachable in  $ep$  scattering but becomes physical for  $e^+e^-$  annihilations or pion pion scattering.

It was in fact from an analysis of the proton form factors that new important ideas emerged, leading to the prediction of the existence of vector mesons, the  $\rho$  meson in particular. The Yukawa theory of strong interaction introduces in the lagrangian a term  $g\phi\bar{\psi}\gamma_5\psi$  where  $g \sim 1$ . This means that a proton is equally a proton, a nucleon plus a pion, or any number of pions. The situation is not likely to lead to simple calculable results but, in a simplistic way, we might try to understand the photon-proton coupling as due to the contributions shown in fig. 4.9.

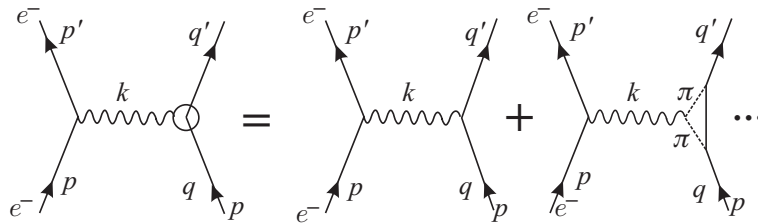


**Fig. 4.9.** Contributions to the electron-proton scattering amplitude.

Analysis of the data on  $ep$  scattering suggested quite a long time ago that the amplitude should be dominated by a two pion state with  $J^{PC} = 1^{--}$  of mass around 800 MeV, as shown in fig. 4.10, as well as by other possible states.

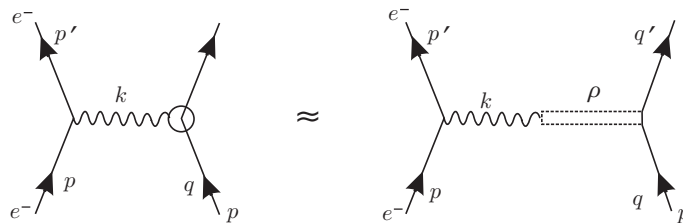


**Fig. 4.10.** The  $\rho$  meson contribution to the electron-proton scattering amplitude.

The existence of the vector mesons was soon confirmed in pion-pion scattering experiment, that is in the study of the mass spectrum of two and three pions in reactions such as  $\pi + p \rightarrow 2\pi + N$  and reactions in which three pions, forming the  $\omega^0$  meson, are produced in the final state. Later, the  $\rho$  meson was observed in  $e^+e^-$  annihilations as we will discuss soon. All of this became later better understood in terms of quarks.

## 4.9 Cross sections for $J=1/2$ particles

This is a very brief outline of how the modulus squared of a matrix element  $\mathfrak{M}$  containing fermions is calculated. We will limit ourselves to the common case in which the polarization of the particles is not observed. This means that we must

sum over the final state spin orientations and average over the initial ones. The latter is equivalent to summing also and dividing by the possible values  $2J + 1 = 2$  for spin  $1/2$ . For every fermion in the process we will typically have a term  $\bar{u}(p_f, s_f)\Gamma u(p_i, s_i)$  in  $\mathfrak{M}$ .  $u(p)$  here is the so called particle, *i.e.* positive energy spinor obeying the Dirac equation  $(\not{p} - m)u(p, s) = 0$ , while the antiparticle is negative energy spinor  $v$  obeying the Dirac equation  $(\not{p} + m)v(p, s) = 0$ .  $v$  spinors rather than  $u$  spinors can appear in  $\mathfrak{M}$ .  $\Gamma$  is a combination of  $\gamma$ -matrices. We want to calculate

$$\sum_{s_f, s_i} |\mathfrak{M}|^2$$

that is

$$\sum_{s_f, s_i} |\bar{u}(p_f, s_f)\Gamma u(p_i, s_i)|^2 = \sum_{s_f, s_i} [\bar{u}(p_f, s_f)\Gamma u(p_i, s_i)][\bar{u}(p_i, s_i)\bar{\Gamma}u(p_f, s_f)],$$

where  $\bar{\Gamma} = \gamma^0\Gamma^\dagger\gamma^0$ . With the normalization for spinors  $\bar{u}u = \bar{v}v = 2m$  and the completeness relation  $\sum_s u_\alpha(p, s)\bar{u}_\beta(p, s) - v_\alpha(p, s)\bar{v}_\beta(p, s) = \delta_{\alpha\beta}$ , the polarization sum above is given by the trace:

$$\sum_{s_f, s_i} |\bar{u}(p_f, s_f)\Gamma u(p_i, s_i)|^2 = \text{Tr}(\not{p}_f + m)\Gamma(\not{p}_i + m)\bar{\Gamma}.$$

Finally, the cross section for scattering of two spin  $1/2$  particles labelled 1, 2 into two spin  $1/2$  particles labelled a, b is given by:

$$d\sigma = \frac{1}{4} \frac{1}{|\mathbf{v}_1 - \mathbf{v}_3|} \frac{1}{2E_1} \frac{1}{2E_2} \sum_{\text{spins}} |\mathfrak{M}|^2 \frac{d^3\mathbf{p}_a}{2E_a(2\pi)^3} \frac{d^3\mathbf{p}_b}{2E_b(2\pi)^3} \times \\ (2\pi)^4 \delta^4(p_1 + p_2 - p_a - p_b)$$

where the additional factor  $1/4$  accounts for the average and not the sum over the initial spins. Likewise for the decay of a fermion of mass  $M$  and 4-momentum  $P$  into three fermions labelled 1, 2, 3, the decay rate is:

$$d\Gamma = \frac{1}{2} \frac{1}{2M} \sum_{\text{spins}} |\mathfrak{M}|^2 \frac{d^3\mathbf{p}_1}{2E_1(2\pi)^3} \frac{d^3\mathbf{p}_2}{2E_2(2\pi)^3} \frac{d^3\mathbf{p}_3}{2E_3(2\pi)^3} \times \\ (2\pi)^4 \delta^4(P - p_1 - p_2 - p_3)$$

#### 4.10 $e^+e^- \rightarrow \pi^+\pi^-$

What is new for this process is the electron, whose spin we cannot ignore. Referring to fig. 4.11, the amplitude for the process

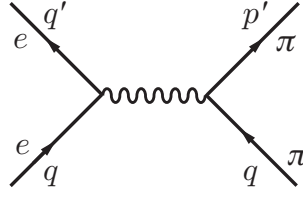


Fig. 4.11. Amplitude for  $e^+e^- \rightarrow \pi^+\pi^-$ .

is given by

$$\mathfrak{M} = J_e^\mu A_\mu \frac{1}{s} J_\pi^\nu A_\nu.$$

Summing over the polarization of the intermediate photon,  $\sum A_\mu A_\nu = g_{\mu\nu}$ , we find

$$\mathfrak{M} = J^\mu(e) J_\mu(\pi) \frac{1}{s}.$$

The electron current above is the 4-vector  $J_e^\mu = e\bar{u}(q')\gamma^\mu u(q)$ . I ignore  $i$  and signs, since I do all to first order only. The pion current  $J_\pi^\mu$  is  $e(p - p')_\mu$ , see eq. (4.3). Thus  $\mathfrak{M} = e^2 (\bar{u}(q')\gamma^\mu u(q)(p' - p)_\mu) / s$  and

$$|\mathfrak{M}|^2 = \frac{e^4}{s^2} (\bar{u}(q')\gamma^\mu u(q)(p' - p)_\mu) (\bar{u}(q')\gamma^\nu u(q)(p' - p)_\nu)$$

to be averaged over initial spins. The sum over the electron spin orientations is the tensor

$$T_e^{\mu\nu} = 4 (q'^\mu q^\nu + q'^\nu q^\mu - (q'q - m^2)g_{\mu\nu}).$$

Dividing by 4 ( $= (2s_1 + 1)(2s_2 + 1)$ ) and neglecting the electron mass gives

$$\overline{|\mathfrak{M}|^2} = \frac{e^4}{s^2} (q'P qP + qP q'P - q'q PP); \quad P = p' - p.$$

In the CM, with  $W = \sqrt{s}$ :

$$\begin{aligned} E_e = E'_e = E_\pi = E'_\pi &= W/2 \\ \vec{q} = -\vec{q}'; \quad |\vec{q}| &= W/2 \\ \vec{p} = -\vec{p}' \end{aligned}$$

Therefore

$$P = (0, 2\vec{p}); \quad PP = 4|\vec{p}|^2; \quad qq' = 2|\vec{q}|^2 = 2E_\pi^2$$

After a little algebra

$$\overline{|\mathfrak{M}|^2} = \frac{e^4 p_\pi^2}{2E_\pi^2} \sin^2 \theta.$$

From eq. (3.2):

$$d\sigma = \frac{1}{32\pi s} \frac{p_{\text{out}}}{p_{\text{in}}} \overline{|\mathfrak{M}|^2} d\cos\theta$$

we get

$$\frac{d\sigma}{d\cos\theta} = \frac{1}{32\pi s} \frac{p_{\text{out}}}{p_{\text{in}}} \frac{e^4 p_\pi^2}{2E_\pi^2} \sin^2\theta = \frac{\pi\alpha^2}{4s} \beta^3 \sin^2\theta$$

and

$$\sigma(e^+e^- \rightarrow \pi^+\pi^-) = \frac{\pi\alpha^2}{3s} \beta^3$$

The computed cross section is correct for a point-like pion. From Lorentz invariance, the most general form of the pion current is

$$J^\mu(\pi) = e(p - p')^\mu \times F(s)$$

where the arbitrary function  $F(s)$  or  $F_\pi(s)$  is called the pion form factor. For  $e\pi$  scattering we would write  $F_\pi(t)$ . By definition,  $F_\pi(s=0) = F_\pi(t=0) = 1$ . With the form factor, the cross section is given by:

$$\sigma(e^+e^- \rightarrow \pi^+\pi^-) = \frac{\pi\alpha^2}{3s} \beta^3 |F_\pi(s)|^2$$

The form factor is dominated by the  $\rho$  pole, in the simplest form:

$$|F_\pi|^2 \propto \frac{(\Gamma_\rho/2)^2}{(s^{1/2} - m_\rho)^2 - (\Gamma_\rho/2)^2}$$

#### 4.11 $e^+e^- \rightarrow \mu^+\mu^-$

The amplitude for  $e^-\mu^- \rightarrow \mu^-e^-$  scattering is shown at left in fig. 4.12 and the corresponding matrix element is given by:

$$\mathfrak{M} = -e^2 \bar{u}(p') \gamma_\mu u(p) \bar{u}(q') \gamma_\mu u(q) \frac{1}{k^2}, \quad k = p - p'$$

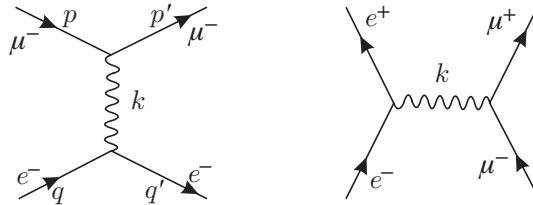


**Fig. 4.12.** Amplitudes for  $e^-\mu^- \rightarrow \mu^-e^-$  and  $e^+e^- \rightarrow \mu^+\mu^-$ .

The sums over spins can be put in the form

$$\sum_{\text{spins}} |\mathfrak{M}|^2 = \frac{e^4}{k^4} T_e^{\mu\nu} T_{\mu\nu}^{\text{muon}}$$

The electron tensor is

$$\begin{aligned} T_e^{\mu\nu} &= \frac{1}{2} \text{Tr}(p' \gamma^\mu p \gamma^\nu + m^2 \gamma^\mu \gamma^\nu) \\ &= 2(p'^\mu p^\nu + p'^\nu p^\mu - (p' \cdot p - m^2) g^{\mu\nu}) \end{aligned}$$

with  $m$  the electron mass and a very similar result follows for  $T^{\text{muon}}$

$$T_{\mu\nu}^{\text{muon}} = 2(q'_\mu q_\nu + q'_\nu q_\mu - (q' \cdot q - M^2)g_{\mu\nu})$$

with  $M$  the muon mass. The rest of the calculation is trivial. We only write the extreme relativistic result, *i.e.*  $M, m \ll \sqrt{s}$  or  $M, m = 0$ , using the variables  $s, t, u$

$$\begin{aligned} s &= (p + q)^2 = 2(p \cdot q) = 2(p' \cdot q') \\ t &= (p - p')^2 = -2(p \cdot p') = -2(q \cdot q') \\ u &= (p - q')^2 = -2(p \cdot q') = -2(q' \cdot p) \end{aligned}$$

$$\sum_{\text{spins}} |\mathfrak{M}|^2 = 2e^4 \frac{s^2 + u^2}{t^2}$$

This result applies also to  $e^+e^- \rightarrow \mu^+\mu^-$  scattering by turning around appropriately the external lines or *crossing the amplitude*. In the present case this amounts to the substitutions  $p' \leftrightarrow -q$  or  $s \leftrightarrow t$  in the last result giving

$$\sum_{\text{spins}} |\mathfrak{M}|^2 = 2e^4 \frac{t^2 + u^2}{s^2}$$

for  $e^+e^- \rightarrow \mu^+\mu^-$  scattering. Performing the phase space integration, remembering a factor of  $1/4$  for the initial spin states and with  $\alpha = e^2/4\pi$  we find

$$\frac{d\sigma}{d\Omega} = \frac{\alpha^2}{2s} \frac{t^2 + u^2}{s^2}. \quad (4.17)$$

In the CM, for all masses negligible, all particles have the same energy  $E$  and the variables  $s, t, u$  can be written in term of  $E$  and the scattering angle as

$$\begin{aligned} s &= 2p \cdot q = 4E^2 \\ t &= -2p \cdot p' = -2E^2(1 - \cos \theta) \\ u &= -2p \cdot q' = -2E^2(1 + \cos \theta) \end{aligned}$$

from which

$$\left. \frac{d\sigma}{d\Omega} \right|_{\text{CM}} = \frac{\alpha^2}{4s} (1 + \cos^2 \theta)$$

and

$$\sigma(e^+e^- \rightarrow \mu^+\mu^-) = \frac{4\pi\alpha^2}{3s} \frac{\beta_\mu(3 - \beta_\mu^2)}{2}$$

putting back the threshold dependence on  $\beta_\mu$  due to the muon mass.

### 4.12 Bhabha scattering: $e^+e^- \rightarrow e^+e^-$

For completeness we give the result for the Bhabha process, *i.e.*  $e^+e^- \rightarrow e^+e^-$ . Two amplitudes contribute, the exchange and annihilation diagrams, see for instance fig. 4.5 in section 4.4. The cross section correspondingly contains three terms due, respectively to the two amplitudes and their interference term.

$$\frac{d\sigma}{d\Omega} = \frac{\alpha^2}{2s} \left[ \frac{s^2 + u^2}{t^2} + \frac{t^2 + u^2}{s^2} + \frac{2u^2}{ts} \right].$$

The first term, being due to one photon exchange, exhibit the usual divergence  $1/t^2$  or  $1/\sin^4\theta/2$ . The second term is identical to the result in eq. (4.17) above and the last is the interference contribution.

## 5 $e^+e^- \rightarrow \text{Hadrons, R, Color etc}$

### 5.1 $e^+e^- \rightarrow \text{Hadrons}$

If only  $\rho$ , first  $\sigma$  becomes large and then  $\sigma \rightarrow 0$  faster than  $1/s$ .

$$\sigma(e^+e^- \rightarrow \pi^+\pi^-) = \frac{12\pi}{s} \Gamma_{ee} \Gamma_{\text{res}} \frac{M_{\text{res}}^2}{(M_{\text{res}}^2 - s)^2 + M_{\text{res}}^2 \Gamma^2}$$

$$\lim_{s \rightarrow \infty} \sigma(\text{hadrons}) \propto \frac{1}{s^3}$$

$$\sigma(ep)_{\text{elastic}} \sim \sigma_{\text{Rutherford}} \times |f(\rho)|^2 \sim \frac{\text{const}}{t^4}$$

#### 5.1.1 Final remarks

## 6 The Weak Interaction. I

### 6.1 Introduction

The study of the weak interaction begins with the discovery of beta decay of nuclei  $(A, Z) \rightarrow (A, Z - 1) + e^-$ . Soon it became clear that the electron emitted in beta decay had a continuous spectrum with

$$0 \leq E_e \leq M(A, Z) - M(A, Z - 1) = E_0.$$

In the early days of quantum mechanics physicists were ready to abandon *old* prejudices and non other than Bohr proposed that energy conservation might not apply at atomic or nuclear scale. Pauli knew better and preferred to propose the existence of a new particle, later called neutrino by Fermi – the small neutral particle. The properties of the neutrino were to be:  $J=1/2$ ,  $m=0$ ,  $Q=0$  and its interaction with matter small enough to make it undetectable. Following QED, Fermi proposed that the beta decay processes be due to an effective four fermion interaction, similar to the electromagnetic case, but with the four fermion operators taken at the same space time point, fig. 6.1.

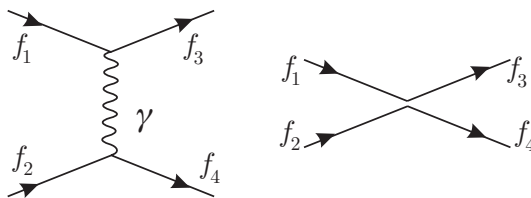


**Fig. 6.1.** The effective Fermi 4-fermion coupling, right, compared to QED, left. The small gap between vertices reminds us that the 4-fermion interaction is an effective theory with a coupling constant of dimension -2, about which we will do something.

Consider the simplest case of  $n \rightarrow p + e^- + \nu$  or better the crossed process  $p + e^- \rightarrow n + \nu$ . The matrix element is taken as

$$\mathfrak{M} = G \bar{\Psi}_n \gamma_\mu \Psi_p \bar{\Psi}_e \gamma_\mu \Psi_\nu \quad (6.1)$$

with  $G$  a coupling constant to be determined experimentally. If the proton and neutron mass are large wrt the momenta involved in the decay, the terms in  $\gamma_1$ ,  $\gamma_2$ , and  $\gamma_3$  do not contribute and (6.1) reduces to:

$$\mathfrak{M} = G \Psi_n^* \Psi_p \Psi_e^* \Psi_\nu. \quad (6.2)$$

For  $\sum_{\text{spins}} |\mathfrak{M}|^2 = 1$  we find the electron spectrum for allowed Fermi transitions:

$$\frac{d\Gamma}{dp_e} = \frac{G^2}{\pi^3} p_e^2 (E - E_0)^2.$$

The Kurie plot is a graph of the experimentally determined quantity  $\sqrt{d\Gamma/dp_e}/p_e$  versus  $E_e$ . According to (6.1), the graph should be a straight line and this is indeed the case. Note that if  $m(\nu)$  is different from zero the spectrum ends before  $E_0$  and is not a straight line near the end point. The so called Kurie plot is shown in fig. 6.2.

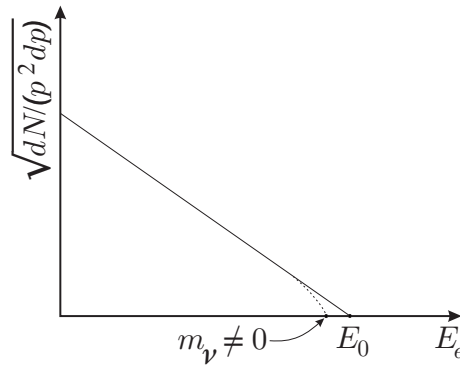


**Fig. 6.2.** A plot of the quantity  $\sqrt{d\Gamma/dp_e}/p_e$  versus  $E_e$ . Accurate experiments have shown that nuclear  $\beta$ -decay data agrees with the Fermi prediction. Also indicated is the spectrum shape and the end point,  $E_0 - m_\nu$ , for a non zero neutrino mass.

We can crudely integrate the differential rate above, putting  $p_e = E_e$ , *i.e.* neglecting the electron mass. We also neglect corrections due to the atomic electrons, which distort the electron wave function. In this way we obtain

$$\Gamma = \frac{1}{\tau} = \frac{G^2 E_0^5}{30\pi^3}.$$

We can thus extract the value of  $G$ ,  $G \approx 10^{-5} m_p^{-2}$ . This value can be obtained from the measured  $\beta$ -decay lifetimes of several different nuclides. Experimental evidence thus supports the existence of the neutrino and the validity of the effective Fermi interaction. Including the above mentioned corrections, as well as radiative corrections, and using the so called super allowed Fermi transitions (decays of nuclei where only the vector part contributes, *i.e.*  $0 \rightarrow 0$  transitions between members of an isospin multiplet) the very precise value below is obtained:

$$G_{\text{F}} (\beta \text{ decay}) = 1.166\,399(2) \times (0.9751 \pm 0.0006) \text{ GeV}^{-2}$$

whose significance we will discuss later.

## 6.2 Parity and Charge Conjugation

In 1957 it was experimentally proved that parity,  $P$ , is violated in weak interactions. In general, the experimental observation that the expectation value of a pseudo

scalar is different from zero implies that parity is violated. In order for this to happen however interference between two amplitudes, one even under  $P$  and one odd under  $P$  is necessary. If only one amplitude  $A$  contributes to a process, whether even or odd under  $P$ ,  $|A|^2$  is even and no parity violation is observable. If on the other hand the amplitude has an even part and an odd part,  $A = A^+ + A^-$ , then  $|A|^2 = |A^+|^2 + |A^-|^2 + 2\Re(A^{+*}A^-)$  and  $2\Re(A^{+*}A^-)$  is odd under  $P$ .

The three 1957 experiments are extremely simple and beautiful and should be understood in their experimental details. Here we will only briefly recall their principle and understand them in terms of measuring a pseudoscalar quantity and understand the result in terms of neutrino helicity when possible. In the beta decay process  $^{60}\text{Co} \rightarrow ^{60}\text{Ni} + e + \nu$  correlations between the Co nucleus spin and the direction of the decay electron are observed, resulting in  $\langle \mathbf{J} \cdot \mathbf{p}_e \rangle \neq 0$ . The experiment is shown in principle in fig. 6.3.

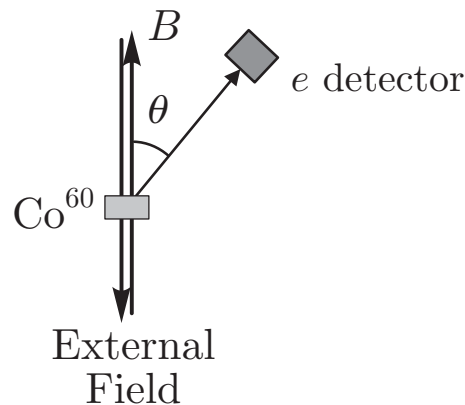


**Fig. 6.3.** The experiment of C. S. Wu *et al.*. The probability of  $^{60}\text{Co}$  an electron along or opposite to  $\mathbf{B}$  is different.

The pseudoscalar with non-zero average observed is  $\mathbf{B} \cdot \mathbf{p}_e$ . Since the magnetic field aligns the cobalt spin,  $\mathbf{B} \cdot \mathbf{p}_e$  is equivalent to  $\mathbf{J} \cdot \mathbf{p}_e$ . For negative electron helicity and positive anti-neutrino helicity, the favored configuration is shown in fig. 6.4.

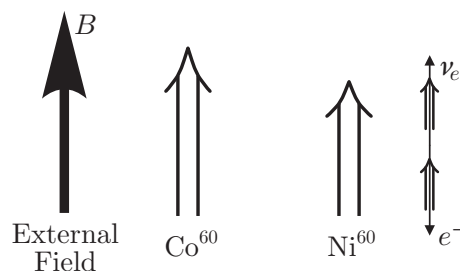


**Fig. 6.4.** Favored orientation of initial,  $J=5$ , and final,  $J=4$  nuclear spins and of the electron and anti-neutrino helicities and momenta in the decay of  $^{60}\text{Co}$ .

Parity violation was also observed in the decay chain  $\pi \rightarrow \mu \rightarrow e$ , fig 6.5.

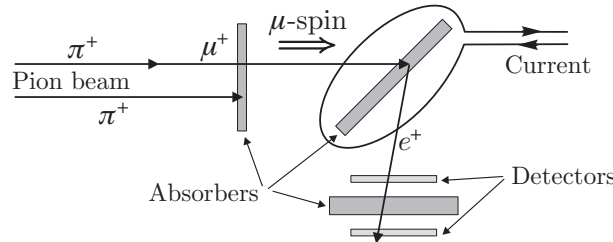


**Fig. 6.5.** The Garwin and Lederman experiment,

Note that in both cases neutrinos are involved. Parity violation was also observed in the decay  $\Lambda \rightarrow p\pi^-$ , a process with no neutrino, by observing correlations of the form  $p_1 \cdot p_2 \times p_3$  which is a pseudoscalar, fig. 6.6. \_\_\_\_\_ Fig. 6????

Soon thereafter it was directly proven that electrons emitted in beta decay have helicity  $\mathcal{H}=-1$  and also that  $\mathcal{H}(\nu)=-1$  in beta decay and in pion decay. A non vanishing value of the helicity is by itself proof of  $P$  and  $C$  violation.

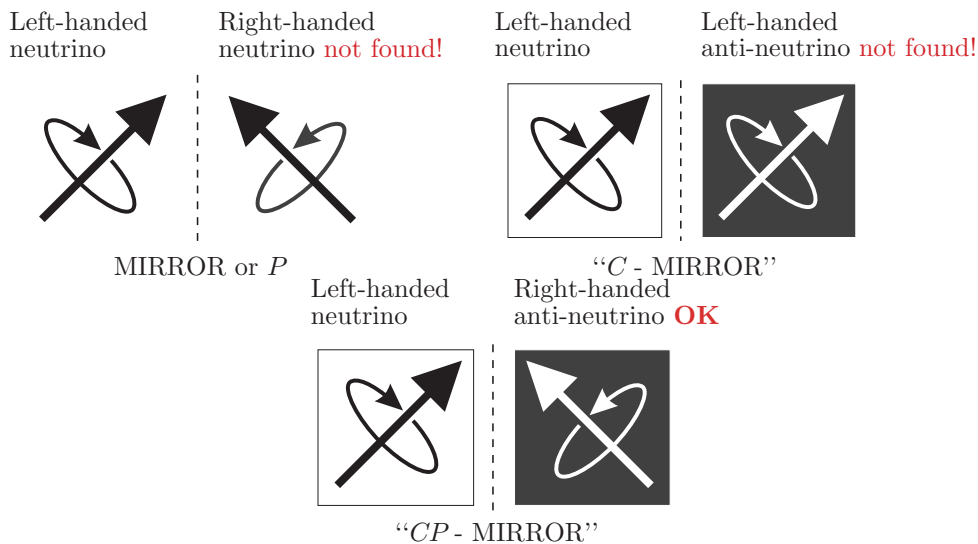


**Fig. 6.7.**  $P$ ,  $C$  and  $CP$  on a neutrino.

### 6.3 Helicity and left-handed particles

We define the helicity of a spin 1/2 particle as the eigenvalue of the helicity operator

$$\mathcal{H} = \frac{1}{2} \vec{\sigma} \cdot \hat{p}, \quad \hat{p} = \frac{\vec{p}}{p}$$

The operator  $\mathcal{H}$  commutes with the Hamiltonian and therefore the helicity is a good quantum number. It is not, however a Lorentz-invariant quantity for a massive particle. If a particle of given helicity moves with a velocity  $\beta < 1$  we can overtake it and find its helicity flipped around.

The operators  $O_{\pm} = (1 \pm \gamma^5)/2$  are projection operators:

$$\begin{aligned} O_{\pm}^2 &= O_{\pm} \\ O_+O_- &= O_-O_+ = 0. \end{aligned}$$

For a spin 1/2 particle with  $\beta = p/E$  approaching 1 the states  $O_{\pm}$  have positive and negative helicity. It is usual to define the spinors

$$\begin{aligned} u_L &= O_-u \\ u_R &= O_+u \end{aligned}$$

for  $m=0$ ,  $u_L$  has negative helicity. A particle with negative helicity has the spin antiparallel to the direction of motion and is called a left-handed particle, from which the  $L$  in  $u_L$ . Similarly  $u_R$  has positive helicity and corresponds to a right-handed particle.

## 6.4 The V–A interaction

The series of experiments at the end of the 50's lead to a new form of the effective weak interaction:

$$\frac{G}{\sqrt{2}} \bar{u} \gamma_{\mu} (1 - \gamma^5) u \bar{u} \gamma_{\mu} (1 - \gamma^5) u \quad (6.3)$$

where for the moment we do not specify to what particles the four spinors belong. The factor  $1/\sqrt{2}$ , introduced for historical reasons, maintains the value of the Fermi constant  $G$ . Recall that  $\bar{u} \gamma^{\mu} u$  and  $\bar{u} \gamma^{\mu} \gamma^5 u$  transform respectively as a vector (V) and an axial vector (A), from which the name V–A. The form of the interaction suggests that we put it in the form of a current  $\times$  current interaction in analogy with electromagnetism. We remain to face of course the problem that a four fermion interaction is a very divergent theory but we will ultimately couple the currents via a massive vector field which in the end will allow us to describe weak interactions with a renormalizable theory. For now we maintain the Fermi form and we write the effective lagrangian as

$$\mathcal{L} = \frac{G}{\sqrt{2}} J_{\mu}^{+}(x) J^{+\mu}(x) + \text{h.c.}$$

with

$$J_{\mu}^{+} = (\bar{\nu} e)_{\mu} + (\bar{p} n)_{\mu}$$

where, for instance,

$$(\bar{\nu}e)_\mu = \bar{u}(\nu)\gamma_\mu(1 - \gamma^5)u(e).$$

The superscript ‘+’ reminds us that the current is a charge raising current, corresponding to the transitions  $n \rightarrow p$  and  $e^- \rightarrow \nu$  in beta decay. The two currents are taken at the same space time point  $x$ .

The presence of the factor  $1 - \gamma^5$  in the current requires that all fermions participating in a weak process be left-handed and all antifermions be right-handed. For neutrino which are massless we expect neutrino to always have negative helicity and anti neutrino to have positive helicity.

This has been verified experimentally both for neutrinos in  $\beta$ -decay, which we call electron-neutrinos or  $\nu_e$  And for neutrinos from the decay  $\pi \rightarrow \mu\nu$ , the muon-neutrinos or  $\mu\nu$ . These experimental results have greatly contributed to establishing the “ $V - A$ ” interaction.

We consider now the purely leptonic weak processes.

## 6.5 Muon Decay

Before writing a matrix element and computing the muon decay, we must discuss more some neutrino properties. We have seen that there appears to be a conservation law of leptonic number, which accounts for the observed properties of weak processes. The experimental observation that the electron in muon decay is not monochromatic is in agreement with lepton number conservation requiring that two neutrinos be created in muon decay. Spin also requires three fermions in the final state, *i.e.* two neutrinos!

The introduction of an additive quantum requires that we distinguish particle and antiparticles. A consistent assignment of leptonic number to muons, electrons and neutrinos is

$$\begin{array}{llll} \text{Particles} & e^- & \mu^- & \nu & L=1 \\ \text{Antiparticles} & e^+ & \mu^+ & \bar{\nu} & L=-1 \end{array}$$

with the beta decay and muon decay reactions being

$$\begin{array}{l} n \rightarrow pe^-\bar{\nu} \\ \mu^- \rightarrow e^-\bar{\nu}\nu \end{array}$$

The absence of the transition  $\mu \rightarrow e\gamma$  is not however explained by any property of the weak interaction and we are lead to postulate that in nature there are two independently conserved lepton numbers:  $L_e$  and  $L_\mu$ . We also have to postulate two

kind of neutrinos:  $\nu_e$  and  $\nu_\mu$ . Then the assignment of  $L_e$  and  $L_\mu$  is:

Particle	$L_e$	$L_\mu$
$e^-$ , $\nu_e$	1	0
$e^+$ , $\bar{\nu}_e$	-1	0
$\mu^-$ , $\nu_\mu$	0	1
$\mu^+$ , $\bar{\nu}_\mu$	0	-1

and the reactions above become

$$n \rightarrow pe^- \bar{\nu}_e$$

$$\mu^- \rightarrow e^- \bar{\nu}_e \nu_\mu$$

The amplitude for muon decay is shown in fig. 6.8.

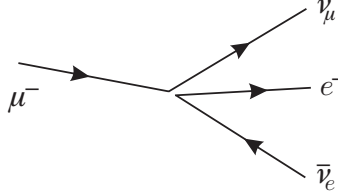


**Fig. 6.8.** Amplitude for muon decay. The gap between vertices reminds us that the 4-fermion interaction is the limit of a more complete theory.

From now on we will indicate the spinors with the particle symbol. The muon decay matrix element is:

$$\mathfrak{M} = \frac{G}{\sqrt{2}} \bar{\nu}_\mu \gamma^\alpha (1 - \gamma^5) \mu \bar{e} \gamma_\alpha (1 - \gamma^5) \nu_e$$

and summing over the spin orientations

$$\begin{aligned} \sum_{\text{spins}} |\mathfrak{M}|^2 &= 128G^2 (\mu \cdot \bar{\nu}_e) (e \cdot \nu_\mu) = 128G^2 (Pk_1)(pk_2) \\ &= 128G^2 P^\alpha p^\beta k_{1\alpha} k_{2\beta} \end{aligned}$$

where the term before the last defines the 4-momenta of the four particles. The decay rate, in the muon rest frame, is given by

$$\begin{aligned} d\Gamma &= \frac{1}{2} \frac{1}{2M_\mu} \sum_{\text{spins}} |\mathfrak{M}|^2 \frac{d^3p}{2E_e(2\pi)^3} \frac{d^3k_1}{2E_{\bar{\nu}_e}(2\pi)^3} \frac{d^3k_2}{2E_{\nu_\mu}(2\pi)^3} \\ &\quad \times (2\pi)^4 \delta^4(P - p - k_1 - k_2) \end{aligned}$$

The neutrinos are not (observable) observed, therefore we integrate over their momenta:

$$\begin{aligned} d\Gamma &= \frac{G^2}{4M_\mu} \frac{d^3p}{2E_e(2\pi)^3} \frac{(2\pi)^4}{2^2(2\pi)^6} P^\alpha p^\beta \\ &\quad \times \int k_{1\alpha} k_{2\beta} \frac{d^3k_1}{E_{\bar{\nu}_e}} \frac{d^3k_2}{E_{\nu_\mu}} \delta^4(q - k_1 - k_2). \end{aligned}$$

with  $q = P - p$  and, after integration over the  $\delta$ -function,  $q = k_1 + k_2$ . The integral is a function of  $q$  only and its most general form is:

$$\begin{aligned} I_{\alpha\beta} &= \int k_{1\alpha} k_{2\beta} \frac{d^3 k_1 d^3 k_2}{E_1 E_2} \delta^4(q - k_1 - k_2) \\ &= A(q^2 g_{\alpha\beta} + 2q_\alpha q_\beta) + B(q^2 g_{\alpha\beta} - 2q_\alpha q_\beta) \end{aligned}$$

where the last two terms are orthogonal to each other. Multiplying both sides by  $q^2 g^{\alpha\beta} - 2q^\alpha q^\beta$  gives:

$$\begin{aligned} B \times 4q^4 &= \int k_{1\alpha} k_{2\beta} (q^2 g^{\alpha\beta} - 2q^\alpha q^\beta) \dots \\ &= \int [q^2 (k_1 k_2) - 2(q k_1)(q k_2)] \dots = 0 \end{aligned}$$

(remember  $k_1^2 = k_2^2 = 0$  and  $q = k_1 + k_2$ ) *i.e.*  $B=0$ . Multiplying by  $q^2 g^{\alpha\beta} + 2q^\alpha q^\beta$  gives

$$\begin{aligned} A \times 12q^4 &= q^4 \int \frac{d^3 k_1}{E_1} \frac{d^3 k_2}{E_2} \delta^4(q - k_1 - k_2) \\ &= q^4 \int \frac{d^3 k_1}{E_1 E_2} \delta(E - E_1 - E_2) = \frac{4\pi}{2} q^4 \end{aligned}$$

where we have used  $q = (E, \mathbf{q})$  and computed the last integral in the system where  $\mathbf{q}=0$ , *i.e.*  $|\mathbf{k}_1| = |\mathbf{k}_2| = E_1 = E_2$  and  $dE = dE_1 + dE_2 = 2dk_1$ . Finally

$$I_{\alpha\beta} = \frac{1}{6} \pi (q^2 g_{\alpha\beta} + 2q_\alpha q_\beta)$$

from which

$$d\Gamma = \frac{G^2}{\pi^4 48 M_\mu} [(q^2 (Pp) + 2(Pq)(pq))] \frac{1}{E} \mathbf{p}^2 dp d\Omega$$

Neglecting the electron mass and introducing  $x = E/(2M_\mu)$ , the electron spectrum can be expressed as

$$d\Gamma = \frac{G^2 M_\mu^5}{96\pi^3} x^2 (3 - 2x) dx$$

and, integrating over the spectrum,

$$\Gamma = \frac{G^2 M_\mu^5}{192\pi^3}. \quad (6.4)$$

Accurate measurements of the muon lifetime allow determining the Fermi coupling constant  $G$ . One must however include radiative corrections. (6.4) then becomes:

$$\Gamma = \frac{G^2 M_\mu^5}{192\pi^3} \left(1 - \frac{\alpha}{2\pi} (\pi^2 - 25/4)\right)$$

From  $\tau_\mu = (2.19703 \pm 0.00004) \times 10^{-6}$  s,  $G = (1.16639 \pm 0.00001) \times 10^{-5}$  GeV<sup>-2</sup>. Given the experimental accuracy, we cannot forget the radiative corrections,  $\sim 4.2 \times 10^{-3}$ .

It is not necessary however to go to the next order. If we allow both V-A and V+A couplings, the muon decay spectrum is:

$$d\Gamma = 12\Gamma[(1-x) - \frac{2}{9}\rho(3-4x)]x^2 \quad (6.5)$$

where  $\rho = 0.75$  for pure V-A.

$$d\Gamma = \frac{G^2 M_\mu^5}{96\pi^3} x^2 (3-2x) dx$$

For pure V+A interaction,  $\rho = 0$  and

$$d\Gamma = \frac{G^2 M_\mu^5}{96\pi^3} 6x^2 (1-x) dx$$

whose integral is equal to (6.5). Experimentally,  $\rho = 0.7518 \pm 0.0026$ , '63-64. The two spectra, with correct relative normalization, are shown in fig. 6.9.

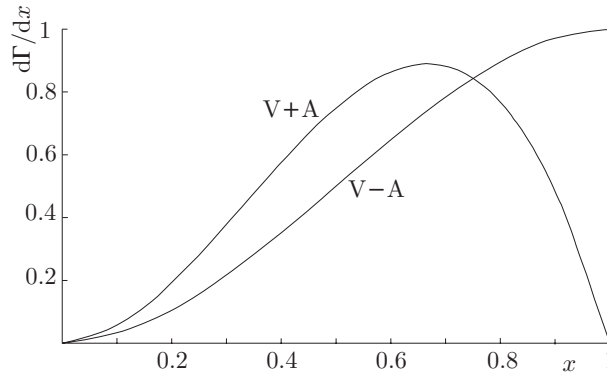


**Fig. 6.9.** Electron spectrum in  $\mu$ -decay for pure V-A and V+A coupling.

There is a strong correlation between the direction of emission of the electron and the spin of the muon. The favoured,  $x \sim 1$ , and unfavoured,  $0 < x \ll 1$ , kinematical configurations are shown in fig. 6.10 for the V-A coupling.

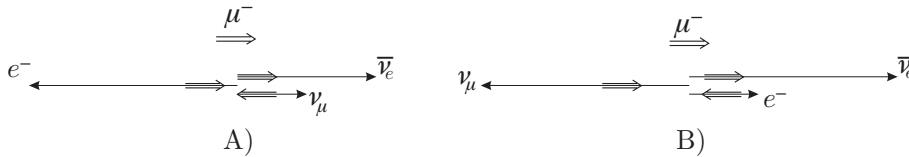


**Fig. 6.10.** Muon spin-electron direction correlation. A. favoured configuration,  $p_e = M_\mu/2$ . B.  $p_e \ll M_\mu/2$ . The '⇒' arrows indicate spin orientations

For  $x = 1$ , conservation of angular momentum requires that the electron in  $\mu^-$  decay be emitted in the direction opposite to the muon spin, while for small  $x$  the electron is along the spin. We thus expect the electron direction in average to tell us the muon spin orientation. Calculations of the electron angular distribution

integrated over  $x$  gives:

$$\frac{d\Gamma}{\Gamma} = \frac{1}{2} \left(1 - \frac{1}{3} \cos \theta\right) d \cos \theta \quad (6.6)$$

where  $\theta$  is the angle between the electron momentum and the muon spin, both in the CM of the muon. This was first observed in 1957 by Garwin and Lederman. The correlation becomes stronger if a cut  $x > x_{\min}$  is experimentally imposed. Note that (6.6) implies that  $P$  is violated, since we observe that the expectation value of a pseudoscalar is non zero,  $\langle \sigma \cdot p \rangle = \langle \cos \theta \rangle \neq 0$ . The correlation also violates  $C$  since it changes sign for the charge conjugated process  $\mu^+ \rightarrow e^+ \bar{\nu}_\mu \nu_e$ .

The results above, apart from being a confirmation of the structure of the weak coupling for muon decay, have great practical importance in determining the muon ‘‘anomaly’’  $a_\mu = (g_\mu - 2)/2$  by measuring the difference between cyclotron frequency and spin precession frequency in a magnetic field which is proportional to  $a$ . The decay electron provides a measurement of the spin direction in time while muons are made to circulate in a storage ring. Another application of this effect is the so called  $\mu$ MR (muon magnetic resonance), where the precession frequency allows to probe crystalline fields, used among other things to understand the structure of high  $T_c$  superconducting materials.

## 6.6 Semileptonic weak decays

We have somewhat literally taken the weak interaction form of eq. (6.3) and written in a pure  $V-A$  form for the muon decay. Agreement with experiment ultimately fully justifies doing so. This is not the case for nuclear  $\beta$ -decay, typical being neutron decay as well as many other processes:  $\pi^\pm \rightarrow \pi^0 e^\pm \nu(\bar{\nu})$ ,  $\pi \rightarrow \ell \nu$ ,  $\Lambda \rightarrow p e^- \bar{\nu}$ ,  $K \rightarrow \mu \nu$ ,  $K \rightarrow \pi \ell \nu$  and so on. For neutron decay, for instance, we find that the amplitudes has the form

$$\frac{G}{\sqrt{2}} \bar{u}_p \gamma_\mu (1 - \eta \gamma^5) u_n \bar{u}_e \gamma_\mu (1 - \gamma^5) u_\nu$$

with  $\eta = 1.253 \pm 0.007$ .

## 6.7 Quarks and the weak current

Since the lepton term does not have complications we propose that for quarks, the weak interaction retains the simple lepton form. For  $u$  and  $d$  quarks we assume:

$$J_\mu^+(u, d) = \bar{u}_u \gamma_\mu (1 - \gamma^5) u_d.$$

The complications arise when we need the matrix element

$$\langle p | J_\mu^+(u, d) | n \rangle$$

although apparently nothing happens for the vector part of the current. We will in the following use the notations:

$$J_\alpha(\text{leptons, hadrons}) = L_\alpha + H_\alpha$$

$$\mathfrak{M} = \frac{G}{\sqrt{2}} L_\alpha H^\alpha$$

since  $\mu$  is used for muon.

$$L_\alpha = \langle \bar{\ell} | O_\alpha | \nu_\ell \rangle e^{-ikx}$$

$$H_\alpha = \langle f | O'_\alpha | i \rangle e^{-iqx}$$

$$k = p_\ell - p_\nu$$

$$q = p_f - p_i$$

$$L_\alpha = \bar{u}(p_\ell) \gamma_\alpha (1 - \gamma_5) u(p_\nu)$$

$$H_\alpha = V_\alpha + A_\alpha = u(p_f) \gamma_\alpha (G_V - G_A \gamma_5) u(p_i)$$

with  $G_V$  and  $G_A$  of order 1 but not necessarily equal to 1.

We now introduce the isospinor

$$q = \begin{pmatrix} u \\ d \end{pmatrix}, \quad \bar{q} = \begin{pmatrix} -d \\ u \end{pmatrix}$$

and recall the pion isospin wave functions:

$$\pi^+ = u\bar{d}, \quad \pi^0 = \frac{u\bar{u} - d\bar{d}}{\sqrt{2}}, \quad \pi^- = \bar{u}d$$

The  $ud$  current is an isovector, since  $1/2 \otimes 1/2 = 0 \oplus 1$  and clearly the third component is non-zero. The electromagnetic current, which is a Lorentz vector has an isoscalar and an isovector part as we derive in the following. Using the isospinor  $q$  we can write neutral and charged currents as

$$\begin{aligned} \bar{u} \gamma_\alpha d &= \bar{q} \gamma_\alpha \tau^+ q \\ \bar{d} \gamma_\alpha u &= \bar{q} \gamma_\alpha \tau^- q \\ \frac{\bar{u} \gamma_\alpha u - \bar{d} \gamma_\alpha d}{\sqrt{2}} &= \bar{q} \gamma_\alpha \tau_3 q \end{aligned}$$

or equivalently as

$$V_\alpha(u, d) = \bar{q} \gamma_\alpha \vec{\tau} q.$$

$\tau_{1,2,3}$  are the Pauli matrices and

$$\tau_{\pm} = \frac{\tau_1 \pm i\tau_2}{2}$$

The electromagnetic interaction between quarks and the electromagnetic field which defines the electromagnetic quark current is given by:

$$eA_{\alpha}(\frac{2}{3}\bar{u}\gamma_{\alpha}u - \frac{1}{3}\bar{d}\gamma_{\alpha}d) = eA_{\alpha}(\frac{1}{2}\bar{q}\gamma_{\alpha}\tau_3q + \frac{1}{6}\bar{q}\gamma_{\alpha}q).$$

The isoscalar part of the electric current contains more terms due to the other quarks. If isospin invariance holds, the matrix elements of the em and weak currents must be the same functions of  $q^2$ . In particular the current  $\bar{u}\gamma_{\alpha}d$  must be conserved, or transverse, just as the em current:

$$\partial^{\alpha}\bar{u}\gamma_{\alpha}d = 0 \quad \text{or} \quad q^{\alpha}\bar{u}\gamma_{\alpha}d = 0$$

This conservation of the vector part of the weak hadronic current is usually referred to as CVC. CVC requires that the vector coupling constant remains unmodified by hadronic complications.<sup>7</sup> No similar results applies to the axial vector current. The latter turns out to be ‘partially’ conserved, this being called PCAC.  $\partial^{\alpha}\bar{u}\gamma_{\alpha}\gamma_5d$  is small, more precisely  $\partial^{\alpha}\bar{u}\gamma_{\alpha}\gamma_5d \sim m_{\pi}$ . The pion mass can in the appropriate context be considered small.

## 6.8 Pion Decay

Charged pion decays to  $\ell\nu$  and  $\pi^0\ell\nu$ , where  $\ell$  stands for  $e$  or  $\mu$  are due to the interaction

$$\frac{G}{\sqrt{2}} L_{\alpha}H^{\alpha}$$

with

$$H_{\alpha} = V_{\alpha} + A_{\alpha}$$

### 6.8.1 Pion decay to lepton plus neutrino

For  $\pi^+ \rightarrow \ell^+ + \nu$ , the matrix element of  $V_{\alpha}$  equals 0. For the axial part we set  $\langle 0 | A_{\alpha} | \pi \rangle = f_{\pi} \phi_{\pi} p_{\alpha}$  where  $f_{\pi}$  is an arbitrary constant with dimensions of an energy and  $p_{\alpha}$  is the pion 4-momentum.  $f_{\pi}$  is infact a form factor, function of the 4-momentum transfer squared  $q^2$  between initial and final state, in this case just the pion mass squared.

<sup>7</sup>This strictly applies to the term  $\bar{u}\gamma_{\alpha}d$ . In the electromagnetic current of proton etc, there are two ff,  $f_1$  and  $f_2$ . For  $f_1(q^2)$  the relation  $f_1(q^2 = 0) = 1$  holds. Likewise  $G_V(n \rightarrow p) = 1$  at  $q^2 = 0$ .

From

$$p_\pi = p_\ell + p_\nu$$

and  $(\not{p} - m)u=0$  we have

$$\mathfrak{M} = \frac{G}{\sqrt{2}} f_\pi m_\ell \phi_\pi \bar{u}_\nu (1 + \gamma_5) u_\ell.$$

The proportionality of  $\mathfrak{M}$  to  $m_\ell$  is just a consequence of angular momentum conservation which forbids the decay of a spin zero pion into a negative helicity neutrino and a positive helicity anti electron moving in opposite directions.

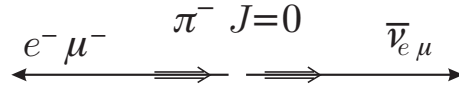


**Fig. 6.11.** Angular momenta in  $\pi \rightarrow \ell\nu$  decays.

From the above

$$\sum_{\text{spins}} |\mathfrak{M}|^2 = \frac{G^2}{2} f_\pi^2 m_\ell^2 8(p_\nu p_\ell) = 4G^2 f_\pi^2 m_\ell^2 m_\pi E_\nu$$

and using

$$\Gamma = \frac{1}{2m} \sum_{\text{spins}} |\mathfrak{M}|^2 \Phi_p$$

with  $\Phi_p$  the phase space volume equal to  $E_\nu/(4\pi m_\pi)$ , we finally find

$$\Gamma = \frac{G^2 f_\pi^2 m_\ell^2 m_\pi}{8\pi} \left(1 - \frac{m_\ell^2}{m_\pi^2}\right)^2.$$

The ratio between muon and electron decays does not depend on  $f_\pi$  and is given by:

$$\frac{\Gamma(\pi \rightarrow e\nu)}{\Gamma(\pi \rightarrow \mu\nu)} = \left(\frac{m_e}{m_\mu}\right)^2 \left(\frac{1 - m_e^2/m_\pi^2}{1 - m_\mu^2/m_\pi^2}\right)^2 \cong 1.3 \times 10^{-4},$$

in agreement with observation.

From the measured pion lifetime and the above results for the width, ignoring decay to  $e\nu$  and  $\pi^0 e\nu$  which contribute very little to the total width, one finds  $f_\pi=130$  MeV.

### 6.8.2 $\pi^\pm$ decay to $\pi^0$ , electron and neutrino

For the decays  $\pi^\pm \rightarrow \pi^0 e^\pm \nu(\bar{\nu})$ , the axial part of the hadronic current gives no contribution. The vector weak current transforms as an isovector and therefore must have the same form as the electromagnetic current discussed in section 4.4, in particular must be transverse. In the limit of exact isospin invariance, the charged

and neutral pion masses are identical and the general form  $J_\alpha = a(p_i - p_f) + b(p_i + p_f)$  reduces to  $(p_i + p_f)$  requiring that  $\partial_\alpha J^\alpha = 0$ .

The decay amplitude is given by:

$$\mathfrak{M} = \frac{G}{\sqrt{2}} G \phi_i \phi_f \sqrt{2} p^\alpha \bar{\nu} \gamma_\alpha (1 - \gamma_5) e$$

with  $p = p_i + p_f$ , from which

$$\Gamma = \frac{G^2 \Delta^4}{30\pi^3} \left( 1 - \frac{5m_e^2}{\Delta^2} - \frac{3\Delta}{2m_\pi} \right)$$

The factor  $\sqrt{2}$  in the matrix element comes from

$$\langle \pi^0 | V_\alpha^- | \pi^+ \rangle = \langle \pi^0 | \bar{d} \gamma_\alpha u | \pi^+ \rangle = \langle \pi^0 | T^- | \pi^+ \rangle = \sqrt{2}$$

where  $u$  and  $d$  are the quark fields and  $T^-$  is the isospin lowering operator.

An alternate way, but the same of course, is by using the pion quark wave functions:

$$|\pi^+\rangle = |u\bar{d}\rangle; \quad |\pi^0\rangle = |(d\bar{d} - u\bar{u})/\sqrt{2}\rangle; \quad |\pi^-\rangle = |\bar{u}d\rangle$$

Then  $\langle \pi^0 | u^\dagger d | \pi^+ \rangle = \langle (d\bar{d} - u\bar{u})/\sqrt{2} | -u\bar{u} + d\bar{d} \rangle = 2/\sqrt{2} = \sqrt{2}$ . Remember that  $I_- \bar{u} = -\bar{d}$  but  $I_- u = d$ , etc.

Matrix element for superallowed Fermi  $0^+ \rightarrow 0^+$  transitions between members of an isospin triplet are the same as for pion decay, *i.e.*  $\sqrt{2}$ . For neutron  $\beta$ -decay the matrix element of the vector current is 1, computed for instance from  $\sqrt{T(T+1) - T_3(T_3+1)}$ , with  $T_3 = -1/2$ .

## 6.9 Inverse muon decay.

The process  $\nu_e e \rightarrow \nu_\mu \mu$  can be observed experimentally. However of the two processes

$$\begin{aligned} \nu_e + e^- &\rightarrow \nu_\mu + \mu^- \\ \bar{\nu}_e + e^- &\rightarrow \bar{\nu}_\mu + \mu^- \end{aligned}$$

the first is not allowed by the weak interaction. If instead the leptons in the final state are the same as in the initial state, both reactions are possible, mediated by 'exchange' and 'annihilation' amplitudes as indicated in fig. 6.12.

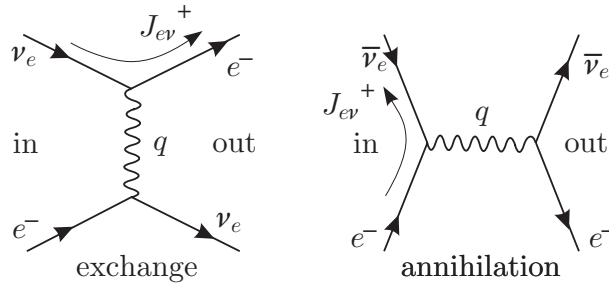


**Fig. 6.12.** Amplitudes for  $\nu_e e \rightarrow \nu_e e$  scattering. The + superscript indicates that the current is a charge raising operator.

The diagram on the right applies also to production of  $\mu^- \bar{\nu}_\mu$ . The respective cross sections are trivial to calculate. Neglecting all masses, in the center of mass we find:

$$\frac{d\sigma}{d\Omega} \Big|_{\nu e^-} = \frac{G^2 s}{4\pi^2}$$

$$\frac{d\sigma}{d\Omega} \Big|_{\bar{\nu} e^-} = \frac{G^2 s}{16\pi^2} (1 + \cos \theta)^2,$$

where  $\theta$  is the angle between incident and scattered electron. The different angular distribution in the two cases can be understood in terms of helicities and angular momentum conservation which results in a suppression of the scattering cross section in the backward direction for incident antineutrinos.

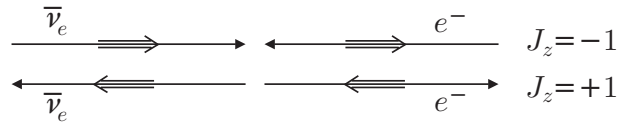


**Fig. 6.13.** Backward  $\bar{\nu}_e e$  scattering is forbidden by angular momentum conservation.

The total cross section is given by:

$$\sigma(\nu e^-) = \frac{G^2 s}{\pi}$$

$$\sigma(\bar{\nu} e^-) = \frac{G^2 s}{3\pi}.$$

The second result in both cases is valid also for  $\bar{\nu}_e e^- \rightarrow \bar{\nu}_\mu \mu^-$ . The results can also be rewritten for  $\nu_\mu e$  processes.<sup>8</sup>

<sup>8</sup>Why only left-handed  $\nu$ 's? Because they are the only ones that couple to something. But than do they still exist, right-handed  $\nu$ 's? Perhaps. Makes no difference!!

## 7 STRANGENESS

### 7.1 Discovery

1940, ~50 years ago. In few thousand pictures, ~1000  $\pi$ 's, observe production of particles which decay in few cm.  $c=30$  cm/ns, 1 cm at  $\gamma\sim 3$  corresponds to  $\tau\sim 10^{-10}$  s.  $\tau(\text{V-particles})\sim 10^{-10}$  to  $10^{-8}$  s. *i.e.* typical of weak interactions.

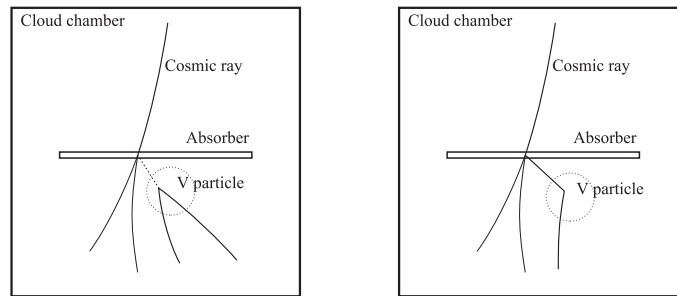


**Fig. 7.1.** Schematic drawings of production and decay of V particles.

Production:

$$\begin{aligned}
 N_{\text{events}} &= N_{\text{in}} \times \sigma \times \frac{\text{nucleons}}{\text{cm}^2} \\
 &= N_{\text{in}} \times \sigma \times \frac{\text{g}}{\text{cm}^2} \times \frac{6 \times 10^{23}}{\text{g}} \\
 &= 10^3 \times 10^{-26} \times 1 \times 6 \times 10^{23} \\
 &= 6
 \end{aligned}$$

or few events in 1000 pictures with  $\sigma \sim \sigma_{\text{strong}}$ . Therefore production time  $\sim 10^{-23}$ , decay time  $\sim 10^{-10}$ . Decay is  $\sim 10^{13}$  times slower than production.

Decays of V-particles

$$\Lambda^0 \rightarrow \pi^- p$$

$$\Lambda^0 \rightarrow \pi^0 n$$

$$\Sigma^\pm \rightarrow \pi^\pm n$$

$$K^\pm, K^0 \rightarrow 2\pi$$

$$K^\pm, K^0 \rightarrow \pi \ell \nu$$

...

### 7.2 A New Quantum Number and Selection Rule

Introduce  $S$ , an additive QN – *i.e.* a charge – a multiplicative QN was tried first and rejected – with appropriate assignments and selection rule: SI conserve  $S$ , if  $\Delta S \neq 0$ ,

WI are only process.  $S$ , for strangeness is carried by the new (strange) particles and is zero for pions, nucleons *etc.*

$S$  is assigned as follows:

$$\begin{aligned} S|\Lambda, \Sigma \dots\rangle &= -1|\Lambda, \Sigma \dots\rangle \\ S|K^+, K^0\rangle &= +1|K^+, K^0\rangle \\ S|K^-, \bar{K}^0\rangle &= -1|K^+, K^0\rangle \end{aligned}$$

than all observed strong production reactions satisfy  $\Delta S=0$ .

Associate production:

$$\begin{aligned} \pi^- p &\rightarrow \Lambda^0 K^0 \\ \pi^- p &\rightarrow \Sigma^- K^+ \\ \pi N &\rightarrow K^+ K^- N \\ &\dots \end{aligned}$$

Reactions with  $|\Delta S| \neq 0$  proceed via the WI.

### 7.3 Charge and $I_3$

I		$I_3$	B	Q
1/2	p	+1/2	1	+1
	n	-1/2	1	0
1	$\pi^+$	+1	0	+1
1	$\pi^0$	0	0	0
1	$\pi^-$	-1	0	-1

from which clearly the charge is linear in  $I_3$ , or  $Q = I_3 + \text{const.}$  where the constant is different for baryons and mesons, and clearly can be taken as  $B/2$ .

$$Q = I_3 + \frac{B}{2}.$$

This relation is valid for all known non-strange baryon and mesons. For instance, for  $I=3/2$ ,  $B=1$  the four states should have charges:  $+2e$ ,  $+e$ ,  $0$  and  $-e$  as observed for the  $\Delta \pi N$  resonance. The relation also implies that non-strange baryons occur in half integer iso-spin multiplets. Note also that  $\langle Q \rangle$  is  $1/2$  for baryons and zero for mesons. The situation is reversed for strange particles. First we must examine whether is possible to assign a value of  $B$  to them. Since all strange particles heavier than the proton, called hyperons, decay ultimately to a proton, we can assign to

them  $B=1$  and take  $B$  as conserved. Then we have:

$$\langle Q \rangle = \begin{cases} 0 & \text{for hyperons} \\ \pm 1/2 & \text{for mesons} \end{cases}$$

The relation above between charge and  $I_3$  can be generalized to

$$Q = I_3 + \frac{B + S}{2} = I_3 + \frac{Y}{2}.$$

This is the Gell-Mann–Nishijima formula and the definition of the quantum number  $Y$ , the hypercharge. Now we have to make some observations. The existence of  $\Sigma^\pm$ , puts the  $\Sigma$ 's in an iso-triplet and predicts the existence of a  $\Sigma^0$ , discovered soon after the prediction. The  $K$ -mesons are more complicated. They must belong to two iso- doublets:

$$K = \begin{pmatrix} K^+ \\ K^0 \end{pmatrix} \quad \bar{K} = \begin{pmatrix} K^- \\ \bar{K}^0 \end{pmatrix}$$

and for the first time we encounter a neutral particles which is not self-charge conjugate, since under  $C$ ,  $S$  changes sign.

#### 7.4 Selection rules for hyperon decays

In  $\Lambda^0$  decay the initial I-spin is 0 and the final states  $\pi^- p$  and  $\pi^0 n$  have  $I_3=-1/2$ . I-spin is not conserved in weak interaction as we already know from  $\beta$ -decay. However the weak current has a precise I-spin structure (*e. g.*  $I_+$ ) in that case. In  $\Lambda^0$  decay, from the observation above, the weak interaction can transform as an  $I=1/2, 3/2$  state. If the weak interaction induces only  $\Delta I=1/2$  transitions than the  $\pi N$  final state has  $I, I_3=1/2, -1/2$  and we can write:

$$|\pi, N, I = 1/2, I_3 = -1/2\rangle = \sqrt{\frac{2}{3}}|\pi^- p\rangle - \sqrt{\frac{1}{3}}|\pi^0 n\rangle$$

leading to  $\Gamma(\pi^- p)/\Gamma(\pi^0 n)=2$ . For  $\Delta I=3/2$  the  $\pi N$  state is

$$|\pi, N, I = 1/2, I_3 = -1/2\rangle = \sqrt{\frac{1}{3}}|\pi^- p\rangle + \sqrt{\frac{2}{3}}|\pi^0 n\rangle$$

or  $\Gamma(\pi^- p)/\Gamma(\pi^0 n)=1/2$ . Experimentally,  $\Gamma(\pi^- p)/\Gamma(\pi^0 n)=1.85$ , after correcting for the small phase space difference.  $\Delta I=1/2$  appears to dominate although some  $\Delta I=3/2$  amplitude is clearly necessary. Before examining other cases we discuss briefly parity violation in  $\Lambda$  decay. If the spin of the  $\Lambda$  is  $1/2$ , than the  $\pi N$  final state can be in an  $L=0, 1$  state and the decay amplitude can be written as:

$$A(\Lambda \rightarrow \pi^- p) = S + P\vec{\sigma} \cdot \hat{p}$$

where  $S$  and  $P$  are the  $S$ - and  $P$ -wave amplitudes and  $\sigma$  the Pauli spin operator, acting on the proton spin in its CM. All this from  $P(\pi p) = P(\pi)P(p)(-1)^L$ . Then

$$d\Gamma(\theta) \propto (|S|^2 + |P|^2 + 2\Re SP^* \cos \theta) d\cos \theta \propto (1 + \alpha \cos \theta) d\cos \theta$$

with  $\alpha = 2\Re SP^*/(|S|^2 + |P|^2)$ . Experimentally  $\alpha=0.64$  for  $\pi^-p$  and  $\alpha=0.65$  for  $\pi^0n$ . The maximum value of  $\alpha$  is 1. Still 0.65 is a rather strong  $P$  violation.

## 7.5 Measuring the spin of the $\Lambda^0$

Consider the reaction  $\pi^-p \rightarrow \Lambda^0 + K^0$  with pions interacting in an unpolarized proton target at rest. In the lab, we chose the quantization axis  $z$  along the incident pion. Then  $L_z=0$  and  $J_z = s_z(p) = \pm 1/2$ , where the two. We choose only  $\Lambda$ 's produced forward. Then again  $L_z=0$  and the  $\Lambda$  has  $J, J_z=J, M=s_\Lambda, 1/2$ . Finally we consider the  $\pi^-p$  state from decay. From conservation of angular momentum it also has  $J, M=s_\Lambda, 1/2$ . The possible values of  $L$  for the two particles are given by  $L = s_\Lambda \pm 1/2$ , the last 1/2 coming from the proton spin. Both values are allowed because parity is not conserved in the decay. We explicitly derive the angular distribution of the decay proton for  $s_\Lambda=1/2$  and give the result for other cases.

For  $L=1$  or  $P$ -waves and  $M = 1/2$ , the  $\pi p$  wave function is:

$$\begin{aligned} \psi_P &= \sqrt{\frac{2}{3}} Y_1^{+1} \begin{pmatrix} 0 \\ 1 \end{pmatrix} - \sqrt{\frac{1}{3}} Y_1^0 \begin{pmatrix} 1 \\ 0 \end{pmatrix} \\ &= -\sqrt{\frac{2}{3}} \sqrt{\frac{3}{8\pi}} \sin \theta \begin{pmatrix} 0 \\ 1 \end{pmatrix} - \sqrt{\frac{1}{3}} \sqrt{\frac{3}{4\pi}} \cos \theta \begin{pmatrix} 1 \\ 0 \end{pmatrix} \\ &= \frac{1}{\sqrt{4\pi}} \left( -\sin \theta \begin{pmatrix} 0 \\ 1 \end{pmatrix} - \cos \theta \begin{pmatrix} 1 \\ 0 \end{pmatrix} \right) \end{aligned}$$

where we have dropped the  $\phi$  dependence in the spherical harmonics  $Y_l^m$  since the initial state is unpolarized and the azimuthal dependence has to drop out in the end. The Pauli spinors are the spin wave functions of the proton. For  $S$ -waves we have:

$$\psi_S = \frac{1}{\sqrt{4\pi}} \begin{pmatrix} 1 \\ 0 \end{pmatrix}.$$

The amplitude for decay to  $\pi p$  is:

$$A_{\pi-p} = A_P + A_S = P\psi_P + S\psi_S$$

where  $S$  and  $P$  come from the dynamics of the decay interaction and are in general complex. Finally:

$$f_+(\theta) = |A_P + A_S|^2 = \frac{1}{4\pi} (|P|^2 + |S|^2 - 2\Re SP^* \cos \theta)$$

For  $M = s_z(p) = -1/2$  the same calculation gives

$$\psi_P = \frac{1}{\sqrt{4\pi}} \left( \cos \theta \begin{pmatrix} 0 \\ 1 \end{pmatrix} - \sin \theta \begin{pmatrix} 1 \\ 0 \end{pmatrix} \right)$$

and therefore

$$f_-(\theta) = \frac{1}{4\pi} (|P|^2 + |S|^2 + 2\Re SP^* \cos \theta).$$

The complete angular distribution is given just by  $f_+ + f_-$ , since the initial state is a statistical mixture of spin up and spin down and the interference term therefore vanishes. For  $s_\Lambda=1/2$  the decay is therefore isotropic. For higher  $\Lambda$  spins the same calculation can be repeated. The results are:

$\Lambda$ spin	Angular distribution
1/2	1
3/2	$1 + 3 \cos^2 \theta$
5/2	$1 - 2 \cos^2 \theta + 5 \cos^4 \theta$

## 7.6 $\Sigma$ decays

We must study three processes:

$$\begin{aligned} \Sigma^- &\rightarrow \pi^- n, & \text{amplitude: } A^- \\ \Sigma^+ &\rightarrow \pi^+ n, & \text{amplitude: } A^+ \\ \Sigma^+ &\rightarrow \pi^0 p, & \text{amplitude: } A^0 \end{aligned}$$

If the interaction transforms as an isospinor, *i.e.*  $\Delta I = 1/2$ , by the same methods used for the  $\Lambda$  case we find the following relation:

$$A^+ - \sqrt{2}A^0 = A^-$$

which applies both to  $S$ -waves and  $P$ -waves. The  $P$  violating parameter  $\alpha$  is proportional to  $\Re SP^*$  where  $S$  and  $P$  are required to be real by  $T$ -invariance. Final state interaction however introduces factors of  $e^{i\phi(\pi N)}$ .  $\phi(\pi N)$  are the  $\pi N$  scattering phases for  $i=1/2$  and  $S$ - or  $P$ -waves at the energy corresponding to the  $\Sigma$  mass. These phases are quite small and can be neglected in first approximation.  $S$ - and  $P$ -waves are however orthogonal and the  $A$ s can be drawn in an  $x, y$  plane, where one axis is the  $P(S)$ -wave component and the other the  $S(P)$ -wave part. Experimentally  $\alpha_- \sim \alpha_+ \sim 0$ , while  $\alpha_0 \sim 1$ . We can thus draw  $A_+(A_-)$  along the  $x(y)$  axes while  $A_0$  lies at  $45^\circ$  in the plane, see fig. 7.2.

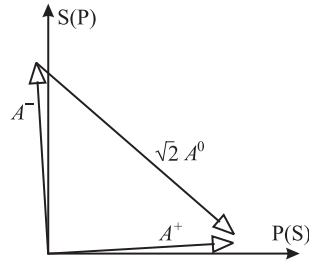


**Fig. 7.2.** The amplitudes  $A^+$ ,  $\sqrt{2}A^0$  and  $A^-$  in  $\Sigma \rightarrow \pi N$  decays.

Finally the very close equality of  $\Gamma^- = \Gamma(\Sigma^- \rightarrow \pi^- n)$  with  $\Gamma^+$  and  $\Gamma^0$  ensures that the triangle in the  $S, P$  plane closes as required by the relation between amplitudes obtained using the  $\Delta I=1/2$  assumption. A more complete analysis shows clearly that there is very little room left for  $\Delta I=3/2$ .

## 7.7 Computing the amplitudes

We want to compute the decay amplitude for a process due to an interaction transforming as an iso-tensor corresponding to some value of the isospin  $I_H$ . We need that part of the matrix element that contains the iso-spin QN's. Consider the case in which the final state is two particles labeled 1 and 2, the initial state is one particle of i-spin  $I$  and the interaction has i-spin  $I_H$ , *i.e.*:

$$\langle I^{(1)}, I^{(2)}, I_3^{(1)}, I_3^{(2)} | T | I, I_3 \rangle$$

Formally this means to find all isoscalar in the product  $(I^{(1)} \otimes I^{(2)}) \otimes I_H \otimes I$  and express the results in terms of appropriate reduced matrix elements in the Wigner-Eckart theorem sense. That is we consider the interaction itself as a sort of object of i-spin  $I_H$  and proceed requiring i-spin invariance. For the case  $\Sigma \rightarrow \pi N$ ,  $I^{(1)}=1$ ,  $I^{(2)}=2$  and  $I(\pi N)=1/2, 3/2$ . Similarly,  $I_H \otimes I$  also contains  $I=1/2, 3/2$ , in all cases the  $I_3$  values being the appropriate ones for the three possible final state. There are 2 scalars in the total product or two reduced matrix elements, connecting  $I=3/2$  to  $3/2$  and  $1/2$  to  $1/2$ , which we call  $A_3$  and  $A_1$ . Expressing  $A^+$ ,  $A^0$  and  $A^-$  in terms of  $A_3$  and  $A_1$  is a matter of Clebsch-Gordan coefficients which we do.

$$\begin{aligned} |\pi^- n\rangle &= |3/2, 3/2\rangle \\ |\pi^+ n\rangle &= \sqrt{1/3} |3/2, 1/2\rangle + \sqrt{2/3} |1/2, 1/2\rangle \\ |\pi^0 p\rangle &= \sqrt{2/3} |3/2, 1/2\rangle - \sqrt{1/3} |1/2, 1/2\rangle \end{aligned}$$

Note in the decomposition of the  $\Sigma \otimes I_H$  we get exactly the same answer as for the first two lines, since we always have a  $\Sigma^+$  in the initial state. We therefore trivially

read out the result:

$$\begin{aligned} A^- &= A_3 \\ A^+ &= 1/3(A_3 + 2A_1) \\ A^0 &= 1/3(\sqrt{2}A_3 - \sqrt{2}A_1) \end{aligned}$$

Multiply the third line by  $\sqrt{2}$  and add:

$$A^+ + \sqrt{2}A^0 = A_3 \equiv A_3$$

This relation is not quite the same as the one announced, in fact it is equivalent. We have used the more common sign convention in use today for the C-G coefficients. The case for  $\Delta I = 3/2$  reduces to find all scalars in the product  $(I = 1/2, 3/2) \otimes (I = 1/2, 3/2, 5/2)$ . There are two, corresponding to the reduced matrix element  $B_1$  and  $B_3$ .

## 7.8 $K$ decays

The situation becomes strikingly clear for the two pion decays of kaons. Consider:

$$K^{+,0} \rightarrow \pi\pi.$$

The initial state has  $I=1/2$ ,  $I_3=\pm 1/2$ . Also the spin of the  $K$  is zero, therefore  $L(2\pi)=0$ . The two pion state must be totally symmetric which means  $I_{2\pi}=0$  or 2. For  $K^0 \rightarrow \pi^+\pi^-$  or  $\pi^0\pi^0$ ,  $I_3(2\pi)=0$ , thus if  $\Delta I=1/2$  holds  $I(2\pi)=0$  and  $\text{BR}(\pi^+\pi^-)=2 \times \text{BR}(\pi^0\pi^0)$  in good, not perfect, agreement with observation. For  $\pi^+\pi^0$ ,  $I_3$  is 1, therefore  $I(2\pi)=2$  and the decay is not allowed for  $\Delta I=1/2$  and it can only proceed by  $\Delta I=3/2$ . Experimentally  $\Gamma(K^0 \rightarrow 2\pi)=1.1 \times 10^{10}$  and  $\Gamma(K^+ \rightarrow 2\pi)=1.6 \times 10^7 \text{ s}^{-1}$ . Therefore  $\Gamma^0/\Gamma^+=655$  and  $A_{3/2}/A_{1/2} = 1/\sqrt{655} = 0.04$  which is a clear indication of the suppression of  $\Delta I=3/2$  transitions.

## 8 The Weak Interaction II. $CP$

### 8.1 Introduction

The origin of  $CP$  violation, to my mind, is one of the two most important questions to be understood in particle physics (the other one being the origin of mass). In the meantime we are finally getting proof - after 51 years of hard work - that  $\mathcal{C}\mathcal{P}$  belongs to the weak interaction with 6 quarks and a unitary mixing matrix. Last June 1999, “kaon physicists” had a celebratory get together in Chicago. Many of the comments in these lectures reflect the communal reassessments and cogitations from that workshop. It is clear that a complete experimental and theoretical *albeit* phenomenological solution of the  $CP$  violation problem will affect in a most profound way the fabric of particle physics.

### 8.2 Historical background

It is of interest, at this junction, to sketch with broad strokes this evolution. With hindsight, one is impressed by how the  $K$  mesons are responsible for many of the ideas which today we take for granted.

1. Strangeness which led to quarks and the *flavor* concept.
2. The  $\tau$ - $\theta$  puzzle led to the discovery of parity violation.
3. The  $\Delta I = 1/2$  rule in non leptonic decays, approximately valid in kaon and all strange particle decays, still not quite understood.
4. The  $\Delta S = \Delta Q$  rule in semileptonic decays, fundamental to quark mixing.
5. Flavor changing neutral current suppression which led to 4 quark mixing - GIM mechanism, charm.
6.  $CP$  violation, which requires 6 quarks - KM, beauty and top.

### 8.3 $K$ mesons and strangeness

$K$  mesons were possibly discovered in 1944 in cosmic radiation<sup>(5)</sup> and their decays were first observed in 1947<sup>(6)</sup> A pair of two old cloud chamber pictures of their decay is on the website

[http://hepweb.rl.ac.uk/ppUKpics/pr\\_971217.html](http://hepweb.rl.ac.uk/ppUKpics/pr_971217.html)

demonstrating that they come both in neutral and charged versions. The two pictures are shown in fig. 1.

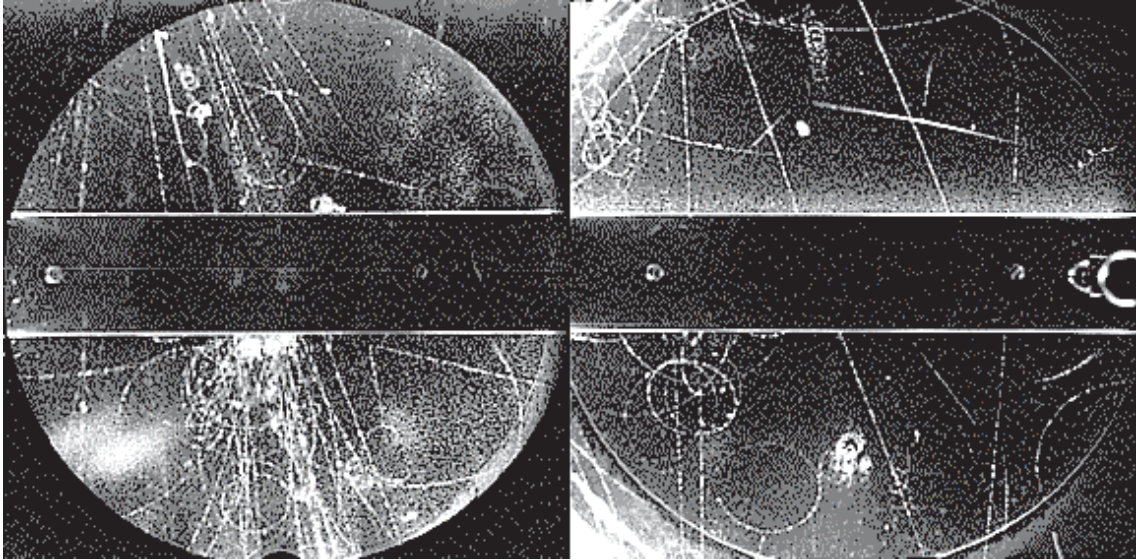


**Fig. 8.1.** *K* discovery

On December 1947 Rochester and Butler (Nature **106**, 885 (1947)) published Wilson chamber pictures showing evidence for what we now call  $K^0 \rightarrow \pi^+ \pi^-$  and  $K^+ \rightarrow \pi^+ \pi^0$ .

### 8.3.1 The Strange Problem

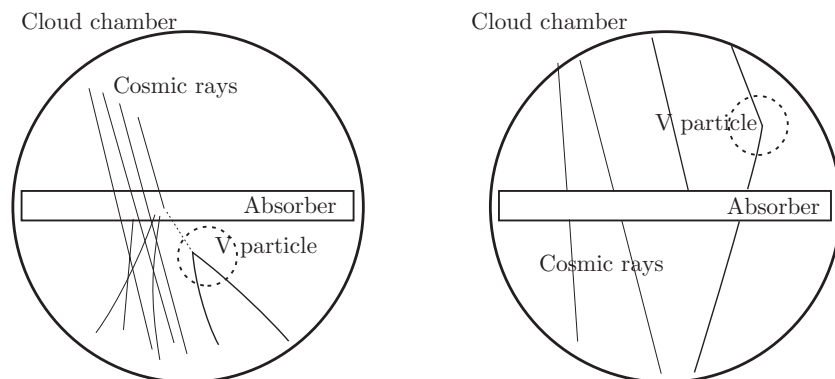


**Fig. 8.2.** Production and decay of V particles.

In few triggered pictures,  $\sim 1000$  nuclear interactions, a few particles which decay in few cm were observed. A typical strong interaction cross section is  $(1 \text{ fm})^2 = 10^{-26} \text{ cm}^2$ , corresponding to the production in a  $1 \text{ g/cm}^2$  plate of:

$$N_{\text{events}} = N_{\text{in}} \times \sigma \times \frac{\text{nucleons}}{\text{cm}^2} = 10^3 \times 10^{-26} \times 1 \times 6 \times 10^{23} = 6$$

Assuming the V-particles travel a few cm with  $\gamma\beta\sim 3$ , their lifetime is  $\mathcal{O}(10^{-10}$  s), typical of weak interactions. We conclude that the decay of V-particles is weak while the production is strong, strange indeed since pions and nucleons appear at the beginning and at the end!! This strange property of *K* mesons and other particles, the hyperons, led to the introduction of a new quantum number, the strangeness,  $S$ !<sup>(7)</sup> Strangeness is conserved in strong interactions, while 12 first order weak interaction can induce transitions in which strangeness is changed by one unit.

Today we describe these properties in terms of quarks with different “flavors”, first suggested in 1964 independently by Gell-Mann and Zweig,<sup>(8)</sup> reformulating the  $SU(3)$  flavor, approximate, global symmetry. The “normal particles” are bound states of quarks:  $q\bar{q}$ , the mesons, or  $qqq$ , baryons, where

$$q = \begin{pmatrix} u \\ d \end{pmatrix} = \begin{pmatrix} \text{up} \\ \text{down} \end{pmatrix}.$$

*K*'s, hyperons and hypernuclei contain a strange quark,  $s$ :

$$\begin{aligned} K^0 &= d\bar{s} & \bar{K}^0 &= \bar{d}s \\ K^+ &= u\bar{s} & K^- &= \bar{u}s \\ S &= +1 & S &= -1. \end{aligned}$$

The assignment of negative strangeness to the  $s$  quark is arbitrary but maintains today the original assignment of positive strangeness for  $K^0$ ,  $K^+$  and negative for the  $\Lambda$  and  $\Sigma$  hyperons and for  $\bar{K}^0$  and  $K^-$ . Or, mysteriously, calling negative the charge of the electron.

An important consequence of the fact that *K* mesons carry strangeness, a new additive quantum number, is that *the neutral K and anti neutral K meson are distinct particles!!!*

$$C|K^0\rangle = |\bar{K}^0\rangle, \quad S|K^0\rangle = |K^0\rangle, \quad S|\bar{K}^0\rangle = -|\bar{K}^0\rangle$$

An apocryphal story says that upon hearing of this hypothesis, Fermi challenged Gell-Mann to devise an experiment which shows an observable difference between the  $K^0$  and the  $\bar{K}^0$ . Today we know that it is trivial to do so. For example, the process  $p\bar{p} \rightarrow \pi^- K^+ \bar{K}^0$ , produces  $\bar{K}^0$ 's which in turn can produce  $\Lambda$  hyperons while the  $K^0$ 's produced in  $p\bar{p} \rightarrow \pi^+ K^- K^0$  cannot.

Another of Fermi's question was:

if you observe a  $K \rightarrow 2\pi$  decay, how do you tell whether it is a  $K^0$  or a  $\bar{K}^0$ ? Since the '50's *K* mesons have been produced at accelerators, first amongst them was the Cosmotron.

## 8.4 Parity Violation

Parity violation,  $\bar{R}$ , was first observed through the  $\theta$ - $\tau$  decay modes of  $K$  mesons. Incidentally, the  $\tau$  there is not the heavy lepton of today, but is a charged particle which decays into three pions,  $K^+ \rightarrow \pi^+\pi^+\pi^-$  in today's language. The  $\theta$  there refers to a neutral particle which decays into a pair of charged pions,  $K^0 \rightarrow \pi^+\pi^-$ .

The studies of those days were done mostly in nuclear emulsions and JLF contributed also long strands of her hair to make the reference marks between emulsion plates, to enable tracking across plates... The burning question was whether these two particles were the same particle with two decay modes, or two different ones. And if they were the same particle, how could the two different final states have opposite parity?

This puzzle was originally not so apparent until Dalitz advanced an argument which says that one could determine the spin of  $\tau$  by looking at the decay distribution of the three pions in a ‘‘Dalitz’’ (what he calls phase space) plot, which was in fact consistent with  $J=0$ .

The spin of the  $\theta$  was inferred to be zero because it did not like to decay into a pion and a photon (a photon cannot be emitted in a  $0 \rightarrow 0$  transition). For neutral  $K$ 's one of the principal decay modes are two or three pions.

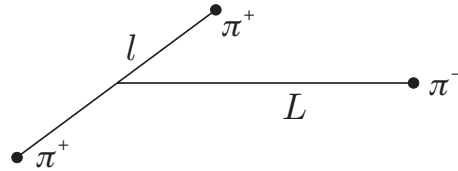


**Fig. 8.3.** Definition of  $l$  and  $L$  for three pion decays of  $\tau^+$ .

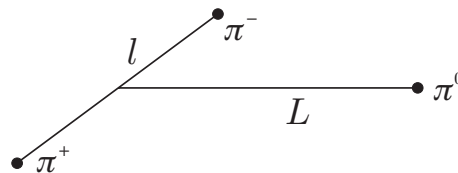


**Fig. 8.4.** Definition of  $l$  and  $L$  for  $K^0 \rightarrow \pi^+\pi^-\pi^0$ .

The relevant properties of the neutral two and three pion systems with zero total angular momentum are given below.

1.  $\ell = L = 0, 1, 2 \dots$
2.  $\pi^+\pi^-, \pi^0\pi^0$ :  $P = +1, C = +1, CP = +1$ .

3.  $\pi^+\pi^-\pi^-$ :  $P = -1$ ,  $C = (-1)^l$ ,  $CP = \pm 1$ , where  $l$  is the angular momentum of the charged pions in their center of mass. States with  $l > 0$  are suppressed by the angular momentum barrier.
4.  $\pi^0\pi^0\pi^0$ :  $P = -1$ ,  $C = +1$ ,  $CP = -1$ . Bose statistics requires that  $l$  for any identical pion pair be even in this case.

Note that the two pion and three pion states have opposite parity, except for  $\pi^+\pi^-\pi^0$  with  $\ell, L$  odd.

## 8.5 Mass and CP eigenstates

While the strong interactions conserve strangeness, the weak interactions do not. In fact, not only do they violate  $S$  with  $\Delta S = 1$ , they also violate charge conjugation,  $C$ , and parity,  $P$ , as we have just seen. However, at the end of the 50's, the weak interaction does not manifestly violate the combined  $CP$  symmetry. For now let's assume that  $CP$  is a symmetry of the world. We define an arbitrary, unmeasurable phase by:

$$CP|K^0\rangle = |\bar{K}^0\rangle$$

Then the simultaneous mass and  $CP$  eigenstates are:<sup>(9)</sup>

$$|K_1\rangle \equiv \frac{|K^0\rangle + |\bar{K}^0\rangle}{\sqrt{2}} \quad |K_2\rangle \equiv \frac{|K^0\rangle - |\bar{K}^0\rangle}{\sqrt{2}}, \quad (8.1)$$

where  $K_1$  has  $CP=+1$  and  $K_2$  has  $CP=-1$ .

While  $K^0$  and  $\bar{K}^0$  are degenerate states in mass, as required by  $CPT$  invariance, the weak interactions, which induces to second order  $K^0 \leftrightarrow \bar{K}^0$  transitions, induces a small mass difference between  $K_1$  and  $K_2$ ,  $\Delta m$ . We expect that  $\Delta m \sim \Gamma$ , at least as long as real and imaginary parts of the amplitudes of fig. 8.5 are about equal, since the decay rate is proportional to the imaginary part and the real part contributes to the mass difference. Dimensionally,  $\Gamma = \Delta m = G^2 m_\pi^5 = 5.3 \times 10^{-15}$  GeV, in good agreement with measurements. The  $K_1$  mass is the expectation value

$$\langle K_1 | H | K_1 \rangle$$

. With  $K_1 = (K^0 + \bar{K}^0)/\sqrt{2}$  and analogously for  $K_2$ , we find

$$m_1 - m_2 = \langle K^0 | H | \bar{K}^0 \rangle + \langle \bar{K}^0 | H | K^0 \rangle,$$

$\delta m$  is due to  $K^0 \leftrightarrow \bar{K}^0$  transitions induced by a  $\Delta S=2$  interaction.

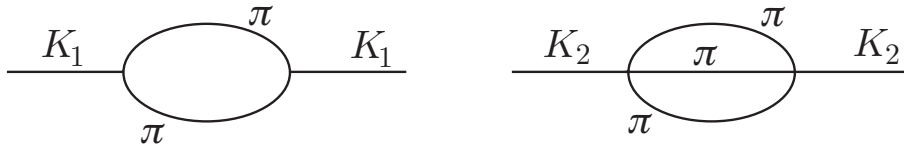


**Fig. 8.5.** Contributions to the  $K_1$ - $K_2$  mass difference.

## 8.6 $K_1$ and $K_2$ lifetimes and mass difference

If the total Hamiltonian conserves  $CP$ , *i.e.*  $[H, CP] = 0$ , the decays of  $K_1$ 's and  $K_2$ 's must conserve  $CP$ . Thus the  $K_1$ 's with  $CP = 1$ , must decay into two pions (and three pions in an  $L = \ell = 1$  state, surmounting an angular momentum barrier -  $\sim(kr)^2(KR)^2 \sim 1/100$  and suppressed by phase space,  $\sim 1/1000$ ), while the  $K_2$ 's with  $CP = -1$ , must decay into three pion final states.

Phase space for 3 pion decay is smaller by  $32\pi^2$  plus some, since the energy available in  $2\pi$  decay is  $\sim 220$  MeV, while for three  $\pi$ s decay is  $\sim 90$  MeV, the lifetime of the  $K_1$  is much much shorter than that of the  $K_2$ .

Lederman *et al.*<sup>(10)</sup> observed long lived neutral kaons in 1956, in a diffusion cloud chamber at the Cosmotron.

Today we have  $\tau_1 = (0.8959 \pm 0.0006) \times 10^{-10}$  s and :<sup>†</sup>

$$\begin{aligned}
 \Gamma_1 &= (1.1162 \pm 0.0007) \times 10^{10} \text{ s}^{-1} \\
 \Gamma_2 &= (1.72 \pm 0.02) \times 10^{-3} \times \Gamma_1 \\
 \Delta m = m(K_2) - m(K_1) &= (0.5296 \pm 0.0010) \times 10^{10} \text{ s}^{-1} \\
 &= (3.489 \pm 0.008) \times 10^{-6} \text{ eV} \\
 \Delta m / (\Gamma_1 + \Gamma_2) &= 0.4736 \pm 0.0009.
 \end{aligned} \tag{8.2}$$

---

<sup>†</sup>We use natural units, *i.e.*  $\hbar = c = 1$ . Conversion is found using  $\hbar c = 197.3 \dots$  MeV  $\times$  fm.

### Unit Conversion

To convert from	to	multiply by
1/MeV	s	$6.58 \times 10^{-22}$
1/MeV	fm	197
1/GeV <sup>2</sup>	mb	0.389

## 8.7 Strangeness oscillations

The mass eigenstates  $K_1$  and  $K_2$  evolve in vacuum and in their rest frame according to

$$|K_{1,2}\rangle t, = |K_{1,2}\rangle t = 0, e^{-i m_{1,2} t - t \Gamma_{1,2}/2} \quad (8.3)$$

If the initial state has definite strangeness, say it is a  $K^0$  as from the production process  $\pi^- p \rightarrow K^0 \Lambda^0$ , it must first be rewritten in terms of the mass eigenstates  $K_1$  and  $K_2$  which then evolve in time as above. Since the  $K_1$  and  $K_2$  amplitudes change phase differently in time, the pure  $S=1$  state at  $t=0$  acquires an  $S=-1$  component at  $t > 0$ . From (8.1) the wave function at time  $t$  is:

$$\begin{aligned} \Psi(t) = & \sqrt{1/2} [e^{(i m_1 - \Gamma_1/2)t} |K_1\rangle + e^{(i m_2 - \Gamma_1/2)t} |K_2\rangle] = \\ & 1/2 [(e^{(i m_1 - \Gamma_1/2)t} + e^{(i m_2 - \Gamma_2/2)t}) |K^0\rangle + \\ & (e^{(i m_1 - \Gamma_1/2)t} - e^{(i m_2 - \Gamma_2/2)t}) |\bar{K}^0\rangle]. \end{aligned}$$

The intensity of  $K^0$  ( $\bar{K}^0$ ) at time  $t$  is given by:

$$\begin{aligned} I(K^0 (\bar{K}^0), t) = & |\langle K^0 (\bar{K}^0) | \Psi(t) \rangle|^2 = \\ & \frac{1}{4} [e^{-t\Gamma_1} + e^{-t\Gamma_2} + (-)2e^{-t(\Gamma_1+\Gamma_2)/2} \cos \Delta m t] \end{aligned}$$

which exhibits oscillations whose frequency depends on the mass difference, see fig. 8.6.

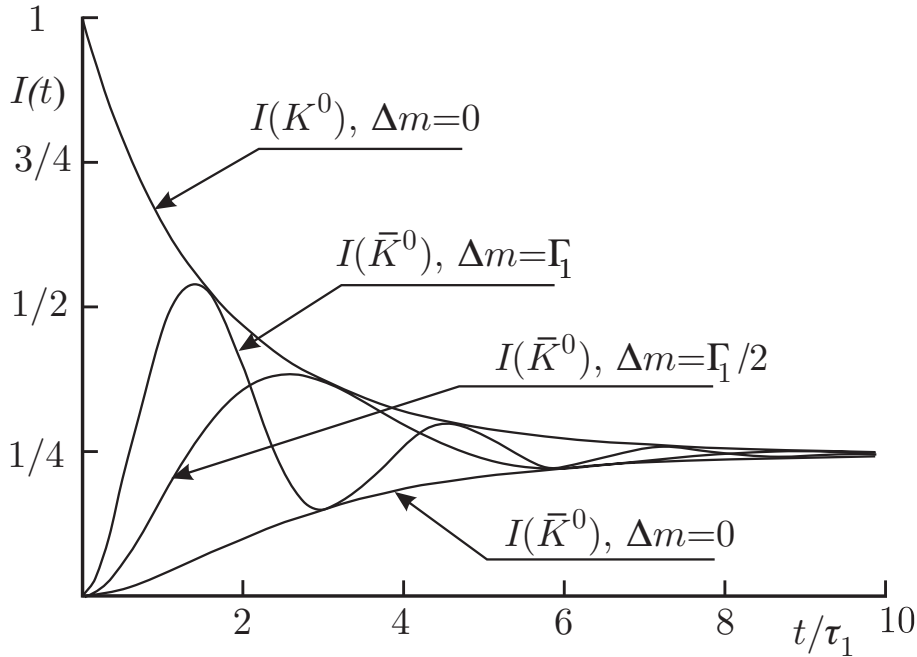


Fig. 8.6. Evolution in time of a pure  $S=1$  state at time  $t=0$

The appearance of  $\bar{K}^0$ 's from an initially pure  $K^0$  beam can be detected by the production of hyperons, according to the reactions:

$$\begin{aligned}\bar{K}^0 p &\rightarrow \pi^+ \Lambda^0, & \rightarrow \pi^+ \Sigma^+, & \rightarrow \pi^0 \Sigma^+, \\ \bar{K}^0 n &\rightarrow \pi^0 \Lambda^0, & \rightarrow \pi^0 \Sigma^0, & \rightarrow \pi^- \Sigma^-.\end{aligned}$$

The  $K_L$ - $K_S$  mass difference can therefore be obtained from the oscillation frequency.

## 8.8 Regeneration

Another interesting, and extremely useful phenomenon, is that it is possible to regenerate  $K_1$ 's by placing a piece of material in the path of a  $K_2$  beam. Let's take our standard reaction,

$$\pi^- p \rightarrow K^0 \Lambda^0,$$

the initial state wave function of the  $K^0$ 's is

$$\Psi(t=0) \equiv |K^0\rangle = \frac{|K_1\rangle + |K_2\rangle}{\sqrt{2}}.$$

Note that it is composed equally of  $K_1$ 's and  $K_2$ 's. The  $K_1$  component decays away quickly via the two pion decay modes, leaving a virtually pure  $K_2$  beam.

A  $K_2$  beam has equal  $K^0$  and  $\bar{K}^0$  components, which interact differently in matter. For example, the  $K^0$ 's undergo elastic scattering, charge exchange etc. whereas the  $\bar{K}^0$ 's also produce hyperons via strangeness conserving transitions. Thus we have an apparent rebirth of  $K_1$ 's emerging from a piece of material placed in the path of a  $K_2$  beam! See fig. 8.7.

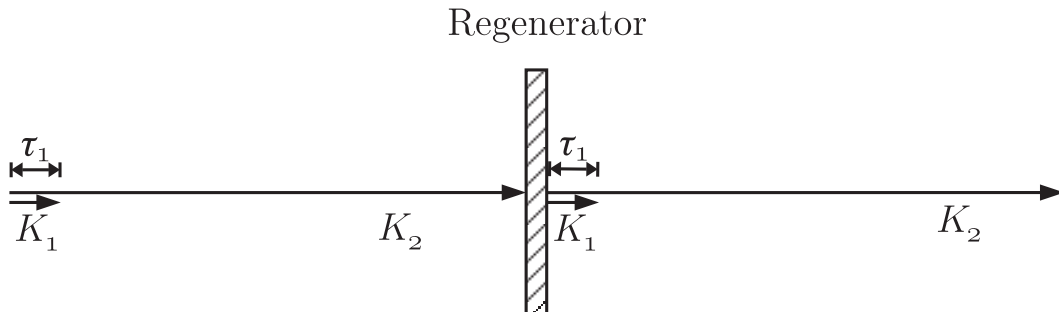


**Fig. 8.7.**  $K_1$  regeneration

Virtually all past and present experiments, with the exception of a couple which will be mentioned explicitly, use this method to obtain a source of  $K_1$ 's (or  $K_S$ 's, as we shall see later).

Denoting the amplitudes for  $K^0$  and  $\bar{K}^0$  scattering on nuclei by  $f$  and  $\bar{f}$  respectively, the scattered amplitude for an initial  $K_2$  state is given by:

$$\begin{aligned} \sqrt{1/2}(f|K^0\rangle - \bar{f}|\bar{K}^0\rangle) &= \frac{f + \bar{f}}{2\sqrt{2}}(|K^0\rangle - |\bar{K}^0\rangle) + \frac{f - \bar{f}}{2\sqrt{2}}(|K^0\rangle + |\bar{K}^0\rangle) \\ &= 1/2(f + \bar{f})|K_2\rangle + 1/2(f - \bar{f})|K_1\rangle. \end{aligned}$$

The so called regeneration amplitude for  $K_2 \rightarrow K_1$ ,  $f_{21}$  is given by  $1/2(f - \bar{f})$  which of course would be 0 if  $f = \bar{f}$ , which is true at infinite energy.

Another important property of regeneration is that when the  $K_1$  is produced at non-zero angle to the incident  $K_2$  beam, regeneration on different nuclei in a regenerator is incoherent, while at zero degree the amplitudes from different nuclei add up coherently.

The intensity for coherent regeneration depends on the  $K_1$ ,  $K_2$  mass difference. Precision mass measurements have been performed by measuring the ratio of coherent to diffraction regeneration. The interference of  $K_1$  waves from two or more regenerators has also allowed us to determine that the  $K_2$  meson is heavier than the  $K_1$  meson. This perhaps could be expected, but it is nice to have it measured.

Finally we note that the  $K_1$  and  $K_2$  amplitudes after regeneration are coherent and can interfere if  $CP$  is violated.

## 8.9 CP Violation in Two Pion Decay Modes

### 8.9.1 Discovery

For some years after the discovery that  $C$  and  $P$  are violated in the weak interactions, it was thought that  $CP$  might still be conserved.  $CP$  violation was discovered in '64,<sup>(11)</sup> through the observation of the unexpected decay  $K_2 \rightarrow \pi^+\pi^-$ . This beautiful experiment is conceptually very simple, see fig. 8.8.

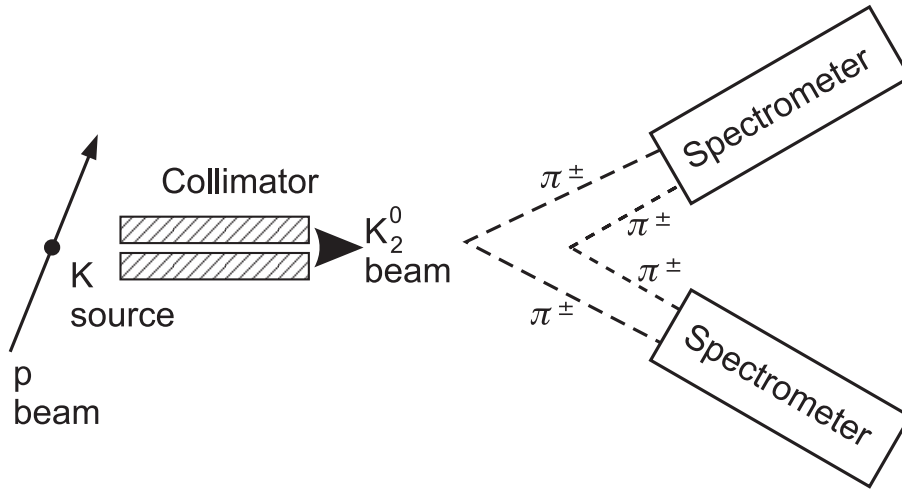


**Fig. 8.8.** The setup of the experiment of Christenson *et al.*.

Let a  $K$  beam pass through a long collimator and decay in an empty space (actually a big helium bag) in front of two spectrometers. We have made a  $K_2$  beam. The  $K_2$  decay products are viewed by spark chambers and scintillator hodoscopes in the spectrometers placed on either side of the beam.

Two pion decay modes are distinguished from three pion and leptonic decay modes by the reconstructed invariant mass  $M_{\pi\pi}$ , and the direction  $\theta$  of their resultant momentum vector relative to the beam. In the mass interval 494-504 MeV an excess of 45 events collinear with the beam ( $\cos\theta > 0.99997$ ) is observed. For the intervals 484-494 and 504-514 there is no excess, establishing that  $K_2$ s decay into two pions, with a branching ratio of the order of  $2 \times 10^{-3}$ .

$CP$  is therefore shown to be violated! The  $CP$  violating decay  $K_L \rightarrow \pi^0 \pi^0$  has also been observed.

### 8.9.2 $K^0$ Decays with $CP$ Violation

Since  $CP$  is violated in  $K$  decays, the mass eigenstates are no more  $CP$  eigenstate and can be written, assuming  $CPT$  invariance, as:

$$\begin{aligned}
 K_S &= \left( (1 + \epsilon) |K^0\rangle + (1 - \epsilon) |\bar{K}^0\rangle \right) / \sqrt{2(1 + |\epsilon|^2)} \\
 K_L &= \left( (1 + \epsilon) |K^0\rangle - (1 - \epsilon) |\bar{K}^0\rangle \right) / \sqrt{2(1 + |\epsilon|^2)}
 \end{aligned}$$

Another equivalent form, in terms of the  $CP$  eigenstate  $K_1$  and  $K_2$  is:

$$|K_S\rangle = \frac{|K_1\rangle + \epsilon |K_2\rangle}{\sqrt{1 + |\epsilon|^2}} \quad |K_L\rangle = \frac{|K_2\rangle + \epsilon |K_1\rangle}{\sqrt{1 + |\epsilon|^2}} \quad (8.4)$$

with  $|\epsilon| = (2.259 \pm 0.018) \times 10^{-3}$  from experiment. Note that the  $K_S$  and  $K_L$  states are not orthogonal states, contrary to the case of  $K_1$  and  $K_2$ . If we describe an

arbitrary state  $a|K^0\rangle + b|\bar{K}^0\rangle$  as

$$\psi = \begin{pmatrix} a \\ b \end{pmatrix}.$$

its time evolution is given by

$$i\frac{d}{dt}\psi = (\mathbf{M} - i\mathbf{\Gamma}/2)\psi$$

where  $\mathbf{M}$  and  $\mathbf{\Gamma}$  are  $2\times 2$  hermitian matrices which can be called the mass and decay matrix.  $CPT$  invariance requires  $M_{11} = M_{22}$ , *i.e.*  $M(K^0) = M(\bar{K}^0)$ , and  $\Gamma_{11} = \Gamma_{22}$ .  $CP$  invariance requires  $\arg(\Gamma_{12}/M_{12})=0$ . The relation between  $\epsilon$  and  $\mathbf{M}$ ,  $\mathbf{\Gamma}$  is:

$$\frac{1 + \epsilon}{1 - \epsilon} = \sqrt{\frac{M_{12} - \Gamma_{12}/2}{M_{12}^* - \Gamma_{12}^*/2}}.$$

$K_S$  and  $K_L$  satisfy

$$(\mathbf{M} - i\mathbf{\Gamma})|K_{S,L}\rangle = (M_{S,L} - i\Gamma_{S,L})|K_{S,L}\rangle$$

where  $M_{S,L}$  and  $\Gamma_{S,L}$  are the mass and width of the physical neutral kaons, with values given earlier for the  $K_1$  and  $K_2$  states.

Equation (8.3) is rewritten as:

$$|K_{S,L}\rangle_t = |K_{S,L}\rangle_{t=0}, e^{-iM_{S,L}t - \Gamma_{S,L}/2t}$$

$$\frac{d}{dt}|K_{S,L}\rangle = -i\mathcal{M}_{S,L}|K_{S,L}\rangle$$

with

$$\mathcal{M}_{S,L} = M_{S,L} - i\Gamma_{S,L}/2$$

and the values of masses and decay widths given in eq. (8.2) belong to  $K_S$  and  $K_L$ , rather than to  $K_1$  and  $K_2$ . We further introduce the so called superweak phase  $\phi_{\text{SW}}$  as:

$$\phi_{\text{SW}} = \text{Arg}(\epsilon) = \tan^{-1} \frac{2(M_{K_L} - M_{K_S})}{\Gamma_{K_S} - \Gamma_{K_L}} = 43.63^\circ \pm 0.08^\circ.$$

A superweak theory, is a theory with a  $\Delta S=2$  interaction, whose sole effect is to induce a  $CP$  impurity  $\epsilon$  in the mass eigenstates. Since 1964 we have been asking the question: is  $CP$  violated directly in  $K^0$  decays, *i.e.* is the  $|\Delta S|=1$  amplitude  $\langle \pi\pi | K_2 \rangle \neq 0$  or the only manifestation of  $\bar{C}\bar{P}$  is to introduce a small impurity of  $K_1$  in the  $K_L$  state, via  $K^0 \leftrightarrow \bar{K}^0$ ,  $|\Delta S|=2$  transitions?

Wu and Yang,<sup>(12)</sup> have analyzed the two pion decays of  $K_S$ ,  $K_L$  in term of the isospin amplitudes:

$$\begin{aligned} A(K^0 \rightarrow 2\pi, I) &= A_I e^{i\delta_I} \\ A(\bar{K}^0 \rightarrow 2\pi, I) &= A_I^* e^{i\delta_I} \end{aligned}$$

where  $\delta_I$  are the  $\pi\pi$  scattering phase shifts in the  $I=0, 2$  states. W-Y chose an arbitrary phase, by defining  $A_0$  real. They also introduce the ratios of the amplitudes for  $K$  decay to a final state  $f_i$ ,  $\eta_i = A(K_L \rightarrow f_i)/A(K_S \rightarrow f_i)$ :

$$\begin{aligned} \eta_{+-} &\equiv |\eta_{+-}| e^{-i\phi_{+-}} = \frac{\langle \pi^+ \pi^- | K_L \rangle}{\langle \pi^+ \pi^- | K_S \rangle} = \epsilon + \epsilon' \\ \eta_{00} &\equiv |\eta_{00}| e^{-i\phi_{00}} = \frac{\langle \pi^0 \pi^0 | K_L \rangle}{\langle \pi^0 \pi^0 | K_S \rangle} = \epsilon - 2\epsilon', \end{aligned}$$

with

$$\epsilon' = \frac{i}{2\sqrt{2}} e^{i(\delta_2 - \delta_0)} \frac{\Re A_2}{A_0} \frac{\Im A_2}{\Re A_2}$$

Since  $\delta_2 - \delta_0 \sim 45^\circ$ ,  $\text{Arg}(\epsilon') \sim 135^\circ$  *i.e.*  $\epsilon'$  is orthogonal to  $\epsilon$ . Therefore, in principle, only two real quantities need to be measured:  $\Re\epsilon$  and  $\Re(\epsilon'/\epsilon)$ , *with sign*.

In terms of the measurable amplitude ratios,  $\eta$ ,  $\epsilon$  and  $\epsilon'$  are given by:

$$\begin{aligned} \epsilon &= (2\eta_{+-} + \eta_{00})/3 \\ \epsilon' &= (\eta_{+-} - \eta_{00})/3 \\ \text{Arg}(\epsilon) &= \phi_{+-} + (\phi_{+-} - \phi_{00})/3. \end{aligned}$$

$\epsilon'$  is a measure of direct  $CP$  violation and its magnitude is  $\mathcal{O}(A(K_2 \rightarrow \pi\pi)/A(K_1 \rightarrow \pi\pi))$ .

Our question above is then the same as: is  $\epsilon' \neq 0$ ? Since 1964, experiments searching for a difference in  $\eta_{+-}$  and  $\eta_{00}$  have been going on.

If  $\eta_{+-} \neq \eta_{00}$  the ratios of branching ratios for  $K_{L,S} \rightarrow \pi^+ \pi^-$  and  $\pi^0 \pi^0$  are different.

The first measurement of  $\text{BR}(K_L \rightarrow \pi^0 \pi^0)$ , *i.e.* of  $|\eta_{00}|^2$  was announced by Cronin in 1965.....

Most experiments measure the quantity  $\mathcal{R}$ , the so called double ratio of the four rates for  $K_{L,S} \rightarrow \pi^0 \pi^0$ ,  $\pi^+ \pi^-$ , which is given, to lowest order in  $\epsilon$  and  $\epsilon'$  by:

$$\mathcal{R} \equiv \frac{\Gamma(K_L \rightarrow \pi^0 \pi^0)/\Gamma(K_S \rightarrow \pi^0 \pi^0)}{\Gamma(K_L \rightarrow \pi^+ \pi^-)/\Gamma(K_S \rightarrow \pi^+ \pi^-)} \equiv \left| \frac{\eta_{00}}{\eta_{+-}} \right|^2 = 1 - 6\Re(\epsilon'/\epsilon).$$

Observation of  $\mathcal{R} \neq 0$  is proof that  $\Re(\epsilon'/\epsilon) \neq 0$  and therefore of “direct”  $CP$  violation, *i.e.* that the amplitude for  $|\Delta S|=1$ ,  $CP$  violating transitions

$$A(K_2 \rightarrow 2\pi) \neq 0.$$

All present observations of *CP* violation,  $\mathcal{CR}$ , *i.e.* the decays  $K_L \rightarrow 2\pi$ ,  $\pi^+\pi^-\gamma$  and the charge asymmetries in  $K_{\ell 3}$  decays are examples of so called “indirect” violation, due to  $|\Delta S|=2$   $K^0 \leftrightarrow \bar{K}^0$  transitions introducing a small *CP* impurity in the mass eigenstates  $K_S$  and  $K_L$ .

Because of the smallness of  $\epsilon$  (and  $\epsilon'$ ), most results and parameter values given earlier for  $K_1$  and  $K_2$  remain valid after the substitution  $K_1 \rightarrow K_S$  and  $K_2 \rightarrow K_L$ .

### 8.9.3 Experimental Status

We have been enjoying a roller coaster ride on the last round of *CP* violation precision experiments. One of the two, NA31, was performed at CERN and reported a tantalizing non-zero result:<sup>(13)</sup>

$$\Re(\epsilon'/\epsilon) = (23 \pm 6.5) \times 10^{-4}.$$

NA31 alternated  $K_S$  and  $K_L$  data taking by the insertion of a  $K_S$  regenerator in the  $K_L$  beam every other run, while the detector collected both charged and neutral two pion decay modes simultaneously. The other experiment, E731 at Fermilab, was consistent with no or very small direct  $\mathcal{CR}$ .<sup>(14)</sup>

$$\Re(\epsilon'/\epsilon) = (7.4 \pm 5.9) \times 10^{-4}.$$

E731 had a fixed  $K_S$  regenerator in front of one of the two parallel  $K_L$  beams which entered the detector which, however, collected alternately the neutral and charged two pion decay modes.

Both collaborations have completely redesigned their experiments. Both experiments can now observe both pion modes for  $K_S$  and  $K_L$  simultaneously. Preliminary results indicate that in fact the answer to the above question is a resounding NO!!! The great news in HEP for 2001 is that both experiment observe a significant non zero effect. Combining their results, even though the agreement is not perfect, value of  $\epsilon'$  is  $17.8 \pm 1.8 \times 10^{-4}$ , which means that there definitely is direct *CP* violation. The observed value is  $\sim 10\sigma$  away from zero.

## 8.10 *CP violation in two pion decay*

### 8.10.1 Outgoing Waves

In order to compute weak decay processes we need matrix elements from the parent state to outgoing waves of the final products, in states with definite quantum

numbers, such as

$$\begin{aligned}\langle (2\pi)_I^{\text{out}} | T | K^0 \rangle &= A e^{i\delta_I} \\ \langle (2\pi)_I^{\text{out}} | T | \bar{K}^0 \rangle &= \bar{A} e^{i\delta_I} \quad I = 0, 2.\end{aligned}$$

We derive in the following the reason why the scattering phase  $\delta_I$  appear in the above formulae.

The  $S$  matrix is unitary and, from  $T$ -invariance of the lagrangian, symmetric. In the following the small  $T$  violation from  $CP$  violation and  $CPT$ -invariance is neglected.

We first find the relation between amplitudes for  $i \rightarrow f$  and the reversed transition  $i \rightarrow f$  which follows from unitarity  $S^\dagger S = S S^\dagger = 1$  in the approximation that  $A_{fi}$  are small.

We write:

$$S = S^0 + S^1, \quad |S^0| \gg |S^1|$$

$S^0$  and  $S^1$  are chosen so as to satisfy:

$$\begin{aligned}S_{fi}^0 &= 0 & S_{ii'}^0 &\neq 0 & S_{ff'}^0 &\neq 0 \\ S_{fi}^1 &\neq 0 & S_{ii'}^1 &= 0 & S_{ff'}^1 &= 0\end{aligned}$$

where  $i, i' (f, f')$  are from groups of initial (final) states. we also have

$$S_{fi} = S_{fi}^1 \quad S_{ii'} = S_{ii'}^0 \quad S_{ff'} = S_{ff'}^0$$

From unitarity

$$(S^0 + S^1)^\dagger (S^0 + S^1) = 1$$

and neglecting  $S^{1\dagger} S^1$

$$S^{0\dagger} S^0 = 1$$

$$S^{0\dagger} S^1 + S^{1\dagger} S^0 = 0$$

*i.e.*

$$S^1 = -S^0 S^{1\dagger} S^0$$

$$S_{fi}^1 = -S_{ff'}^0 S_{f'i'}^{1\dagger} S_{i'i}^0$$

$$S_{fi}^1 = -S_{ff'}^0 S_{i'f'}^* S_{i'i}^0$$

since, see above,  $S_{fi} = S_{fi}^1$ . The  $ii$  and  $ff$  elements of  $S^0$  are given by  $e^{2i\delta_i}$  and  $e^{2i\delta_f}$ , where  $\delta_i$  and  $\delta_f$  are the scattering phases. Then

$$S_{fi} = -e^{2i(\delta_i + \delta_f)} S_{if}^*$$

. Using the (approximate) symmetry of  $S$ , see above,

$$S_{fi} = -e^{2i(\delta_i + \delta_f)} S_{fi}^*$$

which means ( $S$  and  $S^*$  differ in phase by  $2(\delta_i + \delta_f + \pi)$ )

$$\arg S_{fi} = \delta_i + \delta_f + \pi$$

and, from  $S = 1 + iT$  etc., see page 21 of the notes,

$$\arg A_{fi} = \delta_i + \delta_f.$$

The decay amplitude to an out state with definite  $L, T$  etc., ( $\delta_i=0!$ ) therefore is:

$$A_{L,T,\dots} e^{i\delta_{L,T,\dots}}$$

which justifies the appearance of the  $\pi\pi$  scattering phases in the amplitudes used for computing  $\Re(\epsilon'/\epsilon)$ .

## 8.11 CP Violation at a $\phi$ -factory

### 8.11.1 $\phi$ ( $\Upsilon'''$ ) production and decay in $e^+e^-$ annihilations

The cross section for production of a bound  $q\bar{q}$  pair of mass  $M$  and total width  $\Gamma$  with  $J^{PC} = 1^{--}$ , a so called vector meson  $V$ , ( $\phi$  in the following and the  $\Upsilon(4S)$  later) in  $e^+e^-$  annihilation, see fig. 8.9, is given by:

$$\sigma_{q\bar{q},\text{res}} = \frac{12\pi}{s} \frac{\Gamma_{ee}\Gamma M^2}{(M^2 - s)^2 + M^2\Gamma^2} = \frac{12\pi}{s} B_{ee} B_{q\bar{q}} \frac{M^2\Gamma^2}{(M^2 - s)^2 + M^2\Gamma^2}$$

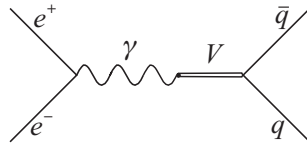


**Fig. 8.9.** Amplitude for production of a bound  $q\bar{q}$  pair

The  $\phi$  meson is an  $s\bar{s}$   $^3S_1$  bound state with  $J^{PC}=1^{--}$ , just as a photon and the cross section for its production in  $e^+e^-$  annihilations at 1020 MeV is

$$\sigma_{s\bar{s}}(s = (1.02)^2 \text{ GeV}^2) \sim \frac{12\pi}{s} B_{ee}$$

$$= 36.2 \times (1.37/4430) = 0.011 \text{ GeV}^{-2} \sim 4000 \text{ nb},$$

compared to a total hadronic cross section of  $\sim(5/3) \times 87 \sim 100$  nb.

The production cross section for the  $\Upsilon(4S)$  at  $W=10,400$  MeV is  $\sim 1$  nb, over a background of  $\sim 2.6$  nb.

The Frascati  $\phi$ -factory, DAΦNE, will have a luminosity  $\mathcal{L} = 10^{33} \text{ cm}^{-2} \text{ s}^{-1} = 1 \text{ nb}^{-1}\text{s}^{-1}$ . Integrating over one year, taken as  $10^7 \text{ s}$  or one third of a calendar year, we find

$$\int_{1 \text{ y}} \mathcal{L} dt = 10^7 \text{ nb}^{-1},$$

corresponding to the production at DAΦNE of  $\sim 4000 \times 10^7 = 4 \times 10^{10}$   $\phi$  meson per year or approximately  $1.3 \times 10^{10}$   $K^0, \bar{K}^0$  pairs, a large number indeed.

One of the advantages of studying  $K$  mesons at a  $\phi$ -factory, is that they are produced in a well defined quantum state. Neutral  $K$  mesons are produced as collinear pairs, with  $J^{PC} = 1^{--}$  and a momentum of about  $110 \text{ MeV}/c$ , thus detection of one  $K$  announces the presence of the other and gives its direction.

Since in the reaction:

$$e^+e^- \rightarrow \text{“}\gamma\text{”} \rightarrow \phi \rightarrow K^0\bar{K}^0$$

we have

$$C(K^0\bar{K}^0) = C(\phi) = C(\gamma) = -1.$$

we can immediately write the 2- $K$  state. Define  $|i\rangle = |K\bar{K}\rangle_{t=0}$ ,  $C=-1$ . Then  $|i\rangle$  must have the form:

$$|i\rangle = \frac{|K^0\rangle_{\mathbf{p}}, |\bar{K}^0\rangle_{-\mathbf{p}} - |\bar{K}^0\rangle_{\mathbf{p}}, |K^0\rangle_{-\mathbf{p}}}{\sqrt{2}}$$

From eq. (8.4), the relations between  $K_S, K_L$  and  $K^0, \bar{K}^0$ , to lowest order in  $\epsilon$ , we find:

$$|K_S (K_L)\rangle = \frac{(1+\epsilon)|K^0\rangle + (-)(1-\epsilon)|\bar{K}^0\rangle}{\sqrt{2}}.$$

$$|K^0 (\bar{K}^0)\rangle = \frac{|K_S\rangle + (-)|K_L\rangle}{(1+(-)\epsilon)\sqrt{2}}$$

from which

$$|i\rangle = \frac{1}{\sqrt{2}} (|K_S - \mathbf{p}\rangle |K_L \mathbf{p}\rangle - |K_S \mathbf{p}\rangle |K_L - \mathbf{p}\rangle)$$

so that the neutral kaon pair produced in  $e^+e^-$  annihilations is a pure  $K^0, \bar{K}^0$  as well as a pure  $K_S, K_L$  for *all times*, in vacuum. What this means, is that if at some time  $t$  a  $K_S (K_L, K^0, \bar{K}^0)$  is recognized, the other kaon, if still alive, is a  $K_L (K_S, \bar{K}^0, K^0)$ .

The result above is correct to all orders in  $\epsilon$ , apart from a normalization constant, and holds even without assuming  $CPT$  invariance.

The result also applies to  $e^+e^- \rightarrow B^0\bar{B}^0$  at the  $\Upsilon(4S)$ .

### 8.11.2 Correlations in $K_S, K_L$ decays

To obtain the amplitude for decay of  $K(\mathbf{p})$  into a final state  $f_1$  at time  $t_1$  and of  $K(-\mathbf{p})$  to  $f_2$  at time  $t_2$ , see the diagram below, we time evolve the initial state in the usual way:

$$|t_1 \mathbf{p}; t_2 -\mathbf{p}\rangle = \frac{1 + |\epsilon^2|}{(1 - \epsilon^2)\sqrt{2}} \times \\ \left( |K_S(-\mathbf{p})\rangle |K_L(\mathbf{p})\rangle e^{-i(\mathcal{M}_S t_2 + \mathcal{M}_L t_1)} - \right. \\ \left. |K_S(\mathbf{p})\rangle |K_L(-\mathbf{p})\rangle e^{-i(\mathcal{M}_S t_1 + \mathcal{M}_L t_2)} \right)$$



**Fig. 8.10.**  $\phi \rightarrow K_L, K_S \rightarrow f_1, f_2$ .

where  $\mathcal{M}_{S,L} = M_{S,L} - i\Gamma_{S,L}/2$  are the complex  $K_S, K_L$  masses.

In terms of the previously mentioned ratios  $\eta_i = \langle f_i | K_L \rangle / \langle f_i | K_S \rangle$  and defining  $\Delta t = t_2 - t_1$ ,  $t = t_1 + t_2$ ,  $\Delta \mathcal{M} = \mathcal{M}_L - \mathcal{M}_S$  and  $\mathcal{M} = \mathcal{M}_L + \mathcal{M}_S$  we get the amplitude for decay to states 1 and 2:

$$A(f_1, f_2, t_1, t_2) = \langle f_1 | K_S \rangle \langle f_2 | K_S \rangle e^{-i\mathcal{M}t/2} \times \left( \eta_1 e^{i\Delta \mathcal{M} \Delta t/2} - \eta_2 e^{-i\Delta \mathcal{M} \Delta t/2} \right) / \sqrt{2}. \quad (8.5)$$

This implies  $A(e^+e^- \rightarrow \phi \rightarrow K^0 \bar{K}^0 \rightarrow f_1 f_2) = 0$  for  $t_1 = t_2$  and  $f_1 = f_2$  (Bose statistics).

For  $t_1 = t_2$ ,  $f_1 = \pi^+ \pi^-$  and  $f_2 = \pi^0 \pi^0$  instead,  $A \propto \eta_{+-} - \eta_{00} = 3 \times \epsilon'$  which suggest a (unrealistic) way to measure  $\epsilon'$ .

The intensity for decay to final states  $f_1$  and  $f_2$  at times  $t_1$  and  $t_2$  obtained taking the modulus squared of eq. (8.5) depends on magnitude and argument of  $\eta_1$  and  $\eta_2$  as well as on  $\Gamma_{L,S}$  and  $\Delta \mathcal{M}$ . The intensity is given by

$$I(f_1, f_2, t_1, t_2) = |\langle f_1 | K_S \rangle|^2 |\langle f_2 | K_S \rangle|^2 e^{-\Gamma_S t/2} \times \\ \left( |\eta_1|^2 e^{\Gamma_S \Delta t/2} + |\eta_2|^2 e^{-\Gamma_S \Delta t/2} - 2|\eta_1||\eta_2| \cos(\Delta m t + \phi_1 - \phi_2) \right)$$

where we have everywhere neglected  $\Gamma_L$  with respect to  $\Gamma_S$ .

Thus the study of the decay of  $K$  pairs at a  $\phi$ -factory offers the unique possibility of observing interference pattern in time, or space, in the intensity observed at two different points in space.

This fact is the source of endless excitement and frustration to some people.

Rather than studying the intensity above, which is a function of two times or distances, it is more convenient to consider the once integrated distribution. In particular one can integrate the intensity over all times  $t_1$  and  $t_2$  for fixed time difference  $\Delta t = t_1 - t_2$ , to obtain the intensity as a function of  $\Delta t$ . Performing the integrations yields, for  $\Delta t > 0$ ,

$$I(f_1, f_2; \Delta t) = \frac{1}{2\Gamma} |\langle f_1 | K_S \rangle \langle f_2 | K_S \rangle|^2 \\ \times \left( |\eta_1|^2 e^{-\Gamma_L \Delta t} + |\eta_2|^2 e^{-\Gamma_S \Delta t} - \right. \\ \left. 2|\eta_1||\eta_2| e^{-\Gamma \Delta t / 2} \cos(\Delta m \Delta t + \phi_1 - \phi_2) \right)$$

and a similar expression is obtained for  $\Delta t < 0$ . The interference pattern is quite different according to the choice of  $f_1$  and  $f_2$  as illustrated in fig. 8.11.

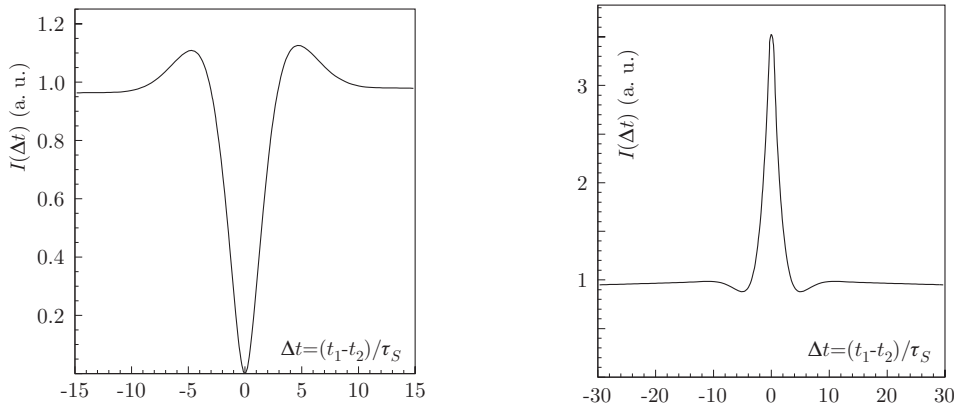


**Fig. 8.11.** Interference pattern for  $f_{1,2} = \pi^+ \pi^-$ ,  $\pi^0 \pi^0$  and  $\ell^-, \ell^+$ .

The strong destructive interference at zero time difference is due to the antisymmetry of the initial  $KK$  state, decay amplitude phases being identical. The destructive interference at zero time difference becomes constructive since the amplitude for  $K^0 \rightarrow \ell^-$  has opposite sign to that for  $\bar{K}^0 \rightarrow \ell^+$  thus making the overall amplitude symmetric. One can thus perform a whole spectrum of precision “kaon-interferometry” experiments at DAΦNE by measuring the above decay intensity distributions for appropriate choices of the final states  $f_1, f_2$ . Four examples are listed below.

- With  $f_1 = f_2$  one measures  $\Gamma_S, \Gamma_L$  and  $\Delta m$ , since all phases cancel. Rates can be measured with a  $\times 10$  improvement in accuracy and  $\Delta m$  to  $\sim \times 2$ .

- With  $f_1 = \pi^+ \pi^-$ ,  $f_2 = \pi^0 \pi^0$ , one measures  $\Re(\epsilon'/\epsilon)$  at large time differences, and  $\Im(\epsilon'/\epsilon)$  for  $|\Delta t| \leq 5\tau_s$ . Fig. 8.11 shows the interference pattern for this case.

- With  $f_1 = \pi^+ \ell^- \nu$  and  $f_2 = \pi^- \ell^+ \nu$ , one can measure the  $CPT$ -violation parameter  $\delta$ , see our discussion later concerning tests of  $CPT$ . Again the real part of  $\delta$  is measured at large time differences and the imaginary part for  $|\Delta t| \leq 10\tau_s$ . Fig. 8.11 shows the interference pattern

For  $f_1 = 2\pi$ ,  $f_2 = \pi^+\ell^-\nu$  or  $\pi^-\ell^+\nu$  small time differences yield  $\Delta m$ ,  $|\eta_{\pi\pi}|$  and  $\phi_{\pi\pi}$ , while at large time differences, the asymmetry in  $K_L$  semileptonic decays provides tests of  $T$  and  $CPT$ . The *vacuum regeneration* interference is shown in fig. 8.12.

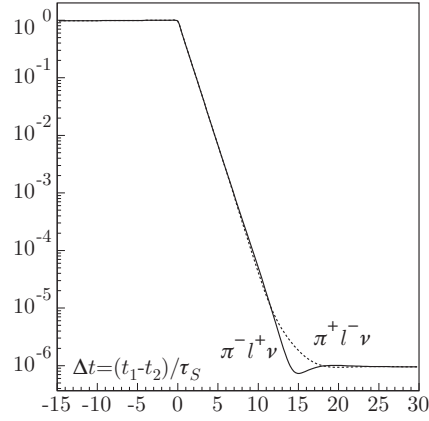


**Fig. 8.12.** Interference pattern for  $f_1 = 2\pi$ ,  $f_2 = \ell^\pm$

## 8.12 CP Violation in Other Modes

### 8.12.1 Semileptonic decays

$K$ -mesons also decay semileptonically, into a hadron with charge  $Q$  and strangeness zero, and a pair of lepton-neutrino. These decays at quark levels are due to the elementary processes

$$\begin{aligned} s &\rightarrow W^- u \rightarrow \ell^- \bar{\nu} u \\ \bar{s} &\rightarrow W^+ \bar{u} \rightarrow \ell^+ \nu \bar{u}. \end{aligned}$$

Physical  $K$ -mesons could decay as:

$$\begin{aligned} K^0 &\rightarrow \pi^- \ell^+ \nu, \quad \Delta S = -1, \quad \Delta Q = -1 \\ \bar{K}^0 &\rightarrow \pi^+ \ell^- \bar{\nu}, \quad \Delta S = +1, \quad \Delta Q = +1 \\ \bar{K}^0 &\rightarrow \pi^- \ell^+ \nu, \quad \Delta S = +1, \quad \Delta Q = -1 \\ K^0 &\rightarrow \pi^+ \ell^- \bar{\nu}, \quad \Delta S = -1, \quad \Delta Q = +1. \end{aligned}$$

In the standard model,  $SM$ ,  $K^0$  decay only to  $\ell^-$  and  $\bar{K}^0$  to  $\ell^+$ . This is commonly referred to as the  $\Delta S = \Delta Q$  rule, experimentally established in the very early days of strange particle studies. Semileptonic decays enable one to know the strangeness of the decaying meson - and for the case of pair production to “tag” the strangeness of the other meson of the pair.

Assuming the validity of the  $\Delta S = \Delta Q$  rule, the leptonic asymmetry

$$\mathcal{A}_\ell = \frac{\ell^- - \ell^+}{\ell^- + \ell^+}$$

in  $K_L$  or  $K_S$  decays is

$$2\Re\epsilon \simeq \sqrt{2}|\epsilon| = (3.30 \pm 0.03) \times 10^{-3}.$$

The measured value of  $\mathcal{A}_\ell$  for  $K_L$  decays is  $(0.327 \pm 0.012)\%$ , in good agreement with the above expectation, a proof that  $CP$  violation is, mostly, in the mass term.

In strong interactions strangeness is conserved. The strangeness of neutral  $K$ -mesons can be tagged by the sign of the charge kaon (pion) in the reaction

$$p + \bar{p} \rightarrow K^0(\bar{K}^0) + K^{-(+)} + \pi^{+(-)}.$$

### 8.13 CP violation in $K_S$ decays

$CP$  violation has only been seen in  $K_L$  decays ( $K_L \rightarrow \pi\pi$  and semileptonic decays). This is because, while it is easy to prepare an intense, pure  $K_L$  beam, thus far it has not been possible to prepare a pure  $K_S$  beam.

However, if the picture of  $\mathcal{QR}$  we have developed so far is correct, we can predict quite accurately the values of some branching ratios and the leptonic asymmetry.

It is quite important to check experimentally such predictions especially since the effects being so small, they could be easily perturbed by new physics outside the standard model.

#### 8.13.1 $K_S \rightarrow \pi^0\pi^0\pi^0$

At a  $\phi$ -factory such as DAΦNE, where  $\mathcal{O}(10^{10})$  tagged  $K_S/\gamma$  will be available, one can look for the  $\mathcal{QR}$  decay  $K_S \rightarrow \pi^0\pi^0\pi^0$ , the counterpart to  $K_L \rightarrow \pi\pi$ .

The branching ratio for this process is proportional to  $|\epsilon + \epsilon'_{000}|^2$  where  $\epsilon'_{000}$  is a quantity similar to  $\epsilon'$ , signalling direct  $CP$  violation. While  $\epsilon'_{000}/\epsilon$  might not be as suppressed as the  $\epsilon'/\epsilon$ , we can neglect it to an overall accuracy of a few %. Then  $K_S \rightarrow \pi^+\pi^-\pi^0$  is due to the  $K_L$  impurity in  $K_S$  and the expected BR is  $2 \times 10^{-9}$ . The signal at DAΦNE is at the 30 event level. There is here the possibility of observing the  $CP$  impurity of  $K_S$ , never seen before.

The current limit on  $\text{BR}(K_S \rightarrow \pi^+\pi^-\pi^0)$  is  $3.7 \times 10^{-5}$ .

#### 8.13.2 $\text{BR}(K_S \rightarrow \pi^\pm \ell^\mp \nu)$ and $\mathcal{A}_\ell(K_S)$

The branching ratio for  $K_S \rightarrow \pi^\pm \ell^\mp \nu$  can be predicted quite accurately from that of  $K_L$  and the  $K_S$ - $K_L$  lifetimes ratio, since the two amplitudes are equal assuming

*CPT* invariance. In this way we find

$$\begin{aligned}\text{BR}(K_S \rightarrow \pi^\pm e^\mp \nu) &= (6.70 \pm 0.07) \times 10^{-4} \\ \text{BR}(K_S \rightarrow \pi^\pm \mu^\mp \nu) &= (4.69 \pm 0.06) \times 10^{-4}\end{aligned}$$

The leptonic asymmetry in  $K_S$  (as for  $K_L$ ) decays is  $2\Re\epsilon = (3.30 \pm 0.03) \times 10^{-3}$ .

Some tens of leptonic decays of  $K_S$  have been seen recently by CMD-2 at Novosibirsk resulting in a value of BR of 30% accuracy, not in disagreement with expectation. The leptonic asymmetry  $\mathcal{A}_\ell$  in  $K_S$  decays is not known. At DAΦNE an accuracy of  $\sim 2.5 \times 10^{-4}$  can be obtained. The accuracy on BR would be vastly improved.

This is again only a measurement of  $\epsilon$ , not  $\epsilon'$ , but the observation for the first time of *CP* violation in two new channels of  $K_S$  decay would be nonetheless of considerable interest.

## 8.14 *CP violation in charged K decays*

Evidence for direct *CP* violation can be also be obtained from the decays of charged  $K$  mesons. *CP* invariance requires equality of the partial rates for  $K^\pm \rightarrow \pi^\pm \pi^+ \pi^-$  ( $\tau^\pm$ ) and for  $K^\pm \rightarrow \pi^\pm \pi^0 \pi^0$  ( $\tau'^\pm$ ).

With the luminosities obtainable at DAΦNE one can improve the present rate asymmetry measurements by two orders of magnitude, although *alas* the expected effects are predicted from standard calculations to be woefully small.

One can also search for differences in the Dalitz plot distributions for  $K^+$  and  $K^-$  decays in both the  $\tau$  and  $\tau'$  modes and reach sensitivities of  $\sim 10^{-4}$ . Finally, differences in rates in the radiative two pion decays of  $K^\pm$ ,  $K^\pm \rightarrow \pi^\pm \pi^0 \gamma$ , are also proof of direct *CP* violation. Again, except for unorthodox computations, the effects are expected to be very small.

## 8.15 Determinations of Neutral Kaon Properties

### 8.16 CPLEAR

The CPLEAR experiment<sup>(15)</sup> studies neutral  $K$  mesons produced in equal numbers in proton-antiproton annihilations at rest:

$$\begin{aligned}p\bar{p} \rightarrow K^- \pi^+ K^0 & \quad \text{BR} = 2 \times 10^{-3} \\ \rightarrow K^+ \pi^- \bar{K}^0 & \quad \text{BR} = 2 \times 10^{-3}\end{aligned}$$

The charge of  $K^\pm(\pi^\pm)$  tags the strangeness  $S$  of the neutral  $K$  at  $t=0$ . CPLEAR has presented several results<sup>(16,17)</sup> from studying  $\pi^+\pi^-$ ,  $\pi^+\pi^-\pi^0$  and  $\pi^\pm\ell^\mp\bar{\nu}(\nu)$  final states. Of particular interest is their measurement of the  $K_L-K_S$  mass difference  $\Delta m$  because it is independent of the value of  $\phi_{+-}$ , unlike in most other experiments.

They also obtain improved limits on the possible violation of the  $\Delta S = \Delta Q$  rule, although still far from the expected SM value of about  $10^{-7}$  arising at higher order.

The data require small corrections for background asymmetry  $\sim 1\%$ , differences in tagging efficiency,  $\varepsilon(K^+\pi^-) - \varepsilon(K^-\pi^+) \sim 10^{-3}$  and in detection,  $\varepsilon(\pi^+e^-) - \varepsilon(\pi^-e^+) \sim 3 \times 10^{-3}$ . Corrections for some regeneration in the detector are also needed.

### 8.16.1 $K^0(\bar{K}^0) \rightarrow e^+(e^-)$

Of particular interest are the study of the decays  $K^0(\bar{K}^0) \rightarrow e^+(e^-)$ . One can define the four decay intensities:

$$\left. \begin{array}{l} I^+(t) \text{ for } K^0 \rightarrow e^+ \\ \bar{I}^-(t) \text{ for } \bar{K}^0 \rightarrow e^- \end{array} \right\} \Delta S = 0$$

$$\left. \begin{array}{l} \bar{I}^+(t) \text{ for } \bar{K}^0 \rightarrow e^+ \\ I^-(t) \text{ for } K^0 \rightarrow e^- \end{array} \right\} |\Delta S| = 2$$

where  $\Delta S = 0$  or 2 means that the strangeness of the decaying  $K$  is the same as it was at  $t=0$  or has changed by 2, because of  $K^0 \leftrightarrow \bar{K}^0$  transitions. One can define four asymmetries:

$$A_1(t) = \frac{I^+(t) + \bar{I}^-(t) - (\bar{I}^+(t) + I^-(t))}{I^+(t) + \bar{I}^-(t) + \bar{I}^+(t) + I^-(t)}$$

$$A_2(t) = \frac{\bar{I}^-(t) + \bar{I}^+(t) - (I^+(t) + I^-(t))}{\bar{I}^-(t) + \bar{I}^+(t) + I^+(t) + I^-(t)}$$

$$A_T(t) = \frac{\bar{I}^+(t) - I^-(t)}{\bar{I}^+(t) + I^-(t)}, \quad A_{CPT}(t) = \frac{\bar{I}^-(t) - I^+(t)}{\bar{I}^-(t) + I^+(t)}$$

From the time dependence of  $A_1$  they obtain:  $\Delta m = (0.5274 \pm 0.0029 \pm 0.0005) \times 10^{10} \text{ s}^{-1}$ , and  $\Delta S = \Delta Q$  is valid to an accuracy of

$$(12.4 \pm 11.9 \pm 6.9) \times 10^{-3}.$$

Measurements of  $A_T$ , which they insist in calling a direct test of the validity of  $T$  but for me is just a test of  $CP$  invariance or lack of it, involves comparing  $T$  “conjugate” processes (which in fact are just  $CP$  conjugate) is now hailed as a direct measurement of  $T$  violation. The expected value for  $A_T$  is  $4 \times \Re \epsilon = 6.52 \times 10^{-3}$ . The CPLEAR result is  $A_T = (6.6 \pm 1.3 \pm 1.6) \times 10^{-3}$ . In other words, just as expected from the  $CP$  impurity of  $K$ s.

### 8.16.2 $\pi^+\pi^-$ Final State

From an analysis of  $1.6 \times 10^7$   $\pi^+\pi^-$  decays of  $K^0$  and  $\bar{K}^0$  they determine  $|\eta_{+-}| = (2.312 \pm 0.043 \pm 0.03 \pm 0.011_{\tau_S}) \times 10^{-3}$  and  $\phi_{+-} = 42.6^\circ \pm 0.9^\circ \pm 0.6^\circ \pm 0.9^\circ_{\Delta m}$ . Fig. 8.13 shows the decay intensities of  $K^0$  and  $\bar{K}^0$ .

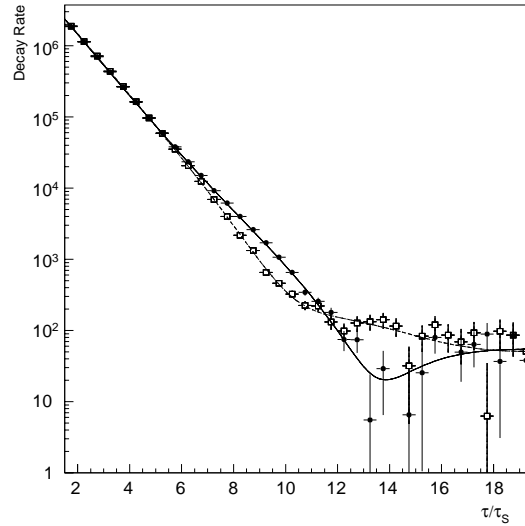


**Fig. 8.13.** Decay distributions for  $K^0$  and  $\bar{K}^0$

Fig. 8.14 is a plot of the time dependent asymmetry  $A_{+-} = (I(\bar{K}^0 \rightarrow \pi^+\pi^-) - \alpha I(K^0 \rightarrow \pi^+\pi^-)) / (I(\bar{K}^0 \rightarrow \pi^+\pi^-) + \alpha I(K^0 \rightarrow \pi^+\pi^-))$ .

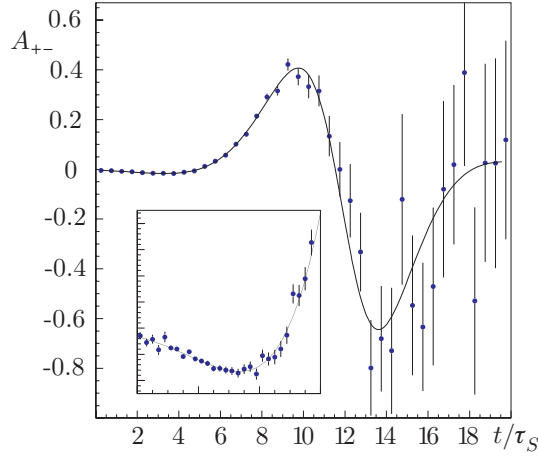


Fig. 8.14. Difference of decay distributions for  $K^0$  and  $\bar{K}^0$

## 8.17 E773 at FNAL

E773 is a modified E731 setup, with a downstream regenerator added. Results have been obtained on  $\Delta m$ ,  $\tau_S$ ,  $\phi_{00} - \phi_{+-}$  and  $\phi_{+-}$  from a study of  $K \rightarrow \pi^+ \pi^-$  and  $\pi^0 \pi^0$  decays!<sup>(18)</sup>

### 8.17.1 Two Pion Final States

This study of  $K \rightarrow \pi\pi$  is a classic experiment where one beats the amplitude  $A(K_L \rightarrow \pi\pi|_i) = \eta_i A(K_S \rightarrow \pi\pi)$  with the coherently regenerated  $K_S \rightarrow \pi\pi$  amplitude  $\rho A(K_S \rightarrow \pi\pi)$ , resulting in the decay intensity

$$I(t) = |\rho|^2 e^{-\Gamma_S t} + |\eta|^2 e^{-\Gamma_L t} + 2|\rho||\eta| e^{-\Gamma t} \cos(\Delta m t + \phi_\rho - \phi_{+-})$$

Measurements of the time dependence of  $I$  for the  $\pi^+ \pi^-$  final state yields  $\Gamma_S$ ,  $\Gamma_L$ ,  $\Delta m$  and  $\phi_{+-}$ . They give:  $\tau_S = (0.8941 \pm 0.0014 \pm 0.009) \times 10^{-10}$  s. With  $\phi_{+-} = \phi_{SW} = \tan^{-1} 2\Delta m / \Delta\Gamma$  and  $\Delta m$  free:

$$\Delta m = (0.5297 \pm 0.0030 \pm 0.0022) \times 10^{10} \text{ s}^{-1}.$$

Including the uncertainties on  $\Delta m$  and  $\tau_S$  and the correlations in their measurements they obtain:  $\phi_{+-} = 43.53^\circ \pm 0.97^\circ$

From a simultaneous fit to the  $\pi^+ \pi^-$  and  $\pi^0 \pi^0$  data they obtain  $\Delta\phi = \phi_{00} - \phi_{+-} = 0.62^\circ \pm 0.71^\circ \pm 0.75^\circ$ , which combined with the E731 result gives  $\Delta\phi = -0.3^\circ \pm 0.88^\circ$ .

### 8.17.2 $K^0 \rightarrow \pi^+ \pi^- \gamma$

From a study of  $\pi^+ \pi^- \gamma$  final states  $|\eta_{+-\gamma}|$  and  $\phi_{+-\gamma}$  are obtained. The time dependence of the this decay, like that for two pion case, allows extraction of the corresponding parameters  $|\eta_{+-\gamma}|$  and  $\phi_{+-\gamma}$ . The elegant point of this measurement is that because interference is observed (which vanishes between orthogonal states) one truly measures the ratio

$$\eta_{+-\gamma} = \frac{A(K_L \rightarrow \pi^+ \pi^- \gamma, \text{CR})}{A(K_S \rightarrow \pi^+ \pi^- \gamma, \text{CP OK})}$$

which is dominated by E1, inner bremsstrahlung transitions. Thus again one is measuring the  $CP$  impurity of  $K_L$ . Direct  $CP$  could contribute via E1, direct photon emission  $K_L$  decays, but it is not observed within the sensitivity of the measurement.

The results obtained are:<sup>(19)</sup>  $|\eta_{+-\gamma}| = (2.362 \pm 0.064 \pm 0.04) \times 10^{-3}$  and  $\phi_{+-\gamma} = 43.6^\circ \pm 3.4^\circ \pm 1.9^\circ$ . Comparison with  $|\eta_{+-}| \sim |\epsilon| \sim 2.3$ ,  $\phi_{+-} \sim 43^\circ$  gives excellent agreement. This implies that the decay is dominated by radiative contribution and that all one sees is the  $CP$  impurity of the  $K$  states.

## 8.18 Combining Results for $\Delta m$ and $\phi_{+-}$ from Different Experiments

The CPLEAR collaboration<sup>(20)</sup> has performed an analysis for obtaining the best value for  $\Delta m$  and  $\phi_{+-}$ , taking properly into account the fact that different experiments have different correlations between the two variables. The data<sup>(16,17,18,21–27)</sup> with their correlations are shown in fig. 8.15.

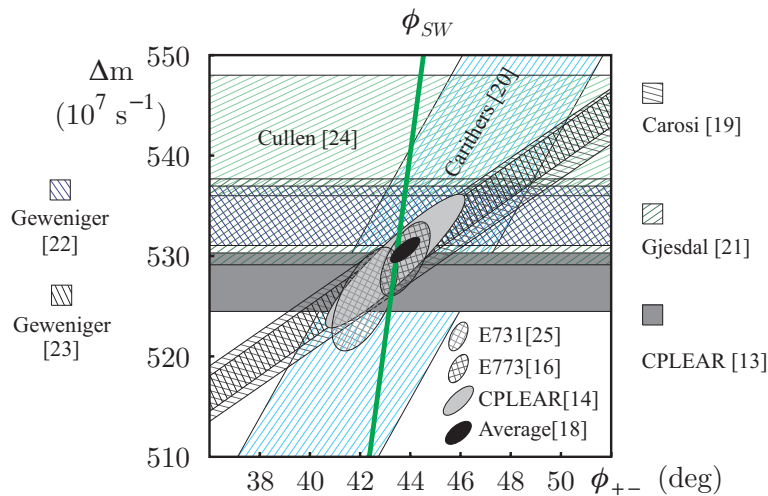


**Fig. 8.15.** A compilation of  $\Delta m$  and  $\phi_{+-}$  results, from ref. 20

A maximum likelihood analysis of all data gives

$$\begin{aligned}\Delta m &= (530.6 \pm 1.3) \times 10^7 s^{-1} \\ \phi_{+-} &= 43.75^\circ \pm 0.6^\circ.\end{aligned}$$

Note that  $\phi_{+-}$  is very close to the *superweak phase*  $\phi_{SW}=43.44^\circ\pm 0.09^\circ$ .

### 8.19 Tests of *CPT* Invariance

In local field theory, *CPT* invariance is a consequence of quantum mechanics and Lorentz invariance. Experimental evidence that *CPT* invariance might be violated would therefore invalidate our belief in either or both QM and L-invariance. We might not be so ready to abandon them, although recent ideas,<sup>(28)</sup> such as distortions of the metric at the Planck mass scale or the loss of coherence due to the properties of black holes might make the acceptance somewhat more palatable. Very sensitive tests of *CPT* invariance, or lack thereof, can be carried out investigating the neutral *K* system at a  $\phi$ -factory.

*CPT* invariance requires  $M_{11} - M_{22} = M(K^0) - M(\bar{K}^0) = 0$ . CPLEAR finds a limit for the mass difference of  $1.5 \pm 2.0 \times 10^{-18}$ . KTEV, using a combined values of the  $\tau_s$ ,  $\Delta m$ ,  $\phi_{SW}$ , and  $\Delta\phi = (-0.01 \pm 0.40)$  obtained the bound that  $(M(K^0) - M(\bar{K}^0))/\langle M \rangle = (4.5 \pm 3) \times 10^{-19}$ , with some simplifying assumptions. If we note that  $m_K^2/M_{\text{Planck}}$  is approximately a few times  $10^{-20}$  it is clear that we are probing near that region, and future experiments, especially at a  $\phi$ -factory is very welcome for confirmation.

### 8.20 Three Precision *CP* Violation Experiments

Three new experiments: NA48<sup>(29)</sup> in CERN, KTEV<sup>(30)</sup> at FNAL and KLOE<sup>(31)</sup> at LNF, have begun taking data, with the primary aim to reach an ultimate error in  $\Re(\epsilon'/\epsilon)$  of  $\mathcal{O}(10^{-4})$ .

The sophistication of these experiments takes advantage of our experience of two decades of fixed target and  $e^+e^-$  collider physics. Fundamental in KLOE is the possibility of continuous self-calibration while running, via processes like Bhabha scattering, three pion and charged *K* decays.

### 8.21 KTEV

The major improvements of KTeV are: CsI crystal calorimeter, simultaneous measurements of all four modes of interest.

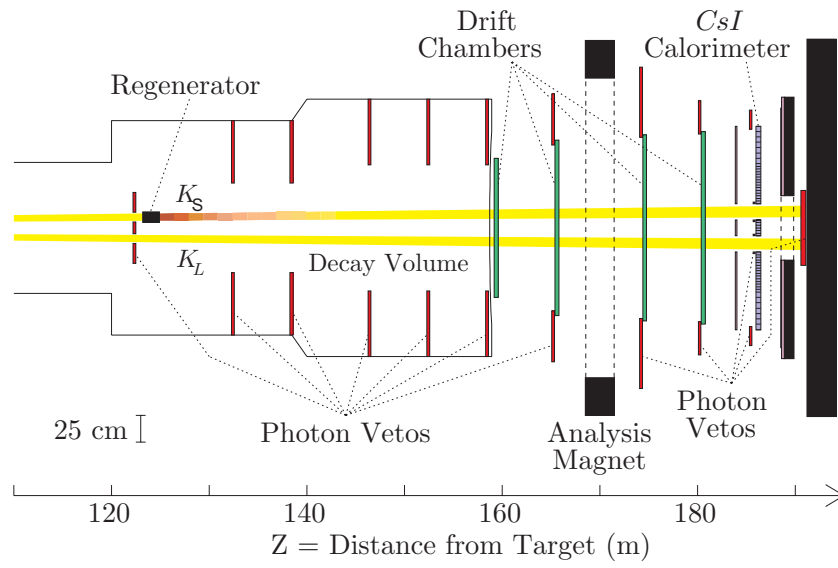


**Fig. 8.16.** Plan view of the KTeV experiment. Note the different scales.

Their result is  $\Re(\epsilon'/\epsilon) = 0.00207 \pm 0.00028$  (Jul 2001)

## 8.22 NA48

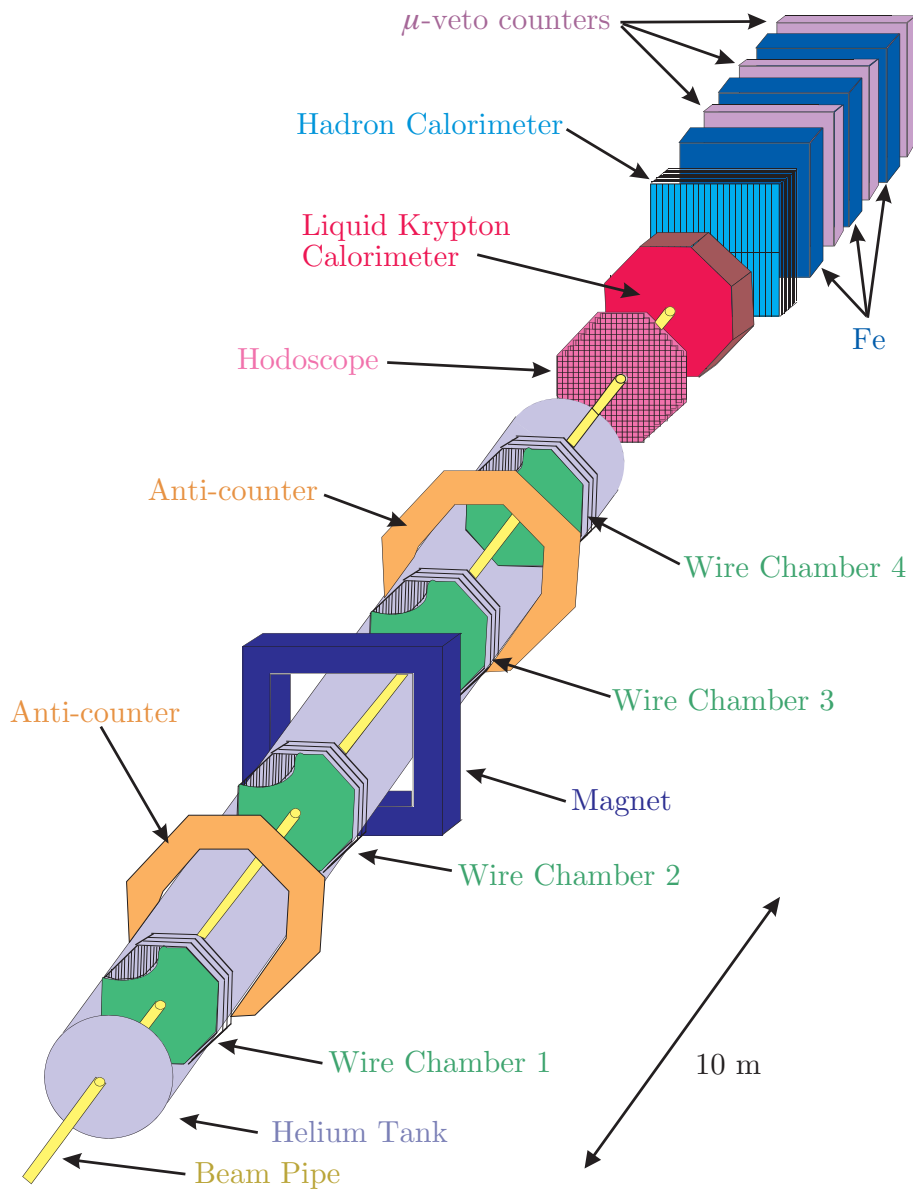


**Fig. 8.17.** The NA48 experiment at CERN

Their result is  $\Re(\epsilon'/\epsilon) = 0.00153 \pm 0.00026$  (Jul 2001)

## 8.23 KLOE

The KLOE detector<sup>(32)</sup> designed by the KLOE collaboration and under construction by the collaboration at the Laboratori Nazionali di Frascati, is shown in cross section in fig. 8.18. The KLOE detector looks very much like a collider detector and will be operated at the DAΦNE collider recently completed at the Laboratori Nazionali di Frascati, LNF.

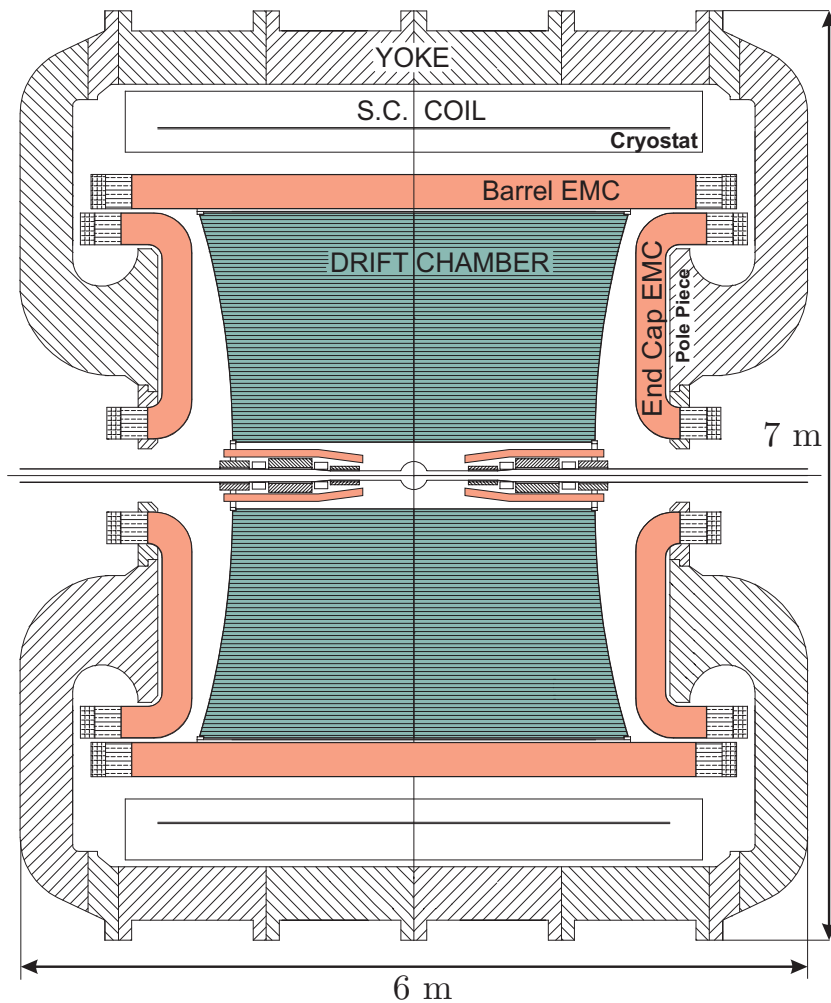


**Fig. 8.18.** Cross section of the KLOE experiment.

The main motivation behind the whole KLOE venture is the observation of direct  $CP$  violation from a measurement of  $\Re(\epsilon'/\epsilon)$  to a sensitivity of  $10^{-4}$ . A pure  $K_S$  beam is unique of  $\phi$ -factory.<sup>(33,34)</sup> A result from KLOE would be quite welcome in the present somewhat confused situation. KLOE is still waiting for DAΦNE to deliver adequate luminosity.

## 9 Quark Mixing

### 9.1 GIM and the $c$ -quark

Quite some time ago Cabibbo mixing was extended to 2 quark families  $u, d$  and  $c, s$  by GIM. In addition to defining mixing in a more formal way, GIM mixing solved the problem of the absence of the decay  $K_L \rightarrow \mu^+ \mu^-$ . All this at the cost of postulating the existence of a fourth quark, called the charm quark. The  $c$ -quark did not exist at

the time and was discovered in 1974 in an indirect way and two years later explicitly. The postulate that quarks appear on the charged weak current as

$$J_\mu^+ = (\bar{u} \ \bar{c})\gamma_\mu(1 - \gamma_5)\mathbf{V} \begin{pmatrix} d \\ s \end{pmatrix},$$

with  $\mathbf{V}$  a unitary matrix, removes the divergence in the box diagram of fig. 9.1, since the amplitudes with  $s \rightarrow u \rightarrow d$  and  $s \rightarrow c \rightarrow d$  cancel out.

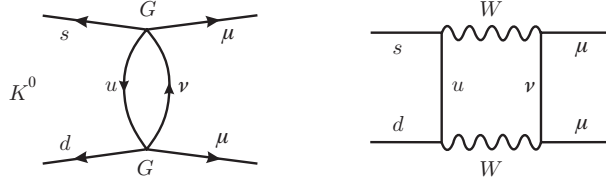


**Fig. 9.1.** Diagrams 9.1 for  $K_L \rightarrow \mu^+ \mu^-$ . Left in the Fermi four fermion style, right with the  $W$  boson. To the graph on the left we add we must add another with the  $c$  quark in place of  $u$ .

I mean 9.1. The process  $K \rightarrow \mu^+ \mu^-$  is expected to happen to second order in weak interactions, as shown in fig. 9.1 to the left. In the Fermi theory the amplitude is quadratically divergent. If however we can justify the introduction of a cut-off  $\Lambda$ , then the amplitude is computable in terms of a new effective coupling  $G_{\text{eff}} = G^2 \Lambda^2$ . The graph at right suggest that the cut-off is  $M_W$  and  $G_{\text{eff}} \sim 6 \times 10^{-7} \text{ GeV}^{-2}$ .

We compute the rates for  $K^\pm \rightarrow \mu^\pm \nu$  and  $K_L \rightarrow \mu^+ \mu^-$  from:

$$\Gamma \propto G^2 \Delta^5$$

where  $\Delta = M_K - \sum_{i=\text{out}} m_i$ . Factors as  $f_K$  and  $\sin \theta_C$  cancel in the ratio, for which we find:

$$\frac{\Gamma_{\mu\mu}}{\Gamma_{\mu\nu}} = \frac{\sim 10^{-15}}{\sim 10^{-12}} = 10^{-3}.$$

Both  $K^\pm \rightarrow \mu^\pm \nu$  and  $K \rightarrow \mu^+ \mu^-$  are (mildly) helicity suppressed. We crudely estimate in this way  $\text{BR}(\mu^+ \mu^-) \sim 10^{-3}$ , to be compared with  $\text{BR}(\mu^+ \mu^-) = 7 \times 10^{-9}$ .

## 9.2 The $K_L$ - $K_S$ mass difference and the $c$ -quark mass

We can go further and use a similar graph to describe  $K^0 \rightarrow \bar{K}^0$  transition. It becomes possible in this way to compute the  $K_S$ - $K_L$  mass difference. Again the quadratic divergence of the box diagram amplitude is removed. The low energy part of the integral over the internal momentum is however non-zero because of the  $c$  mass, where we neglect the  $u$  mass.

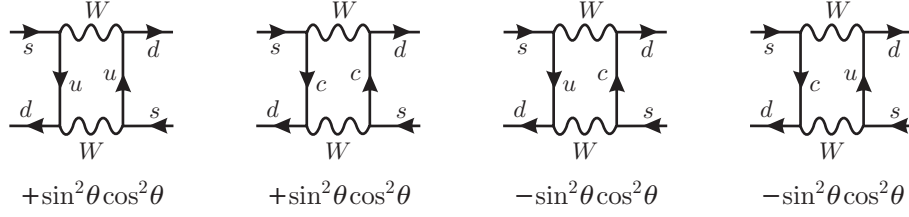


**Fig. 9.2.** The four terms of the  $K^0 \rightarrow \bar{K}^0$  amplitude in the GIM scheme.

From fig. 9.2 we can write an effective  $\Delta S = 2$  interaction for  $s\bar{d} \rightarrow d\bar{s}$  for the form:

$$\mathcal{H}_{\Delta S=2, \text{ eff}} = G_2 \bar{s} \gamma_\alpha (1 - \gamma_5) d \bar{d} \gamma_\alpha (1 - \gamma_5) s$$

with

$$G_2 = \frac{1}{16\pi^2} G^2 (m_c - m_u)^2 \sin^2 \theta \cos^2 \theta = \frac{1}{16\pi^2} G^2 m_c^2 \sin^2 \theta \cos^2 \theta$$

Finally:

$$\Delta M_{L,S} \simeq \frac{4m_c^2 \cos^2 \theta}{3\pi m_\mu^2} \Gamma(K^+ \rightarrow \mu^+ \nu)$$

from which  $m_c$  is of order of 1 GeV. The  $t$  quark does in fact contribute significantly...

### 9.3 6 quarks

The Standard Model has a *natural* place for  $CP$  violation (Cabibbo, Kobayashi and Maskawa). In fact, it is the discovery of  $CP$  violation which inspired KM<sup>(35)</sup> to expand the original Cabibbo<sup>(36)</sup> -GIM<sup>(37)</sup>  $2 \times 2$  quark mixing matrix, to a  $3 \times 3$  one, which allows for a phase and therefore for  $CP$  violation. This also implied an additional generation of quarks, now known as the  $b$  and  $t$ , matching the  $\tau$  in the SM. According to KM the six quarks charged current is:

$$J_\mu^+ = (\bar{u} \ \bar{c} \ \bar{t}) \gamma_\mu (1 - \gamma_5) \mathbf{V} \begin{pmatrix} d \\ s \\ b \end{pmatrix}$$

where  $\mathbf{V}$  is a  $3 \times 3$  unitary matrix:  $\mathbf{V}^\dagger \mathbf{V} = 1$ . Since the relative phases of the 6 quarks are arbitrary,  $\mathbf{V}$  contains 3 real parameter, the Euler angles, plus a phase factor, allowing for  $CP$ . We can easily count the number of 'rotations in the  $3 \times 3$  CKM

matrix. For the original case of Cabibbo, there is just one rotation, see fig. 9.3

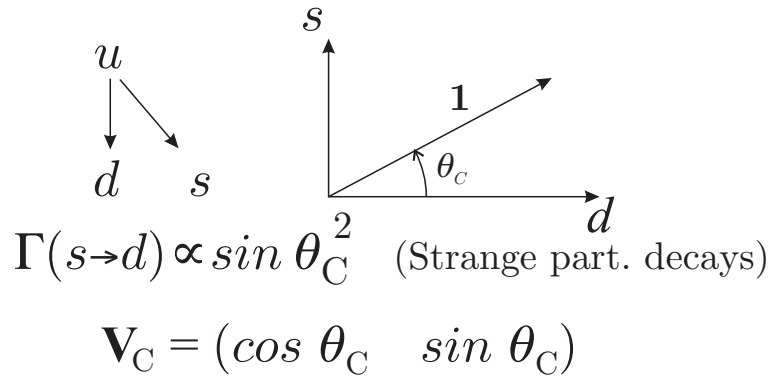


**Fig. 9.3.** Cabibbo mixing.

For the four quark case of GIM, there is still only one angle, see fig. 9.4, since the rotation is in the  $s - d$  “space”.

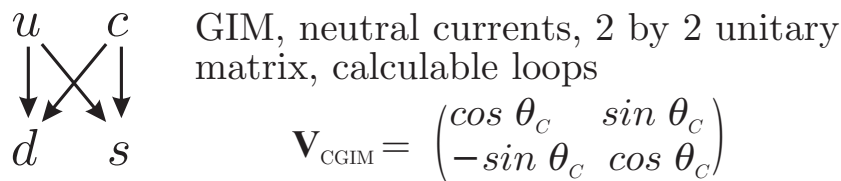


**Fig. 9.4.** GIM mixing.

The charged and neutral currents are given by

$$J_\mu^+(udcs) = \bar{u}(\cos \theta_C d + \sin \theta_C s) + \bar{c}(-\sin \theta_C d + \cos \theta_C s)$$

$$J_\mu^0 = \bar{d}d + \bar{s}s \quad - \quad \text{No FCNC: } K^0 \rightarrow \mu\mu \text{ suppression.}$$

Note that there are no flavor changing neutral currents. For six quarks we need one angle for  $b \rightarrow u$  transitions and also one for  $b \rightarrow c$  transitions, fig. 9.5. Note that there

is still a phase, which we cannot get from geometry.

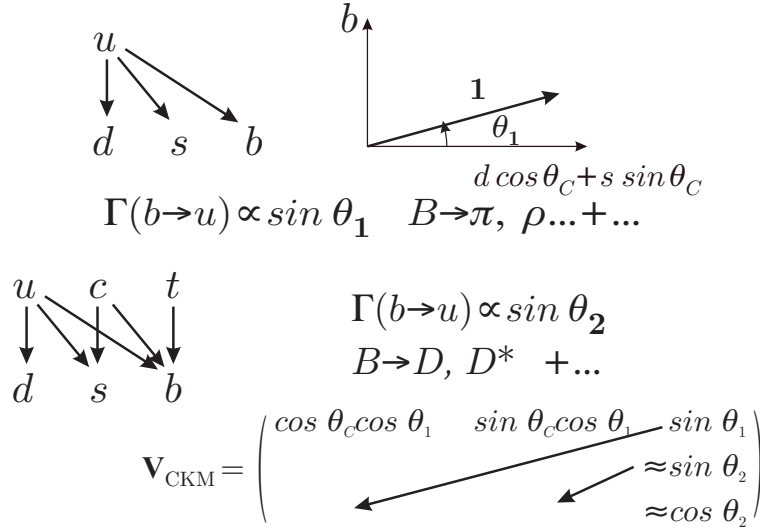


Fig. 9.5. Kobayashi and Maskawa mixing.

These geometric illustrations are justified by counting parameters in an  $n \times n$  unitary matrix.  $2n^2$  real numbers define a complex matrix, of which  $n^2$  are removed requiring unitarity.  $2n - 1$  phases are unobservable and can be reabsorbed in the definition of  $2n - 1$  quark fields. In total we are left with  $(n - 1)^2$  parameters. In  $n$  dimensions there are  $n(n - 1)/2$  orthogonal rotation angles since there are

$$n - 1 + n - 2 + \dots + 1 = n(n - 1)/2$$

planes. Thus a  $n \times n$  unitary matrix contains  $n(n - 1)/2$  rotations and  $(n - 1)(n - 2)/2$  phases. For  $n = 3$  we have three angles and one phase.

The complete form of the matrix, in the Maiani notation, is:

$$\begin{pmatrix} c_{12}c_{13} & s_{12}c_{13} & c_{13}e^{-i\delta} \\ -s_{12}c_{23} - c_{12}s_{23}s_{13}e^{i\delta} & c_{12}c_{23} - s_{12}s_{23}s_{13}e^{i\delta} & s_{23}c_{13} \\ s_{12}s_{23} - c_{12}c_{23}s_{13}e^{i\delta} & -c_{12}s_{23} - s_{12}c_{23}s_{13}e^{i\delta} & c_{23}c_{13} \end{pmatrix}$$

with  $c_{12} = \cos \theta_{12} = \cos \theta_C$ , etc.

While a phase can be introduced in the unitary matrix  $\mathbf{V}$  which mixes the quarks

$$\begin{pmatrix} d' \\ s' \\ b' \end{pmatrix} = \begin{pmatrix} V_{ud} & V_{us} & V_{ub} \\ V_{cd} & V_{cs} & V_{cb} \\ V_{td} & V_{ts} & V_{tb} \end{pmatrix} \begin{pmatrix} d \\ s \\ b \end{pmatrix},$$

the theory does not predict the magnitude of any of the four parameters. The constraint that the mixing matrix be unitary corresponds to the original Cabibbo

assumption of a universal weak interaction. Our present knowledge of the magnitude of the  $V_{ij}$  elements is given below.

$$\begin{pmatrix} 0.9745 - 0.9757 & 0.219 - 0.224 & 0.002 - 0.005 \\ 0.218 - 0.224 & 0.9736 - 0.9750 & 0.036 - 0.047 \\ 0.004 - 0.014 & 0.034 - 0.046 & 0.9989 - .9993 \end{pmatrix}$$

The diagonal elements are close but definitely not equal to unity. If such were the case there could be no  $CP$  violation. However, if the violation of  $CP$  which results in  $\epsilon \neq 0$  is explained in this way then, in general, we expect  $\epsilon' \neq 0$ . For *technical* reasons, it is difficult to compute the value of  $\epsilon'$ . Predictions are  $\epsilon'/\epsilon \leq 10^{-3}$ , but cancellations can occur, depending on the value of the top mass and the values of appropriate matrix elements, mostly connected with understanding the light hadron structure.

A fundamental task of experimental physics today is the determination of the four parameters of the CKM mixing matrix, including the phase which results in  $\mathcal{C}\mathcal{P}$ . A knowledge of all parameters is required to confront experiments. Rather, many experiments are necessary to complete our knowledge of the parameters and prove the uniqueness of the model or maybe finally break beyond it.

#### 9.4 Direct determination of the CKM parameters, $V_{us}$

The basic relation is:

$$\Gamma(K \rightarrow \pi \ell \nu) \propto |V_{us}|^2$$

From PDG

	$m$ MeV	$\Delta$ Mev	$10^7 \Gamma$ $10^7 \text{ s}^{-1}$	BR( $e3$ )	$\Gamma(e3)$ $10^6 \text{ s}^{-1}$
$K^\pm$	493.677	358.190	8.07	0.0482	3.89
error	-	-	0.19%	1.24%	1.26%
$K_L$	497.672	357.592	1.93	0.3878	7.50
error	-	-	0.77%	0.72%	1.06%

The above rates for  $K_{e3}$  determine, in principle,  $|V_{us}|^2$  to 0.8% and  $|V_{us}|$  to 0.4%. Yet in PDG

$$|V_{us}| = 0.2196 \pm 1.05\%.$$

The problem is estimating-guessing matrix element corrections due to isospin and  $SU(3)_{\text{flavor}}$  symmetry breaking. Decay rates for  $|i\rangle \rightarrow |f\rangle$  are obtained from the

transition probability density  $\bar{w}_{fi} = |T_{fi}|^2$  ( $S = 1 + iT$ ):

$$\bar{w}_{fi} = (2\pi)^4 \delta^4(p_i - p_f) (2\pi)^4 \delta^4(0) |\mathfrak{M}|^2$$

where

$$\mathfrak{M} = \langle f | \mathcal{H} | i \rangle$$

from which

$$d\Gamma = \frac{1}{8M(2\pi)^3} |\mathfrak{M}|^2 dE_1 dE_2.$$

$\Gamma(\ell 3) \propto G_F^2 \times |V_{us}|^2$  but we must deal with a few details.

1. Numerical factors equivalent to an overlap integral between final and initial state. Symmetry breaking corrections, both isospin and  $SU(3)_F$ .
2. An integral over phase space of  $|\mathfrak{M}|^2$ .
3. Experiment dependent radiative corrections. Or, bad practice, correct the data.

$$\begin{aligned} \langle \pi^0 | J_\alpha^H | K^+ \rangle &= \langle (u\bar{u} - d\bar{d})/\sqrt{2} | u\bar{u} \rangle = 1/\sqrt{2} \\ \langle \pi^- | J_\alpha^H | K^0 \rangle &= \langle d\bar{u} | d\bar{u} \rangle = 1 \\ \langle \pi^+ | J_\alpha^H | \bar{K}^0 \rangle &= \langle \bar{d}u | \bar{d}u \rangle = 1 \\ \langle \pi^+ | J_\alpha^H | K_L \rangle &= -\langle \bar{d}u | \bar{d}u \rangle/\sqrt{2} = -1/\sqrt{2} \\ \langle \pi^- | J_\alpha^H | K_L \rangle &= \langle \bar{d}u | \bar{d}u \rangle/\sqrt{2} = 1/\sqrt{2} \\ \langle \pi^+ | J_\alpha^H | K_S \rangle &= \langle \bar{d}u | \bar{d}u \rangle/\sqrt{2} = 1/\sqrt{2} \\ \langle \pi^- | J_\alpha^H | K_S \rangle &= \langle \bar{d}u | \bar{d}u \rangle/\sqrt{2} = 1/\sqrt{2} \quad (\times f_+(q^2) q_\alpha \langle J^L \rangle^\alpha \dots) \end{aligned}$$

Ignoring phase space and form factor differences:

$$\begin{aligned} \Gamma(K_L \rightarrow \pi^\pm e^\mp \bar{\nu}(\nu)) &= \Gamma(K_S \rightarrow \pi^\pm e^\mp \bar{\nu}(\nu)) \\ &= 2\Gamma(K^\pm \rightarrow \pi^0 e^\pm \bar{\nu}(\bar{\nu})) \end{aligned}$$

An approximate integration gives

$$\Gamma = \frac{G^2 |V_{us}|^2}{768\pi^3} |f_+(0)|^2 M_K^5 (0.57 + 0.004 + 0.14\delta\lambda_+)$$

with  $\delta\lambda = \lambda - 0.0288$ . Integration over phase space gives a leading term  $\propto \Delta^5$ , where  $\Delta = M_K - \sum_f(m)$  and  $(\Delta_+^5 - \Delta_0^5)/\Delta^5 = 0.008$ .

From data,  $\Gamma_0 = (7.5 \pm 0.08) \times 10^6$ ,  $2\Gamma_+ = (7.78 \pm 0.1) \times 10^6$  and  $(2\Gamma_+ - \Gamma_0)/\Sigma = (3.7 \pm 1.5)\%$ . This is quite a big difference, though only  $2\sigma$ , but typical of

violation of I-spin invariance. The slope difference is  $\sim 0.001$ , quite irrelevant. The big problem remains the  $s - u, d$  mass difference. For  $K^0$  the symmetry breaking is  $\propto (m_s - \langle m_{u,d} \rangle)^2$  in accordance with A-G. But then  $(m_s - \langle m_{u,d} \rangle)^2$  acquires dangerous divergences, from a small mass in the denominator. It is argued that it is not a real problem.

Leutwyler and Roos (1985) deal with all these points and radiative corrections. They are quoted by PDG (Gilman *et al.*, 2000), for the value of  $|V_{us}|$ . After isospin violation corrections,  $K^0$  and  $K^+$  values agree to 1%, experimental errors being 0.5%, 0.6%. Reducing the errors on  $\Gamma_+$  and  $\Gamma_0$ , coming soon from KLOE, will help understand whether we can properly compute the corrections.

## 9.5 Wolfenstein parametrization

Nature seems to have chosen a special set of values for the elements of the mixing matrix:  $|V_{ud}| \sim 1$ ,  $|V_{us}| = \lambda$ ,  $|V_{cb}| \sim \lambda^2$  and  $|V_{ub}| \sim \lambda^3$ . On this basis Wolfenstein found it convenient to parameterize the mixing matrix in a way which reflects more immediately our present knowledge of the value of some of the elements and has the  $CP$  violating phase appearing in only two off-diagonal elements, to lowest order in  $\lambda = \sin \theta_{\text{Cabibb}}$  a real number describing mixing of  $s$  and  $d$  quarks. The Wolfenstein<sup>(38)</sup> *approximate* parameterization up to  $\lambda^3$  terms is:

$$\mathbf{V} = \begin{pmatrix} V_{ud} & V_{us} & V_{ub} \\ V_{cd} & V_{cs} & V_{cb} \\ V_{td} & V_{ts} & V_{tb} \end{pmatrix} = \begin{pmatrix} 1 - \frac{1}{2}\lambda^2 & \lambda & A\lambda^3(\rho - i\eta) \\ -\lambda & 1 - \frac{1}{2}\lambda^2 & A\lambda^2 \\ A\lambda^3(1 - \rho - i\eta) & -A\lambda^2 & 1 \end{pmatrix}.$$

$A$ , also real, is close to one,  $A \sim 0.84 \pm 0.06$  and  $|\rho - i\eta| \sim 0.3$ .  $CP$  violation requires  $\eta \neq 0$ .  $\eta$  and  $\rho$  are not very well known. Likewise there is no  $\bar{C}\bar{R}$  if the diagonal elements are unity. The Wolfenstein matrix is not exactly unitary:  $V^\dagger V = 1 + \mathcal{O}(\lambda^4)$ . The phases of the elements of  $\mathbf{V}$  to  $\mathcal{O}(\lambda^2)$  are:

$$\begin{pmatrix} 1 & 1 & e^{-i\gamma} \\ 1 & 1 & 1 \\ e^{-i\beta} & 1 & 1 \end{pmatrix}$$

which defines the angles  $\beta$  and  $\gamma$ .

Several constraints on  $\eta$  and  $\rho$  can be obtained from measurements.  $\epsilon$  can be calculated from the  $\Delta S=2$  amplitude of fig. 9.6, the so called box diagram. At the quark level the calculations is straightforward, but complications arise in estimating the matrix element between  $K^0$  and  $\bar{K}^0$ . Apart from this uncertainties  $\epsilon$  depends

on  $\eta$  and  $\rho$  as  $|\epsilon| = a\eta + b\eta\rho$  a hyperbola in the  $\eta, \rho$  plane as shown in figure 9.6 which is the same as fig. 9.2 but with  $t$  quark included.

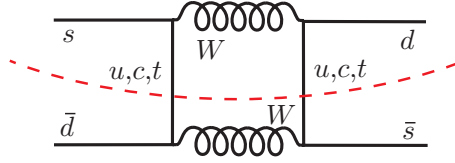


**Fig. 9.6.** Box diagram for  $K^0 \rightarrow \bar{K}^0$

The calculation of  $\epsilon'$  is more complicated. There are three  $\Delta S=1$  amplitudes that contribute to  $K \rightarrow \pi\pi$  decays, given below to lowest order in  $\lambda$  for the real and imaginary parts. They correspond to a  $u$ ,  $c$  and  $t$  quark in the loop and are illustrated in fig. 9.6, just look above the dashed line.

$$A(s \rightarrow u\bar{u}d) \propto V_{us}V_{ud}^* \sim \lambda \quad (9.1)$$

$$A(s \rightarrow c\bar{c}d) \propto V_{cs}V_{cd}^* \sim -\lambda + i\eta A^2\lambda^5 \quad (9.2)$$

$$A(s \rightarrow t\bar{t}d) \propto V_{ts}V_{td}^* \sim -A^2\lambda^5(1 - \rho + i\eta) \quad (9.3)$$

where the amplitude (9.1) correspond to the natural way for computing  $K \rightarrow \pi\pi$  in the standard model and the amplitudes (9.2), (9.3) account for direct  $\mathcal{C}\mathcal{P}$ . If the latter amplitudes were zero there would be no direct  $\mathcal{C}\mathcal{P}$  violation in the standard model. The flavor changing neutral current (FCNC) diagram of fig. 9.7 called the penguin diagram, contributes to the amplitudes (9.2), (9.3). Estimates of  $\Re(\epsilon'/\epsilon)$  range from  $\text{few} \times 10^{-3}$  to  $10^{-4}$ .

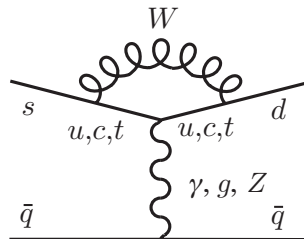


**Fig. 9.7.** Penguin diagram, a flavor changing neutral current effective operator

## 9.6 Unitary triangles

We have been practically inundated lately by very graphical presentations of the fact that the  $CKM$  matrix is unitary, ensuring the renormalizability of the  $SU(2) \otimes U(1)$

electroweak theory. The unitarity condition

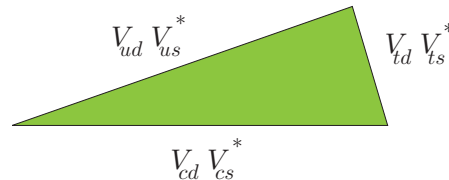
$$V^\dagger V = 1$$

contains the relations

$$\sum_i V_{ij}^* V_{ik} = \sum_i V_{ji}^* V_{ki} = \delta_{jk}$$

which means that if we take the products, term by term of any one column (row) element with the complex conjugate of another (different) column (row) element their sum is equal to 0. Geometrically it means the three terms are sides of a triangle. Two examples are shown below.

1, 2 triangle



1, 3 triangle

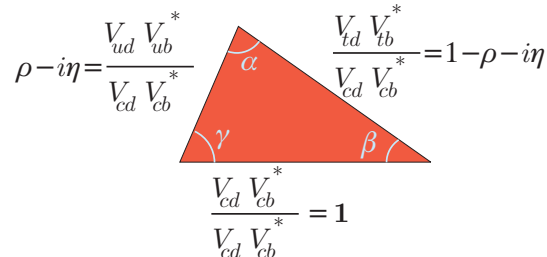


**Fig. 9.8.** The (1,2) and (1,3) Unitarity triangles

The second one has the term  $V_{cd}V_{cb}^*$  pulled out, and many of you will recognize it as a common figure used when discussing measuring  $CP$  violation in the  $B$  system.

Cecilia Jarlskog in 1984 observed that any direct  $CP$  violation is proportional to twice the area which she named  $J$  (for Jarlskog ?) of these unitary triangles, whose areas are of course are equal, independently of which rows/columns one used to form them. In terms of the Wolfenstein parameters,

$$J \simeq A^2 \lambda^6 \eta$$

which according to present knowledge is  $(2.7 \pm 1.1) \times 10^{-5}$ , very small indeed!

This number has been called the price of  $\mathcal{C}\mathcal{P}$ . Its smallness explains why the  $\epsilon'$  experiments are so hard to do, and also why  $B$  factories have to be built in order to study  $CP$  violation in the  $B$  system, despite the large value of the angles in the  $B$  unitary triangle. An illustration of why  $CP$  effects are so small in kaon decays is



case for some rare decays. A classification of measurable quantities according to increasing uncertainties in the calculation of the hadronic matrix elements has been given by Buras<sup>(39)</sup>.

1.  $\text{BR}(K_L \rightarrow \pi^0 \nu \bar{\nu})$ ,
2.  $\text{BR}(K^+ \rightarrow \pi^+ \nu \bar{\nu})$ ,
3.  $\text{BR}(K_L \rightarrow \pi^0 e^+ e^-)$ ,  $\epsilon_K$ ,
4.  $\epsilon'_K$ ,  $\text{BR}(K_L \rightarrow \mu \bar{\mu}]_{\text{SD}})$ , where SD=*short distance* contributions.

The observation  $\epsilon' \neq 0$  remains a unique proof of direct  $\mathcal{C}\mathcal{P}$ . Measurements of 1 through 3, plus present knowledge, over determine the CKM matrix.

Rare  $K$  decay experiments are not easy. Typical expectations for some BR's are:

$$\begin{aligned} \text{BR}(K_L \rightarrow \pi^0 e^+ e^-) \text{, } \mathcal{C}\mathcal{P}[\text{dir}] &\sim (5 \pm 2) \times 10^{-12} \\ \text{BR}(K_L \rightarrow \pi^0 \nu \bar{\nu}) &\sim (3 \pm 1.2) \times 10^{-11} \\ \text{BR}(K^+ \rightarrow \pi^+ \nu \bar{\nu}) &\sim (1 \pm .4) \times 10^{-10} \end{aligned}$$

Note that the uncertainties above reflect our ignorance of the mixing matrix parameters, not uncertainties on the hadronic matrix element which essentially can be "taken" from  $K_{\ell 3}$  decays.

The most extensive program in this field has been ongoing for a long time at BNL and large statistics have been collected recently and are under analysis. Sensitivities of the order of  $10^{-11}$  will be reached, although  $10^{-(12 \text{ or } 13)}$  is really necessary. Experiments with high energy kaon beams have been making excellent progress toward observing rare decays.

## 9.8 Search for $K^+ \rightarrow \pi^+ \nu \bar{\nu}$

This decay,  $CP$  allowed, is best for determining  $V_{td}$ . At present after analyzing half of their data, E781-BNL obtains BR is about  $2.4 \times 10^{-10}$ . This estimate is based on ONE event which surfaced in 1995 from about  $2.55 \times 10^{12}$  stopped kaons. The  $SM$  expectation is about half that value. Some 100 such decays are enough for a first  $V_{td}$  measurements.

## 9.9 $K_L \rightarrow \pi^0 \nu \bar{\nu}$

This process is a "pure" direct  $\mathcal{C}\mathcal{P}$  signal. The  $\nu \bar{\nu}$  pair is an eigenstate of  $CP$  with eigenvalue  $-1$ . Thus  $CP$  is manifestly violated.

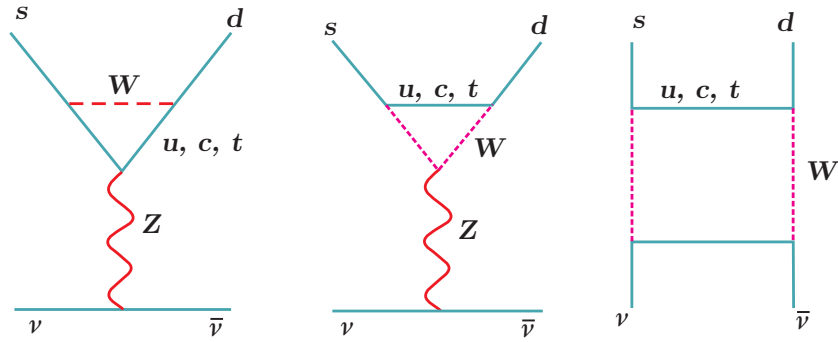


Fig. 9.11. Feynman Diagrams for  $K_L \rightarrow \pi^0 \nu \bar{\nu}$

It is theoretically particularly “pristine”, with only about 1-2% uncertainty, since the *hadronic* matrix element need not be calculated, but is directly obtained from the measured  $K_{\ell 3}$  decays. Geometrically we see it as being the altitude of the  $J_{12}$  triangle.

$$J_{12} = \lambda(1 - \lambda^2/2)\Im(V_{td}V_{ts}^*) \approx 5.6[B(K_L \rightarrow \pi^0 \nu \bar{\nu})]^{1/2}$$

The experimental signature is just a single unbalanced  $\pi^0$  in a hermetic detector. The difficulty of the experiment is seen in the present experimental limit from E799-I,  $\text{BR} <_{\text{pt}5.8, -5, .}$ . The sensitivities claimed for E799-II and at KEK are around  $10^{-9}$ , thus another factor of 100 improvement is necessary. The new FNAL and BNL proposals at the main injector are very ambitious. There is “hope” to make this measurement a reality early in the third millenium.

## 9.10 B decays

### 9.10.1 Introduction

The discovery at Fermilab, in 1977, of the  $\Upsilon$ , with mass of  $\sim 10$  GeV, was immediately taken as proof of the existense of the  $b$  quark, heralded by KM and already so christened:  $b$  for beauty or bottom. The  $b$  quark has  $B$  flavor  $B=-1$ . The fourth  $\Upsilon$  is barely above threshold for decayng into a  $B\bar{B}$  pair, where the  $B$  meson are  $b\bar{u}$ ,  $b\bar{d}$  and their charge conjugate states, in complete analogy to charged and neutral kaons.  $B^0$  and  $\bar{B}^0$  are not self conjugate states. That the  $\Upsilon(4S)$  decays only to  $B^0\bar{B}^0$  pairs was demonstrated by CUSB searching (and not finding) low energy photons from  $B^*$  decays.  $B^0\bar{B}^0$ 's are produced in a  $C$ -odd state as  $K^0\bar{K}^0$  and can be used for  $CP$  studies in the  $B$  system, once the short  $B$  lifetime problem is overcome. CUSB also determined the thresholds for  $B^*B$ ,  $B^*B^*$ ,  $B_s\bar{B}_s$  etc. production.<sup>(40)</sup>

### 9.11 B semileptonic decays

Because of their massiveness,  $B$ 's can decay - weakly - into many more channels than the  $K$ 's. We might recall that we owe the long lifetime of the  $K_L$  to the smallness of the phase space for 3 body decays. The average particle multiplicity in the decay of  $B$  and  $\bar{B}$  is about six. The leptonic modes have a branching ratio of about 25%, with a unique signature, namely a lepton with energy up to half that of the parent  $\Upsilon$ . It was infact through the observation of the sudden appearance of high energy electrons that the existence of the  $b$  quark was unambiguously proved in 1980, since the  $\Upsilon$  after all has  $B=0$ . At quark level beauty decays are:  $b \rightarrow c\ell^-\bar{\nu}$  and  $b \rightarrow u\ell^-\bar{\nu}$  with the selection rule  $\Delta B=\Delta Q$ .  $\bar{b}$  decay to positive leptons.

The endpoint of the lepton spectrum and its shape depend on the flavor of the hadronic system appearing in the final state. We define as  $X_c$  a hadronic system with charm  $C = \pm 1$  and  $U=0$  where  $U$  is the *uppityness*. Likewise  $X_u$  has  $U = \pm 1$  and  $C=0$ . The leptonic decays are:

$$B \rightarrow \ell^\pm + \nu(\bar{\nu}) + X_c$$

$$B \rightarrow \ell^\pm + \nu(\bar{\nu}) + X_u$$

where  $X_c=D, D^* \dots$  with  $\bar{M}(X_c)\sim 2$  GeV and  $X_u=\pi, \rho..$  with  $\bar{M}(X_u)\sim 0.7$  GeV. The expected lepton spectra are shown in figure 9.12.

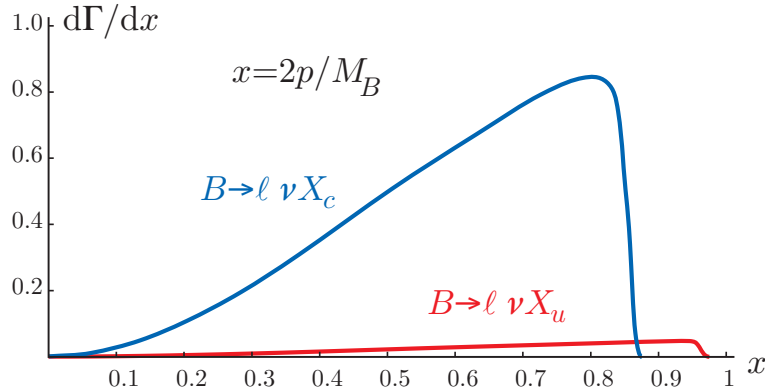


**Fig. 9.12.** Leptonic Spectrum in  $B$  semileptonic decays.

Total decay rates, *i.e.* the inverse of the lifetimes, and branching ratios of  $B$  mesons provide the determination of  $|V_{cb}|$  and  $|V_{ub}|$ . A preferred way is to measure the semileptonic branching ratio by integrating over the whole spectrum. An early determination by CUSB already indicated that  $|V_{ub}/V_{cb}|$  is very small, less than 0.06. However, uncertainties in the calculation of the hadronic matrix elements and the shape of the spectrum near the end pont introduce errors in the extraction of

$|V_{ub}/V_{cb}|$ . Methods (HQET) have been developed to make use of exclusive channels, a good twenty years has been spent in refining such measurements, which still need to be improved!

## 9.12 $B\bar{B}$ Mixing

### 9.12.1 discovery

Just as with  $K$ -mesons, neutral  $B$  mesons are not  $C$  eigenstates and can mix, i.e, transitions  $B^0 \leftrightarrow \bar{B}^0$  are possible. The first observation of mixing was reported by Argus at the DESY DORIS collider running on the  $\Upsilon(4S)$ .

They observed mixing by comparing the  $\ell^+\ell^+$  and  $\ell^-\ell^-$  decay rates from  $B\bar{B}$  pairs. Defining the ratio

$$r = \frac{\ell^+\ell^+ + \ell^-\ell^-}{\ell^+\ell^- + \ell^-\ell^+ + \ell^+\ell^+ + \ell^-\ell^-}$$

$r \neq 0$  is proof of mixing, not however of  $\mathcal{C}\mathcal{P}$ . Today, instead of  $r$ , the  $\chi_d$  parameter, which is a measure of the time-integrated  $B^0$ - $\bar{B}^0$  mixing probability that a produced  $B^0$  ( $\bar{B}^0$ ) decays as  $\bar{B}^0$  ( $B^0$ ), is used. They are related simply by  $r = \chi_d/(1 - \chi_d)$ . The present value of  $\chi_d$  is  $0.172 \pm 0.01$ .

### 9.12.2 Formalism

We define, analogously to the  $K^0\bar{K}^0$  system,

$$\begin{aligned} B_L &= p|B^0\rangle + q|\bar{B}^0\rangle \\ B_H &= p|B^0\rangle - q|\bar{B}^0\rangle \end{aligned}$$

with  $p^2 + q^2 = 1$ . Here L, H stand for light and heavy. The  $B_d$ 's also have different masses but very similar decay widths.

Mixing is calculated in the SM by evaluating the standard ‘‘box’’ diagrams with intermediate  $u, c, t$  and  $W$  states. We define:

$$\Delta M = M_H - M_L, \quad \Delta\Gamma = \Gamma_H - \Gamma_L$$

note that  $\Delta M$  is positive by definition. The ratio  $q/p$  is given by:

$$\begin{aligned} q/p &= (\Delta M - i/2\Delta\Gamma)/2(M_{12} - i/2\Gamma_{12}) = \\ &= 2(M_{12}^* - i/2\Gamma_{12}^*)/(\Delta M - i/2\Delta\Gamma) \end{aligned}$$

where

$$\Gamma_{12} \propto [V_{ub}V_{ud}^* + V_{cb}V_{cd}^*]^2 m_b^2 = (V_{tb}V_{td}^*)^2 m_b^2$$

and  $M_{12} \propto (V_{tb}V_{td}^*)^2 m_t^2$ , so they have almost the same phase.  $x$  and  $y$ , for  $B_d$  and  $B_s$  mesons are:

$$x_{d,s} = \Delta M_{d,s}/\Gamma_{d,s}, \quad y_{d,s} = \Delta\Gamma_{d,s}/\Gamma_{d,s}$$

$y_d$  is less than  $10^{-2}$ , and  $x_d$  is about 0.7, and if we ignore the width difference between the two  $B_d$  states,

$$\left. \frac{q}{p} \right|_{B_d} \approx \frac{(V_{tb}^*V_{td})}{(V_{tb}V_{td}^*)} = e^{-2i\beta}$$

Therefore  $|q/p|_d$  is very close to 1 and since  $2\Re\epsilon_{B_d} \approx 1 - |q/p|_d$ ,  $\epsilon_{B_d}$  is imaginary.  $y_s$  is about 0.2, and  $x_s$  theoretically could be as large as 20, so far only lower bounds are quoted.

$\chi_d$  as defined before, in terms of  $q, p, x, y$  is

$$\chi_d = \frac{1}{2} \left| \frac{q}{p} \right|^2 \frac{x_d^2 - y_d^2/4}{(1 + x_d^2)(1 - y_d^2/4)}$$

which reduces to a good approximation:

$$\chi_d = \frac{x_d^2}{2(1 + x_d^2)},$$

from which one obtains that  $x_d = 0.723 \pm 0.032$ .

In summary, from evaluating the box diagrams, one finds:

$$x_l \propto m_t^2 \tau_{B_l} m_{B_l} |V_{tl}V_{tb}^*|^2.$$

where the subscript  $l$  refers to the light meson partner which makes up the  $B$  meson, i.e.  $l = s$  or  $d$ .<sup>(41)</sup>

An amusing historical note. The surprisingly large amount of mixing seen required that the top mass be larger than the then acceptable value of about 20 GeV. Stretching beyond reason the limits for  $|V_{ub}|$  and the value of  $r$  than known, a lower limit  $M_{\text{top}} \geq 40$  GeV was obtained. The first CUSB limit on  $|V_{ub}|$  already implied  $M_{\text{top}} > 120$  MeV. Theorists were at that time still misled by prejudice and intimidated by very wrong results experimental findings and only had the courage to claim a top mass of  $\sim 40$  GeV.

Using the top mass today known, and  $\Delta M$  measured from the  $B^0\bar{B}^0$  oscillation frequency from experiments at FNAL and LEP, one obtains the estimates  $|V_{td}| = (8.4 \pm 1.4) \times 10^{-3}$  and  $\Im(V_{td}V_{tb}^*) = (1.33 \pm 0.30) \times 10^{-4}$ .

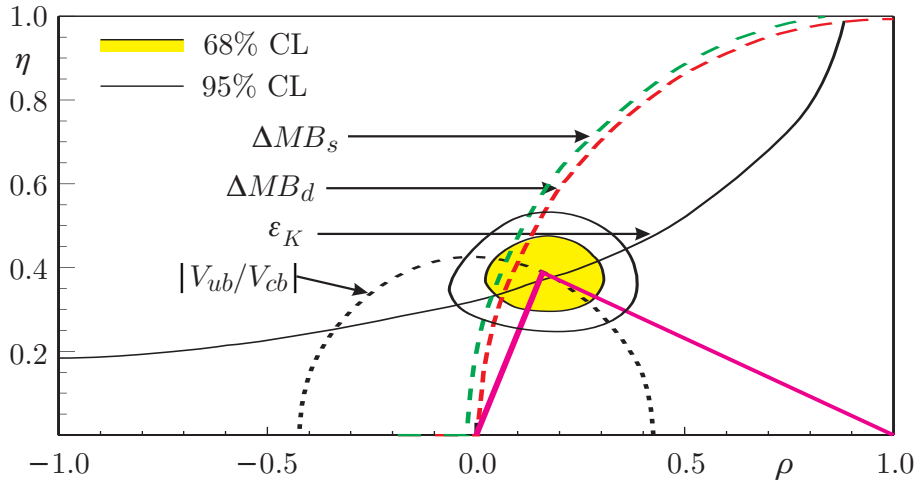


**Fig. 9.13.** Fit to data in the  $\eta$ - $\rho$  plane.

From a fit, shown in fig. 9.13, Parodi *et al.*<sup>(42)</sup> obtain

$$\sin 2\beta = 0.71 \pm 0.13, \quad \sin 2\gamma = 0.85 \pm 0.15.$$

Of course the whole point of the exercise is to measure directly  $\eta$  and  $\rho$  and then verify the uniqueness of the mixing matrix.

### 9.13 CP Violation

Semileptonic decays of  $B$ s allow, in principle, to observe  $\mathcal{C}\mathcal{R}$  by studying the dilepton and total lepton charge asymmetries. This however has turned to be rather difficult because of the huge background and so far yielded no evidence for  $\mathcal{C}\mathcal{R}$  in  $B$ .

We can estimate the magnitude of the leptonic asymmetry from

$$4\Re\epsilon_B = \Im\left(\frac{\Gamma_{12}}{M_{12}}\right) = \frac{|\Gamma_{12}|}{|M_{12}|} \text{Arg}\left(\frac{\Gamma_{12}}{M_{12}}\right)$$

or approximately

$$\frac{m_b^2}{m_t^2} \times \frac{m_c^2}{m_b^2}$$

which is  $\mathcal{O}(10^{-4})$ .

#### 9.13.1 $\alpha$ , $\beta$ and $\gamma$

Sensitivity to  $CP$  violation in the  $B$  system is usually discussed in terms of the 3 interior angles of the  $U_{13}$  triangle.

$$\alpha = \text{Arg}\left(-\frac{V_{td}V_{tb}^*}{V_{ud}V_{ub}^*}\right) \quad \beta = \text{Arg}\left(-\frac{V_{cd}V_{cb}^*}{V_{td}V_{tb}^*}\right) \quad \gamma = \text{Arg}\left(-\frac{V_{ud}V_{ub}^*}{V_{cd}V_{cb}^*}\right)$$

The favorite measurements are asymmetries in decays of neutral  $B$  decays to  $CP$  eigenstates.  $f_{CP}$ , in particular  $J/\psi(1S)K_S$  and possibly  $\pi\pi$ , which allow a clean connection to the CKM parameters. The asymmetry is due to interference of the amplitude  $A$  for  $B^0 \rightarrow J/\psi K_S$  with the amplitude  $A'$  for  $B^0 \rightarrow \bar{B}^0 \rightarrow J/\psi K_S$ .

As in the case in the  $K$  system, direct  $\mathcal{C}\mathcal{P}$  needs interference of two different amplitudes, more precisely amplitudes with different phases. If  $A$  is the amplitude for decay of say a  $B^0$  to a  $CP$  eigenstate, given by  $A = \sum_i A_i e^{i(\delta_i + \phi_i)}$ , the amplitude  $\bar{A}$  for the  $CP$  conjugate process is  $\bar{A} = \sum_i A_i e^{i(\delta_i - \phi_i)}$ . The strong phases  $\delta$  do not change sign while the weak phases ( $CKM$  related) do. Direct  $CP$  violation requires  $|A| \neq |\bar{A}|$ , while indirect  $CP$  violation only requires  $|q/p| \neq 1$ .

The time-dependent  $CP$  asymmetry is:

$$\begin{aligned} a_{f_{CP}}(t) &\equiv \frac{I(B^0(t) \rightarrow J/\psi K_S) - I(\bar{B}^0(t) \rightarrow J/\psi K_S)}{I(B^0(t) \rightarrow J/\psi K_S) + I(\bar{B}^0(t) \rightarrow J/\psi K_S)} \\ &= \frac{(1 - |\lambda_{f_{CP}}|^2) \cos(\Delta Mt) - 2\Im(\lambda_{f_{CP}}) \sin(\Delta Mt)}{1 + |\lambda_{f_{CP}}|^2} \\ &= \Im \lambda_{f_{CP}} \sin(\Delta Mt) \end{aligned}$$

with

$$\lambda_{f_{CP}} \equiv (q/p)(\bar{A}_{f_{CP}}/A_{f_{CP}}), \quad |\lambda_{f_{CP}}| = 1.$$

In the above,  $B^0_{(t)}$  ( $\bar{B}^0_{(t)}$ ) is a state tagged as such at time  $t$ , for instance by the sign of the decay lepton of the other meson in the pair.

The time integrated asymmetry, which vanishes at a  $B$ -factory because the  $B^0\bar{B}^0$  pair is in a  $C$ -odd state, is given by

$$a_{f_{CP}} = \frac{I(B^0 \rightarrow J/\psi K_S) - I(\bar{B}^0 \rightarrow J/\psi K_S)}{I(B^0 \rightarrow J/\psi K_S) + I(\bar{B}^0 \rightarrow J/\psi K_S)} = \frac{x}{1+x^2} \Im \lambda_{f_{CP}}$$

Staring at box diagrams, with a little poetic license one concludes

$$a_{f_{CP}} \propto \Im \lambda_{f_{CP}} = \sin 2\beta.$$

or

$$a_{f_{CP}} \approx 0.5 \sin 2\beta \sim 1$$

The license involves ignoring penguins, which is probably OK for the decay to  $J/\psi K_S$ , presumably a few % correction.

For the  $\pi\pi$  final state, the argument is essentially the same. However the branching ratio for  $B \rightarrow \pi\pi$  is extraordinarily small and penguins *are* important. The asymmetry is otherwise proportional to  $\sin(2\beta + 2\gamma) = -\sin 2\alpha$ . Here we assume  $\alpha + \beta + \gamma = \pi$ , which is something that we would instead like to prove. The angle  $\gamma$

can be obtained from asymmetries in  $B_s$  decays and from mixing, measurable with very fast strange  $B_s$ .

## 9.14 CDF and DØ

CDF at the Tevatron is the first to profit from the idea suggested first by Toni Sanda, to study asymmetries in the decay of tagged  $B^0$  and of  $\bar{B}^0$  to a final state which is a  $CP$  eigenstate. They find

$$\sin 2\beta = 0.79_{-0.44}^{+0.41}, \quad 0.0 \leq \sin 2\beta < 1 \quad \text{at 93\% CL}$$

Their very lucky central value agrees with the aforementioned SM fit, but there is at least a two fold ambiguity in the determination of  $\beta$  which they can not differentiate with their present errors. In the coming Tevatron runs, CDF not only expect to improve the determinations of  $\sin 2\beta$  by a factor of four, so  $\delta \sin 2\beta \approx 0.1$ , but to measure  $\sin(2\alpha)$  from using the asymmetry resulting from  $B^0 \rightarrow \pi^+\pi^-$  interfering with  $\bar{B}^0 \rightarrow \pi^+\pi^-$  to a similar accuracy. Being optimistic, they hope to get a first measurement of  $\sin(\gamma)$  by using  $B_s^0/\bar{B}_s^0 \rightarrow D_s^\pm K^\mp$  from about 700 signal events.

DØ will have the same sensitivity

## 9.15 B-factories

In order to overcome the short  $B$  lifetime problem, and still profit from the coherent state property of  $B$ 's produced on the  $\Upsilon(4S)$ , two asymmetric  $e^+e^-$  colliders have been built, PEP-II and KEKB. The two colliders both use a high energy  $\approx 9$  GeV beam colliding against a low energy,  $\approx 3.1$  GeV, beam so that the center of mass energy of the system is at the  $\Upsilon(4S)$  energy, but the  $B$ 's are boosted in the laboratory, so they travel detectable distances before their demise. In order to produce the large number of  $B^0\bar{B}^0$  pairs, the accelerators must have luminosities on the order of  $3 \times 10^{33} \text{ cm}^{-2}\text{s}^{-1}$ , about one orders of magnitude that of CESR. Both factories have in fact achieved luminosities of  $2 \times 10^{33} \text{ cm}^{-2} \text{ s}^{-1}$  and in SLAC Babar collects  $120 \text{ pb}^{-1}$  per day while Belle gets around 90. Both experiments will have 40% measurements of  $\beta$  by summer 2000 and reach higher accuracy if and when the colliders will achieve and surpass luminosities of  $10^{34}$ .

$B$ -factories will likely provide the best measurements of  $|V_{cb}|$  and  $|V_{cb}|$ .

## 9.16 LHC

The success of CDF shows that LHCb, BTeV, ATLAS and CMS will attain, some day, ten times better accuracy than the almost running ones (including Belle and Babar), so bear serious watching. In particular the possibility of studying very high energy strange B's,  $B_s$  will allow to measure the mixing oscillation frequency which was not possible at LEP.

## 9.17 $CP$ , kaons and $B$ -mesons: the future

$CP$  violation,  $\mathcal{C}\mathcal{P}$  in the following, was discovered in neutral  $K$  decays about 36 years ago, in 1964.<sup>(41)</sup> Two important observations about  $\mathcal{C}\mathcal{P}$  were to follow in the next 10 years. In 1967 Andrej Sakharov<sup>(43)</sup> gave the necessary conditions for baryogenesis: baryon number violation,  $C$  and  $CP$  violation, thermal non-equilibrium. Finally in 1973, Kobayashi and Maskawa<sup>(35)</sup> extended the 1963 mixing idea of Nicola Cabibbo<sup>(36)</sup> and the GIM<sup>(37)</sup> four quark idea to three quark families, noting that  $\mathcal{C}\mathcal{P}$  becomes possible in the standard model.

Since those days  $\mathcal{C}\mathcal{P}$  has been somewhat of a mystery, only observed in kaon decays. While the so-called CKM mixing matrix allows for the introduction of a phase and thus  $\mathcal{C}\mathcal{P}$ , the standard model does not predict its parameters. It has taken 35 years to be able to prove experimentally that  $\Re(\epsilon'/\epsilon) \neq 0$  and quite a long time also to learn how to compute the same quantity from the CKM parameters. In the last few years calculations<sup>(44)</sup> had led to values of  $\Re(\epsilon'/\epsilon)$  of  $\mathcal{O}((4-8) \times 10^{-4})$  with errors estimated to be of the order of the value itself. Experimental results are in the range  $(12-27) \times 10^{-4}$  with errors around 3-4 in the same units. This is considered a big discrepancy by some authors. More recently it has been claimed<sup>(45)</sup> that  $\Re(\epsilon'/\epsilon)$  could well reach values greater than  $20 \times 10^{-4}$ . I would like to discuss in more general terms the question of how to test whether the standard model is consistent with  $\mathcal{C}\mathcal{P}$  observations independently of the value of  $\Re(\epsilon'/\epsilon)$  and where can we expect to make the most accurate measurements in the future.

Quite some time ago by Bjorken introduced the unitarity triangles. Much propaganda has been made about the “ $B$ -triangle”, together with claims that closure of the triangle could be best achieved at  $B$ -factories in a short time. This has proved to be over optimistic, because hadronic complications are in fact present here as well. Cecilia Jarlskog<sup>(46)</sup> has observed that  $\mathcal{C}\mathcal{P}$  effects are proportional to a factor  $J$  which is twice the area of any of the unitarity triangles.  $J$ , called the price of  $\mathcal{C}\mathcal{P}$  by Fred Gilman, does not depend on the representation of the mixing matrix we

use.

In the Wolfenstein approximate parametrization  $J = \lambda^6 A^2 \eta$ , as easily verified. The  $K$  or 1,2 and  $B$  or 1,3 triangles have been shown. The 2,3 triangle is also interesting. In the above  $\lambda=0.2215\pm 0.0015$  is the sine of the Cabibbo angle (up to  $V_{ub}^2 \sim 10^{-5}$  corrections), a real number describing mixing of  $s$  and  $d$  quarks, measured in  $K$  decays since the early days.  $A$ , also real, is obtained from the  $B \rightarrow D \dots$  together with the  $B$ -meson lifetime and is close to one,  $A \sim 0.84 \pm 0.06$ . From  $b \rightarrow u$  transitions  $|\rho - i\eta| \sim 0.3$ .

Present knowledge about  $J$  is poor,  $J = 2.7 \pm 1.1 \times 10^{-5}$ , *i.e.*  $\sim 40\%$  accuracy.  $J$  is a small number and as such subject to effects beyond present physics. The important question is where and when can we expect to get more precise results. Lets call  $J_{mn}$  the area of the triangles corresponding to the  $m^{\text{th}}$  and  $n^{\text{th}}$  columns of  $\mathbf{V}$ .  $J_{12}$  is measured in  $K$  decays<sup>(47)</sup> including  $\lambda^2$  corrections:

$$J_{12} = \lambda(1 - \lambda^2/2)\Im V_{td}V_{ts}^*$$

where the first piece is  $0.219 \pm 0.002$  and the last is equal to  $25.6 \times \sqrt{\text{BR}(K^0 \rightarrow \pi^0 \nu \bar{\nu})}$ . There are no uncertainties in the hadronic matrix element which is taken from  $K_{l3}$  decays.

While the branching ratio above is small,  $3 \times 10^{-11}$ , it is the most direct and clean measure of  $\eta$ , the imaginary part of  $V_{td}$  and  $V_{ub}$ . 100 events give  $J_{12}$  to 5% accuracy! Then the SM can be double checked *e.g.* comparing with  $\epsilon$ , and  $K^+ \rightarrow \pi^+ \nu \bar{\nu}$ , as shown in fig. 9.14 and  $\Re(\epsilon'/\epsilon)$  will be measured and computed to better accuracy.

$B$  decays give  $J_{13}$  from  $|V_{cb}|$ ,  $|V_{ub}|$ ,  $B - \bar{B}$  mixing,  $B \rightarrow J/\psi K$ ,  $B \rightarrow \pi\pi$ . Long terms goals are here 2-3 % accuracy in  $|V_{cb}|$ , 10% for  $|V_{ub}|$ ,  $\sin 2\beta$  to 0.06 and  $\sin 2\alpha$  to 0.1. CDF, who has already measured  $\sin 2\beta$  to 50%, and DØ at FNAL<sup>(48)</sup> offer the best promise for  $\sin 2\beta$ .  $B$ -factories will also contribute, in particular to the measurements of  $|V_{cb}|$  and  $|V_{ub}|$ . It will take a long time to reach 15% for  $J_{13}$ . LHC, with good sensitivity to  $B_s - \bar{B}_s$  mixing, will reach 10% and perhaps 5%.

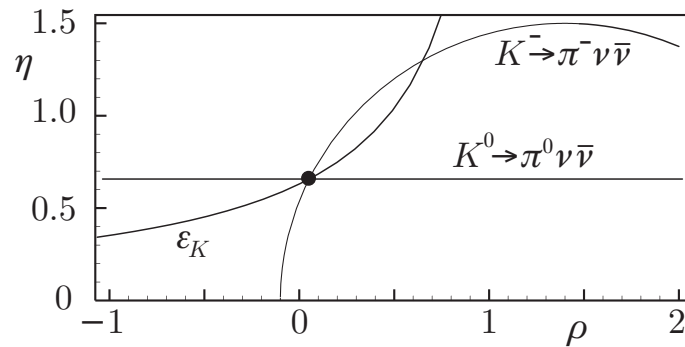


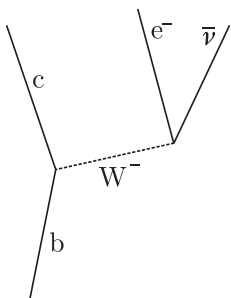
**Fig. 9.14.** Constraints in  $K$  decays.

The branching ratio for  $K^0 \rightarrow \pi^0 \nu \bar{\nu}$  is not presently known. The experience for performing such a measurement is however fully in hand. The uniquely precise way by which this ratio determines  $\eta$ , makes it one of the first priorities of particle physics, at this time. Compared to the very large investments in the study of the  $B$  system, it is a most competitive way of obtaining fundamental and precise results at a small cost.

## 10 The Weak Interaction. III

### 10.1 Beauty Decays

In the following we integrate the four Fermion effective coupling, over the neutrino energies, to obtain the electron spectrum and then over the electron momentum to obtain the total rate. We begin with the decay  $b \rightarrow ce\bar{\nu}$ , as shown in figure 1, which is identical to  $\mu^\pm \rightarrow e^\pm\nu\bar{\nu}$ . The  $W^-$ -boson exchange is shown for convenience in



keeping track of charges and particles and antiparticles, but we do assume its mass to be infinite and therefore use the usual form of the effective lagrangian. The four momenta of  $b$ ,  $c$ ,  $e$  and  $\nu$  are labelled with the same symbol as the corresponding particle. After performing the usual sum over spins, we obtain

**Fig. 10.1.**  $b \rightarrow ce\bar{\nu}$

$$\mathcal{P} \equiv \sum_{spins} |\mathcal{M}|^2 \propto (ce)(\nu b) \quad (10.1)$$

where  $(ab) \equiv a_\mu b^\mu \equiv AB - \vec{a} \cdot \vec{b}$  is the scalar product of the four vectors  $a$  and  $b$ . The 9-fold differential decay rate:

$$d^9\Gamma = \mathcal{P} \frac{d^3p_c}{E_c} \frac{d^3p_e}{E_e} \frac{d^3p_\nu}{E_\nu} \delta^4(b - c - e - \nu)$$

reduces to a 2-fold differential rate after integrating over the delta function variables (4 dimensions reduction) and irrelevant angles (2+1 dimensions reduction), to

$$d^2\Gamma = \mathcal{P} dE_1 dE_2 \quad (10.2)$$

where  $E_1, E_2$  are the energies of any two of the three final state particles. Since we are interested in the electron spectrum we chose  $E_1$  as the electron energy (to good accuracy equal to the momentum). If we choose the (anti)neutrino energy for  $E_2$ , then we can reduce  $\mathcal{P}$  to a polinomial in  $E_\nu$  and easily perform the first integration. We have:

$$(ce) = ((b - e - \nu)e) = (be) - (ee) - (\nu e) = M_b E_e - E_e E_\nu + \vec{p}_\nu \cdot \vec{p}_e,$$

neglecting  $M_e^2 \approx 0$ , where  $\vec{p}_\nu \cdot \vec{p}_e$  is obtained from

$$\begin{aligned} |\vec{p}_\nu + \vec{p}_e|^2 &= |\vec{p}_c|^2 \\ 2\vec{p}_\nu \cdot \vec{p}_e &= |\vec{p}_c|^2 - E_e^2 - E_\nu^2 \\ &= (M_b - E_e - E_\nu)^2 - M_c^2 - E_e^2 - E_\nu^2 \\ &= M_b^2 - M_c^2 - 2M_b E_e - 2M_b E_\nu + 2E_e E_\nu \end{aligned}$$

from which:

$$(ce) = \frac{1}{2}(M_b^2 - M_c^2 - 2M_b E_\nu)$$

and

$$\mathcal{P} \propto \frac{1}{2}(M_b^2 - M_c^2 - 2M_b E_\nu) E_\nu M_b \quad (10.3)$$

Substituting  $y = 2(E_\nu/M_b)$ ,  $\alpha = M_c/M_b$ , we have:

$$d^2\Gamma \propto M_b^5 (1 - y - \alpha^2)y dE_e dy \quad (10.4)$$

The electron spectrum is given by the integral:

$$d\Gamma \propto dE_e \int_{y_{min}(E_e)}^{y_{max}(E_e)} (1 - y - \alpha^2)y dy. \quad (10.5)$$

To obtain the limits of integration, consider the  $\nu, c$  system recoiling against the electron of energy  $E_e$  and momentum  $\vec{p}_e$ , ( $p_e = E_e$ ), in the b rest frame. Then  $M_{\nu,c} = M_b^2 - 2E_e M_b$ , neglecting  $M_e$ , and  $\gamma_{\nu,c} = (M_b - E_e)/M_{\nu,c}$ ,  $(\gamma\beta)_{\nu,c} = E_e/M_{\nu,c}$ . Defining  $E_\nu^*$  as the energy of the neutrino in the  $\nu, c$  rest frame, given by  $(M_{\nu,c}^2 - M_c^2)/(2M_{\nu,c})$  then, in the b rest frame

$$E_\nu \Big|_{min}^{max} = E_\nu^* \gamma_{\nu,c} (1 \pm \beta_{\nu,c})$$

or

$$E_\nu \Big|_{min}^{max} = \frac{M_b^2 - 2EM_b - M_c^2}{2(M_b^2 - 2EM_b)} (M_b - E_e \pm E_e)$$

and, with  $x = 2E_e/M_b$ :

$$y_{min} = 1 - x - \alpha^2, \quad y_{max} = \frac{1 - x - \alpha^2}{1 - x} \quad (10.6)$$

Before performing this integration, we ought to put back all the factors that we have been dropping. To begin with the proper double differential decay width is given by:

$$d^2\Gamma = \frac{G_F^2}{128\pi^5 M_b} \sum_{spins} |\mathcal{M}|^2 8\pi^2 dE_1 dE_2 \quad (10.7)$$

which, for  $M_c = 0$ , integrated over the neutrino momentum, gives the well known electron differential decay rate as:

$$\frac{d\Gamma}{dx} = \frac{G_F^2 M_b^5}{96\pi^3} (3 - 2x)x^2 \quad (10.8)$$

and, integrating over x,

$$\Gamma = \frac{G_F^2 M_b^5}{192\pi^3} \quad (10.9)$$

Without neglecting  $M_c$ , the differential decay rate is:

$$\frac{d\Gamma}{dx} = \frac{G_F^2 M_b^5}{192\pi^3} \times 12 \left[ \frac{1-\alpha^2}{2} \left( \frac{(1-x-\alpha^2)^2}{(1-x)^2} - (1-x-\alpha^2)^2 \right) - \frac{1}{3} \left( \frac{(1-x-\alpha^2)^3}{(1-x)^3} - (1-x-\alpha^2)^3 \right) \right] \quad (10.10)$$

Note that equations (10.8) and (10.9) are the well known results for muon decay, in particular the electron spectrum, given by  $f(x) = x^2(3-2x)$  is maximum at  $x=1$ , that is at the kinematic limit  $p_e = M/2$ . For the case of  $M_c \neq 0$ , the electron spectrum is given by the expression in square bracket in equation (10.10) or by the less cumbersome expression:

$$f(x) = x^2 \frac{(1-x-\alpha^2)^2}{(1-x)^3} [(3-2x)(1-x) + (3-x)\alpha^2], \quad (10.11)$$

which has the general shape of the muon electron spectrum, but rounded off at high momentum and ending at  $p_e^{max} = (M_b^2 - M_c^2)/(2M_b)$  or  $x = 1 - \alpha^2$ , with zero slope. All the results above apply also to  $b \rightarrow ue\bar{\nu}$ , with the substitution  $M_c \rightarrow M_u \approx 0$ .

## 10.2 Charm Decays

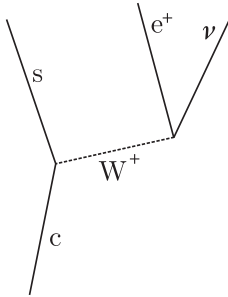


**Fig. 10.2.**  $c \rightarrow se^+\nu$  immediately leads to:

For the case of charmed leptonic decays, the decay amplitude is given in figure 2. Note that the incoming c-quark emits a  $W^+$  boson, while for a b quark a  $W^-$  was emitted. This is required by charge conservation. The net result is that  $e$  and  $\nu$  are charge conjugated in the two processes, while the quarks are not. Examination of the diagram im-

$$\mathcal{P} \equiv \sum_{spins} |\mathcal{M}|^2 \propto (s\nu)(ce) \quad (10.12)$$

We trivially obtain:

$$\mathcal{P} = (s\nu)(ce) \propto M_c^4 (1 - \alpha^2 - x)x \quad (10.13)$$

where  $y = 2(E_\nu/M_c)$ ,  $\alpha = M_s/M_c$  and  $x = 2(E_e/M_c)$ , and

$$d^2\Gamma \propto M_c^6 (1-x-\alpha^2)x dx dy \quad (10.14)$$

For  $M_s = 0$ , i.e.  $\alpha = 0$ , the electron spectrum is given by

$$\frac{d\Gamma}{dx} \propto (1-x)x \int_{1-x}^1 dy = x^2(1-x). \quad (10.15)$$

The electron spectrum from up-like quarks is therefore softer than that for down-like quarks, discussed above. The former peaks at  $x = 2/3$  and vanishes at the kinematic limit. Without neglecting  $M_s$ , the electron spectrum is given by:

$$f(x) = x^2 \frac{(1-x-\alpha^2)^2}{1-x} \quad (10.16)$$

### 10.3 Decay Rate

To obtain the total rate for decay we must integrate equation (10.10). The limits of integrations are now 0 and  $1 - \alpha^2$  and the result is:

$$\Gamma = \frac{G_F^2 M_b^5}{192\pi^3} \times (1 - 8\alpha^2 + 8\alpha^6 - \alpha^8 - 24\alpha^4 \log \alpha).$$

The same result is also obtained integrating equation (10.14) with all the appropriate factors included.

### 10.4 Other Things

#### 10.5 Contracting two indexes.

$$\epsilon^{\alpha\beta\mu\nu} \epsilon_{\alpha\beta\rho\sigma} = 2(\delta_{\nu\rho}\delta_{\mu\sigma} - \delta_{\mu\rho}\delta_{\nu\sigma})$$

therefore

$$\epsilon^{\mu\nu\alpha\beta} \epsilon_{\mu\nu\gamma\delta} a_\alpha b_\beta c^\gamma d^\delta = 2[(bc)(ad) - (ac)(bd)]$$

#### 10.6 Triple Product “Equivalent”.

$$\epsilon_{\alpha\beta\gamma\delta} P^\alpha p_1^\beta p_2^\gamma p_3^\delta = M(\vec{p}_1 \times \vec{p}_2 \cdot \vec{p}_3)$$

in the system where  $P=(M,0)$ .

## 11 Quantum Chromodynamics

## 12 Hadron Spectroscopy

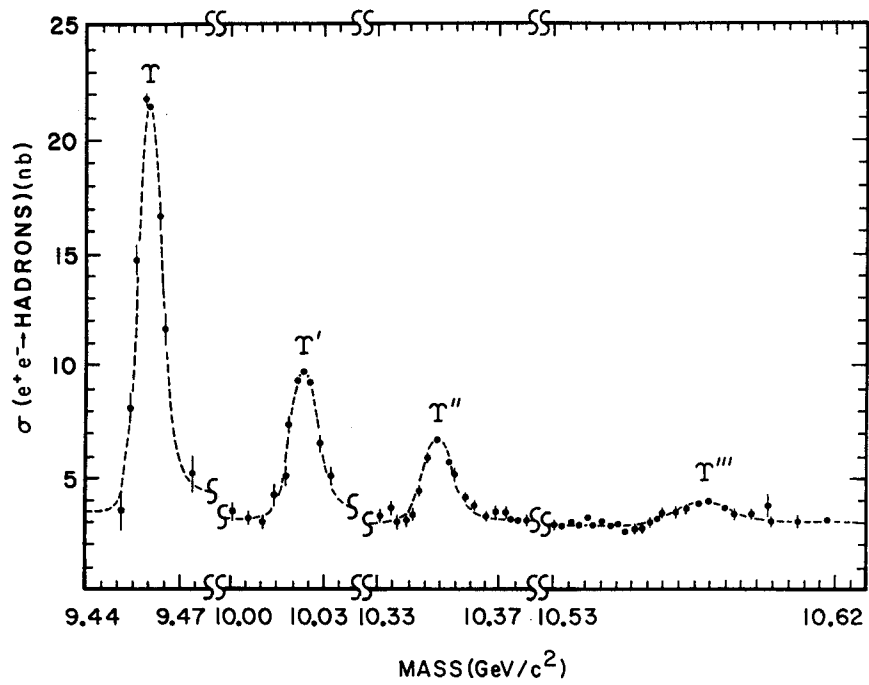


Fig. 12.1. Experimental observation of the 4  $\Upsilon$  mesons, CUSB.

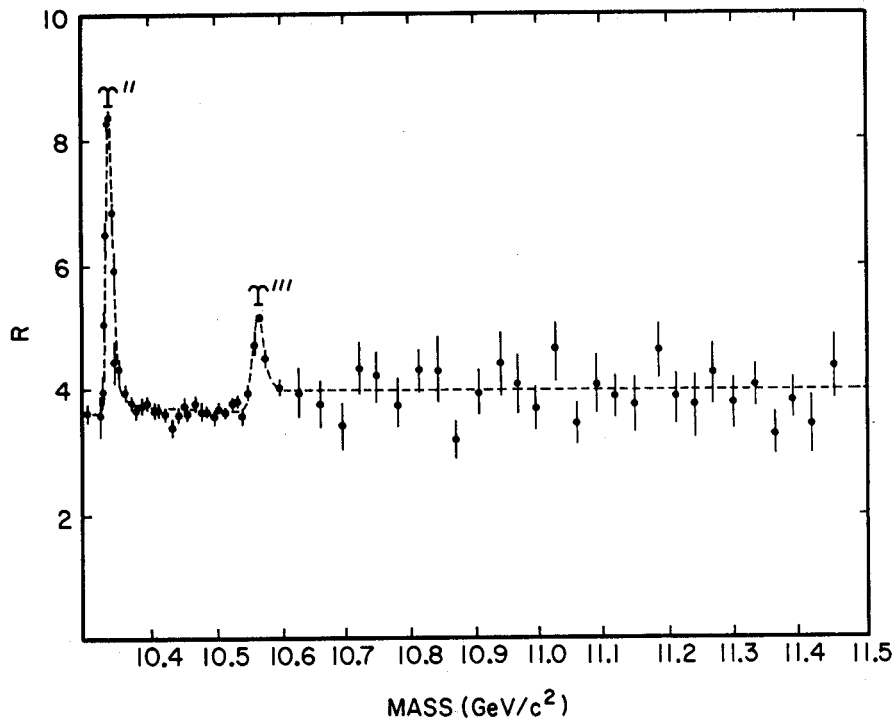
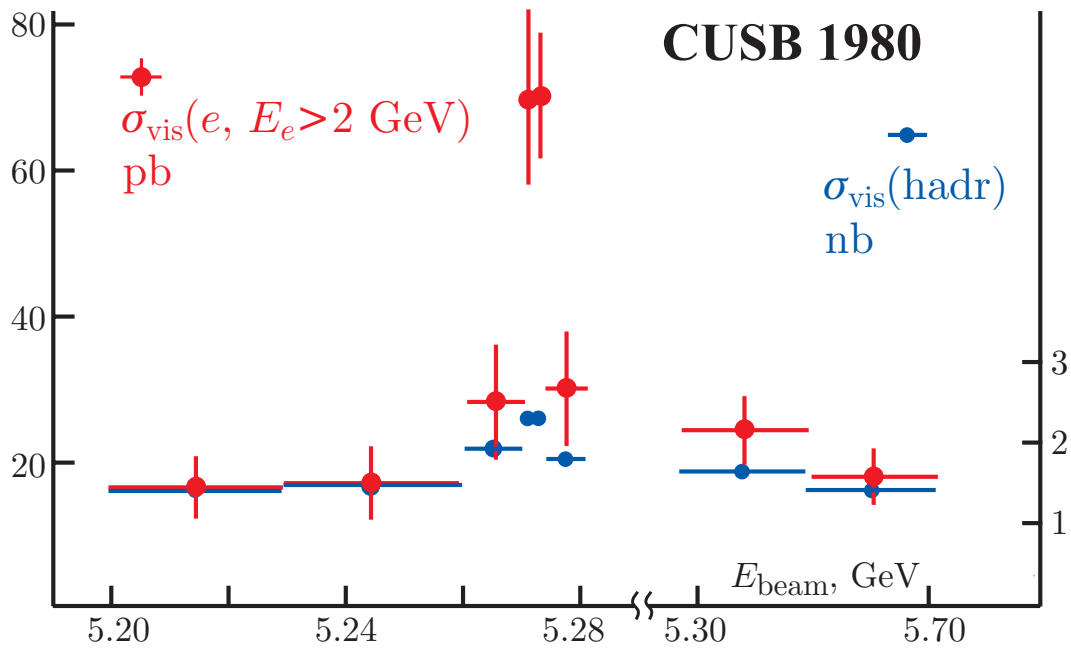
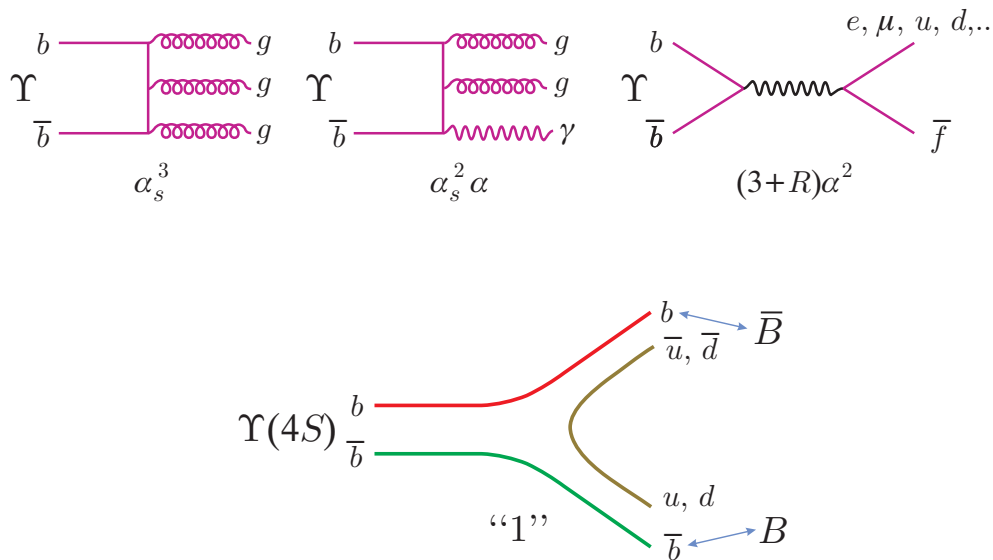


Fig. 12.2.  $R$  below and above the  $B\bar{B}$  threshold, CUSB.





**Fig. 12.5.** Discovery of the  $b$ -quark. The large excess of high energy electrons and positrons at the  $\Upsilon(4s)$  peak signals production of  $b\bar{d}$ ,  $b\bar{u}$ ,  $\bar{b}d$ ,  $\bar{b}u$  mesons, called  $B$  mesons, of mass  $\sim 5.2$  GeV. The  $B$  mesons decay into electrons of maximum energy of  $\sim 2$  GeV.



**Fig. 12.6.** Decay channels for the  $\Upsilon$  mesons. The three diagrams in top are the only available below the  $b$ -flavor threshold. The bottom graphs,  $\Upsilon \rightarrow B\bar{B}$  is kinematically possible only for the fourth  $\Upsilon$ .

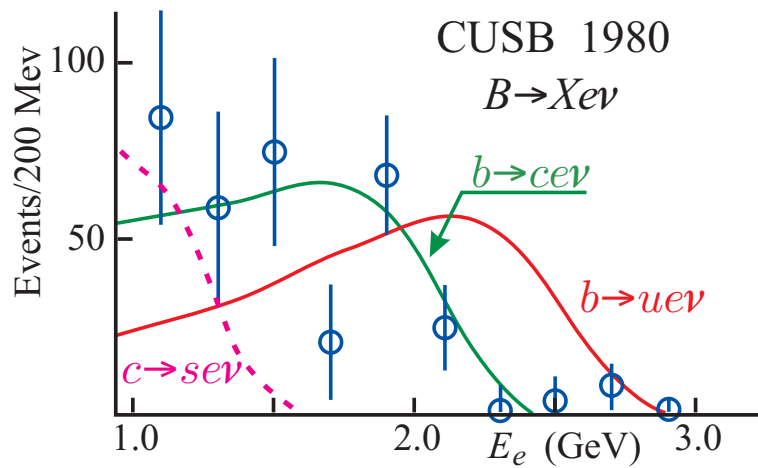


**Fig. 12.7.** Experimental evidence for the suppression of the  $bu$  coupling, see fig. 9.12 and section 9.11, CUSB.

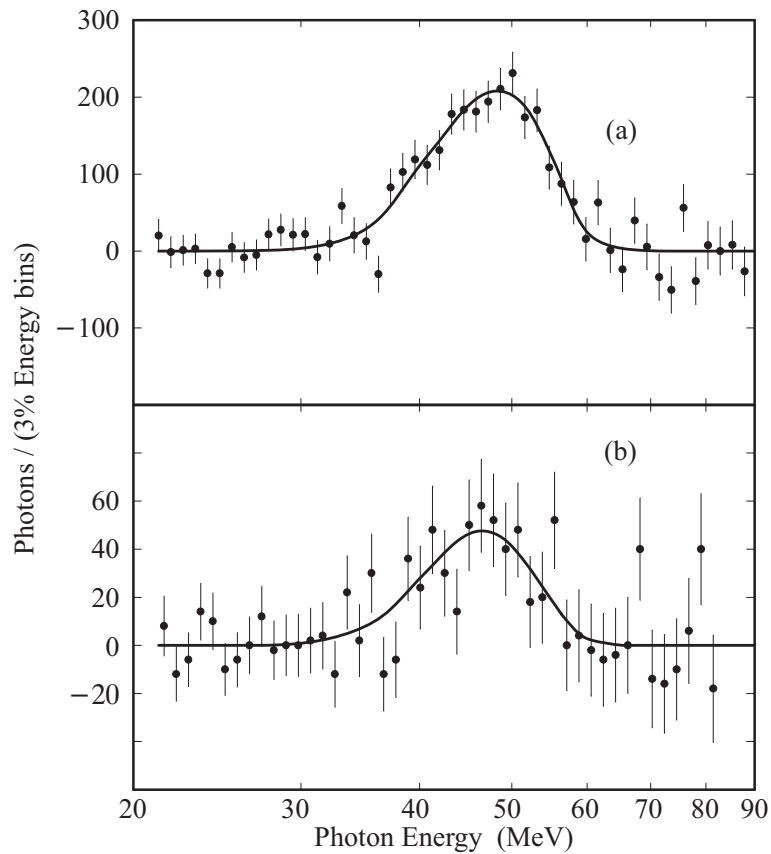


**Fig. 12.8.** Photon spectrum at the  $\Upsilon(5S)$ , continuum subtracted. The signal provided evidence for the existence of the  $B^*$  meson, with  $m(B^*) - m(B) \sim 50$  MeV, CUSB.

**13 High Energy Scattering****14 The Electro-weak Interaction**

# 15 Spontaneous Symmetry Breaking, the Higgs Scalar

## 15.1 Introduction

The potential is illustrated in fig. 15.1.

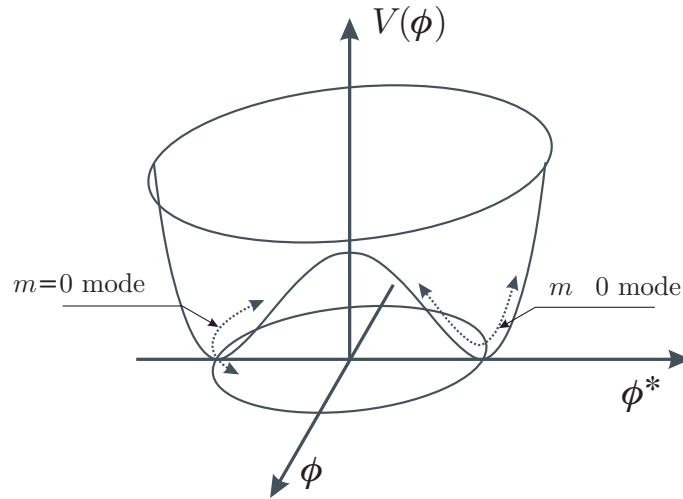


**Fig. 15.1.** The potential.

where the massless mode and the massive mode are indicated.

## 16 Neutrino Oscillation

### 16.1 Introduction

For a long time it was assumed that Pauli's neutrino had zero mass. To date direct measurements are consistent with this assumption. It is of course impossible to prove that a quantity, the neutrino mass in this case, is exactly zero. After experiments required the introduction of a second neutrino,  $\nu_\mu$ , different from the neutrino of  $\beta$ -decay,  $\nu_e$ , neutrinos can exhibit interesting phenomena, mixing and oscillations, if their mass is not zero. There is some evidence that this might be the case. Together with the three neutrino flavors,  $\nu_e$ ,  $\nu_\mu$  and  $\nu_\tau$ , we have introduced three different lepton numbers which appear to be conserved. This implies that in  $\beta$ -decay, only  $\nu_e$  are emitted, while in pion decays almost only  $\nu_\mu$  are produced.

It is possible however to conceive a situation in which

1. The neutrinos have masses
2. The mass eigenstates do not coincide with flavor eigenstates.

Then we can introduce a unitary mixing matrix  $\mathbf{U}$  which connects flavor and mass eigenstates through:

$$\mathbf{V}_f = \mathbf{U}\mathbf{V}_m \quad \mathbf{V}_m = \mathbf{U}^\dagger\mathbf{V}_f \quad (16.1)$$

where

$$\mathbf{V}_f = \begin{pmatrix} \nu_e \\ \nu_\mu \\ \nu_\tau \end{pmatrix} \quad \mathbf{V}_m = \begin{pmatrix} \nu_1 \\ \nu_2 \\ \nu_3 \end{pmatrix}$$

are the flavor and mass neutrino eigenstates. If the masses of the three different neutrinos are different then a beam which at  $t=0$  was in pure flavor state, oscillates into the other flavor species.

### 16.2 Two neutrinos oscillation

We consider in the following oscillations between two neutrinos only, in order to derive relevant formulae which are easier to appreciate. The case of three or more neutrinos is slightly more complicated but follows exactly the same lines. For definiteness we also chose  $\nu_e$  and  $\nu_\mu$  as the flavor states. Eqs. (16.1) can be written as

$$\begin{aligned} |\nu_e\rangle &= \cos\theta|\nu_1\rangle + \sin\theta|\nu_2\rangle & |\nu_\mu\rangle &= -\sin\theta|\nu_1\rangle + \cos\theta|\nu_2\rangle \\ |\nu_1\rangle &= \cos\theta|\nu_e\rangle - \sin\theta|\nu_\mu\rangle & |\nu_2\rangle &= \sin\theta|\nu_e\rangle + \cos\theta|\nu_\mu\rangle. \end{aligned} \quad (16.2)$$

We recall that a unitary  $2 \times 2$  matrix has only one real parameter, the angle  $\theta$ . We consider now the time evolution of a state which at  $t=0$  is a pure flavor eigenstate  $|\nu_e\rangle$ . At time  $t$  the state wave function is

$$\Psi_e(t) = \cos\theta |\nu_1\rangle e^{iE_1 t} + \sin\theta |\nu_2\rangle e^{iE_2 t}$$

where the subscript  $e$  reminds us of the initial state. Substituting for  $|\nu_1\rangle$  and  $|\nu_2\rangle$  their expansion in eqs. (16.2) and projecting out the  $\nu_e$  and  $\nu_\mu$  components we find the amplitudes

$$\begin{aligned} A(\nu_e, t) &= \cos^2\theta e^{iE_1 t} + \sin^2\theta e^{iE_2 t} \\ A(\nu_\mu, t) &= -\cos\theta \sin\theta e^{iE_1 t} + \cos\theta \sin\theta e^{iE_2 t} \end{aligned}$$

and the intensities:

$$\begin{aligned} I(\nu_e, t) &= |A(\nu_e, t)|^2 = \cos^4\theta + \sin^4\theta + 2\cos^2\theta \sin^2\theta \cos|E_1 - E_2|t \\ I(\nu_\mu, t) &= |A(\nu_\mu, t)|^2 = 2\cos^2\theta \sin^2\theta (1 - \cos|E_1 - E_2|t). \end{aligned} \quad (16.3)$$

Using  $\cos^4\theta + \sin^4\theta = 1 - 2\cos^2\theta \sin^2\theta$ ,  $2\sin\theta \cos\theta = \sin 2\theta$  and  $1 - \cos\theta = 2\sin^2\theta/2$ , eqs. (16.3) can be rewritten as:

$$\begin{aligned} I(\nu_e, t) &= 1 - \sin^2 2\theta \sin^2 \frac{E_1 - E_2}{2} t \\ I(\nu_\mu, t) &= \sin^2 2\theta \sin^2 \frac{E_1 - E_2}{2} t. \end{aligned} \quad (16.4)$$

Notice that  $I(\nu_e, t) + I(\nu_\mu, t) = 1$ , as we should expect. Finally we find the mass dependence, expanding  $E(p)$  to first order in  $m$ :

$$E = p + \frac{m^2}{2p}$$

form which

$$E_1 - E_2 = \frac{m_1^2 - m_2^2}{2p} = \frac{\Delta m^2}{2p}$$

and substituting into eqs. (16.4):

$$\begin{aligned} I(\nu_e, t) &= 1 - \sin^2 2\theta \sin^2 \frac{\Delta m^2}{4p} t \\ I(\nu_\mu, t) &= \sin^2 2\theta \sin^2 \frac{\Delta m^2}{4p} t. \end{aligned} \quad (16.5)$$

Using  $1 \text{ MeV} = 10^{15}/197 \text{ m}^{-1}$  and  $E \sim p$  we get:

$$\begin{aligned} I(\nu_e, t) &= 1 - \sin^2 2\theta \sin^2 \frac{1.27 \times \Delta m^2 \times l}{E} t \\ I(\nu_\mu, t) &= \sin^2 2\theta \sin^2 \frac{1.27 \times \Delta m^2 \times l}{E} t. \end{aligned} \quad (16.6)$$

valid if  $E$  is expressed in MeV,  $\Delta m^2$  in  $\text{eV}^2$  and  $l$  in meters.

Therefore, under the assumptions of eq. (16.1), a pure beam of one flavor at  $t = 0$ ,  $\nu_e$  in the example, oscillates into the other flavors and back, with travelled distance. This effect can be checked experimentally. Starting with a  $\nu_e$  beam we can search for the *appearance* of muon neutrinos or the *disappearance* of the initial electron neutrinos. From the magnitude of the effect and its dependence on distance one can obtain the value of the parameters  $\theta$  and  $\Delta m^2$ . In practice the dependence on distance has not been studied so far. Equivalent results can be obtained from studying the dependence on energy of the flavor oscillation. In the limit of very large distance and a sufficiently large energy range of the neutrinos, the initial intensity of the beam will be halved, in the case of only two neutrino flavors.

$$\begin{array}{l} \text{Particles } e^- \quad \mu^- \quad \nu \quad L=1 \\ \text{Antiparticles } e^+ \quad \mu^+ \quad \bar{\nu} \quad L=-1 \end{array}$$

with the beta decay and muon decay reactions being

...

Evidence.

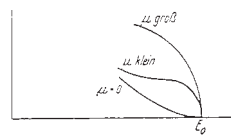
Solar  $\nu$ 's in Cl, more than half, missing. Low  $E$   $\nu_\mu$ 's cannot make  $\mu$ 's. Same in gallium.

Atmospheric  $\nu$ 's.  $\pi \rightarrow \mu + \nu_\mu$ ,  $\mu \rightarrow \nu_\mu \nu_e$

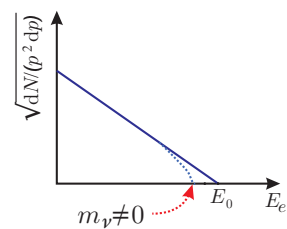
## 17 Neutrino Experiments. A Seminar

### 17.1 The invention of the neutrino

1. Continuous  $\beta$ -spectrum, 1914, 1927
2. **Bohr** as late as '36 thought energy might not be conserved in nuclear physics
3. **Pauli**  $\nu$ , 1930 (-1+3), Dear Radioactive Ladies and Gentlemen...
4. **Fermi**, in Zeitschrift für Physik **88** 161 (1934) (16 January)
5. **Emmy Noether**, 1918, Noether's theorem



From Fermi's paper, in German.



Kurie plot.

### 17.2 Neutrino Discovery

**Bethe & Peierls** 1934.  $\lambda_{\nu\text{-abs}} \sim 10^{19}$  cm, 10 light-years for  $\rho=3$ , will never be observed.

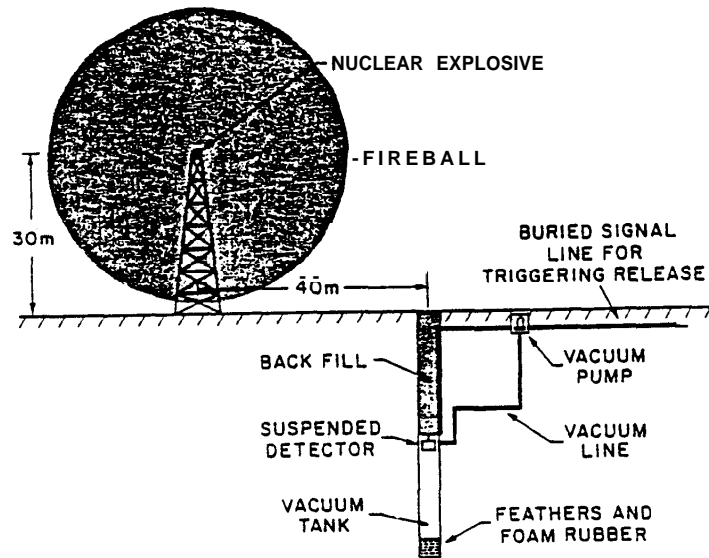
**Reines & Cowan**, try 100 m from an atomic bomb?... Attempt at small breeder, then at large power reactor. June '56 sent a telegram to Pauli to reassure him  $\nu$ 's exist. (24 y vs  $\approx$  40 y for Higgs)

$10^{13}$   $\nu/\text{cm}^2/\text{s} \rightarrow 3$  events/h in  $\sim 1$  ton detector

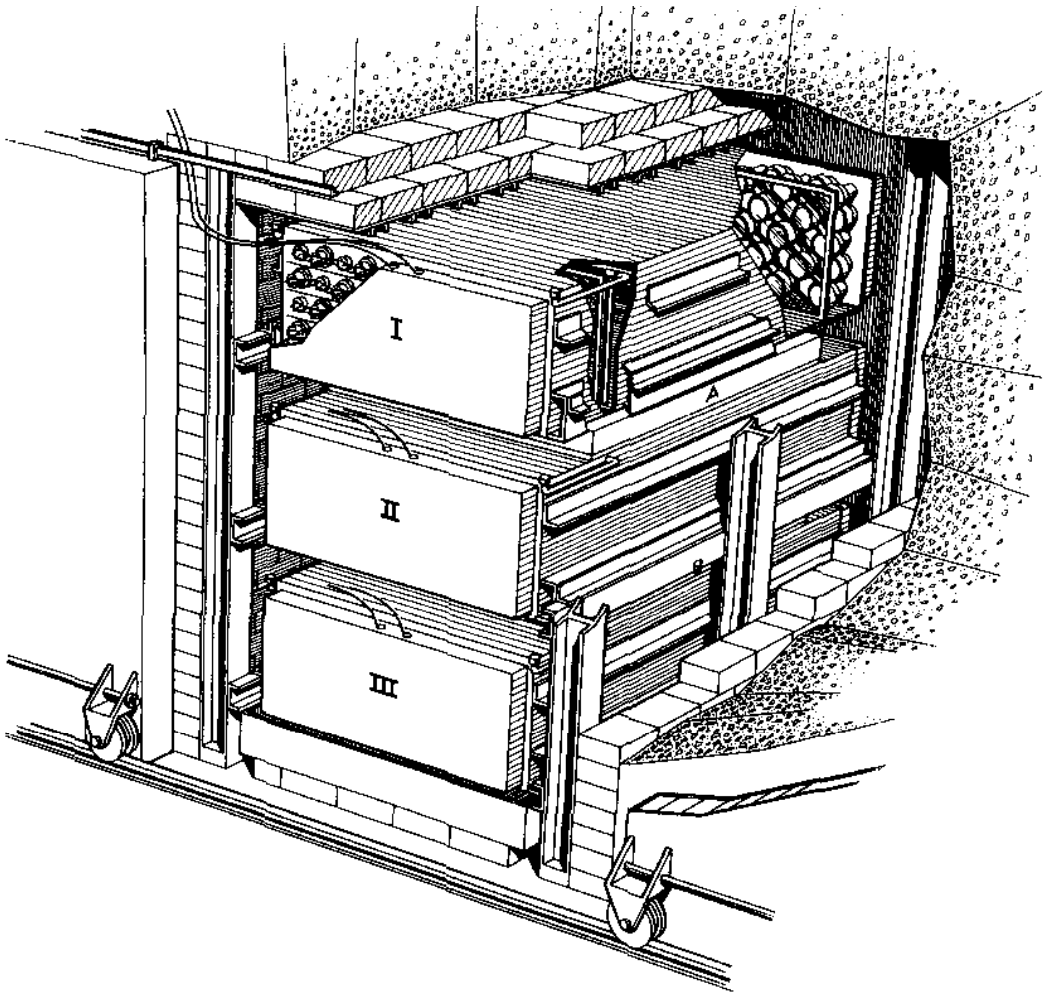


$$N_{\text{ev}}[\text{s}] = f[\text{/cm}^2/\text{s}] \times \sigma[\text{cm}^2] \times V[\text{cm}^3] \times \rho_{\text{H}}[g_{\text{H}_2}/\text{cm}^3] \times N[p/g_{\text{H}_2}]$$

$$N = f \times \sigma \times N \times M$$



The proposed bomb experiment.



Cowan and Reines experiment at a reactor  
1957 to the 70's and on

Reactor:  $\bar{\nu}$ 's, not  $\nu$ 's; R. Davis, '55, chlorine (BMP)

Parity

$$\mu \not\propto \gamma, \quad \nu_e \neq \nu_\mu$$

$\nu_e$  and  $\nu_\mu$  helicity

Observation of  $\nu_\mu$  All the way to the SM where neutrinos have zero mass

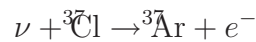
$$m(\nu_e) < 2.8 \text{ eV}, \quad {}^3\text{H} - \beta \text{ decay}$$

Just 3 neutrinos

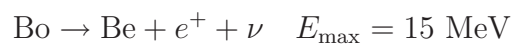
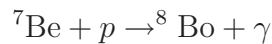
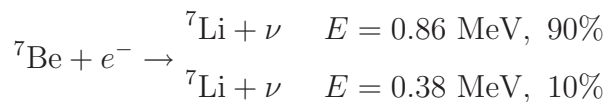
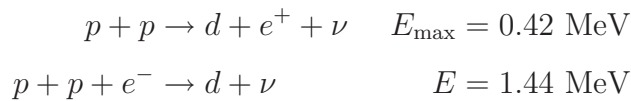
If  $m=0$ , helicity is L-invariant and  $\mathcal{H} = \pm 1$  states are independent.  $\nu_{\text{right}}, \bar{\nu}_{\text{left}}$  need not exist

### 17.3 Something different, neutrinos from the sun

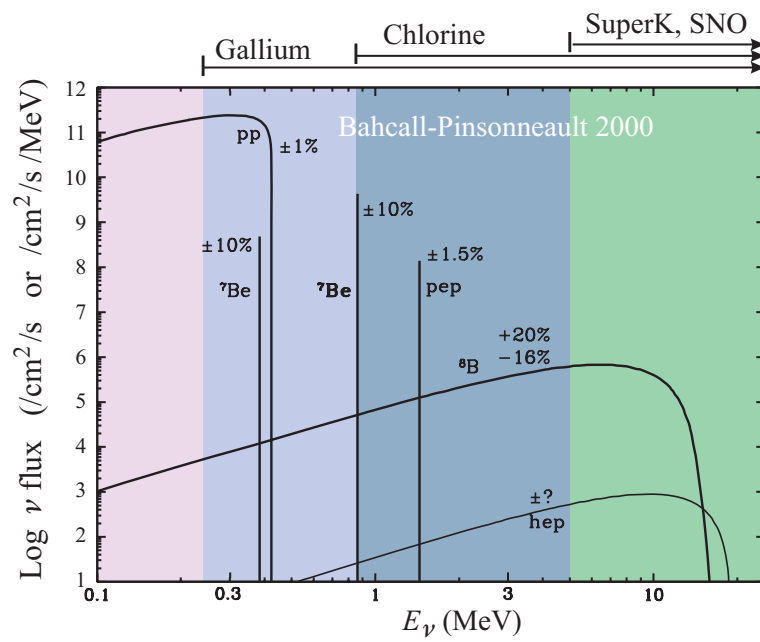
**1964** Look for solar  $\nu$ 's, just to peek inside the sun. 100,000 gallon of tetrachloroethylene - dry cleaning fluid - are enough to observe



as computed in SSM, from the reactions:



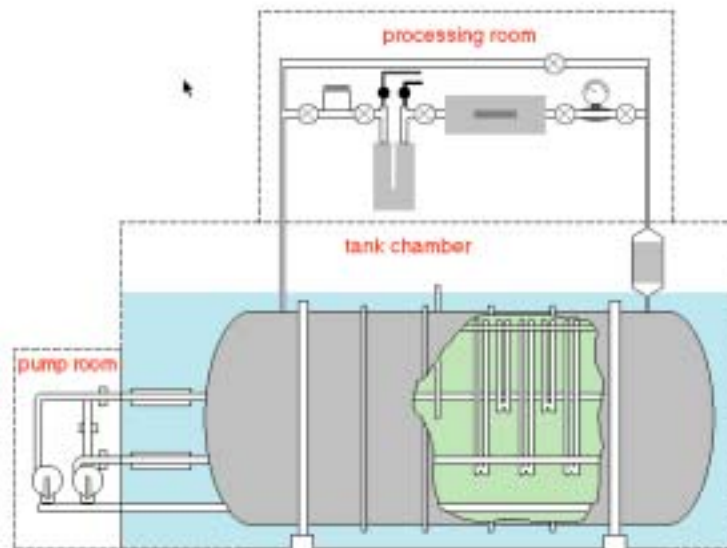
plus all return reactions without  $\nu$ 's.



400 ton  $\text{C}_2\text{H}_2\text{Cl}_4$ . Extract Ar. Count Ar decays

Add and recover Ar (non radioactive) Neutron source check

30 Year Run



Define:  $\text{SNU} \equiv 1 \text{ interaction/sec}/10^{36} \text{ atoms} \approx 1 \text{ int./ton/year}$

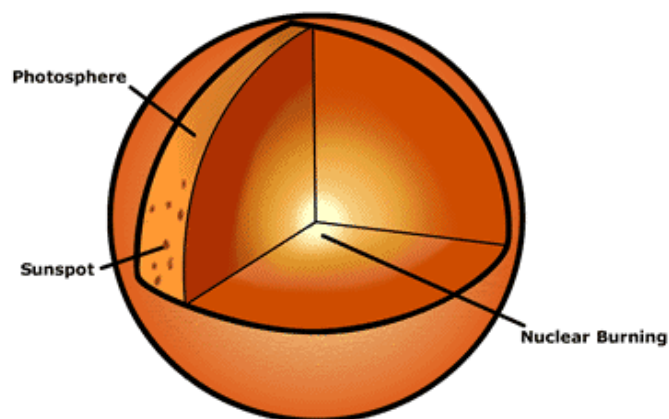
**Ray Davis**, chlorine experiment, expected 7 SNU, gave upper limit of 2.5 by 1968.  $E_\nu > 0.8 \text{ MeV}$

Is the experiment wrong? No, all checks OK!

Is the SSM correct? Doubts but with help of Helioseismology and many checks had to be accepted.

---


$$v_{\text{sound}} \propto T^{1/2} \text{ while } \phi_\nu(^7\text{Be}) \propto T^{10}$$



The sun

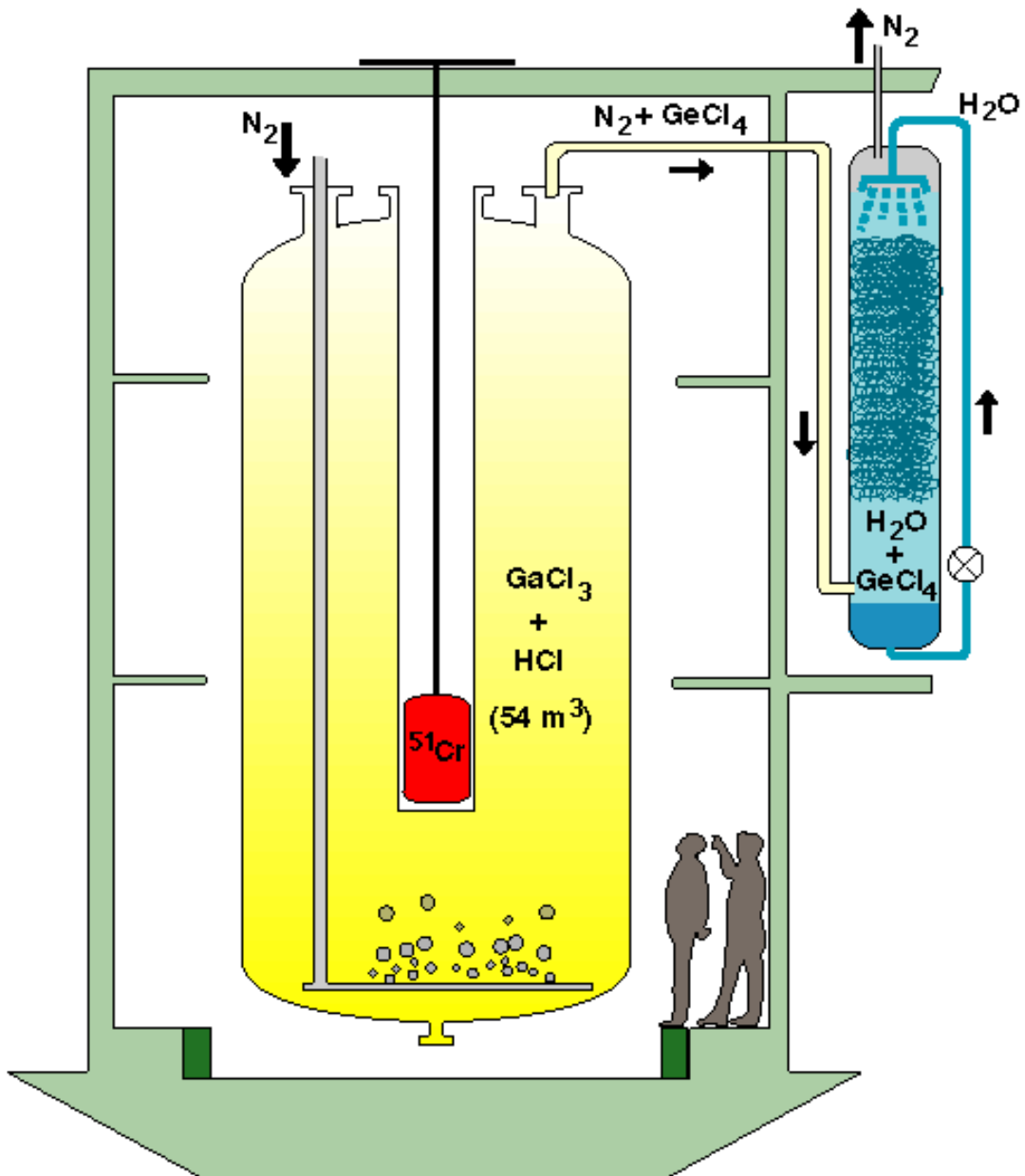
---

## New Experiments

1. Gallex-Sage, Ga,  $E_\nu > 0.25$  MeV
2. K-SuperK, H<sub>2</sub>O,  $E_\nu > 6.5$  MeV

Source	Flux ( $10^{10} \text{ cm}^{-2}\text{s}^{-1}$ )	Cl (SNU)	Ga (SNU)
pp	$5.94 \pm 1\%$	0.0	69.6
pep	$1.39 \times 10^{-2} \pm 1\%$	0.2	2.8
hep	$2.10 \times 10^{-7}$	0.0	0.0
<sup>7</sup> Be	$4.80 \times 10^{-1} \pm 9\%$	1.15	34.4
<sup>8</sup> B	$5.15 \times 10^{-4} + 19\%, -14\%$	5.9	12.4
<sup>13</sup> N	$6.05 \times 10^{-2} + 19\%, -13\%$	0.1	3.7
<sup>15</sup> O	$5.32 \times 10^{-2} + 22\%, -15\%$	0.4	6.0
<sup>17</sup> F	$6.33 \times 10^{-4} + 12\%, -11\%$	0.0	0.1
Total		$7.7_{-1.0}^{+1.2}$	$129_{-6}^{+8}$
Observe		$2.6 \pm .23$	$73 \pm 5$

Gallium:  $^{71}\text{Ga} \rightarrow ^{71}\text{Ge}$ : Sage and Gallex



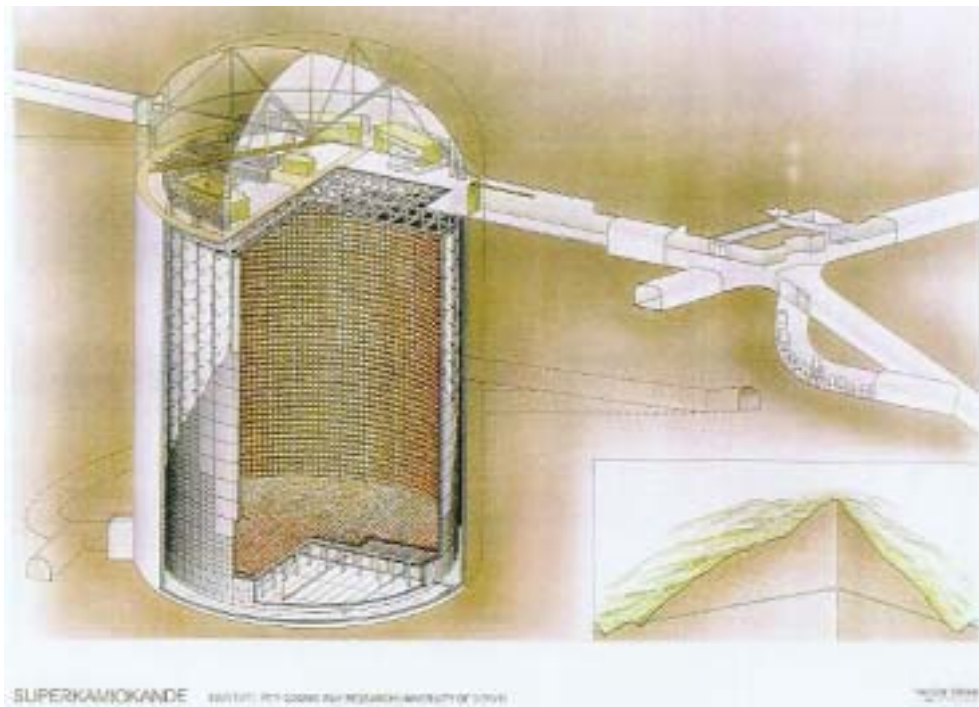
Gallex in the Gran Sasso underground Laboratory.

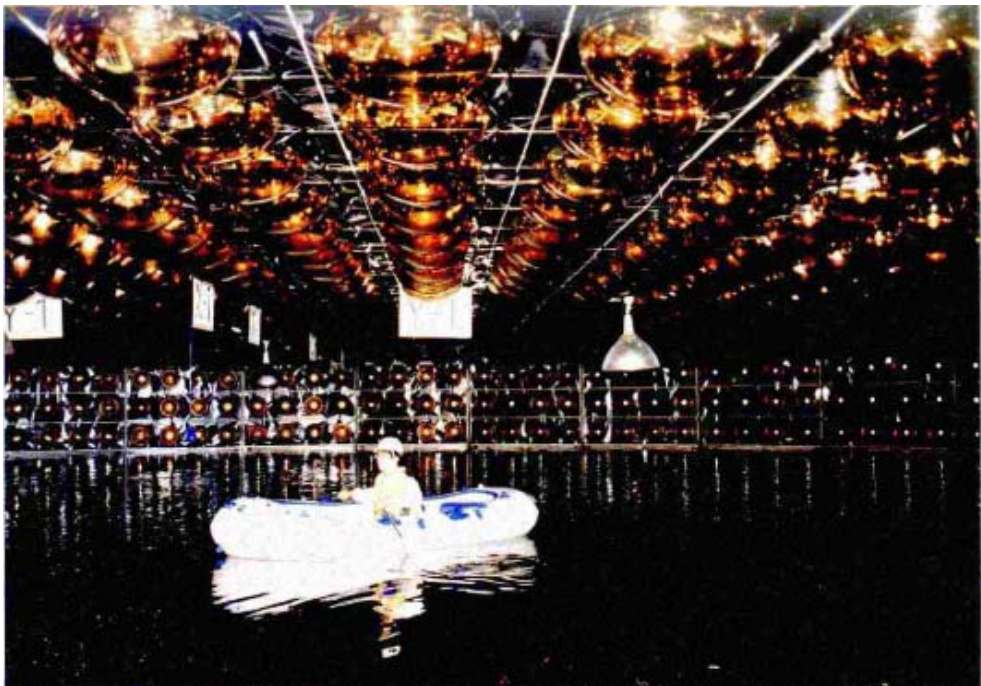
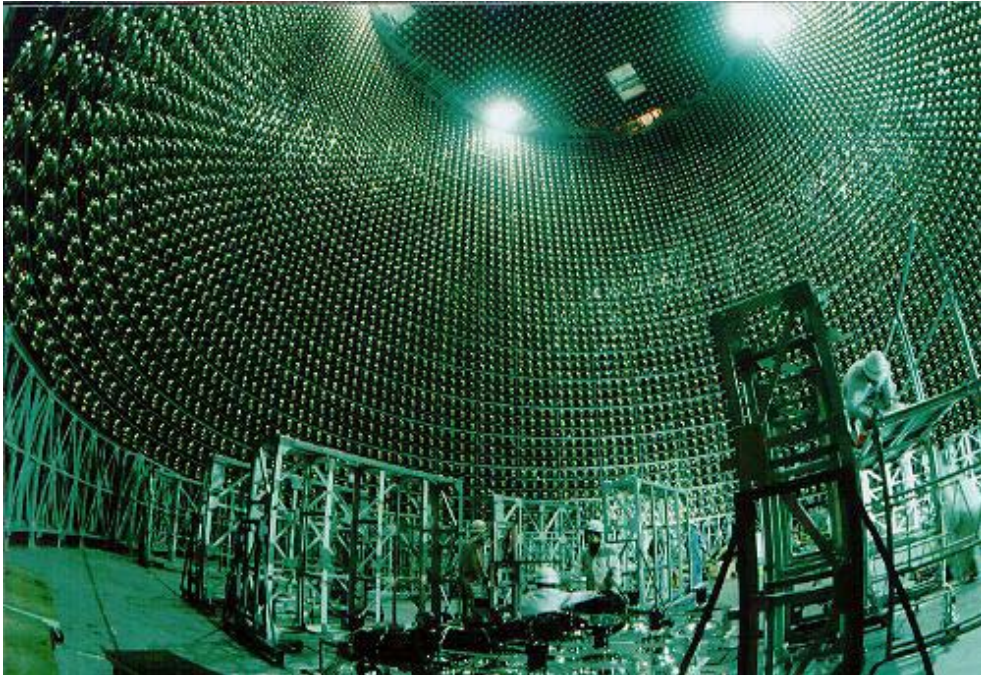
### Are there any $\nu$ from the sun?

Super-Kamiokande. A  $\text{H}_2\text{O}$  Cerenkov detector. 41.4 m  $h$   $\times$  39.3 m  $dia.$  50,000 tons of pure water. 11,200 50 cm dia. PMTs, plus more, outer det.

$\nu$  events point to the sun ok.  $E_{\text{max}} \leq 15$  MeV ok. But:

$$\frac{\text{SuperK } \nu}{\text{SSM}} = 0.44 \pm 0.03$$







## Neutrinos disappear

In the E-W SM, neutrinos have no mass and  $\nu_e \neq \nu_\mu \neq \nu_\tau$

Pontecorvo in '67 had speculated on what could happen if lepton flavor is not conserved and neutrinos have mass.

Mass eigenstates are distinct from flavor eigenstates, and connected by a unitary mixing matrix.

$$\mathbf{V}_f = \mathbf{U}\mathbf{V}_m \quad \mathbf{V}_m = \mathbf{U}^\dagger\mathbf{V}_f$$

where

$$\mathbf{V}_f = \begin{pmatrix} \nu_e \\ \nu_\mu \\ \nu_\tau \end{pmatrix} \quad \mathbf{V}_m = \begin{pmatrix} \nu_1 \\ \nu_2 \\ \nu_3 \end{pmatrix}$$

are the flavor and mass neutrino eigenstates.

Example. Two flavors,  $e, \mu$ ; two masses, 1, 2

$$\begin{aligned} |\nu_e\rangle &= \cos\theta|\nu_1\rangle + \sin\theta|\nu_2\rangle & |\nu_\mu\rangle &= -\sin\theta|\nu_1\rangle + \cos\theta|\nu_2\rangle \\ |\nu_1\rangle &= \cos\theta|\nu_e\rangle - \sin\theta|\nu_\mu\rangle & |\nu_2\rangle &= \sin\theta|\nu_e\rangle + \cos\theta|\nu_\mu\rangle. \end{aligned}$$

If at time  $t = 0$ ,  $\Psi(t) = |\nu_e\rangle$  the state evolves as:

$$\Psi_e(t) = \cos\theta|\nu_1\rangle e^{iE_1 t} + \sin\theta|\nu_2\rangle e^{iE_2 t}.$$

Substitute and project out the  $e, \mu$  amplitudes

$$A(\nu_e, t) = \cos^2 \theta e^{iE_1 t} + \sin^2 \theta e^{iE_2 t}$$

$$A(\nu_\mu, t) = -\cos \theta \sin \theta e^{iE_1 t} + \cos \theta \sin \theta e^{iE_2 t}$$

The intensities then are:

$$I(\nu_e, t) = \cos^4 \theta + \sin^4 \theta + 2 \cos^2 \theta \sin^2 \theta \cos |E_1 - E_2| t$$

$$I(\nu_\mu, t) = 2 \cos^2 \theta \sin^2 \theta (1 - \cos |E_1 - E_2| t).$$

more conveniently

$$I(\nu_e, t) = 1 - \sin^2 2\theta \sin^2 \left( \frac{E_1 - E_2}{2} t \right)$$

$$I(\nu_\mu, t) = \sin^2 2\theta \sin^2 \left( \frac{E_1 - E_2}{2} t \right).$$

or ( $\Delta E = \Delta m^2 / 2E$ ,  $t = l/c$ , using  $\hbar = c = 1$ )

$$I(\nu_e, t) = 1 - \sin^2 2\theta \sin^2 \left( \frac{1.27 \times \Delta m^2 \times l}{E} \right)$$

$$I(\nu_\mu, t) = \sin^2 2\theta \sin^2 \left( \frac{1.27 \times \Delta m^2 \times l}{E} \right).$$

with  $E$  in MeV (GeV),  $\Delta m^2$  in  $\text{eV}^2$  and  $l$  in meters (km).  $\nu_e$  oscillate from 1 to 0 and back and forth...

$\nu_\mu$  appear and then fade and so on...

That of course if

1. You are lucky
2. You are in control of the experiment

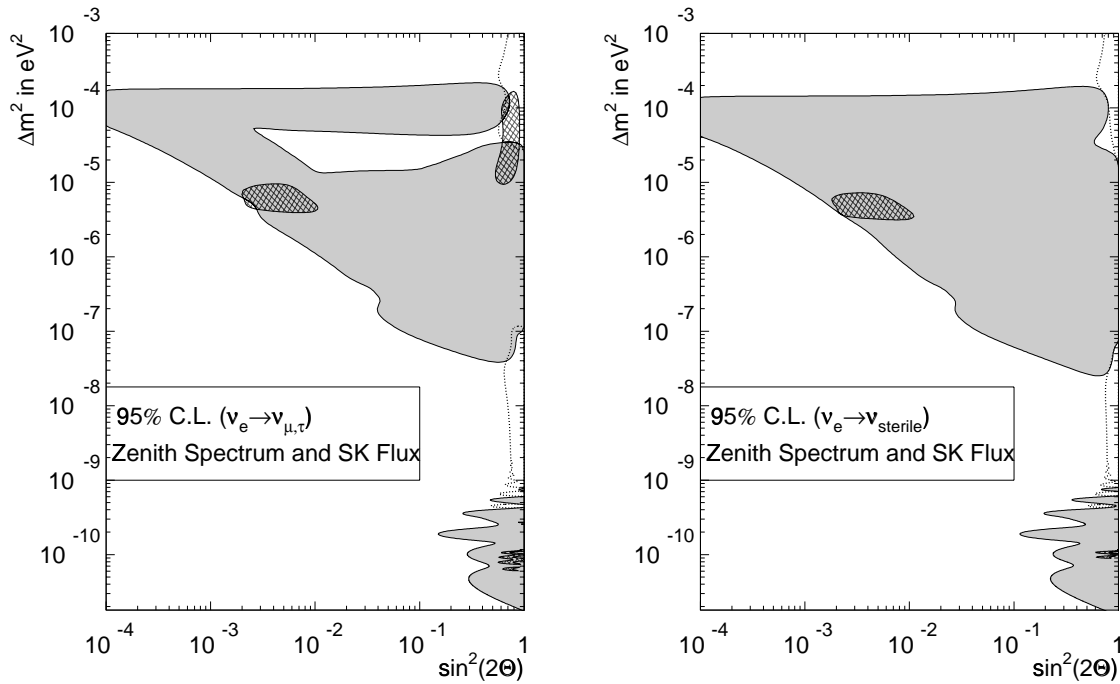
Typically, neutrinos have a continuous spectrum. Then in average some of the  $\nu_e$  disappear and just as many  $\nu_\mu$  appear. For just two species, the limit is 1/2 disappearance and 1/2 appearance.

With solar neutrinos,  $E < 15$  MeV, the muon (tau) neutrino are not positively observable because  $\nu_\mu + X \rightarrow \mu + X'$  is energetically impossible.

1. This is encouraging but not quite enough...
2. No oscillation has ever been seen, except...
3. The missing neutrinos can be detected by scattering
4. There is more: atmospheric  $\nu$ 's

But, before that, what does one get from solar  $\nu$ 's?

In fact many solutions, must include oscillations in matter (MSW). Wave length changes in matter.



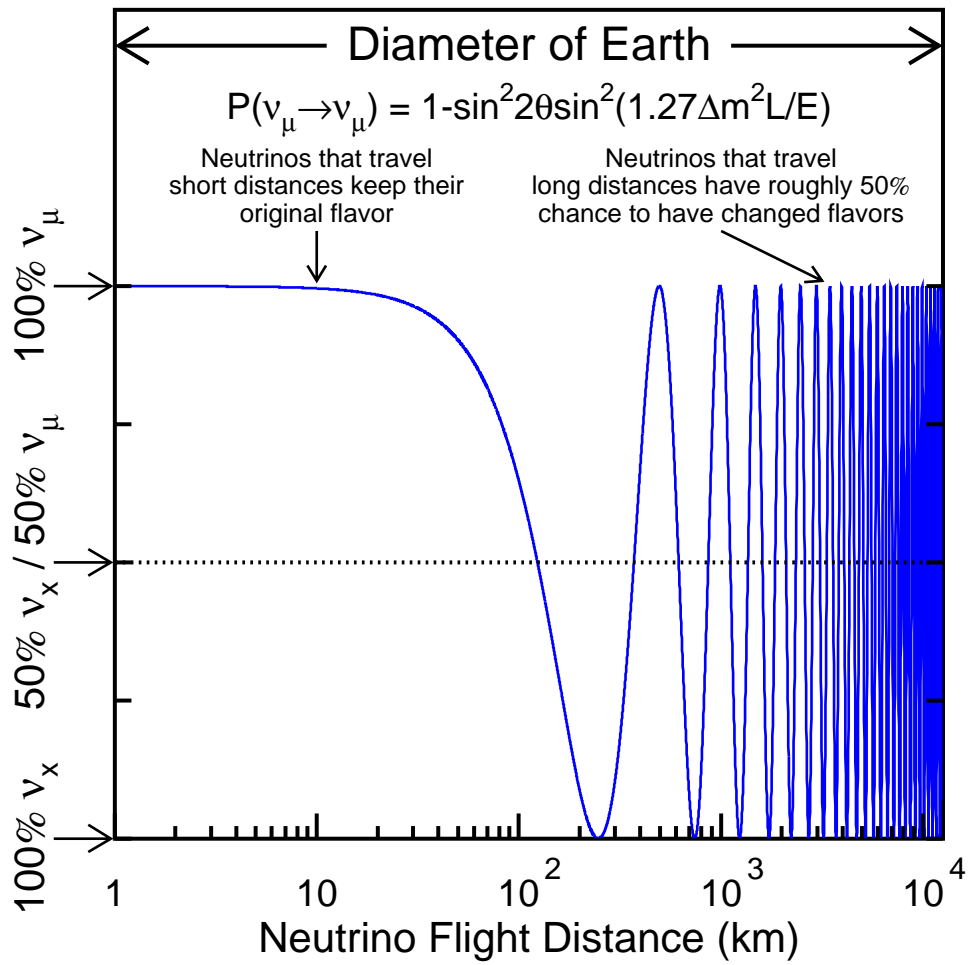
Atmospheric neutrinos

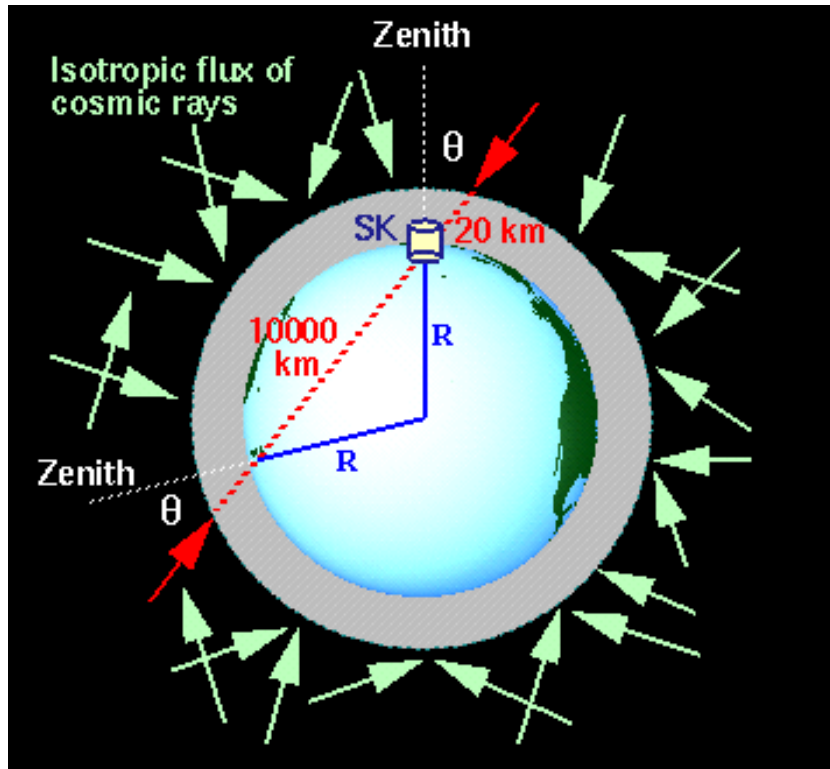
IMB, Kamiokande and **SuperK** find that high energy  $\nu_\mu$  are not twice  $\nu_e$ . High energy  $\nu$ 's come from cosmic rays as:

$$\begin{aligned} \pi &\rightarrow \mu + \nu_\mu \\ \mu &\rightarrow e + \nu_\mu + \nu_e \end{aligned} \quad \Rightarrow \quad 2\nu_\mu + 1\nu_e$$

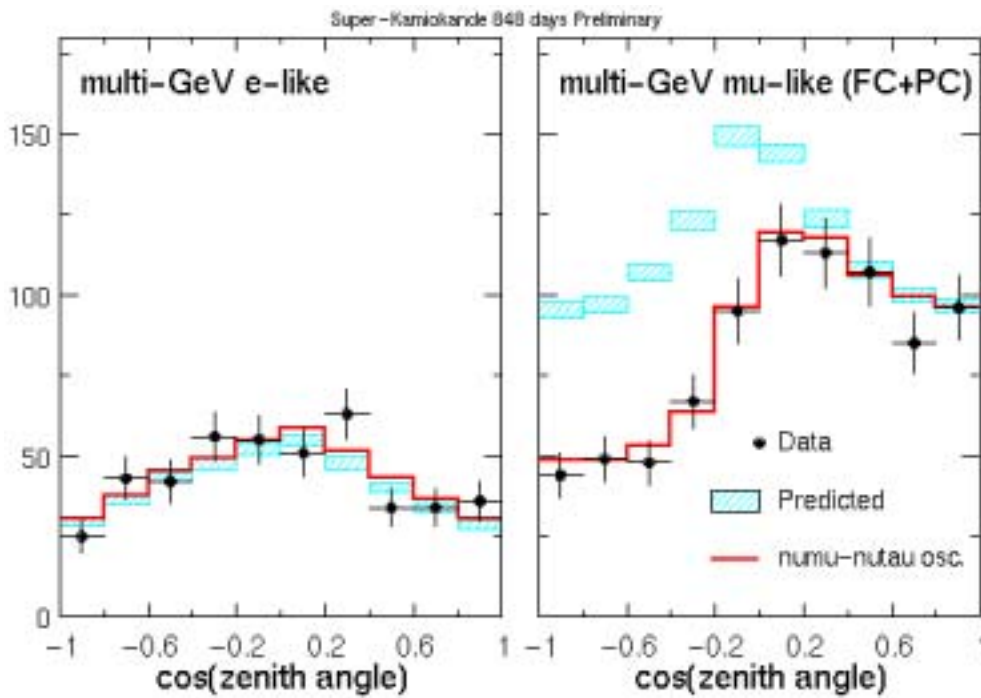
Super-K gives  $(\nu_\mu/\nu_e)_{\text{obs.}}/(\nu_\mu/\nu_e)_{\text{SSM}}=0.63$ . Striking for high  $E$ , upward  $\nu$ 's. Also seen in Macro at Gran Sasso.

The only hint for oscillation

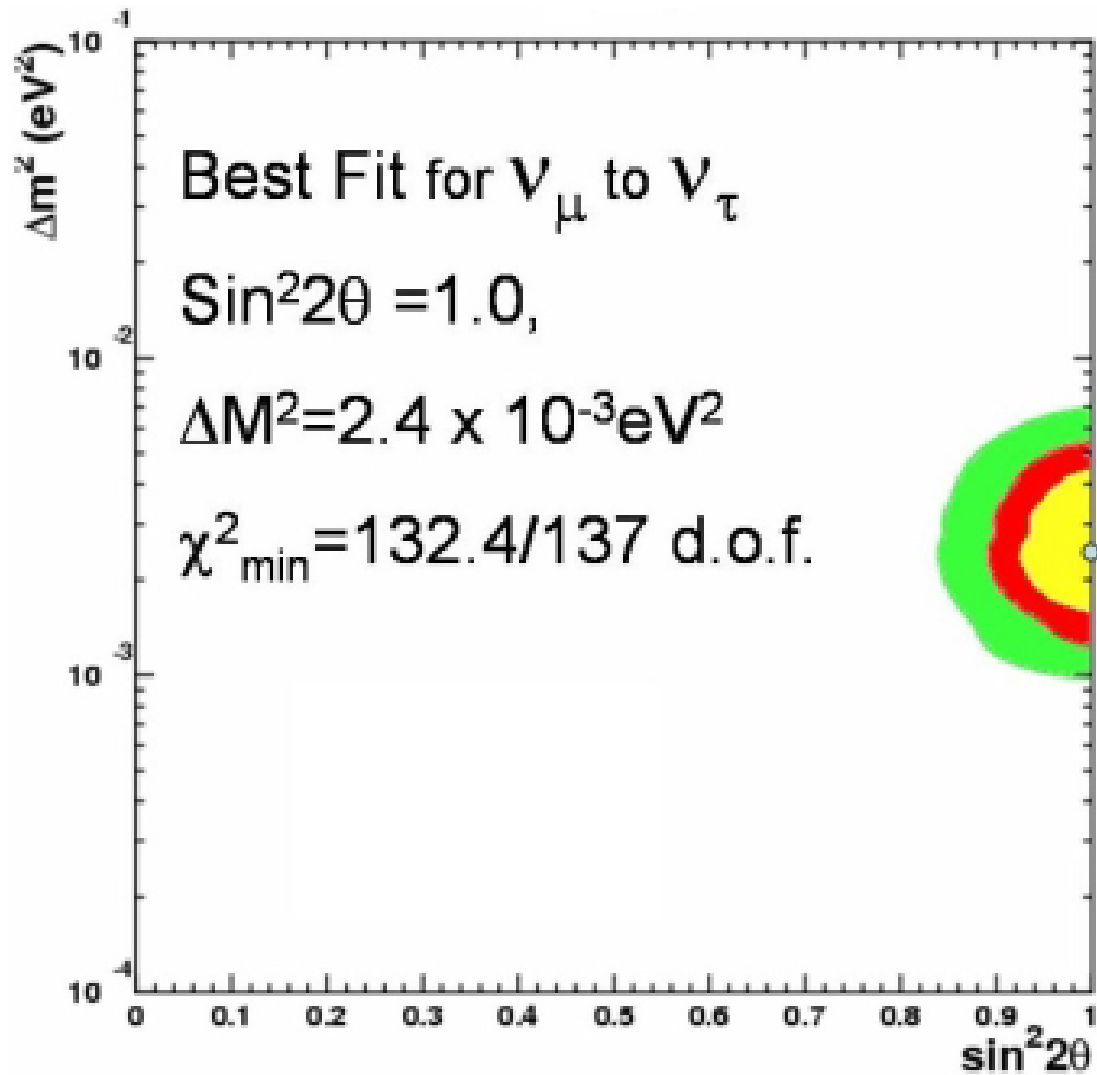




up/dawn



up/dawn

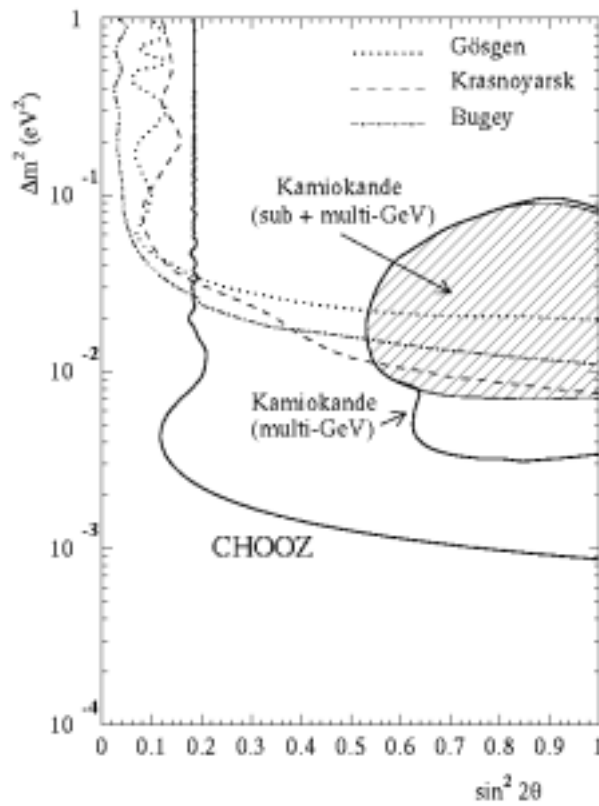
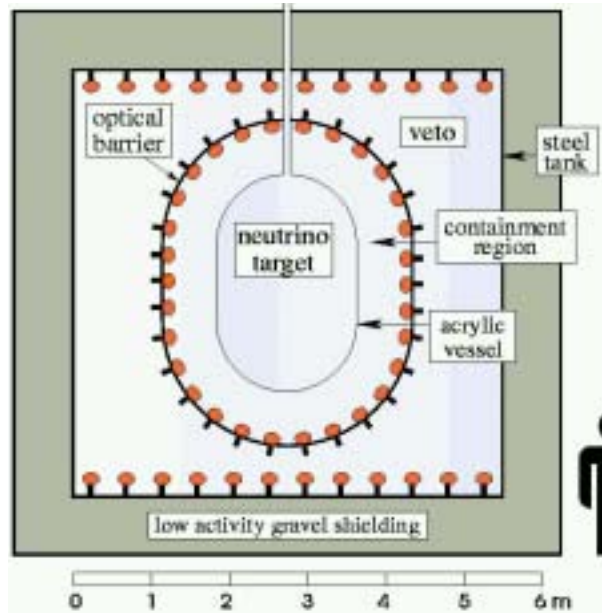


$$\Delta M^2 = 2.4 \times 10^{-3}$$

## 17.4 Reactor and high energy $\nu$ 's

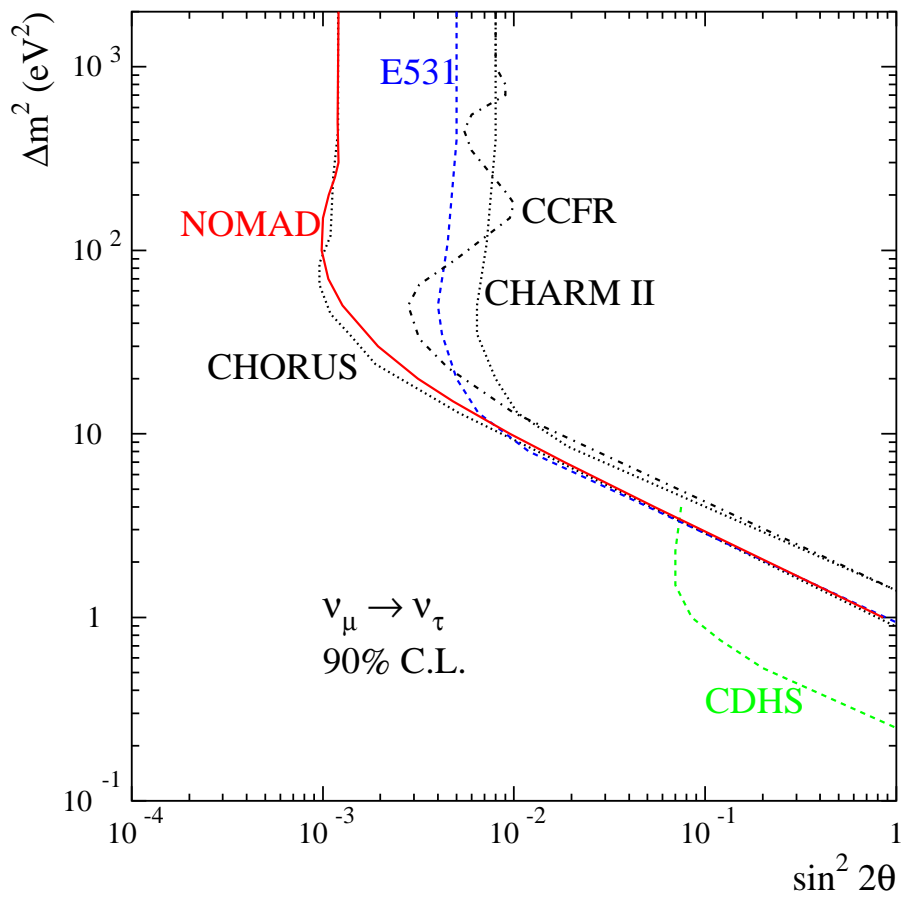
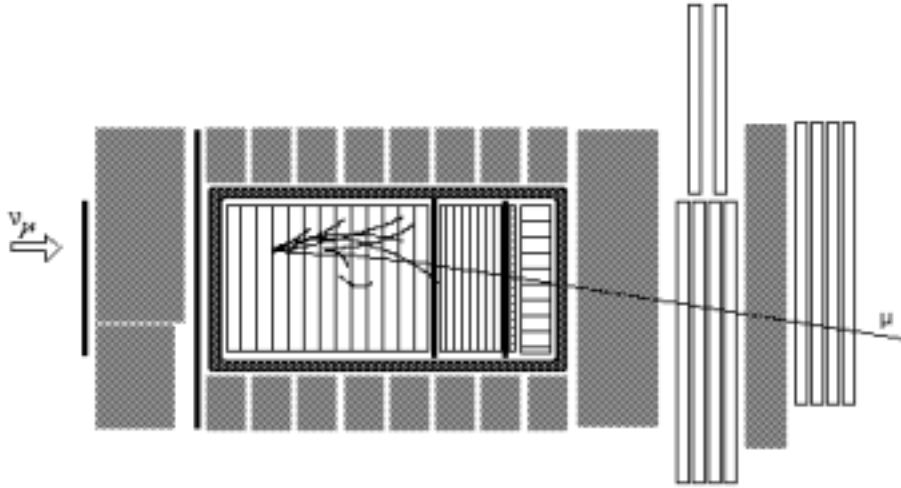
Chooz

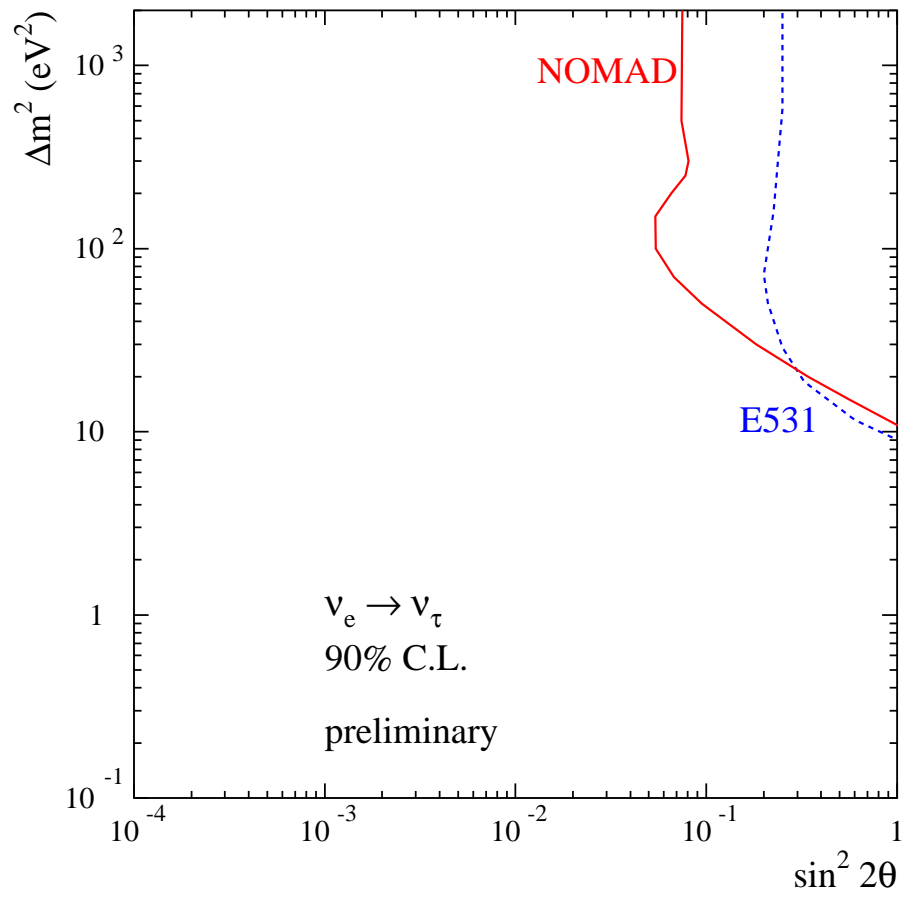
1 km to reactor - 300  $\ell$  liq. scint. Lots of  $\bar{\nu}$ 's



Conventional high energy  $\nu$  beams

Recent example. Nomad, closed. 450 GeV  $p$  produce  $10^{13}$   $\nu_\mu$  every 13 s

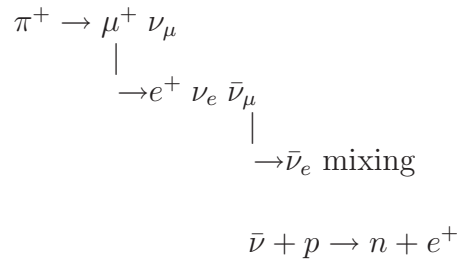




$$\Delta m^2 \lesssim 1 \text{ eV}$$

LSND - Karmen

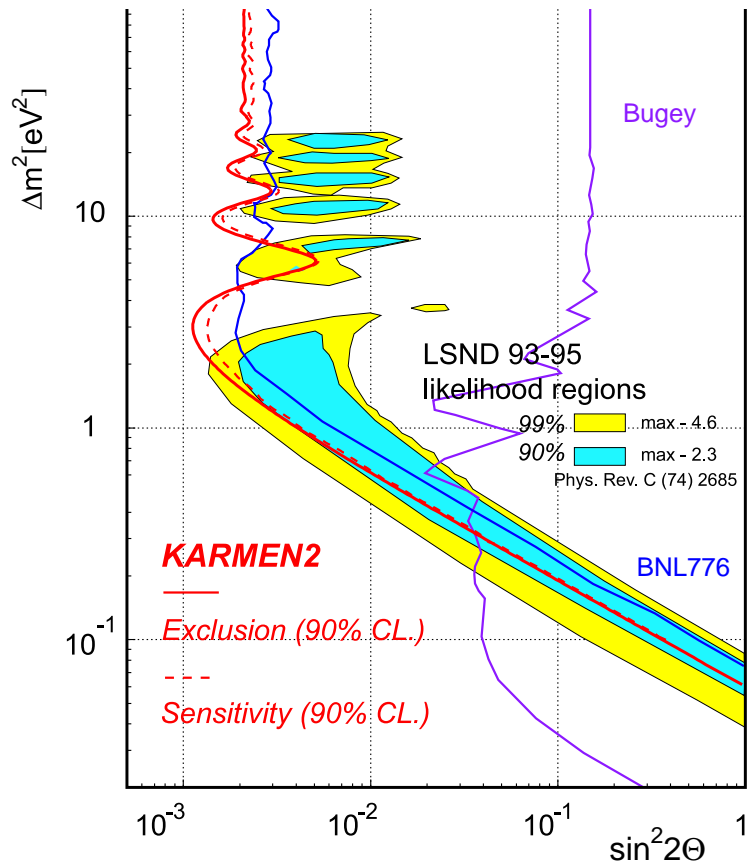
The only appearance experiments



Prompt  $e$  and delayed  $n$  ( $n + p \rightarrow d + \gamma$ )

**LSND**  $51 \pm 20 \pm 8$  events

**Karmen** No signal, lower sensitivity



## 17.5 The missing $\nu$ 's are found

SNO. A new kind of detector

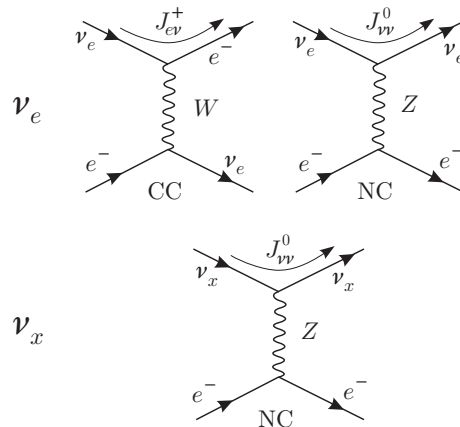
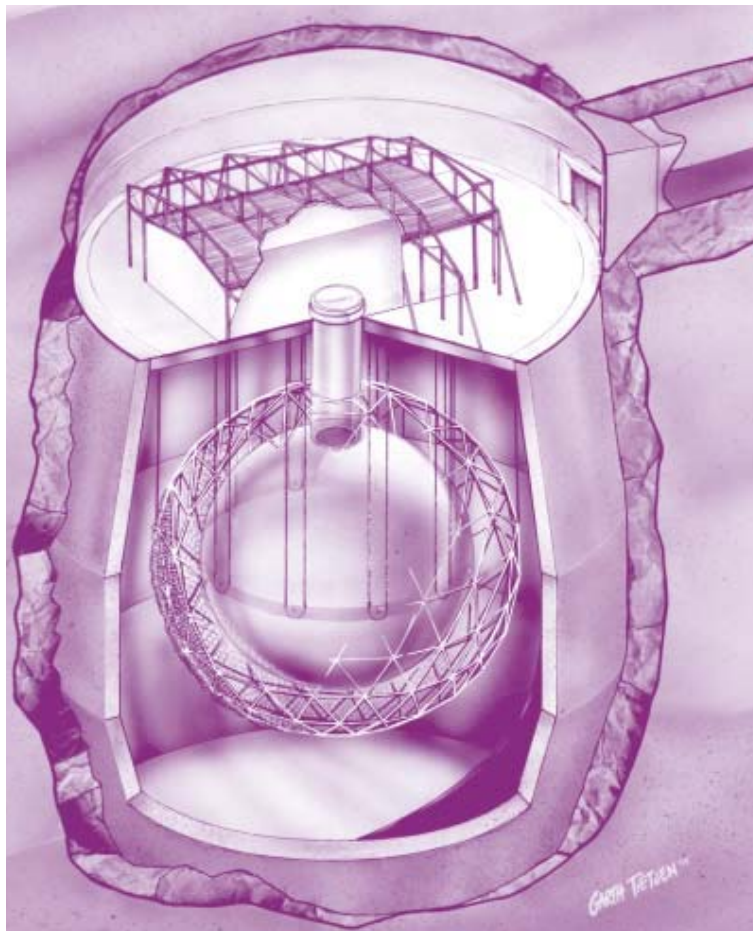
D<sub>2</sub>O Cerenkov - 1000 ton heavy water inside 7000 ton water.

Reactions:

$$\nu e \rightarrow \nu e, \text{ El. scatt, ES}$$

$$\nu_e d \rightarrow p p e^-, \text{ CC}$$

$$\nu d \rightarrow p n \nu, \text{ NC}$$



$$\sigma(\nu_e e \rightarrow \nu_e e) \sim 6.5 \times \sigma(\nu_x e \rightarrow \nu_x e)$$

$$\sigma(\nu_e d \rightarrow p p e) \sim 10 \times \sigma(\nu_e e \rightarrow \nu_e e)$$

From measurements of CC and ES can find flux of  $\nu_e$  and  $\nu_x$  from sun to earth.

$$\phi_{\text{SNO}}^{\text{ES}}(\nu_x) = 2.39 \pm 0.34 \pm 0.15 \times 10^6 \text{ /cm}^2/\text{s}$$

$$\phi_{\text{SNO}}^{\text{CC}}(\nu_e) = 1.75 \pm 0.07 \pm 0.11 \pm 0.05 \times 10^6 \text{ /cm}^2/\text{s}$$

$$\Delta\phi = 1.6 \sigma$$

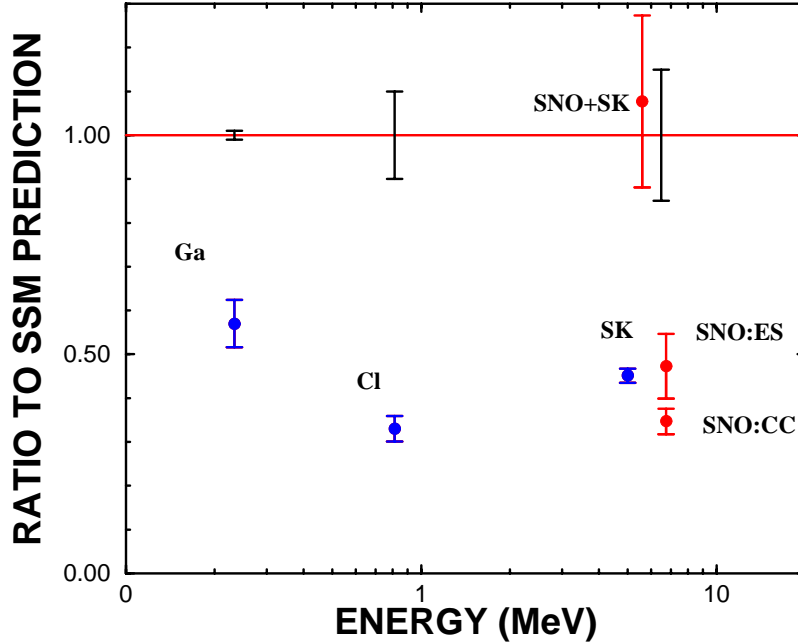
Therefore use SuperK result:

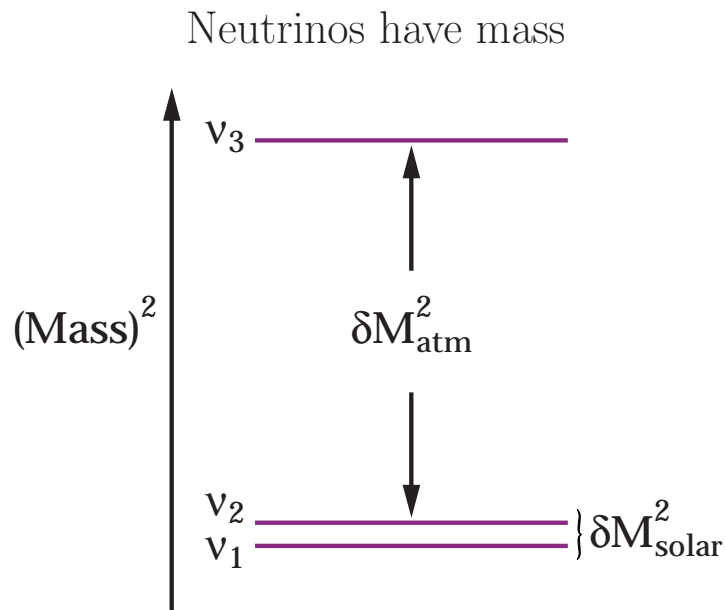
$$\phi_{\text{SK}}^{\text{ES}}(\nu_x) = 2.32 \pm 0.03 \pm 0.108 \times 10^6 \text{ /cm}^2/\text{s}$$

$$\Delta\phi = 3.3 \sigma$$

ES data contain all  $\nu$ 's ( $\nu_e$  favored by 6.5 to 1) while CC data only due to  $\nu_e$ .  
The difference is therefore evidence for non- $e$  neutrinos from the sun.

SNO, LP01, summer 2001: found missing solar  $\nu$ 's





Consistent for solar, atmospheric and reactor data. LSND requires a fourth, sterile neutrino

Most of the detector that led to the above results were not originally meant for measuring neutrino masses.

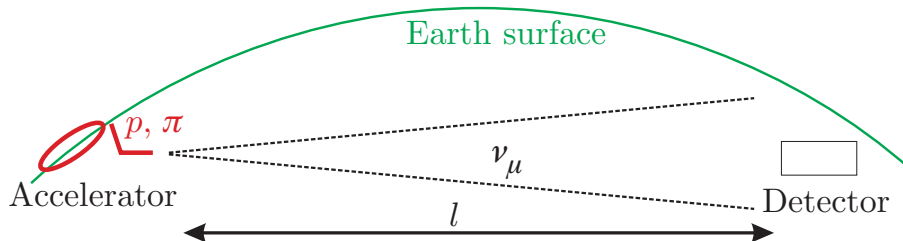
- |                         |                                     |
|-------------------------|-------------------------------------|
| Reactor Experiments     | Verify $\nu$ existence              |
| Underground Experiments | Sun dynamics                        |
|                         | Proton decay                        |
| Accelerator experiments | Verify $\nu$ existence <sup>†</sup> |
|                         | Hadron structure                    |
|                         | E-W parameters                      |

The results were surprising. What is still mostly missing are clear observations of oscillation and appearance of different flavors.

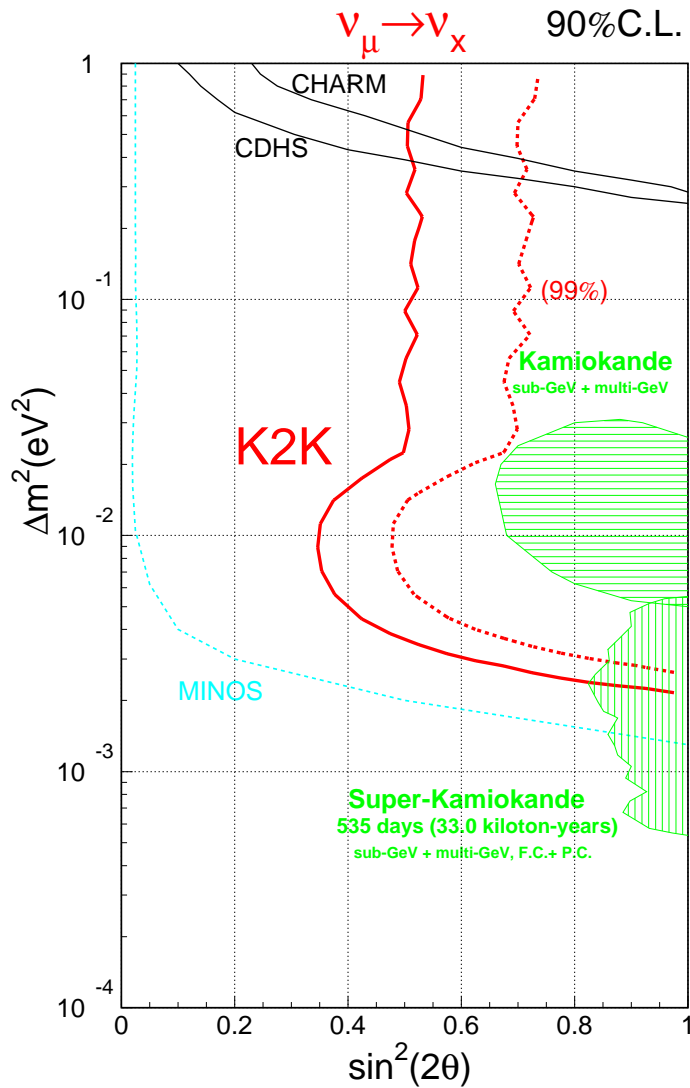
<sup>†</sup>Donut has reported observation of 4  $\nu_\tau \rightarrow \tau$  events.

### 17.6 Future Experiments

The future will be dominated by the so-called long baseline experiments. If  $\Delta m$  is small one needs large  $l$ .



KEK has been sending  $\nu$ 's to SuperK, 250 km away. for a year and events have been observed.



Two new projects are underway. MINOS in the USA,  $l=730$  km to the Soudan Mine site. CERN-Gran Sasso, with  $l=732$ . Ultimately one would like to see the

appearance of  $\nu_\tau$ .

MiniBooNE will begin data taking this year to confirm or otherwise the LSND claim, which seem to need a fourth neutrino.

More sensitive reactor experiments are on the way.

A real time experiment in Gran Sasso will measure the  $^7\text{Be}$  flux in real time by  $\nu - e$  elastic scattering.

There will also be experiments under water: Nestor, Baikal, Dumand. And also under ice, Amanda and over, RAND.

### $\nu_\tau$ appearance at Gran Sasso

$$L=732 \text{ km}, \langle E \rangle=17 \text{ GeV}, \Delta m^2(\text{S-K})=2.4 \times 10^{-3} \text{ eV}^2$$

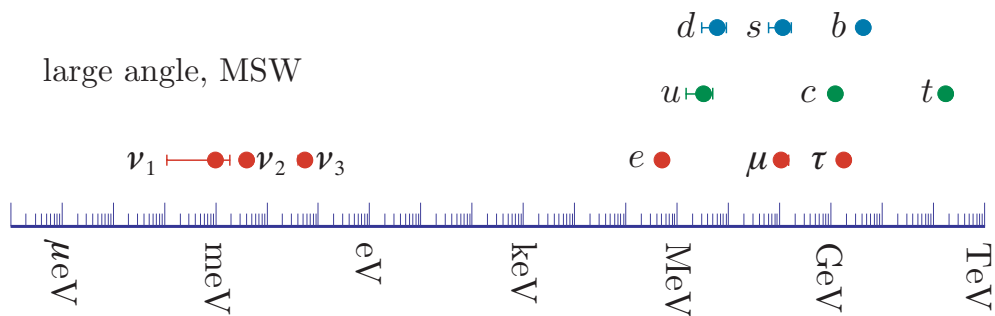
$\Delta m^2, \text{eV} \times 10^3$	5	3.5	2.4	2	1.5	1
$I(\nu_\tau) \text{ au}$	4.3	2.1	1	0.7	0.4	0.17
Events/5 y, Opera	46	23	11	7.5	4.2	2
Years, Icarus	4	8	17	24	43	97

We will know more, but not very soon.

In the meantime we have to change the SM and possibly understand the origin of fermion masses.

Neutrinos have added a new huge span to the values covered.

Theories are around but which is the right way?



## 18 The Muon Anomaly. A Seminar

### 18.1 Introduction

By definition, the gyromagnetic ratio  $g$  of a state of angular momentum  $J$  and magnetic moment  $\mu$  is:

$$g = \frac{\mu}{\mu_0} / \frac{J}{\hbar}.$$

For a particle of charge  $e$  in a state of orbital angular momentum  $\mathbf{L}$  we have:

$$\vec{\mu} = \mu_0 \mathbf{L}, \quad \mu_0 = \frac{e}{2m}, \quad g = 1.$$

For an electron  $g \sim 2$  - the Dirac value,  $\mu_0 = \mu_B = 5.788 \dots \times 10^{-11} \text{ MeV T}^{-1}$  ( $\pm 7$  ppb).

The importance of  $g$  in particle physics is many-fold. A gross deviation from the expected value, 2 for charged spin  $1/2$  Dirac particles, is clear evidence for structure. Thus the electron and the muon ( $g \sim 2.002$ ) are elementary particles while the proton, with  $g_p = 5.6$  is a composite object. For the neutron  $g$  should be zero, measurements give  $g_n = -3.8$

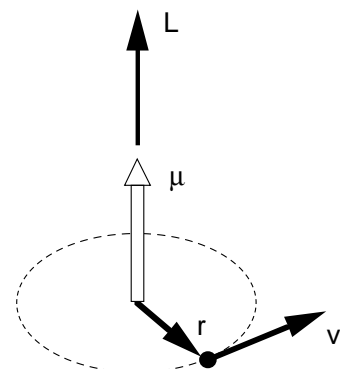
Small deviations from 2,  $\sim 0.1\%$ , appear as consequence of the self interaction of the particles with their own field. Experimental verifications of the computed deviations are a triumph of QED.

We also define the anomaly,  $a = (g - 2)/2$ , a measure of the so called anomalous magnetic moment,  $(g - 2)\mu_0$ .

QED is not all there is in the physical world. The EW interaction contributes to  $a$  and new physics beyond the standard model might manifest itself as a deviation from calculations.

#### Magnetic moment

The classical physics picture of the magnetic moment of a particle in a plane orbit under a central force is illustrated on the side.  $\vec{\mu}$  is along  $\mathbf{L}$ ,  $\mu_0 = q/2m$  and  $g=1$ . This remains true in QM. For an electron in an atom,  $\mu_B = e/2m_e$  is the Bohr magneton.  $\mathbf{L} \parallel \vec{\mu}$  is required by rotational invariance.



When we get to intrinsic angular momentum or spin the classic picture loses meanings and we retain only  $\vec{\mu} \parallel \mathbf{L}$ . We turn now to relativistic QM and the Dirac equation.

### 18.2 $g$ for Dirac particles

In the non-relativistic limit, the Dirac equation of an electron interacting with an electromagnetic field ( $p_\mu \rightarrow p_\mu + eA_\mu$ ) acquires the term

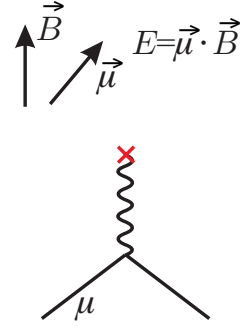
$$\frac{e}{2m} \vec{\sigma} \cdot \mathbf{B} - eA^0$$

which implies that the electron's intrinsic magnetic moment is

$$\vec{\mu} = \frac{e}{2m} \vec{\sigma} \equiv g \frac{e}{2m} \mathbf{S} \equiv g\mu_B \mathbf{S},$$

where  $\mathbf{S} = \vec{\sigma}/2$  is the spin operator and  $g=2$ .

The prediction  $g=2$  for the intrinsic magnetic moment is one of the many triumphs of the Dirac equation.



### 18.3 Motion and precession in a B field

The motion of a particle of momentum  $p$  and charge  $e$  in a uniform magnetic field  $B$  is circular with  $p = 300 \times B \times r$ . For  $p \ll m$  the angular frequency of the circular motion, called the cyclotron frequency, is:

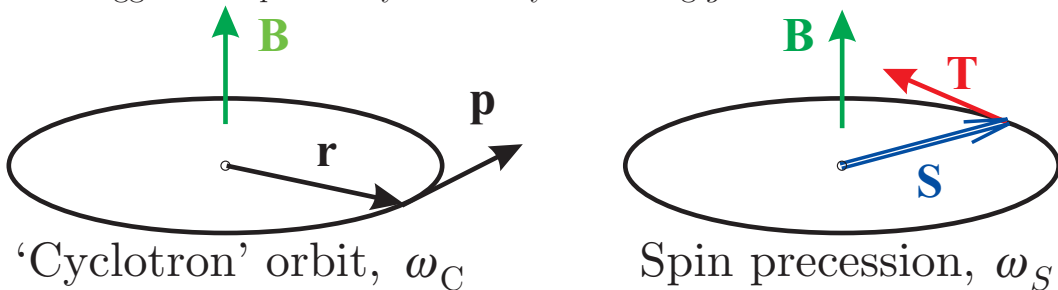
$$\omega_c = \frac{eB}{m}.$$

The spin precession frequency at rest is given by:

$$\omega_s = g \frac{eB}{2m}$$

which, for  $g=2$ , coincides with the cyclotron frequencies.

This suggests the possibility of directly measuring  $g - 2$ .



For higher momenta the frequencies become

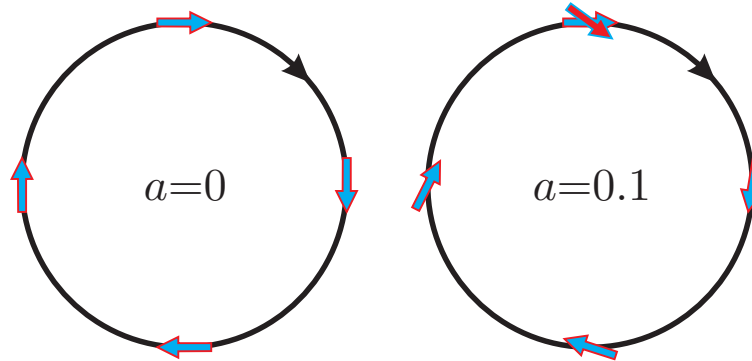
$$\omega_c = \frac{eB}{m\gamma}$$

and

$$\omega_s = \frac{eB}{m\gamma} + a \frac{eB}{m}$$

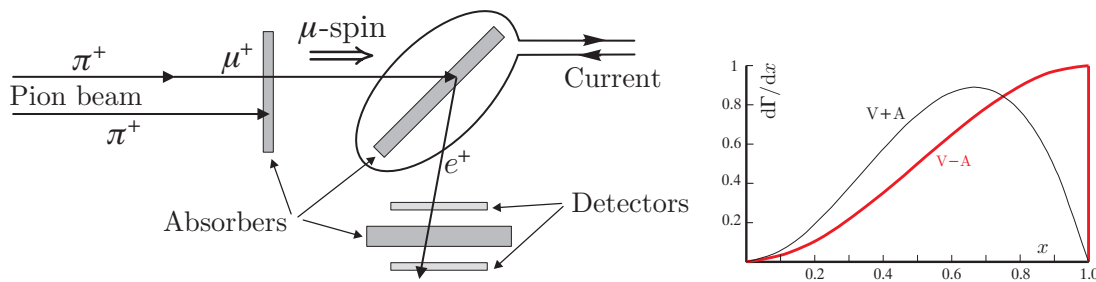
or

$$\omega_a = \omega_s - \omega_c = a \frac{eB}{m} = a\gamma\omega_c$$



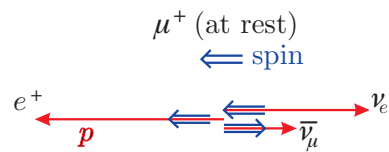
For  $a = 0.1$  ( $\gamma=1$ ), spin rotates wrt momentum by 1/10 turn per turn.

$$\pi \rightarrow \mu \rightarrow e$$



The rate of high energy decay electrons is time modulated with a frequency corresponding to the precession of a magnetic moment  $e/m(\mu)$  or a muon with  $g=2$ . First measurement of  $g(\mu)$ !! Also a proof that  $P$  and  $C$  are violated in both  $\pi\mu\nu$  and  $\mu \rightarrow e\nu\bar{\nu}$  decays.

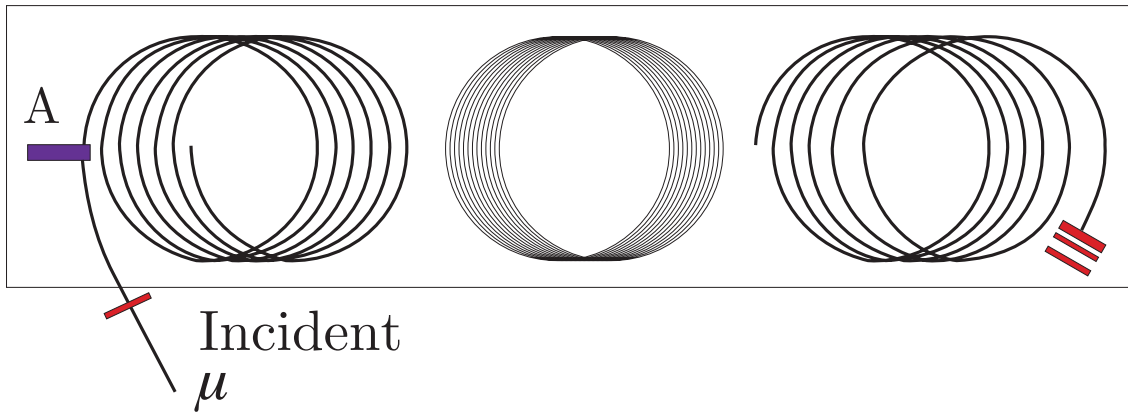
**S-p** correlation fundamental to all muon anomaly experiments



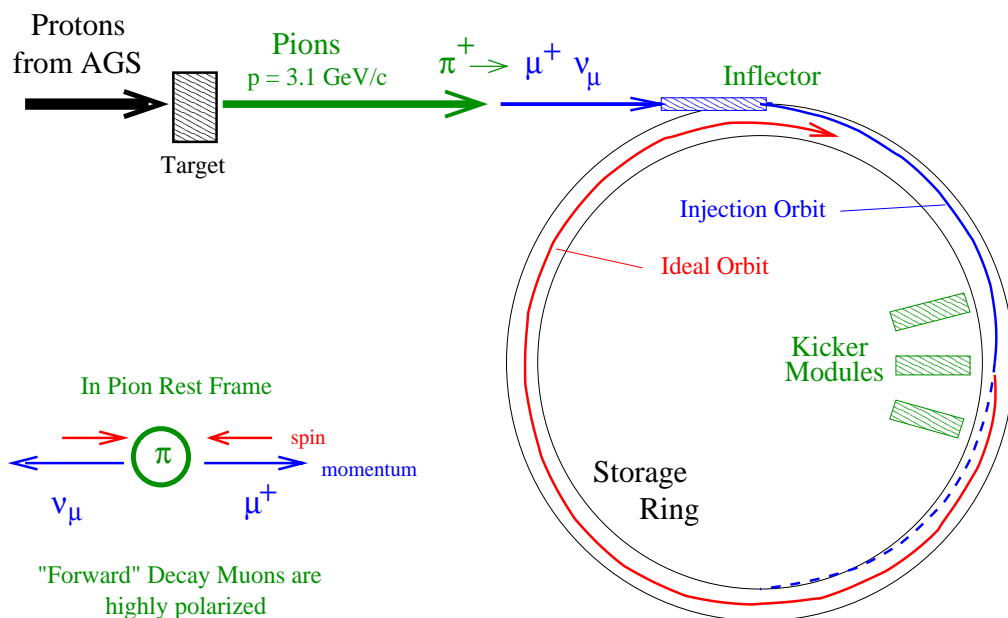
High energy positrons have momentum along the muon spin. The opposite is true for electrons from  $\mu^-$ . Detect high energy electrons. The time dependence of the signal tracks muon precession.

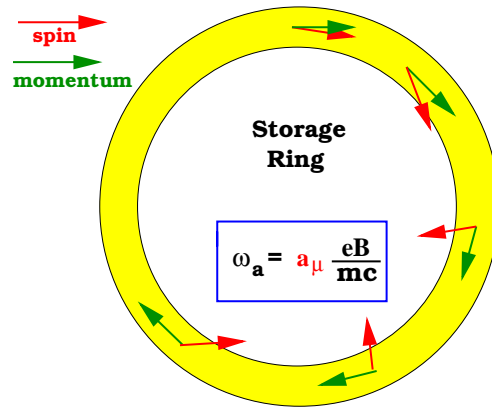
18.4 The first muon  $g - 2$  experiment

## Shaped B field



Performed in CERN, in the sixties. Need more turns, more  $\gamma$ . Next step: a storage ring.

18.5 The BNL  $g-2$  experiment $(g-2)_\mu$  Experiment at BNL



(exaggerated ~20x)

With homogeneous  $\vec{B}$ , all muons precess at same rate

LP01 James Miller - (g-2)<sub>μ</sub> Status: Experiment and Theory 22

With homogeneous  $\vec{B}$ , use quadrupole  $\vec{E}$  to focus and store beam

Spin Precession with  $\vec{B}$  and  $\vec{E}$

$$\vec{\omega}_a = \frac{e}{mc} [a_\mu \vec{B} - (a_\mu - \frac{1}{\gamma^2 - 1}) \vec{\beta} \times \vec{E}]$$

Choose "Magic"  $\gamma = \sqrt{\frac{1+a}{a}} \cong 29.3 \rightarrow$  Minimizes the  $\vec{\beta} \times \vec{E}$  term

- $\gamma \cong 29.3 \rightarrow p_\mu \cong 3.094$
- $B \cong 1.4T \rightarrow$  Storage ring radius  $\cong 7.112m$
- $T_c \cong 149.2ns \quad T_a \cong 4.365\mu s$
- $\gamma\tau \cong 64.38\mu s$

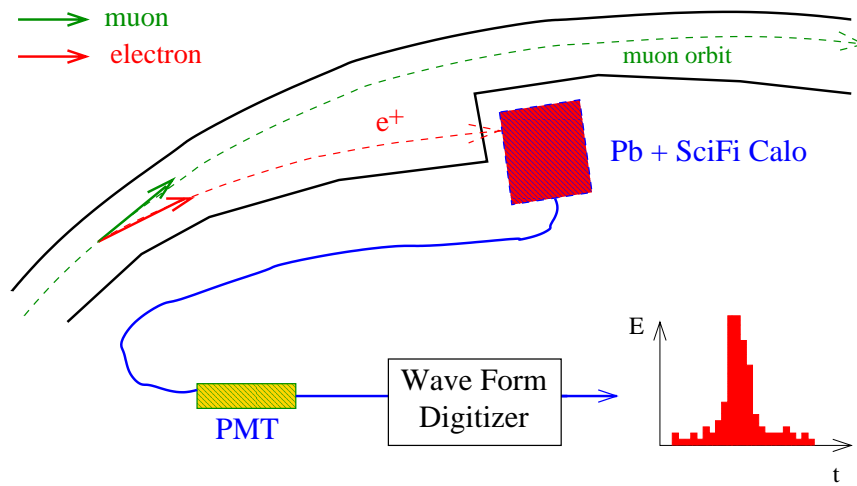
(Range of stored momenta:  $\cong \pm 0.5\%$ )

LP01 James Miller - (g-2)<sub>μ</sub> Status: Experiment and Theory 23

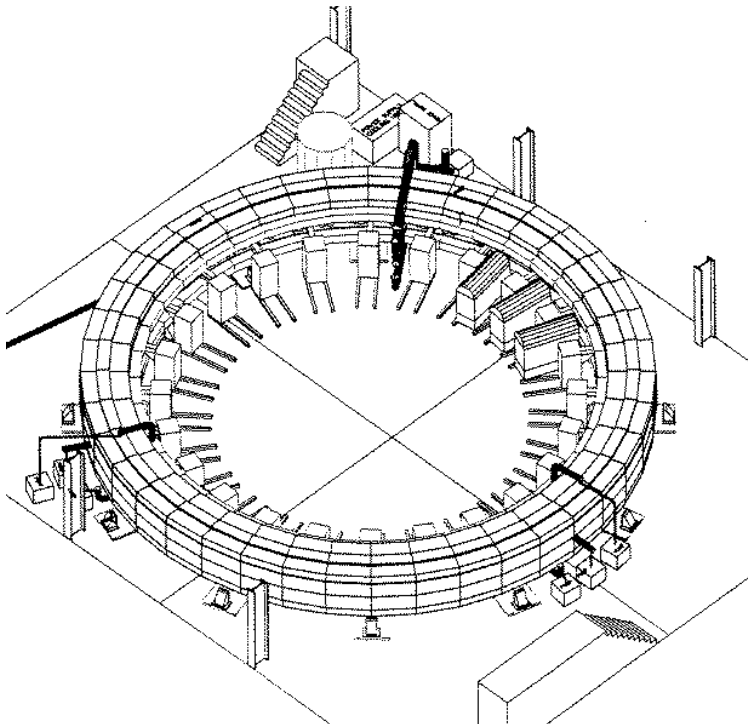
### $\omega_a$ Measurement

- $\mu^+ \rightarrow e^+ \bar{\nu}_\mu \nu_e, \quad 0 < E_e < 3.1GeV$
- Parity Violation  $\rightarrow$  for given  $E_e$ , directions of  $\vec{p}_{e^+}$  and  $\vec{s}_\mu$  are correlated  
 For high values of  $E_e$ ,  $\vec{p}_{e^+}$  is preferentially parallel to  $\vec{s}_\mu$
- number of positrons with  $E > E_{threshold}$   
 $N(t) = N_0(1 + A(E) \cos(\omega_a t + \phi))$

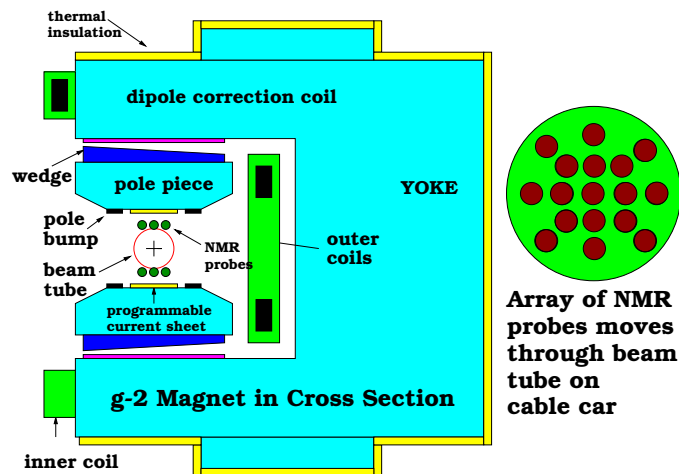
LP01 James Miller - (g-2)<sub>μ</sub> Status: Experiment and Theory 24



LP01 *James Miller -  $(g-2)_\mu$  Status: Experiment and Theory* **25**



LP01 *James Miller -  $(g-2)_\mu$  Status: Experiment and Theory* **26**



LP01 James Miller -  $(g-2)_\mu$  Status: Experiment and Theory 27

Determination of Average B-field ( $\omega_p$ ) of Muon Ensemble

Mapping of B-field

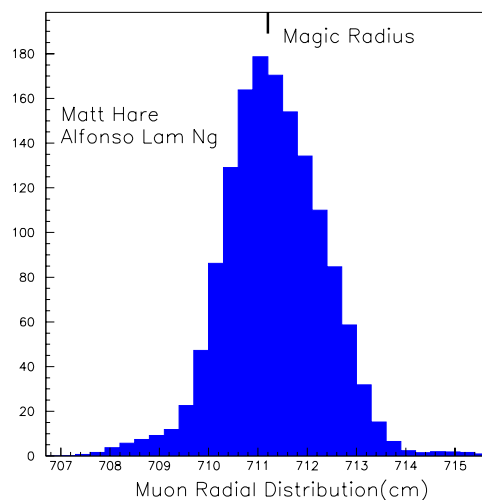
- Complete B-Field map of storage region every 3-4 days  
Beam trolley with 17 NMR probes
- Continuous monitor of B-field with over 100 fixed probes

Determination of muon distribution

- Fit to bunch structure of stored beam vs. time

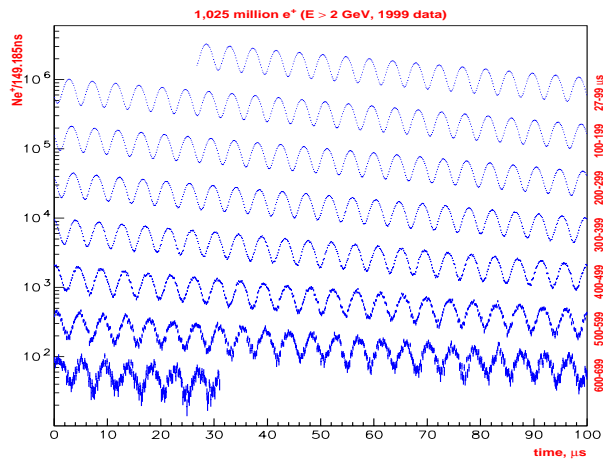
LP01 James Miller -  $(g-2)_\mu$  Status: Experiment and Theory 28

Determination of Muon Distribution



LP01 James Miller -  $(g-2)_\mu$  Status: Experiment and Theory 30

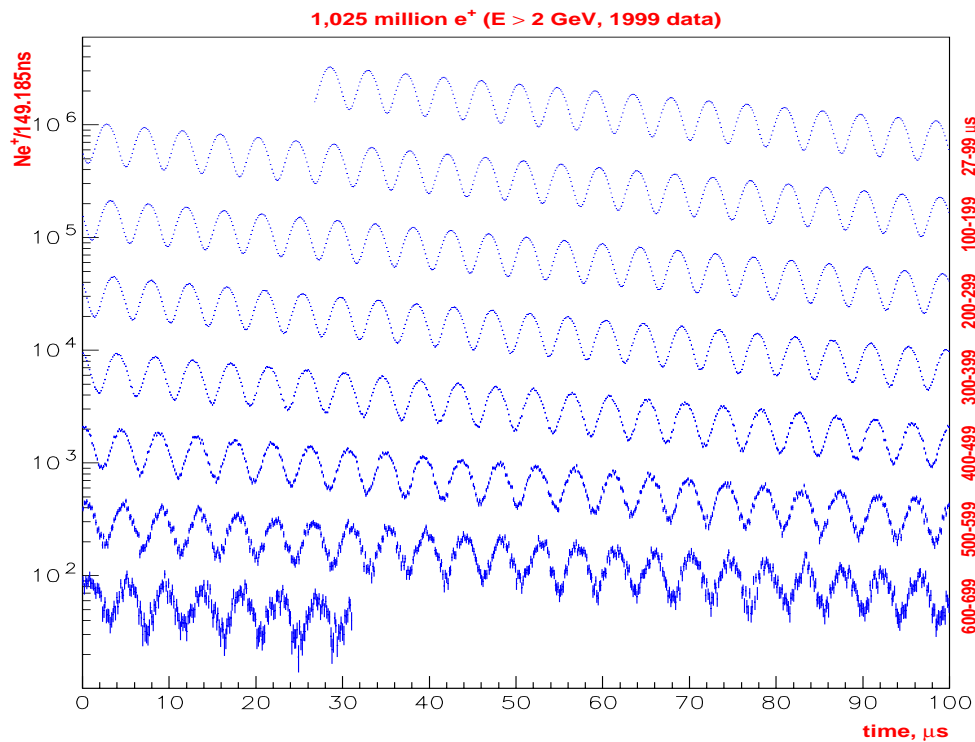
Log plot of 1999  
data ( $10^9$  e+)  
149 ns bins  
100  $\mu$ s segments  
Statistical error:  
$$\frac{\delta\omega_a}{\omega_a} = \frac{\sqrt{2}}{\omega_a \gamma \tau_\mu A \sqrt{N_e}}$$



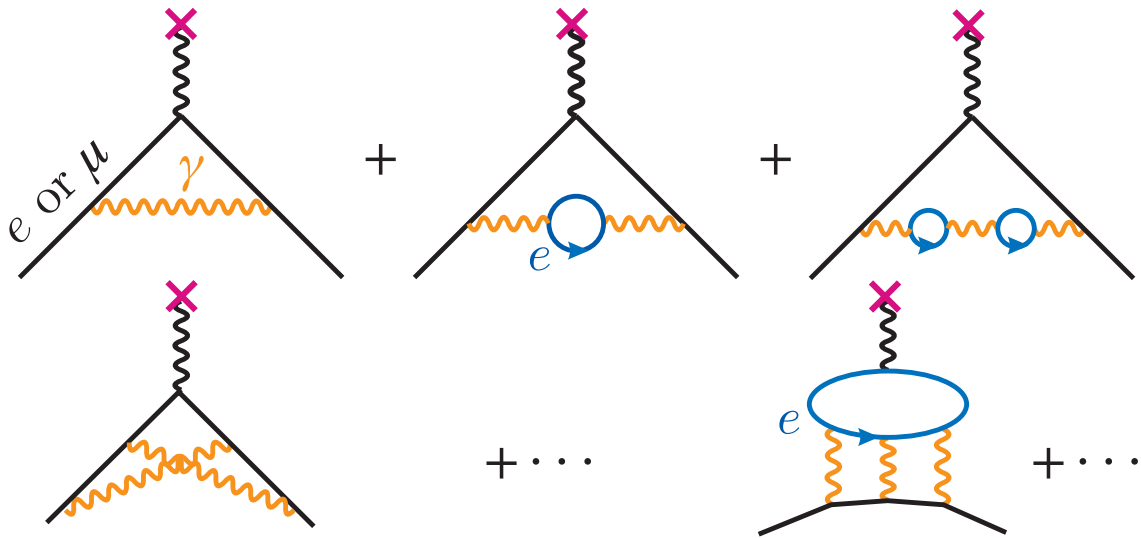
5-parameter function (used to fit to 1998 data)

$$N(t) = N_0 e^{-\lambda t} [1 + A \cos(\omega_a t + \phi)]$$

LP01 James Miller -  $(g-2)_\mu$  Status: Experiment and Theory 32



### 18.6 Computing $a = g/2 - 1$



+  $e \Rightarrow \mu, \tau; u, d, c, s, t, b; W^\pm \dots$

$$a_e = \frac{\alpha}{2\pi} + \dots c_4 \left(\frac{\alpha}{\pi}\right)^4 = (115965215.4 \pm 2.4) \times 10^{-11}$$

Exp,  $e^+$  and  $e^-$ :  $= (\dots 18.8 \pm 0.4) \times 10^{-11}$

Agreement to  $\sim 30$  ppb or  $1.4 \sigma$ . What is  $\alpha$ ?

### 18.7 $a_\mu$

Both experiment and calculation more difficult.  $a_\mu$  is  $m_\mu^2/m_e^2 \sim 44,000$  times more sensitive to high mass states in the diagrams above. Therefore:

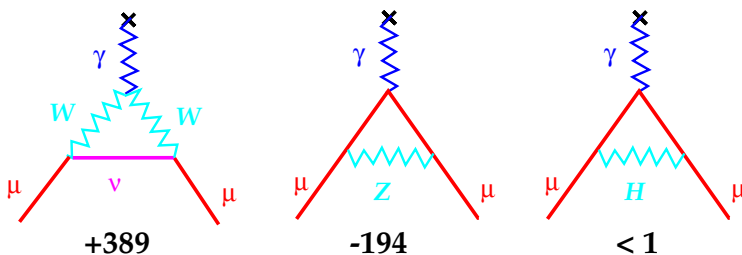
1.  $a_\mu$  can reflect the existence of new particles - and interactions not observed so far.
2. hadrons - pion, etc - become important in calculating its value.

Point 1 is a strong motivation for accurate measurements of  $a_\mu$ .

Point 2 is an obstacle to the interpretation of the measurement.

#### 1. - New Physics

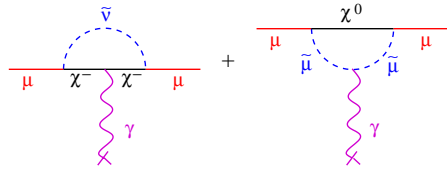
For calibration we take the E-W interaction



$$\langle \phi \rangle = 236 \text{ GeV} \quad M \sim 90$$

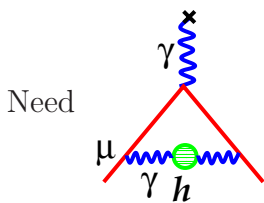
$$\delta a_\mu(\text{EW}) = 150 \times 10^{-11}$$

SUSY

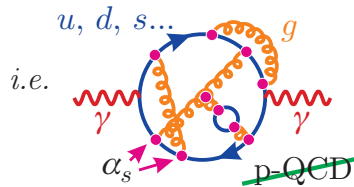


$$\delta a_\mu(\text{SUSY}) \sim 150 \times 10^{-11} \times (100 \text{ GeV}/\tilde{M})^2 \times \tan\beta$$

18.8 HADRONS



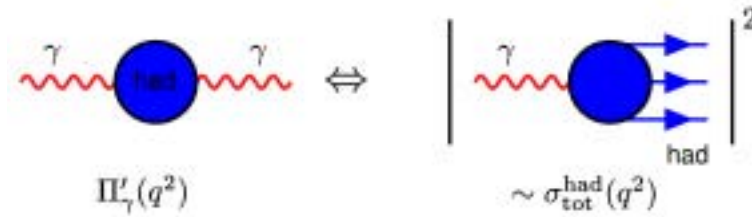
Need



i.e.

which is not calculable at low  $q^2$ .

Instead measure  $\sigma(e^+e^- \rightarrow \text{hadrons})$  and use dispersion relations.



$$\delta a_\mu, (\text{hadr} - 1) \sim 7000 \times 10^{-11}$$

All these effects are irrelevant for  $a_e$

$$a_\mu = \frac{\alpha}{2\pi} + \dots c_4 \left(\frac{\alpha}{\pi}\right)^4 = (116591596 \pm 67) \times 10^{-11}$$

$$\text{Exp, } \mu^+ : \quad = ( \dots 2030 \pm 150) \times 10^{-11}$$

Meas.-comp.= $430 \pm 160$  or  $2.6 \sigma$ ,  $\sim 3.7 \pm 1.4$  ppm; before fall '01

!!!!????

Today

1. H&D: Meas.-comp.= $260 \pm 160$  or  $1.6 \sigma$

2. J: Meas.-comp.= $180 \pm 180$  or  $1.0 \sigma$

Standard Model Value for  $a_\mu$  [1]

$a_\mu(QED)$	=	$116584706(3) \times 10^{-11}$
$a_\mu(HAD; 1)$	=	$6924(62) \times 10^{-11}$ (DH98)
$a_\mu(HAD; > 1)$	=	$-100(6) \times 10^{-11}$ (Except LL)
$a_\mu(HAD; LL)$	=	$-85(25) \times 10^{-11}$
$a_\mu(EW)$	=	$151(4) \times 10^{-11}$
TOTAL	=	$116591596(67) \times 10^{-11}$

[1] Czarnecki, Marciano, Nucl. Phys. B(Proc. Suppl.)76(1999)245

Used by the BNL  $g-2$  experiment for comparison. Addition of above errors in quadrature is questionable.

Light-by-light now is +85

18.9  $\sigma(e^+e^- \rightarrow \pi^+\pi^-)$

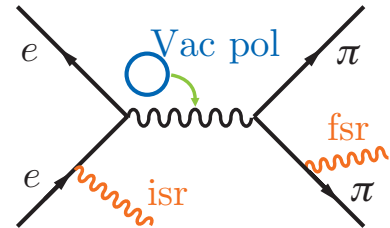
$\delta a_\mu(\text{hadr} - 1) \sim 7000 \times 10^{-11}$

$\sigma(e^+e^- \rightarrow \text{hadrons})$  is dominated below 1 GeV by  $e^+e^- \rightarrow \pi^+\pi^-$ . Low mass  $\pi^+\pi^-$  ( $\rho, \omega$ ) contributes  $\delta a_\mu \sim 5000 \pm 30$ .

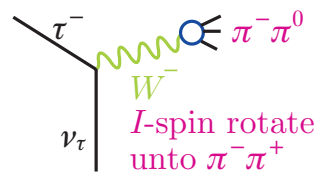
$\sigma(e^+e^- \rightarrow \pi^+\pi^-)$  or ( $\gamma \rightarrow \pi^+\pi^-$ ) is measured:

1. at  $e^+e^-$  colliders, varying the energy
2. in  $\tau$ -lepton decays
3. at fixed energy colliders using radiative return

- 1. - Extensive measurements performed at Novosibirsk. Corrections for efficiency and scale plus absolute normalization (Bhabha,  $e^+e^- \rightarrow e^+e^-$ ) are required for each energy setting. Data must also be corrected for radiation and vacuum polarization.

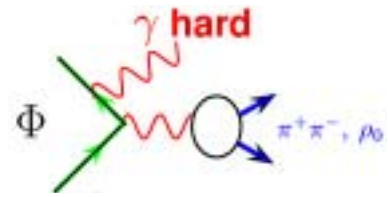


- 2. -  $\tau$  data come mostly from LEP. To get  $\sigma(\text{hadr})$  requires  $I$ -spin breaking,  $M(\rho^\pm) - M(\rho^0)$ ,  $I=0$  contrib... corrections. Radiative corrections are also required.

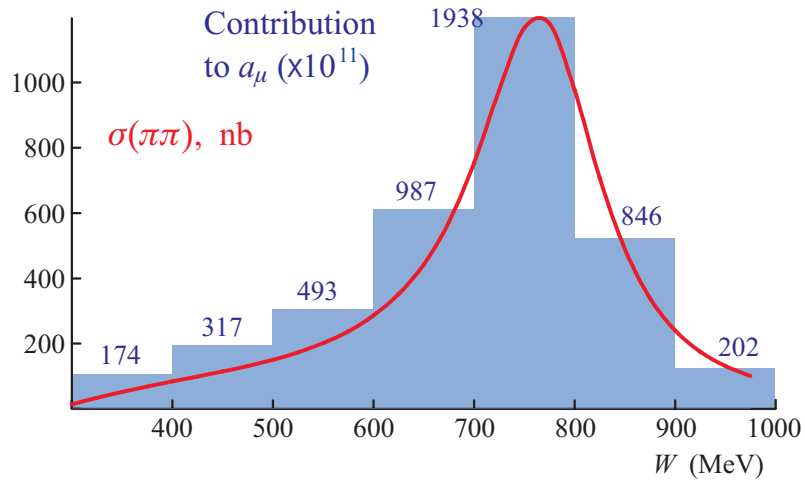
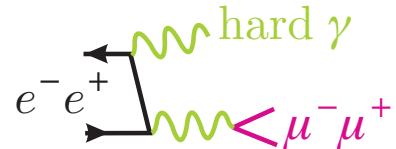


- 3. - The radiative return method is being used by the KLOE collaboration, spear-headed by the Karlsruhe-Pisa groups.

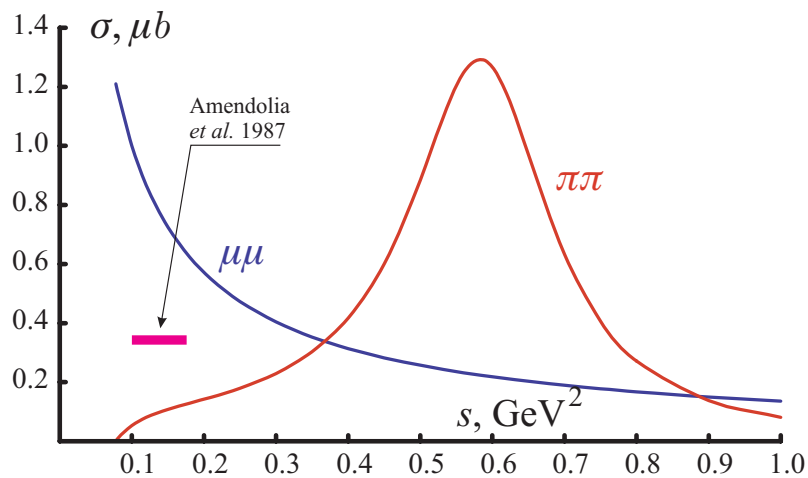
Can turn initial state radiation into an advantage. At fixed collider energy  $W$ , the  $\pi^+\pi^-\gamma$  final state covers the di-pion mass range  $280 < M_{\pi\pi} < W$  MeV. Correction for radiation and vacuum polarization are necessary. All other factors need be obtained only once.

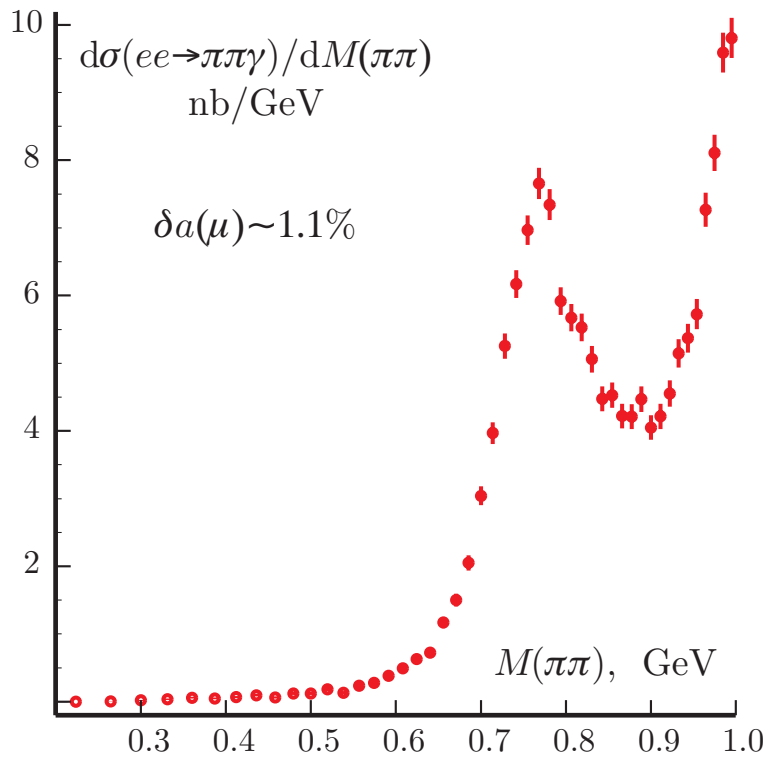
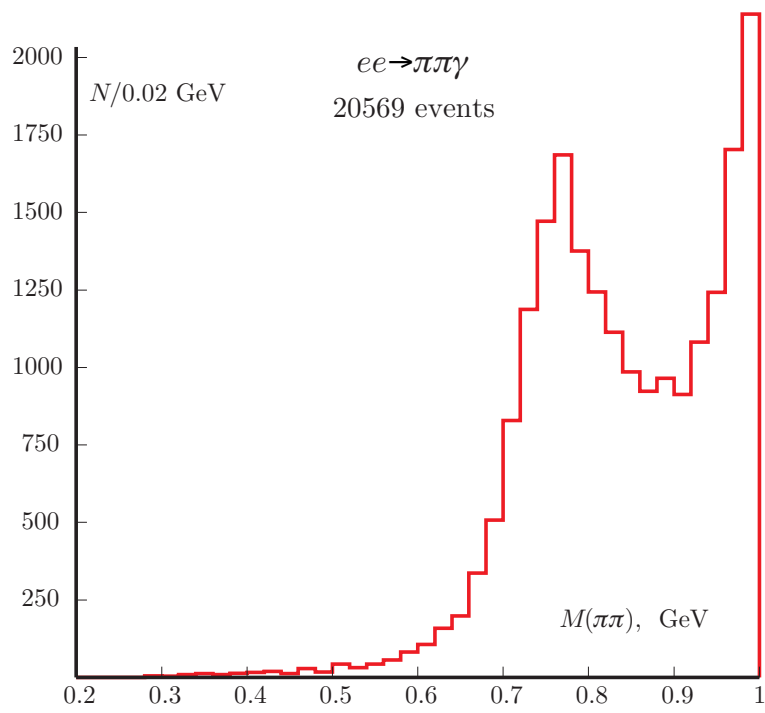


At low mass, di-muon production exceeds that of di-pion. ISR and vacuum polarization cancel.

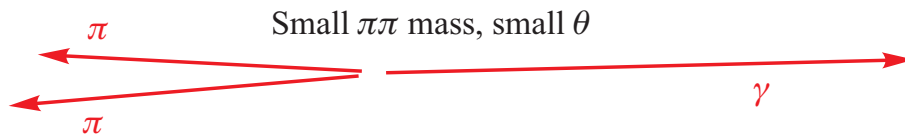
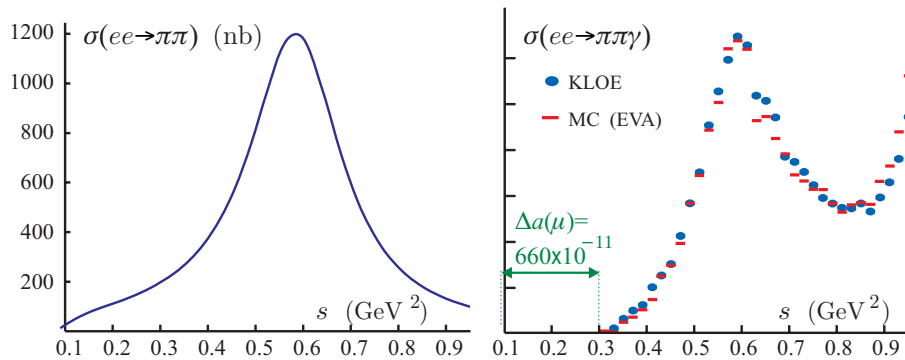


$$\sum(\dots) = 5000$$





Use small angle radiation, higher x-section but miss low  $M_{\pi^+\pi^-}$ .



Unsatisfactory points:

1. Effect is not very compelling.
2. Meas-estimate  $\sim$ EW contribution. What about LEP,  $b \rightarrow s\gamma$ ,  $M_W$ ,  $M_{\text{top}}$ ,  $\Re(\epsilon'/\epsilon)$ ,  $\sin 2\beta \dots$
3. Hadronic corrections difficult, author dependent. Light  $\times$  light sign finally OK?
4. SUSY as a theory is not predictive at present. Too many unknown/free parameters. There is no exp. evidence for it nor a prediction follows from the possible effect in the muon anomaly.

Soon better statistics and both signs muons. Still very exciting at present.

## 19 Higgs Bosons Today. A Seminar

### 19.1 Why are Higgs so popular?

1. No pretense for accuracy or depth
2. A simple reminder of a few things

Higgs and sociology

SSC was justified for its potential for Higgs discovery

TeV-I is today devoted to Higgs: CDF and DØ.

Major portion of US (and world) resources devoted to Higgs search

LHC under construction is commonly justified for Higgs discovery and study.

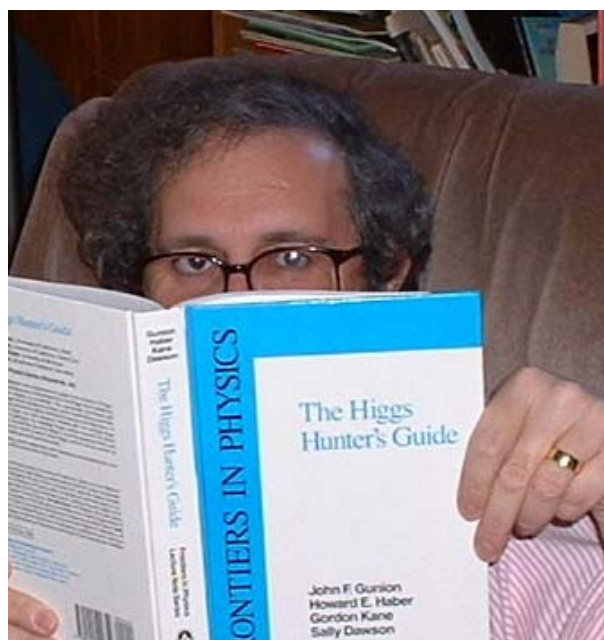
ATLAS and CMS, 2 detectors and 2 collaborations, >3000 physicists

Why?

For example

1. SM is still fine, it just survived the muon anomaly and the measurement of  $\sin 2\beta$  attacks.
2. Is the Higgs fundamental or can it be substituted by something else?
3. If the Higgs is heavy then there something nearby (see MEP)
4. Experiments are big and expensive.
5. Other reasons?

Look-up Michael E Peskin home page



## 19.2 Weak Interaction and Intermediate Boson

S-wave unitarity:

$$\sigma_\ell = \frac{4\pi}{k^2}(2\ell + 1)|a_\ell|^2 \leq \frac{4\pi(2\ell + 1)}{k^2}$$

$$\sigma_{\ell=0} \sim \frac{1}{s} \quad \sigma_F = G^2 s$$

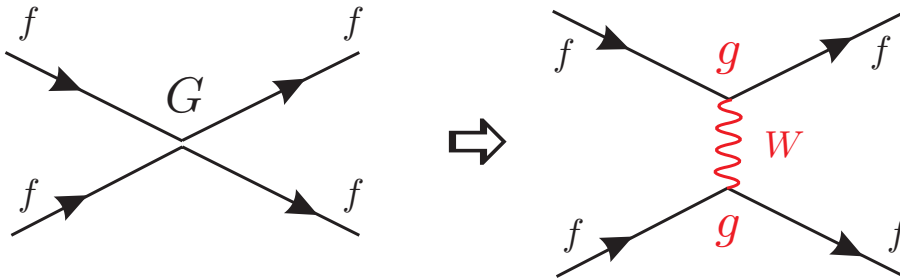
Unitarity bound is violated for:

$$\sigma_F \geq \sigma_{\ell=0} \quad s \geq \frac{1}{G}$$

$$E \geq \sqrt{1/G} \sim 300 \text{ GeV}$$

$\pi=2=1$  above.

But suppose that:



then

$$\frac{d\sigma}{d|t|} \propto \frac{g^4}{(M_W^2 - t)^2}$$

instead of  $d\sigma/d|t| \propto G^2$ . Low energy phenomenology ( $|t|, s \ll M_W^2$ ) requires  $g^2 \approx G \times M_W^2$ .

Late 50's,  $M_W$  few GeV.

Today:  $g^2 \sim 10^{-5} \text{ GeV}^{-2} \times 80^2 \text{ GeV}^2 \sim 0.064 \sim \alpha$ .

This suggest unifying weak and electromagnetic interactions with the help of vector bosons.

EM:  $J_\mu A^\mu$ . Current  $J_\mu$  is a Lorentz vector and is “neutral”

WI  $(V - A)_\mu W^\mu$ . Current  $(V - A)_\mu$  is a Lorentz vector and axial vector, violates parity, is “charged”.

Can one do it all from a local gauge invariance principle?

QED follows from an abelian local U(1) invariance. All of QED follows from  $\partial_\mu \rightarrow \partial_\mu + ieA_\mu$ . The current couples to a massless gauge field  $H = J_\mu A^\mu$ .

WI are more complex, because of  $\Delta Q = \pm 1$ . Minimal group is SU(2) but then you get three gauge fields,  $W^+$ ,  $W^-$  and  $W^0$ !

Neutral currents appear in experiments in the late 60's.

There is another problem with local gauge theories. Gauge bosons ought to be massless. After a real tour de force – Nambu-Goldston-Higgs – spontaneous symmetry breaking is understood and the gauge bosons are allowed to have a mass. But... is the E-W interaction renormalizable?

It turns out it is – t'Hooft-Lee-Veltman – and the E-W interaction the – Glashow-Salam-Weinberg – theory of the so-called Standard Model is finally respectable. It is a local non-abelian gauge theory. The gauge group is  $SU(2) \times U(1)$ . There are two couplings which are related to  $\alpha$  and  $G_F$ .

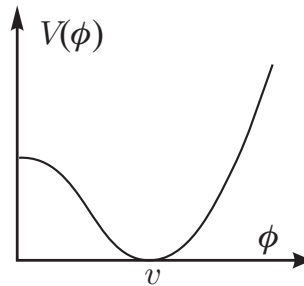
$SU(2)_{\text{w-ispin}} \times U(1)_Y$ : 4 generators  $\Rightarrow$  4 gauge fields:  
 $W^+, W^0, W^-$  and  $B^0$ .

There is also a mixing angle which gets from  $W_\mu^0 - B_\mu^0$  to  $Z_\mu^0 - A_\mu$ , with  $A_\mu$  a massless field, the photon.

Specifically a complex scalar doublet is introduced in the Lagrangian. The manifest initial symmetry is spontaneously broken. The vacuum acquires non zero energy. Or rather the “true” vacuum, the lowest energy state, corresponds to a non zero value of the scalar field  $\phi$ .

One number is well defined,

$$v = \langle \phi \rangle = \sqrt{\frac{1}{\sqrt{2} G}} = 246 \text{ GeV}$$



But because the gauge symmetry is local, three of the degrees of freedom of the Higgs field,  $\phi^+, \phi^0, \bar{\phi}^0$  and  $\phi^-$  become the zero helicity states of the gauge bosons which thus acquire mass.

The vector boson masses are

$$M_W = \frac{1}{\sin \theta} \left( \frac{\pi \alpha}{\sqrt{2} G} \right)^{1/2} = \frac{37.3}{\sin \theta} \text{ GeV}$$

$$M_Z = \frac{M_W}{\cos \theta}$$

One scalar boson survives as an observable elementary particle, it is called the Higgs boson. So all is left to be done is to find the Higgs.

### 19.3 Searching for Higgs. Where?

It would help to know how and where, *i.e.*

1. Mass - at least some guess
2. Production and decays or couplings to the world
3. Anything else

It is typical of the SM that it can relate many things but it has not much predictive power about the many parameters that enter into it. The Higgs mass is certainly one such example.

#### Mass

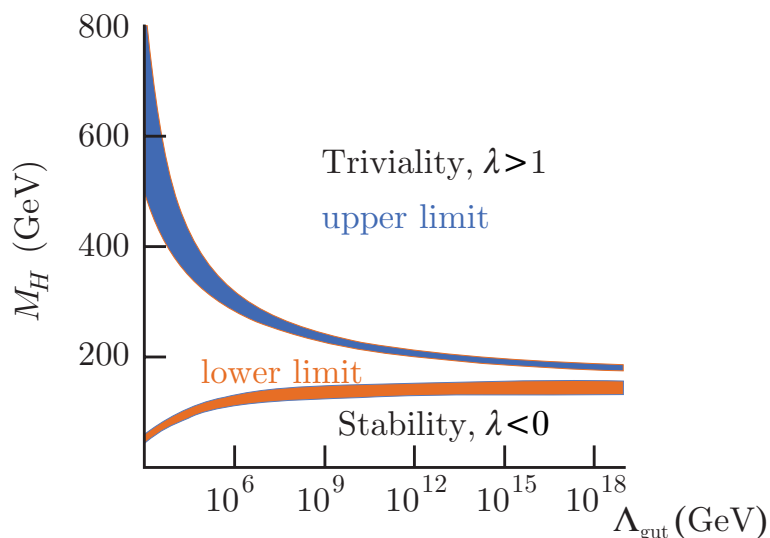
There is no a priori knowledge about the Higgs mass as well as many other things. But... In the Lagrangian we find a quartic coupling  $\lambda\phi^4$ , where  $\lambda$  is an arbitrary dimensionless coupling constant. The Higgs mass is given by  $M_H = v\sqrt{\lambda/2}$ . What is  $\lambda$ ?

From effective  $HH$  coupling,  $M_H > \alpha v$   $M_H > 7.3$  GeV. If  $<$ , the vacuum becomes unstable...! This limit can be somewhat softened.

There is an exception: if  $m_t \sim 80$  GeV the lower bound disappears:  $M_H > 0$  if  $m_t = 80$  GeV. This is just of historical interest.

Upper limits. If  $M_H > 1$  TeV than  $WW$  scattering exceeds unitarity. What, again?

Also for  $M_H \sim 1$  TeV,  $\Gamma_H \sim 1$  TeV...



Higgs mass limit vs new physics scale  $\Lambda$ . Upper unitarity, lower stability.

### Radiative Corrections

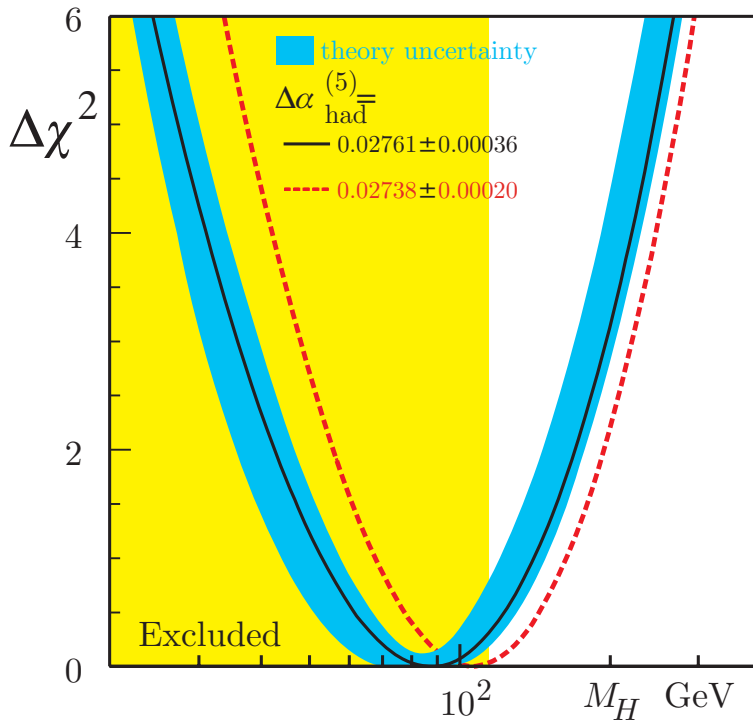
$$M_W = \frac{(\pi\alpha/\sqrt{2}G)^{1/2}}{\sin\theta(1-\Delta r)}$$

Example:

where  $\Delta r$  are the  $SU(2) \times U(1)$  radiative corrections.  $\Delta r = \Delta r_0 - \rho_t/\tan^2\theta + \mathcal{O}(\log M_H/\Lambda)$ .  $\Delta R_0 = 1 - \alpha/\alpha(M_Z) = 0.0664$

$\rho_t = \dots Gm_t^2 \dots = 0.00925 \times (m_t/174.3 \text{ GeV})^2 + \text{logs}$ . PREDICTS  $m_t$ , partly cancels QED.  $\Delta r = 0.0350 \pm 0.0019 \pm 0.0002$ . Last error from  $\alpha(M_Z)$

From  $M_Z, M_W, m_t$ , etc., can find  $M_H$ .

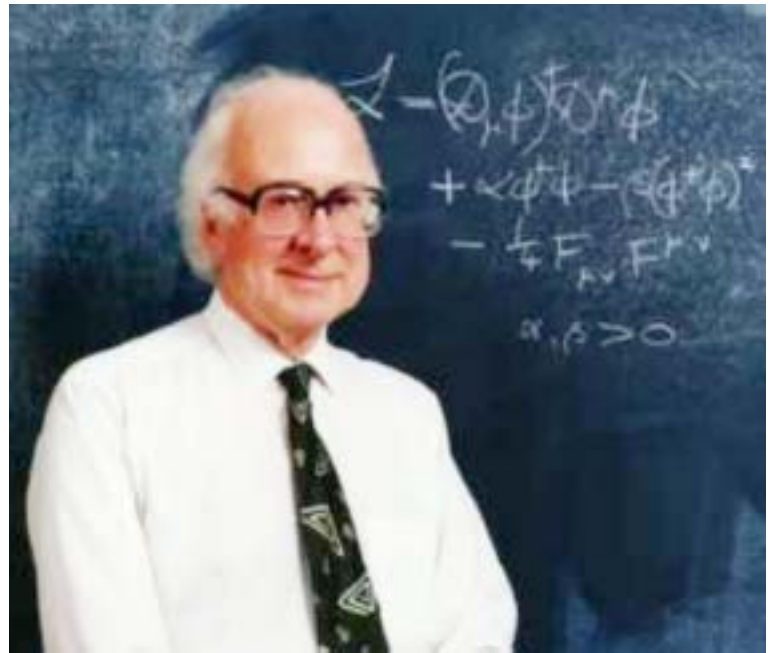


$$M_H = 88^{+53}_{-35} \text{ GeV}$$

$M_H < 196 \text{ GeV}$  (95% CL)

## Breaking Symmetry

Peter Higgs



## Restoring Symmetry



Glashow

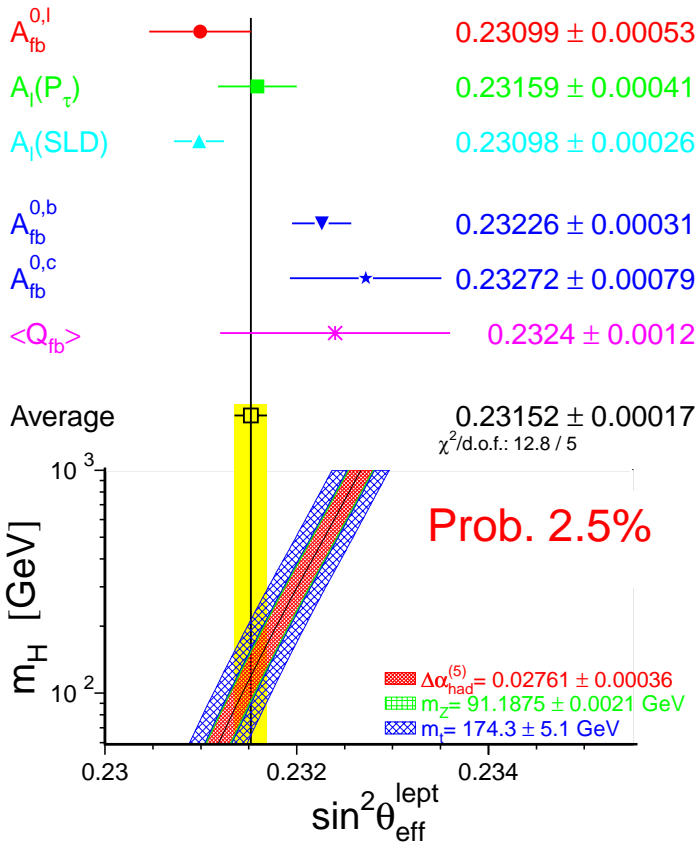


Salam



Weinberg

However...



$\sin^2 \theta_{\text{eff}}^{\text{lept}}$  from only  
 leptons  $.23113 \pm .00021$   
 hadrons  $.23230 \pm .00029$

Either:

- Statistical fluctuation,
- unknown sources of systematic errors,
- or evidence for new physics.

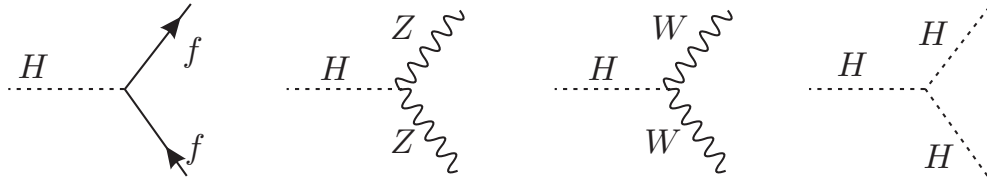
Note:

Only average  $\sin^2 \theta_{\text{eff}}$  consistent with  $m_H$  O(100 GeV) .

### 19.4 Searching for Higgs. How?

#### Production and decay

The Higgs couples universally to fermion and vector bosons



and therefore also to photons and gluons

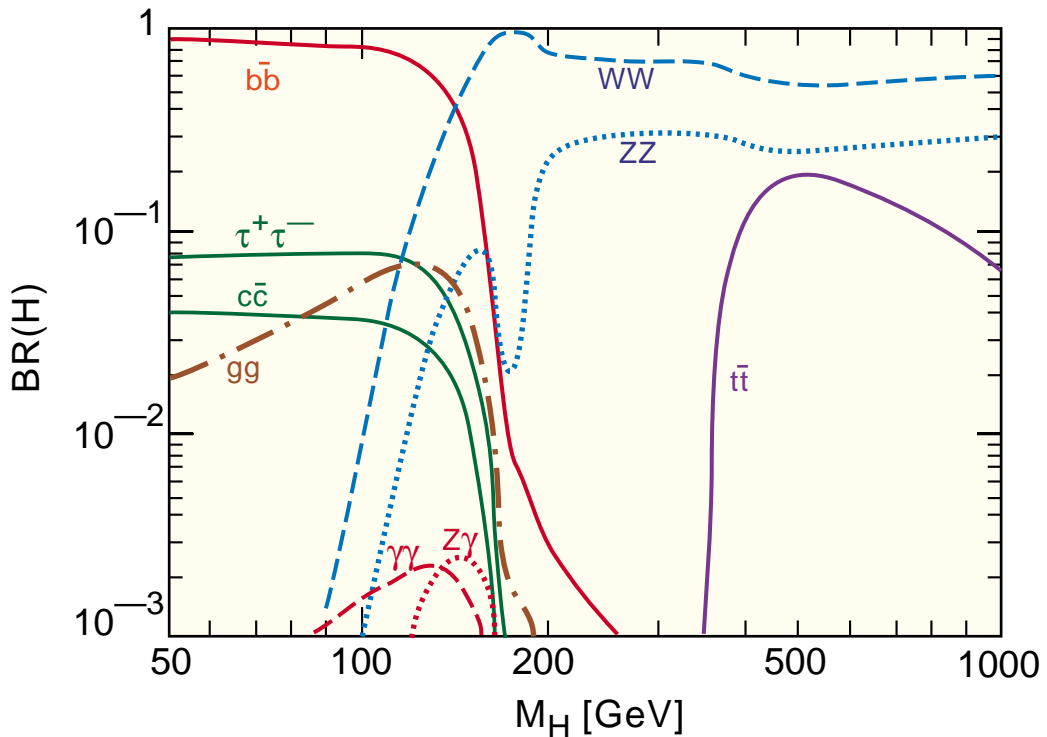


Couplings  $\propto$ (mass). We can choose the best way to detect it!

$$\Gamma(H \rightarrow gg) = \left( \frac{\alpha M_H}{8 \sin^2 \theta} \right) \frac{M_H^2}{M_W^2} \frac{\alpha_s^2}{9\pi^2} \left| \sum_q I(M_H^2/m_q^2) \right|^2$$

$$I(0) = 1, I(\infty) = 0$$

$\Gamma(H \rightarrow \gamma\gamma \dots)$  etc.

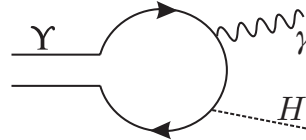


### Yield vs background

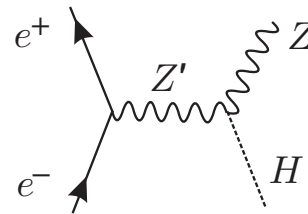
As long as  $\Gamma(H) < 1$  GeV, a rare final state can be better than a a copious one.

1.  $e^+e^- \mu^+\mu^-$  can be measured to few %.
2.  $\gamma\gamma$  could have best resolution for low  $M_H$ , BR lowest.
3.  $\tau\tau$  is characteristic but has no mass resolution.
4. Jet-jet has poor mass resolution but  $b$ -tag might help
5. Missing energy, always an interesting signal, but...

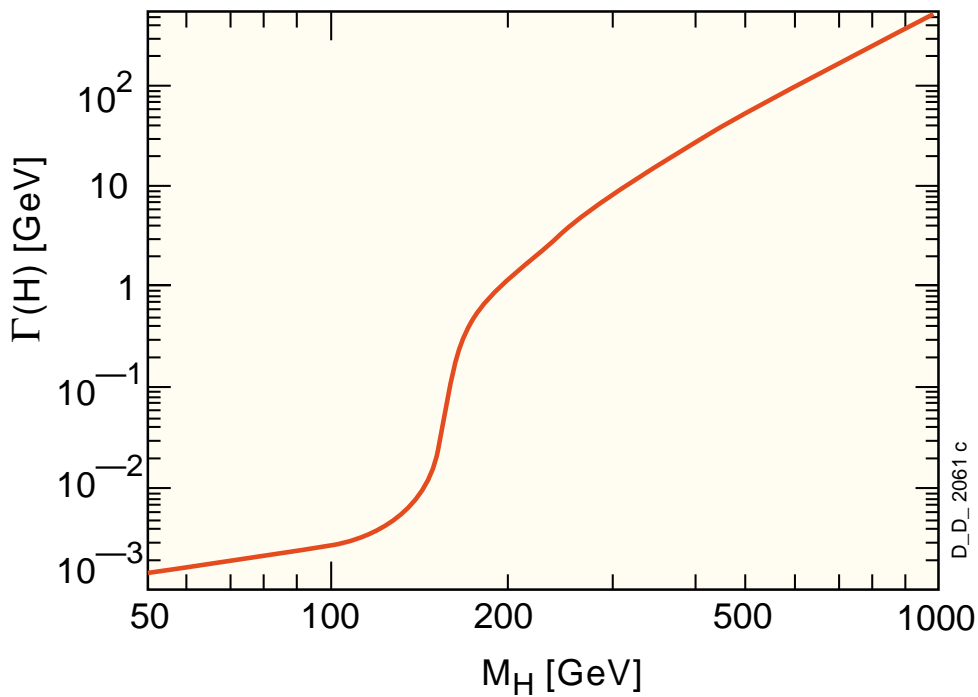
Very light Higgs and axions. Heavy quarks couple more to Higgs. Can search for light Higgs in  $\Upsilon \rightarrow \gamma + H$ . CUSB excluded Higgs with  $M_H < 3-4$  GeV



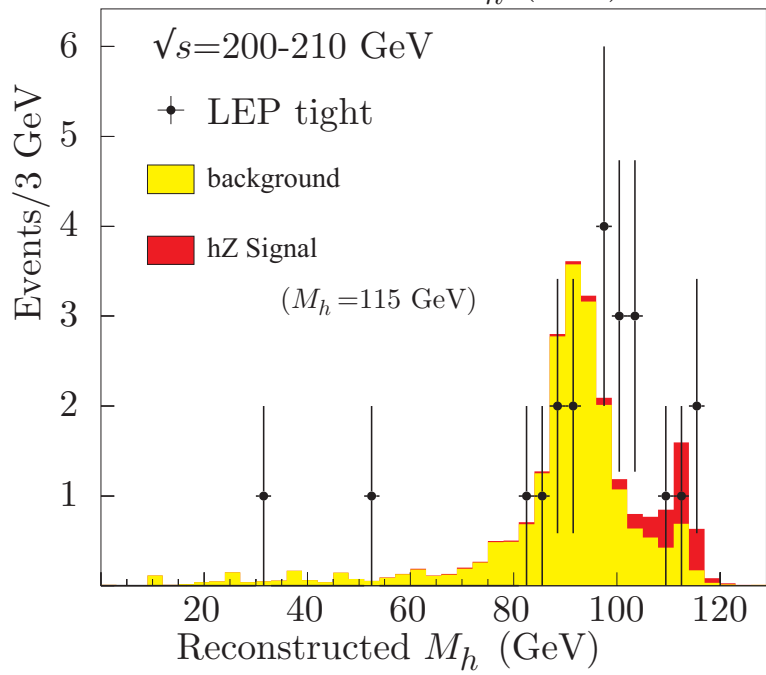
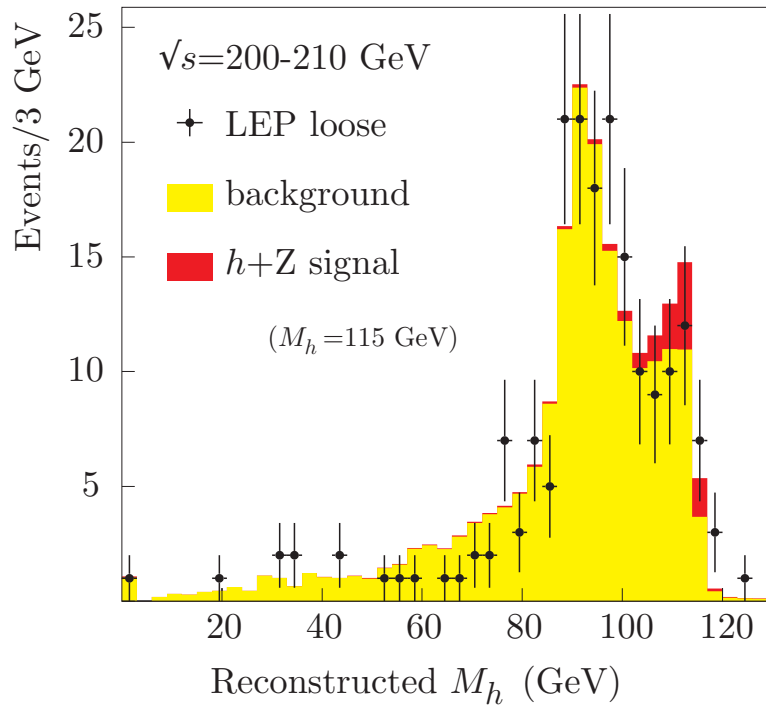
Generic Higgs production at  $e^+e^-$  colliders



Higgs width vs mass



D\_D\_2061c



## LEP EVENTS

	Expt	$E_{cm}$	Decay	$M_H$ (GeV)	$\ln(1 + s/b)$ @115 GeV
1	Aleph	206.7	4-jet	114.3	1.73
2	Aleph	206.7	4-jet	112.9	1.21
3	Aleph	206.5	4-jet	110.0	0.64
4	L3	206.4	E-miss	115.0	0.53
5	Opal	206.6	4-jet	110.7	0.53
6	Delphi	206.7	4-jet	114.3	0.49
7	Aleph	205.0	Lept	118.1	0.47
8	Aleph	208.1	Tau	115.4	0.41
9	Aleph	206.5	4-jet	114.5	0.40
10	Opal	205.4	4-jet	112.6	0.40
11	Delphi	206.7	4-jet	97.2	0.36
12	L3	206.4	4-jet	108.3	0.31
13	Aleph	206.5	4-jet	114.4	0.27
14	Aleph	207.6	4-jet	103.0	0.26
15	Opal	205.4	E-miss	104.0	0.25
16	Aleph	206.5	4-jet	110.2	0.22
17	L3	206.4	E-miss	110.1	0.21
18	Opal	206.4	E-miss	112.1	0.20
19	Delphi	206.7	4-jet	110.1	0.20
20	L3	206.4	E-miss	110.1	0.18

## LEP Limitation

If  $2\sigma$  signal at  $M_H=115$  GeV, it would have taken  $\geq 6\times$  more integrated luminosity to reach a  $5\sigma$  proof of the Higgs existence.

## The Future

The next place where to continue the Higgs hunt is FNAL at the Tevatron operated as collider at  $W = \sqrt{s}=2$  TeV.

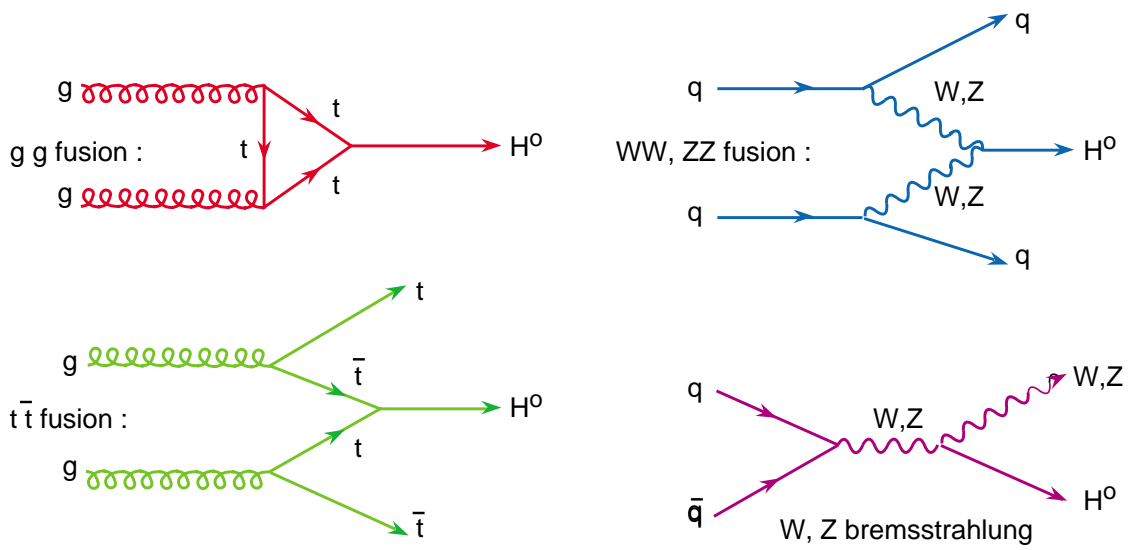
### Lots more to do

Even if a Higgs is found, lots more needs doing: BR's,  $h, H, A, H^\pm$ , ratio of  $v$ 's  
 – see later That is in any case a job for LHC,  $\sqrt{s}=14$  TeV.

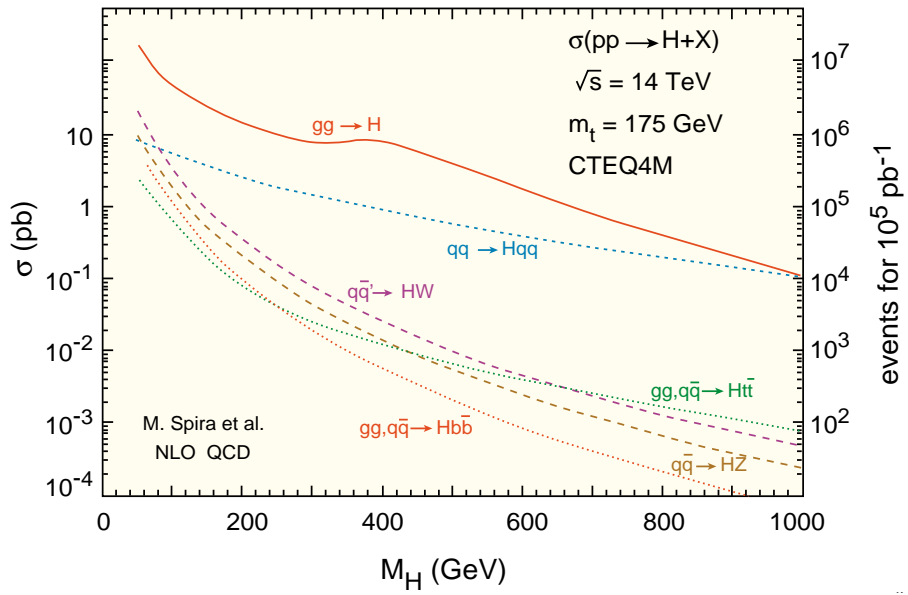
When:

1. CDF and DØ. OK for low mass. 2006??
2. LHC. Atlas and CMS, but it will be a few years before there is an LHC.

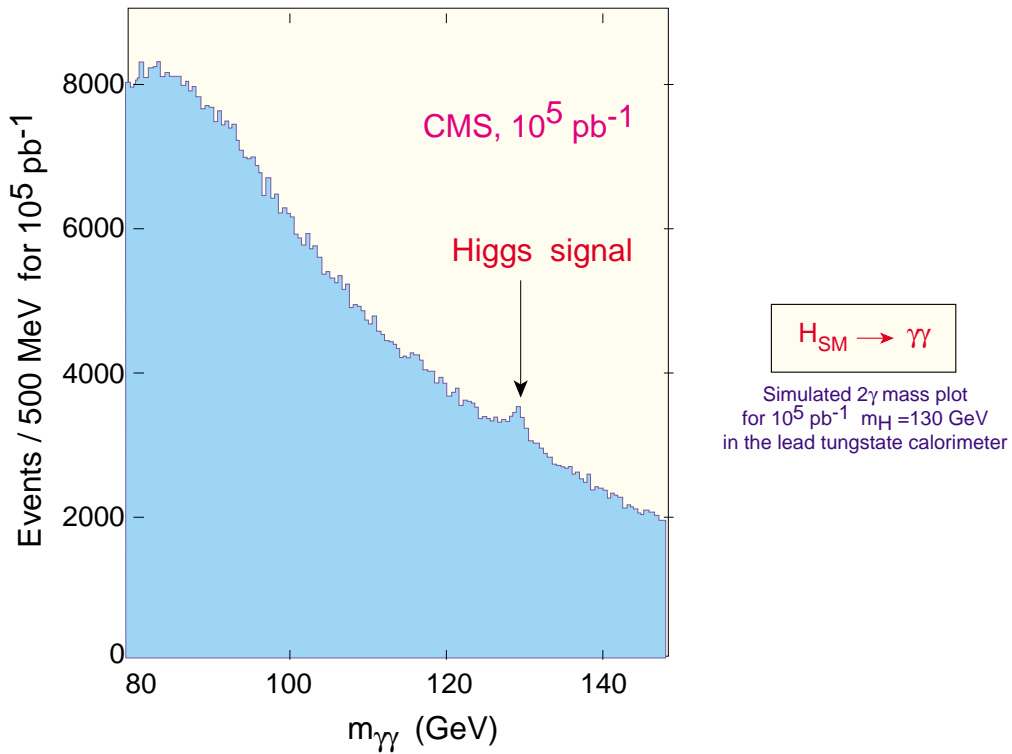
### Higgs production in hadron collisions



### Higgs production in hadron collisions



This is an advertising



## Many Higgs-bosons

Supersymmetry adds more Higgs. In MSSM just one more complex doublet. No new Higgs is necessary for giving mass to additional gauge boson and we now have 5 physical particles:

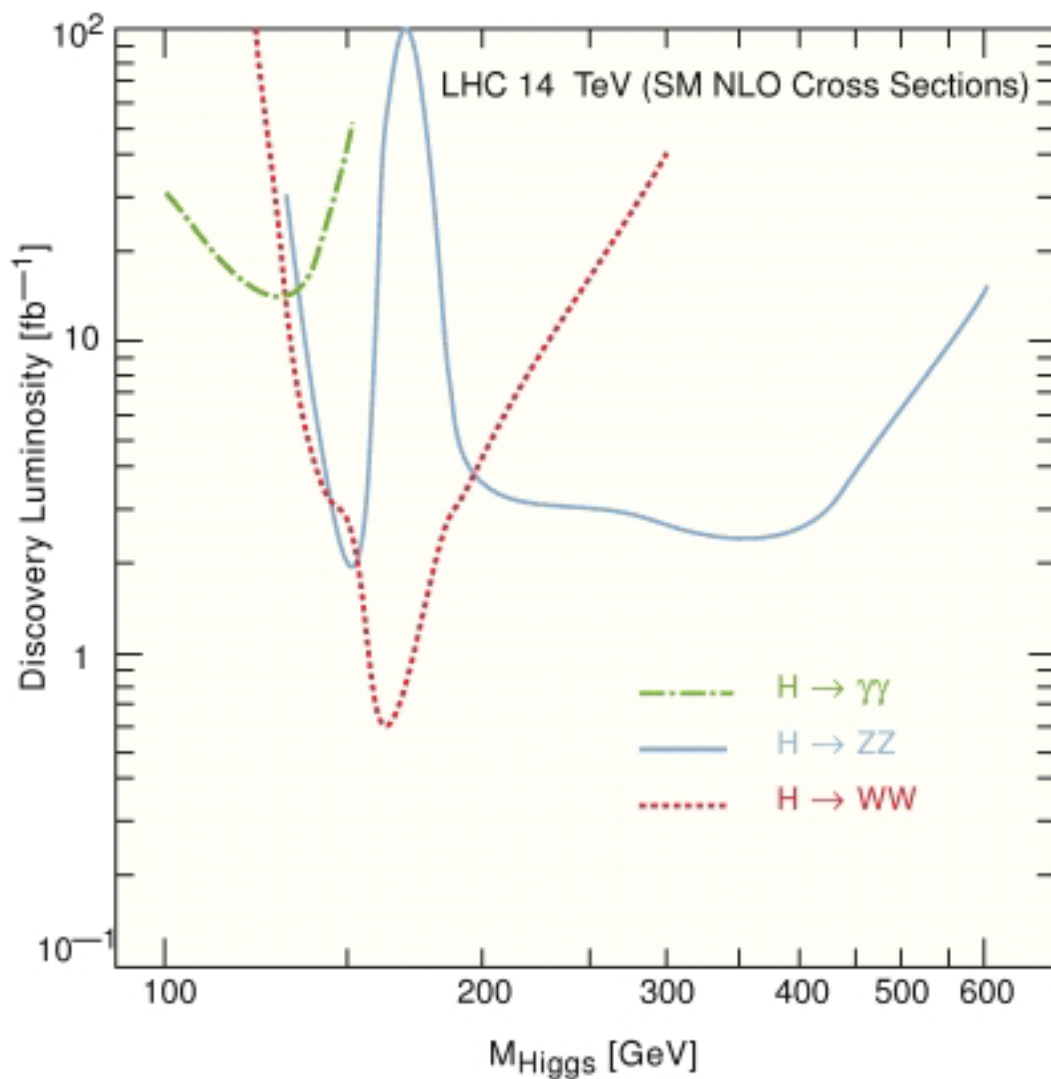
1. Two neutral scalars,  $h^0$ ,  $H^0$
2. One neutral pseudoscalar,  $A^0$
3. Two charged scalars,  $H^+$ ,  $H^-$

At tree level:

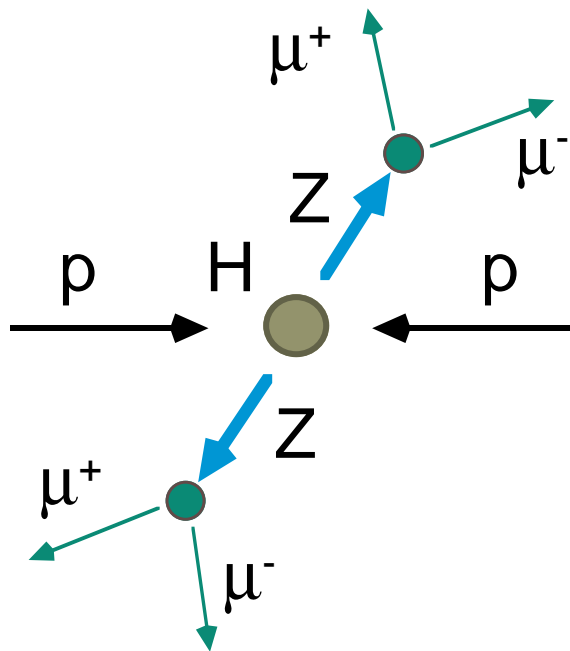
$$M_h \leq M_Z \leq M_H \quad M_A \leq M_H \quad M_{H^\pm} \leq M_{W^\pm}$$

After radiative corrections  $M_h \leq 135$  GeV.

## Energy and Luminosity

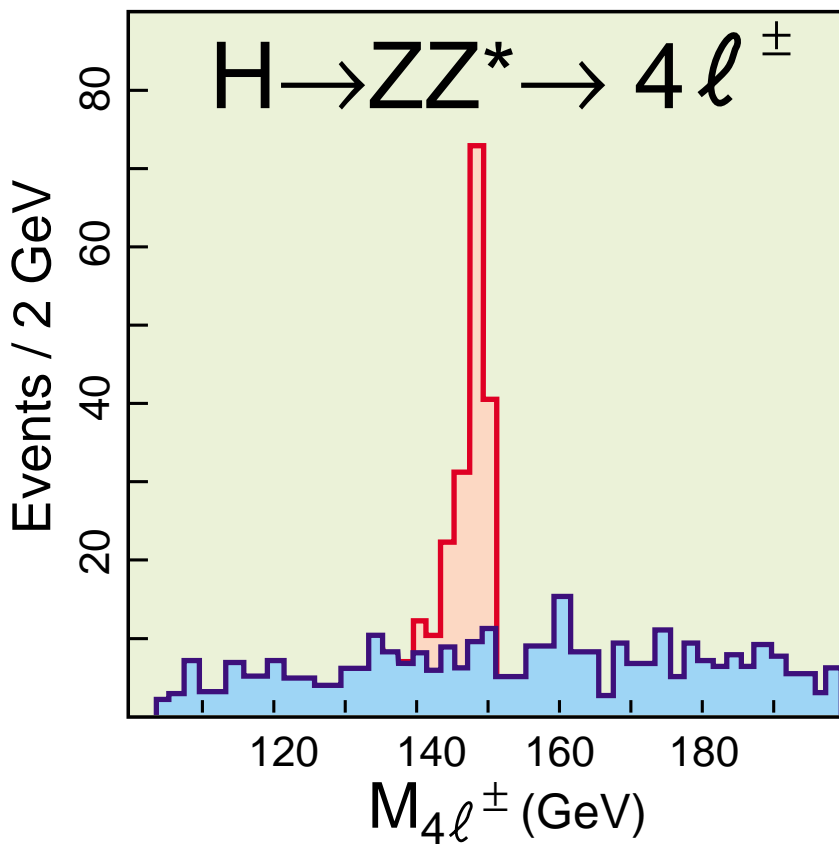


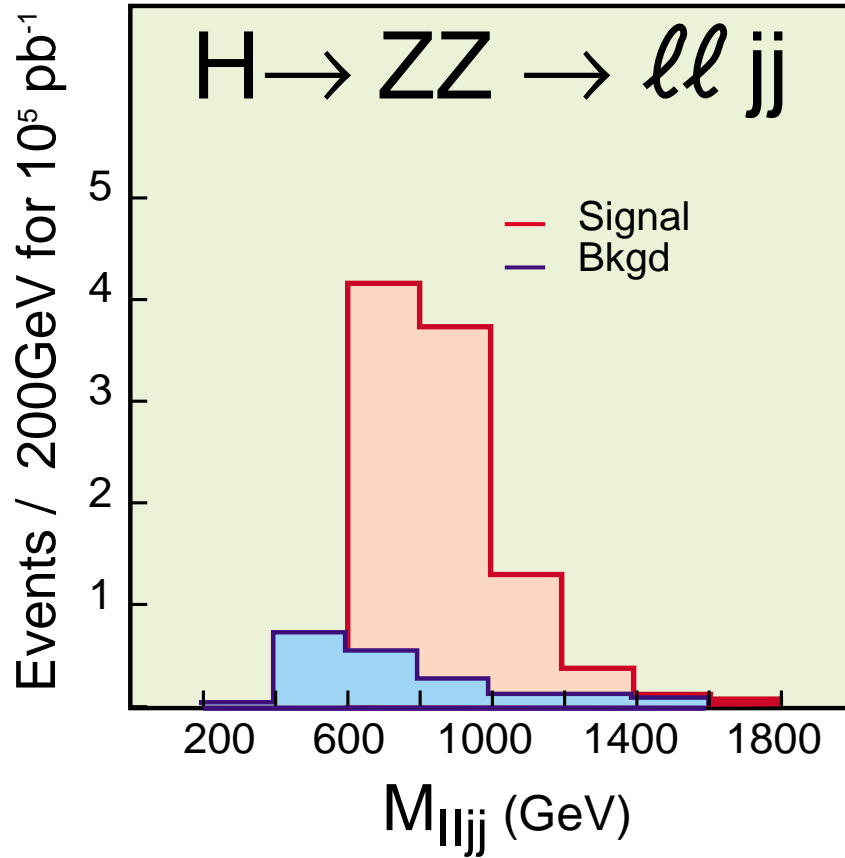
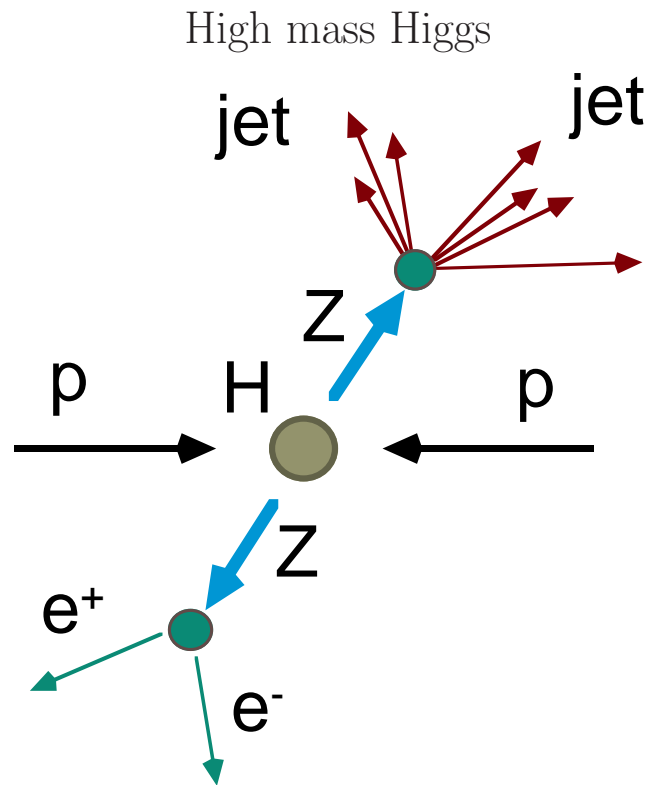
Clean signals



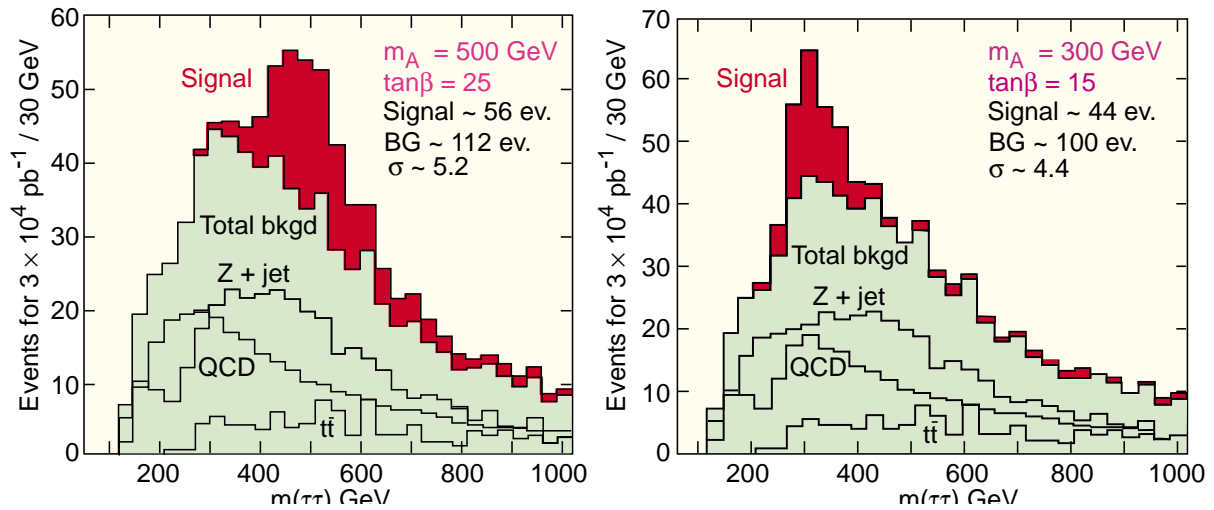
$BR(H \rightarrow 4\mu) 4 \times 10^{-4}$

$BR(H \rightarrow 4\ell) 1.2 \times 10^{-3}$





## Search for A



## What's next

Can the Higgs mass exceed the value from the standard model fit? It has been proven that there are several ways to generate an apparent downward shift of the Higgs mass in the SM fit shown.

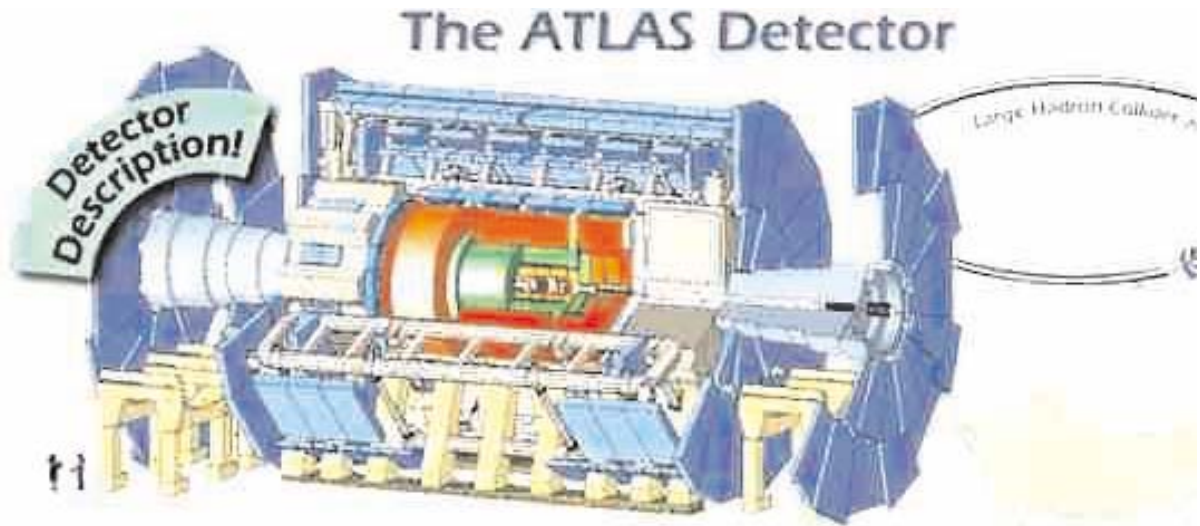
In some models, new fermions and boson with electroweak charge are assumed, in others new vector boson are introduced. It is even possible to reach the same result without new particles.

In this case there are unique predictions in the way the SM parameters should change, within the present constraint.

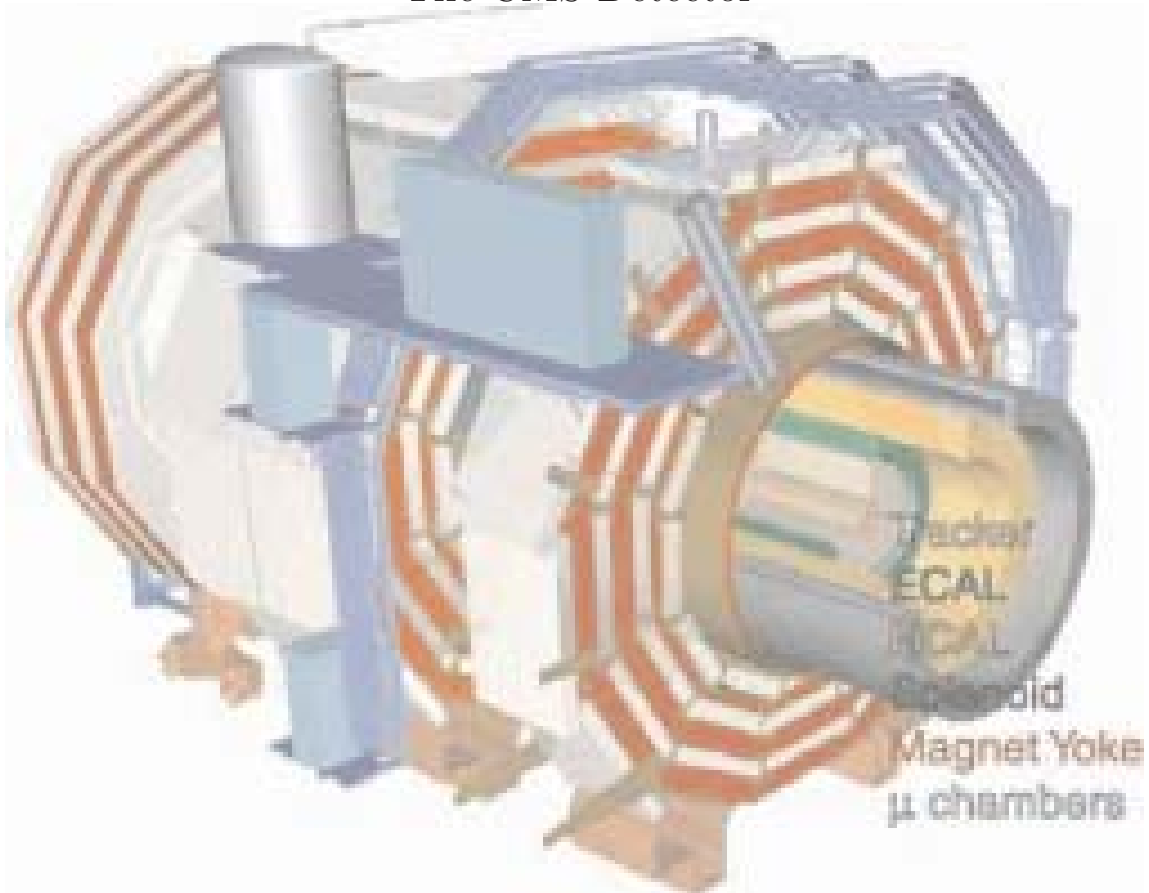
The first possibility is verifiable LHC. The latter could be verified by very precise measurements at a linear collider.

MEANWHILE

---



### The CMS Detector



## 20 App. 1. Kinematics

### 20.1 4-vectors

Le coordinate nello spazio-tempo, uno spazio a quattro dimensioni spesso chiamato lo spazio di Minkowski, sono definite dal vettore contravariante:

$$x^\mu \equiv (x^0, x^1, x^2, x^3) \equiv (t, x, y, z) \equiv (t, \mathbf{r}),$$

dove abbiamo posto  $c=1$  e  $\mathbf{r}$  è un vettore nello spazio euclideo a 3 dimensioni. Useremo spesso la notazione  $|\mathbf{r}| = r$ . Il vettore covariante  $x_\mu$  è dato da

$$x_\mu \equiv (x_0, x_1, x_2, x_3) \equiv (t, -\mathbf{r}) = g_{\mu\nu}x^\nu$$

con

$$g_{\mu\nu} = \begin{pmatrix} 1 & 0 & 0 & 0 \\ 0 & -1 & 0 & 0 \\ 0 & 0 & -1 & 0 \\ 0 & 0 & 0 & -1 \end{pmatrix} \quad (20.1)$$

ed usando la convenzione di somma sugli indici ripetuti. La teoria della relatività speciale richiede che il modulo quadrato del quadrivettore  $x^\mu$ , dato da  $x^\mu x_\mu \equiv x^\mu x^\mu g_{\mu\nu}$ , misurato in sistemi inerziali in moto relativo sia invariante. Come pure è invariante il prodotto scalare di due vettori:  $x^\mu y_\mu$ . Le componenti del vettore  $x'^\mu$  misurate in un sistema  $O'$  in moto rispetto al sistema  $O$ , con velocità  $\beta$  lungo l'asse  $z \equiv x_3$ , con origini coincidenti per  $t=0$  e  $z \parallel z'$ , sono date in  $O$  dalla trasformazione di Lorentz:

$$\begin{pmatrix} x \\ y \\ z \\ t \end{pmatrix} = \begin{pmatrix} 1 & 0 & 0 & 0 \\ 0 & 1 & 0 & 0 \\ 0 & 0 & \gamma & \beta\gamma \\ 0 & 0 & \beta\gamma & \gamma \end{pmatrix} \begin{pmatrix} x' \\ y' \\ z' \\ t' \end{pmatrix} \quad (20.2)$$

dove  $\gamma = (1 - \beta^2)^{-1/2}$ . Trasformazioni di Lorentz per il caso più generale in cui la velocità relativa fra sistemi non sia lungo un asse e gli assi non coincidano per  $t=0$ , si ottengono semplicemente combinando traslazioni e rotazioni tridimensionali in  $O$ ,  $O'$  e la relazione (20.2). La matrice in eq. (20.2) è anche il Jacobiano  $J = \partial(x)/\partial(x')$  della trasformazione di variabili  $x \rightarrow x'$ . Il suo determinante è dato da  $\text{Det}(J)=1$ , per cui l'elemento di volume  $d^4x = dx^0 dx^1 dx^2 dx^3$  è invariante:  $d^4x = d^4x'$ .

Ogni quantità  $a^\mu \equiv (a^0, a^1, a^2, a^3)$  che si trasforma secondo l'equazione (20.2) è un quadrivettore nello spazio di Minkowski. Il quadrivettore energia-impulso, o quadri-impulso,  $p^\mu = (E, \mathbf{p})$  è di fondamentale importanza in fisica delle particelle.

## 20.2 Invariant Mass

Per una particella,  $p^\mu p_\mu = m^2$  è la massa quadrata della particella a riposo ed è un invariante relativistico. Il sistema di riposo è definito da  $\mathbf{p}=0$  e viene spesso chiamato centro di massa, CM. Per un sistema di  $n$  particelle, chiameremo  $p^\mu p_\mu$  la massa invariante quadrata del sistema, dove  $p^\mu = \sum_n p_i^\mu$  è la somma dei quadriimpulsi di tutte le particelle. Riintrucendo esplicitamente la velocità della luce  $c$ , otteniamo la famosa relazione fra massa e energia  $E_0 = mc^2$ , dove il sottoscritto 0 ci ricorda che la relazione è valida nel CM.<sup>9</sup>

## 20.3 Other Concepts

Altre relazioni seguono dalla trasformazione di Lorentz:

$$\begin{aligned}\gamma &= \frac{E}{m} \\ \beta &= \frac{p}{E} \\ \gamma\beta &= \frac{p}{m}\end{aligned}\tag{20.3}$$

Dalla (20.2) si vede come le componenti trasverse al moto del quadrivettore non vengono toccate dalle trasformazioni di Lorentz. Questo permette di scrivere la trasformazione di Lorentz distinguendo solo le componenti longitudinali e trasversali della parte spaziale del quadrivettore come sotto

$$\begin{pmatrix} p_\perp \\ p_\parallel \\ E \end{pmatrix} = \begin{pmatrix} 1 & 0 & 0 \\ 0 & \gamma & \beta\gamma \\ 0 & \beta\gamma & \gamma \end{pmatrix} \begin{pmatrix} p'_\perp \\ p'_\parallel \\ E' \end{pmatrix}\tag{20.4}$$

dove i simboli  $\perp$  e  $\parallel$  stanno, rispettivamente per perpendicolare o trasverso e parallelo o longitudinale. L'elemento di volume nello spazio dei quadriimpulsi,  $dp^4$  è anche esso invariante per trasformazioni di Lorentz. Se il quadriimpulso  $p$  si riferisce ad una particella di massa  $m$ , energia ed impulso non sono indipendenti. Formalmente possiamo imporre la condizione che la particella sia sul cosiddetto *mass shell* introducendo una (distribuzione) funzione  $\delta$ , definita da

$$\begin{cases} \delta(x) = 0 & \text{per } x \neq 0 \\ \int_{-d}^d \delta(x) dx = 1 & \text{per } d > 0 \end{cases}$$

L'elemento di volume con la condizione che il sistema abbia massa  $m$  è quindi  $dp^4 \delta(p^2 - m^2)$ . Integrando su una componente di  $p$ , l'energia, rimuove la funzione

<sup>9</sup>Vedi per esempio L. B. Okun, The Concept of Mass, Physics Today, **42**, 31 (1989).

$\delta$ :

$$d^3p \int dE \delta(p^2 - m^2) = \frac{d^3p}{E} \quad (20.5)$$

L'integrale in eq. (20.5) segue dalla relazione

$$\delta(f(x)) = \sum \frac{\delta(x - x_i)}{\left| \frac{df}{dx} \right|_{x=x_i}}$$

dove  $x_i$  sono le soluzioni di  $f(x) = 0$ . Nel nostro caso

$$\delta(p^2 - m^2) = \frac{\delta(E + \sqrt{\mathbf{p}^2 + m^2}) + \delta(E - \sqrt{\mathbf{p}^2 + m^2})}{2E}$$

L'elemento di volume tridimensionale  $d^3p/E$  é anch'esso un invariante di Lorentz, per costruzione.

Per completezza ricordiamo altre relazioni fondamentali. L'operatore impulso, in rappresentazione di coordinate, è scritto come:

$$p^\mu \rightarrow i \frac{\partial}{\partial x_\mu} \equiv \left( i \frac{\partial}{\partial t}, \frac{1}{i} \nabla \right)$$

e si trasforma come un vettore contravariante:

$$p^\mu p_\mu = - \frac{\partial}{\partial x_\mu} \frac{\partial}{\partial x^\mu} \equiv -\square$$

Il quadrivettore del potenziale elettromagnetico è dato da:

$$A^\mu = (\rho, \mathbf{A}) = g^{\mu\nu} A_\nu$$

e l'equazione di continuità, scritta nella rappresentazione degli impulsi diviene:

$$k^\mu A_\mu = 0.$$

dove  $k^\mu$  è l'impulso portato dal campo elettromagnetico.

## 20.4 Trasformazione di uno spettro di impulsi

È importante in generale trovare la relazione tra lo spettro di impulso dei prodotti di un decadimento in due corpi  $A \rightarrow B + C$ , osservato in sistemi in moto relativo. Incominciamo con considerazioni puramente cinematiche. Nel centro di massa, CM, le due particelle di decadimento si muoveranno in direzioni opposte e con lo stesso impulso. Ripetendo varie volte l'esperimento potremmo costruire la superficie definita dal vettore  $\mathbf{p}$  delle particelle e troviamo che essa è rappresentata da una sfera di raggio  $r = |\mathbf{p}|$ . Ci chiediamo adesso, come apparirebbe questa superficie ad

un osservatore nel sistema del laboratorio, rispetto al quale il CM di  $A$  si muove con velocità  $\beta$ . Qualitativamente la superficie verrà elungata nella direzione di  $\beta$ , mantenendo una simmetria di rotazione attorno a  $\beta$ , e spostata nella direzione di  $\beta$ , perdendo la simmetria rispetto all'origine. Mentre nel CM lo spettro d'impulsi è una linea, cioè le particelle sono monocromatiche, per l'osservatore nel laboratorio vi sarà una banda di valori possibili, compresi tra la distanza massima e minima dei punti dell'ellissoide dal centro della sfera originale, dipendenti dall'angolo di emissione tra  $\mathbf{p}$  e la direzione di  $\beta$ . Le componenti dell'impulso perpendicolari alla velocità rimangono immutate, mentre quella parallela si trasforma secondo la

$$p_{\parallel} = \gamma(p' \cos \theta + \beta E'). \quad (20.6)$$

e nel laboratorio saranno possibili tutti i valori  $p_{\parallel}$  tali che

$$\gamma(-p + \beta E') < p_{\parallel} < \gamma(p + \beta E')$$

Dunque lo spettro d'impulso di una delle due particelle nel laboratorio è rappresentato da un ellissoide. A questo proposito distinguiamo tre casi:

1. quando la massima velocità raggiungibile da una delle particelle è, nel centro di massa, maggiore di  $\beta$ , l'ellissoide ha ancora una porzione nel semispazio in cui le particelle appaiono muoversi 'all'indietro' nel laboratorio (i.e.  $p_{\parallel} < 0$ ).
2. Aumentando la velocità del centro di massa rispetto al laboratorio si arriva fino a che il massimo valore possibile di  $p'_{\parallel}$  è proprio pari a  $\beta E'$ . A questo punto l'ellissoide è tutto contenuto nel semispazio  $p_{\parallel} > 0$  ma tocca ancora l'origine: le particelle che, nel CM, si muovono all'indietro appariranno ferme nel laboratorio.
3. Quando, infine, la velocità del centro di massa è maggiore, in modulo, della velocità massima che ciascuna particella può acquistare, misurata nel CM, allora gli impulsi misurati saranno tutti positivi e le particelle si muoveranno tutte in avanti. In particolare, per particelle di massa nulla, vi saranno sempre particelle emesse in direzione opposta a  $\beta$ , che è equivalente al fatto che la velocità della luce è costante in ogni sistema.

La superficie dell'ellissoide ci chiarifica come gli impulsi siano connessi nei due sistemi, la forma dello spettro di  $p$  è tuttavia il risultato d'interesse di una misura. Per chiarezza, consideriamo un caso concreto, di comune interesse. In un esperimento supponiamo di avere un fascio di mesoni  $\pi^0$ , che decadono in due fotoni. Vogliamo

calcolare lo spettro dell'impulso dei fotoni in funzione dell'energia del  $\pi^0$ . Per fotoni  $p = E$  e possiamo parlare di  $p$  od  $E$ , come più conveniente. Nel CM l'energia dei fotoni è  $m_\pi/2$ , dalla conservazione dell'energia. Inoltre sia  $\theta'$  l'angolo d'emissione del fotone nel centro di massa, misurato rispetto all'impulso del  $\pi$ . Nel laboratorio l'energia dei fotoni è data da:

$$E_\gamma = \gamma_\pi \frac{m_\pi}{2} + \gamma_\pi \beta_\pi \frac{m_\pi}{2} \cos \theta'$$

che, usando l'equazione (20.3) diviene:

$$E_\gamma = \frac{1}{2}(E_\pi + p_\pi \cos \theta') \quad (20.7)$$

L'energia dei fotoni nel laboratorio può quindi variare tra i valori  $E_{min} = (1/2) \times (E_\pi - p_\pi)$  e  $E_{max} = (1/2) \times (E_\pi + p_\pi)$  ed avrà uno spettro piatto. Quest'ultima affermazione segue dal fatto che nel CM la distribuzione angolare è isotropica, cioè  $dN/d \cos \theta' = cost.$  e dall'equazione (20.7),  $dE_\gamma = cost. \times d \cos \theta'$  e quindi  $dN_\gamma/dE = cost.$ <sup>10</sup>

Se i pioni neutri hanno uno spettro di energie dato da  $dN_{\pi^0} = f(E_{\pi^0})dE_{\pi^0}$ , per esempio come mostrato in fig. 2.1, lo spettro dell'energia dei fotoni nel laboratorio è dato da:

$$g(E_\gamma) = \int_{E_\pi^{min}(E_\gamma)}^{\infty} \frac{f(E_\pi)}{p_\pi} dE_\pi = \int_{p_\pi^{min}(E_\gamma)}^{\infty} \frac{f(E_\pi)}{E_\pi} dp_\pi. \quad (20.8)$$

vedi fig. 2.2.

Nell'equazione (20.8), che segue facilmente dalla eq. (20.7) e dalle considerazioni sulla forma dello spettro per decadimento di pioni di energia fissa,  $E_\pi^{min}(E_\gamma)$  è l'energia minima necessaria per un  $\pi^0$  per produrre fotoni di energia  $E_\gamma$ , data da  $E_\gamma + m_\pi^2/4E_\gamma$ . La seconda espressione per  $g(E)$  è più conveniente per integrazione numerica, non avendo lo zero esplicito  $p_\pi = 0$  nel denominatore. Lo spettro  $g(E_\gamma)$  in fig. 2.2 è calcolato numericamente a partire dallo spettro in fig. 2.1. Per semplicità abbiamo posto  $m_{\pi^0} = 140$  MeV. Possiamo notare che lo spettro dei  $\gamma$  ha un massimo a 70 MeV, cioè a  $m_{\pi^0}/2$ . Questo segue in generale dalle equazioni (20.7) e (20.8). Se lo spettro dei pioni non raggiunge il limite  $E_\pi = m_\pi$ , lo spettro dei  $\gamma$  diventa piatto attorno a  $m_{\pi^0}/2$ .

---

<sup>10</sup>Anticipiamo qui che il  $\pi^0$  ha spin nullo e quindi la distribuzione angolare dei  $\gamma$  è isotropica nel CM. Se lo spin delle particelle che decadono fosse diverso da zero ed orientato preferenzialmente in qualche direzione, in generale la distribuzione angolare dei prodotti di decadimento non sarebbe uniforme.

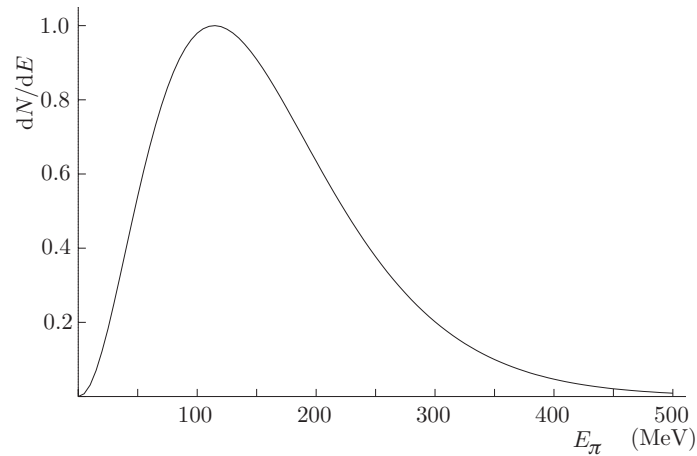


**Fig. 20.1.** Pion energy spectrum  $f(E_\pi)$  in the lab.  $E$  is the kinetic energy.

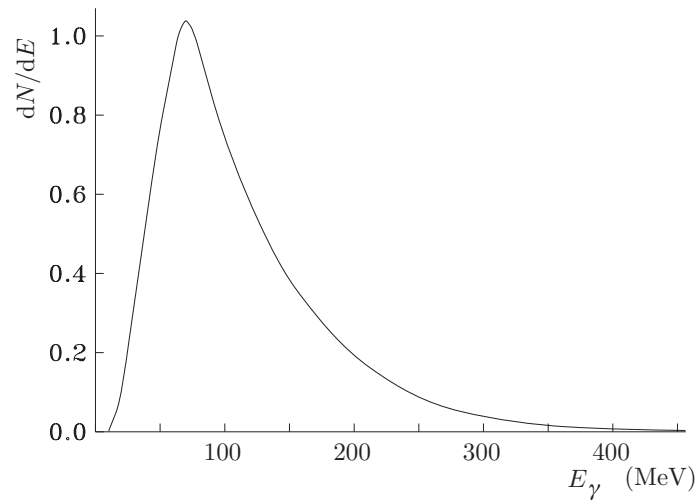


**Fig. 20.2.** Photon spectrum  $g(E_\gamma)$  from decay of pions with the spectrum of fig. 20.1.

## 20.5 Esempi

### 20.5.1 Decadimenti a due corpi

Vogliamo determinare le energie e gli impulsi nel centro di massa delle particelle emesse in un decadimento a due corpi. I quadrimpulsi coinvolti nella reazione sono indicati qui di seguito, calcolati nel CM:

$$\begin{cases} p_0^\mu = (M, 0) & \text{Particella che decade, ferma nel CM} \\ p_1^\mu = (E_1, \mathbf{p}) & \text{Particella di massa } m_1 \\ p_2^\mu = (E_2, -\mathbf{p}) & \text{Particella di massa } m_2. \end{cases}$$

Le due particelle emesse hanno impulso uguale ed opposto per la conservazione della quantità di moto totale. Inoltre ricordiamo che vale:

$$|\mathbf{p}|^2 = m^2 = E^2 - |\mathbf{p}|^2 \quad \text{ovvero} \quad E = \sqrt{m^2 + |\mathbf{p}|^2}$$

Scriviamo, allora, la conservazione dell'energia per la nostra reazione:

$$M = E_1 + E_2 = \sqrt{m_1^2 + |\mathbf{p}|^2} + \sqrt{m_2^2 + |\mathbf{p}|^2}$$

Con un pò di algebra si può ricavare il valore di  $|\mathbf{p}|$  e quindi di  $E_1$  ed  $E_2$ :

$$\begin{aligned} |\mathbf{p}|^2 &= \frac{(M^2 - (m_1 - m_2)^2)(M^2 - (m_1 + m_2)^2)}{4M^2} \\ E_1 &= \frac{M^2 + m_1^2 - m_2^2}{2M} \\ E_2 &= \frac{M^2 - m_1^2 + m_2^2}{2M} \end{aligned} \quad (20.9)$$

che risponde alla domanda. Nel CM, quindi, le energie e gli impulsi delle particelle derivanti da un decadimento a due corpi sono perfettamente fissate.

In pratica questo modo di procedere è laborioso e non necessario. È molto più immediato trovare  $E_1$  ed  $E_2$ , scrivendo la conservazione del quadri-impulso come  $p_1 = p_0 - p_2$ , il cui modulo quadro nel CM di della particella di massa  $M$  immediatamente da:

$$m_1^2 = M^2 + m_2^2 - 2ME_2$$

da cui la terza delle equazioni (20.9). Vedi anche l'esempio 3 più sotto.

### 20.5.2 Decadimenti a tre corpi

Cosideriamo un decadimento a tre corpi:  $M \rightarrow A+B+C$ , nel sistema di riposo di  $M$ . Siano  $M$ ,  $m_a$ ,  $m_b$ ,  $m_c$  le masse delle particelle. Vogliamo trovare la massima energia di ciascuna delle tre particelle finali. Consideriamo per esempio la paricella A. Essa avrà la massima energia quando rincula contro il sistema (B,C) che ha la minima energia interna possibile, cioè quando nel CM di B e C non v'è moto relativo. Questa condizione corrisponde ad un sistema (B,C) con massa invariante  $M_{(A,B)} = m_a + m_b$ . Dalle equazioni (20.9) segue:

$$E_{A, Max} = \frac{M^2 + m_a^2 - (m_b + m_c)^2}{2M}$$

e permutazioni cicliche. L'argomento è intuitivo ma facilmente verificabile.

### 20.5.3 Decadimento $\pi \rightarrow \mu\nu$

Immaginiamo un mesone  $\pi^+$  che decade in volo in un neutrino  $\nu$  ed in un leptone  $\mu$ . Nel sistema del laboratorio misuriamo gli impulsi e le energie dei prodotti del decadimento: quali sono i valori massimi e minimi possibili per tali grandezze? Supponiamo che il mesone iniziale abbia energia  $E_\pi=280$  MeV oppure  $E_\pi=30$  GeV. Le masse delle particelle sono:  $m_\pi=140$  MeV,  $m_\mu=105$  MeV e  $m_\nu=0$  MeV. Dalla seconda e terza eq. (20.9) otteniamo impulsi e energie nel CM.

$$E_\mu = 109.4 \text{ MeV}$$

$$E_\nu = 30.6 \text{ MeV}$$

$$|\mathbf{p}_\nu| = |\mathbf{p}_\mu| = E_\nu = 30.6 \text{ MeV}/c$$

$\gamma$  e  $\beta$ , secondo le eq. (20.3) sono, per le due diverse energie del  $\pi^+$ :

$$\begin{array}{lll} E_\pi = 280 \text{ MeV} & \gamma = 2 & \beta = 0.87 \\ E_\pi = 30 \text{ GeV} & \gamma = 214 & \beta = 0.999989 \simeq 1. \end{array}$$

Per quanto si era visto nel paragrafo 2.2.4, i valori massimi e minimi delle energie e degli impulsi delle particelle “figli” del decadimento si ottengono in corrispondenza delle emissioni in direzioni parallele (o antiparallele) alla linea di volo del mesone  $\pi^+$ , ovvero quando  $\cos\theta' = +1$ . Mettendo i valori opportuni nelle (20.6) si ottengono i seguenti risultati:

$E_\pi = 280$	Muon		Neutrino	
	Max	Min	Max	Min
$p$ (MeV/c)	251.6	129	114.4	7.9
$E$ (MeV)	272	165.6	114.4	7.9

### 20.5.4 Annichilazioni $e^+e^-$

Supponiamo di voler annichilare un elettrone ed un positrone in modo da avere 100 GeV di energia disponibili per la produzione di altre particelle. Si deve calcolare quale energia devono avere le particelle iniziali nel caso in cui esse appartengano a due fasci, e nel caso, invece, in cui un fascio di positroni collida su un bersaglio elettronico fermo. Ricordiamo la definizione di *massa invariante*  $M$  di un insieme di  $N$  particelle:

$$M = \sqrt{\left| \sum_{i=1}^N p_i^\mu \right|^2} \quad (20.10)$$

Per definizione, quindi, essa si conserverà in ogni processo fisico, raggruppando in un'unica legge la conservazione dell'energia e dell'impulso spaziale. In particolare, è utile calcolare il quadrato di  $M$  nel CM, ed imporne la conservazione:

$$M^2 = (E_1 + E_2)^2 - (p_1 + p_2)^2 = m_1^2 + m_2^2 + 2E_1E_2 - 2p_1p_2 \cos \theta = 10000 \text{ GeV}^2$$

Vediamo per primo il caso in cui un fascio collide su un bersaglio fermo. Poniamo pari a zero l'impulso della particella 2 ed assumiamo che le due particelle abbiano la stessa massa  $m$ ; automaticamente, allora, sarà  $E_2 = m_2 = m$  e

$$M^2 = 2m(m + E_1) = 4m^2 + 2mT \simeq 2mT,$$

avendo indicato con  $T$  l'energia cinetica del fascio,  $T = E_1 - m$ , ed avendo trascurato la massa dell'elettrone e del positrone,  $m \simeq 0.5 \text{ MeV}$ . Per ottenere una massa invariante di 100 GeV, si dovrà avere, dunque, un fascio di  $E = M^2/2m = 10000 \text{ GeV}$  ben al di sopra delle capacità degli attuali acceleratori. Consideriamo, invece, ora il caso di due fasci che collidono. Ancora una volta faremo l'assunzione che le masse siano trascurabili rispetto all'energia delle particelle, cioè  $E = p$ . Senza neanche usare la formula sopra,  $M = 2E$ ,  $E = 50 \text{ GeV}$ . Risulta chiaro, da questo Esempio, come sia di gran lunga più conveniente, nonostante le difficoltà pratiche, costruire macchine in cui entrambi i fasci di particelle vengano accelerati. Solo così, infatti, è pensabile di poter raggiungere quelle energie abbastanza alte da permettere di esplorare le zone ancora incognite delle interazioni subnucleari.

### 20.5.5 Angolo minimo tra due fotoni da $\pi^0 \rightarrow \gamma\gamma$

Consideriamo un  $\pi^0$  di energia  $E$  che decade in due fotoni che nel sistema di riposo del pione hanno un impulso  $p^* = m_{\pi^0}/2 = 65.75 \text{ MeV}/c$ . Nel sistema in cui il pione si muove l'angolo dei due gamma è proiettato in avanti, nella direzione di  $\mathbf{p}$ , anche se uno dei fotoni può essere emesso indietro, dato che  $\beta_\gamma = 1$ . Si può facilmente (esercizio per il lettore) dimostrare che l'angolo minimo tra i due  $\gamma$  nel laboratorio corrisponde all'emissione dei due fotoni nel CM a  $90^\circ$ , rispetto alla direzione di moto. Nel laboratorio abbiamo allora  $p_\perp = m_{\pi^0}/2$  e  $p_\parallel = p/2$  e infine  $\theta_{\gamma\gamma} = 2 \arctan(p_\perp/p_\parallel)$ .

### 20.5.6 Energia dei prodotti di decadimenti a tre corpi

Come esercizio, trovare il contorno nel piano  $E_i, E_j, i, j = 1, 2, 3$  che contiene i valori possibile per le energie di due delle tre particelle.

### 20.5.7 2 particelle → 2 particelle

Cosideriamo la reazione  $1+2 \rightarrow 3+4$ . Per particelle senza spin, abbiamo simmetria cilindrica, quindi la reazione è descritta cinematicamente dall'angolo polare di deflessione, essendo dati le masse  $m_1, m_2, m_3, m_4$  e l'energia totale. Una descrizione relativisticamente invariante è data dalla variabile  $t = |p_1 - p_3|^2$ , sempre conoscendo masse ed energia. In generale possiamo introdurre tre invarianti  $s, t, u$ , definiti come

$$\begin{aligned} s &= (p_1 + p_2)^2 = (p_3 + p_4)^2 && \text{massa invariante quadrata} \\ t &= (p_1 - p_3)^2 && \text{modulo quadro del momento trasferito} \\ u &= (p_1 - p_4)^2 && \text{come sopra, incrociato} \end{aligned}$$

Due delle tre variabili descrivono la configurazione cinematica.  $s$  è il quadrato dell'energia totale nel centro di massa, uguale per lo stato iniziale [1,2] e quello finale [3,4]. Le tre variabili soddisfano la relazione

$$s + t + u = m_1^2 + m_2^2 + m_3^2 + m_4^2 \quad (20.11)$$

Questo è facilmente verificato nel CM dove  $\mathbf{p}_1 = -\mathbf{p}_2$  e  $\mathbf{p}_3 = -\mathbf{p}_4$ . Infatti

$$\begin{aligned} s &= (E_1 + E_2)^2 \\ t &= m_1^2 + m_3^2 - 2E_1E_3 + 2\mathbf{p}_1 \cdot \mathbf{p}_3 \\ u &= m_1^2 + m_4^2 - 2E_1E_4 - 2\mathbf{p}_1 \cdot \mathbf{p}_3 \end{aligned}$$

da cui

$$\begin{aligned} s + t + u &= m_1^2 + m_3^2 + m_1^2 + m_4^2 + E_1^2 + E_2^2 + 2E_1(E_2 - E_3 - E_4) \\ &= m_1^2 + m_3^2 + m_1^2 + m_4^2 + E_2^2 - E_1^2 \\ &= m_1^2 + m_2^2 + m_3^2 + m_4^2. \end{aligned}$$

## 20.6 Limite di massa infinita e limite non relativistico

Consideriamo il caso in cui la massa  $M$  di una particella è molto più grande delle altre coinvolte in un processo e dell'energia totale del sistema, nel suo centro di massa, meno il valore di  $M$ . In meccanica classica, nella collisione elastica di un piccola massa con una molto grande, possiamo trascurare nella conservazione dell'energia il cambio di energia dell'oggetto di grande massa ma dobbiamo tener conto correttamente della conservazione dell'impulso. Il caso limite tipico è l'urto elastico di una palla contro un muro. La palla rimbalza con la stessa velocità che aveva prima dell'urto. Energia non viene trasferita al muro ma questo acquista un impulso uguale al cambiamento di impulso della palla, che può raggiungere due volte il suo valore

prima dell'urto. Questo è possibile perchè l'impulso è proporzionale alla velocità  $v$  ed alla massa  $m$  mentre l'energia è proporzionale a  $m$  e  $v^2$ . Nel caso relativistico questo risultato rimane valido. Possiamo dimostrarlo a partire dall'espressione per l'energia di una particella di massa  $M$ :

$$E = \sqrt{M^2 + p^2} = M \sqrt{1 + \frac{p^2}{M^2}} \sim M \left(1 + \frac{1}{2} \frac{p^2}{M^2}\right).$$

L'energia cinetica è data da  $T = E - M \sim p^2/M$ , che è zero per  $M \rightarrow \infty$ ,  $p$  finito. Quindi anche nel caso relativistico abbiamo  $\Delta E=0$  mentre  $\Delta \vec{p} \neq 0$ .

Possiamo applicare questa semplificazione alle collisioni di un elettrone con un protone. Definiamo con gl'indici 1, 2, 3, e 4 le variabili rispettivamente di elettrone incidente, elettrone diffuso, protone iniziale e protone dopo l'urto:

$$\left\{ \begin{array}{ll} E_1, \mathbf{p}_1 & \text{elettrone incidente} \\ E_2, \mathbf{p}_2 & \text{elettrone diffuso} \\ E_3, \mathbf{p}_3 & \text{protone iniziale} \\ E_4, \mathbf{p}_4 & \text{protone dopo l'urto} \end{array} \right. .$$

Per un urto elastico, usando l'approssimazione di cui sopra risulta in

$$\begin{aligned} E_2 &= E_1, |\vec{p}_1| = |\vec{p}_2| \\ E_3 &= E_4, \vec{p}_4 = \vec{p}_3 + \vec{p}_2 - \vec{p}_1 \end{aligned}$$

e per il caso in cui il protone sia a riposo nel sistema di riferimento

$$\begin{aligned} E_2 &= E_1, |\vec{p}_1| = |\vec{p}_2| \\ E_3 &= E_4 = M, \vec{p}_4 = \vec{p}_2 - \vec{p}_1 \end{aligned}$$

Nel caso della collisione di un fotone con un protone a riposo abbiamo:

$$\left\{ \begin{array}{ll} E_\gamma, |\vec{p}_\gamma| = E_\gamma & \text{fotone incidente} \\ E_\gamma, |\vec{p}_\gamma| = E_\gamma & \text{fotone diffuso} \\ M, 0 & \text{protone bersaglio} \\ M, \vec{p}_1 - \vec{p}_2 & \text{protone di rinculo} \end{array} \right.$$

ed il massimo impulso trasferito al bersaglio è  $2 \times E_\gamma$ . L'energia cinetica di rinculo del protone è data, al prim'ordine da  $T = \sqrt{M^2 - (2E_\gamma)^2} - M$ . Per  $E_\gamma \ll M$  troviamo  $T \ll E_{gam}$ , confermando la validità dell'approssimazione. Se  $T \ll M$  possiamo anche usare l'approssimazione non-relativistica  $T = p^2/(2M)$ . Ponendo per esempio  $E_\gamma=10$  MeV/c abbiamo per il massimo impulso di rinculo,  $p_{MAX}=20$  MeV e  $T_{MAX}=40/(2 \times 938) \sim 20/1000=0.02$  MeV, trascurabile rispetto a  $E_\gamma$ , che quindi effettivamente non cambia. Il significato di questo calcolo è che una particelle leggera non può trasferire energia ad una pesante.

Questo risultato è infatti qualitativamente valido anche per particelle leggere di grande energia in urti contro bersaglio fisso. In questo caso per particelle di massa nulla e energia incidente  $E \gg M$  l'energia di rinculo è dell'ordine di  $\sqrt{EM/2}$ . Per esempio nella collisione di un fotone di 1000 GeV contro un protone, l'energia del protone dopo la collisione è  $\sim\sqrt{500}\sim 22$  GeV. Per  $E \rightarrow \infty$ , la frazione di energia di rinculo del bersaglio è data da  $E_R/E = (1/E) \times \sqrt{M/2}$  e quindi tende a zero.

### 20.6.1 Esercizio

Ricavate le relazioni asserite nell'ultimo paragrafo precedente.

## 21 App. 2. $L - J - S$ , $SU(2,3)$ , $g$ , $a$

### 21.1 Orbital angular momentum

From the classical definition of angular momentum

$$\mathbf{L} = \mathbf{r} \times \mathbf{p}$$

by canonical substitution we obtain the *orbital angular momentum operator*  $-i\mathbf{x} \times \vec{\nabla}$  with components  $L_i$ , for example

$$L_z = -i\left(x\frac{\partial}{\partial y} - y\frac{\partial}{\partial x}\right) = -i\frac{\partial}{\partial\phi}.$$

If  $\mathbf{L}$  commutes with the hamiltonian, (particle) states are simultaneous eigenstates of  $\mathbf{L}$  and one of its components, traditionally chosen as  $L_z$ :

$$\mathbf{L}^2|l, m\rangle = l(l+1)|l, m\rangle$$

$$L_z|l, m\rangle = m|l, m\rangle$$

with  $l$  and  $m$  integers and  $m = -l, \dots, l$ , which are  $2l+1$  distinct values. Any state with angular momentum  $l$  can be written as a superposition of  $2l+1$  independent states.  $2l+1$  is the dimension of the representation of the group of operators  $L$ , belonging to the eigenvalue  $l$ . The operators  $L_i$  satisfy the commutation relations

$$[L_i, L_j] = i\epsilon_{ijk}L_k$$

where  $\epsilon_{ijk}$  is the totally antisymmetric tensor, with  $\epsilon_{123} = 1$ . We also recall the *raising and lowering* operators

$$L_{\pm} = L_1 \pm iL_2$$

which operating on a state  $|L, L_3\rangle$  raise or lower the third component by one unit:

$$L_{\pm}|L, L_3\rangle = \sqrt{(L \mp L_3)(L \pm L_3 + 1)}|L, L_3 \pm 1\rangle.$$

The three operators  $L_+$ ,  $L_-$  and  $L_3$  are the three components of  $\mathbf{L}$  in spherical coordinates. These operators, and the equivalent ones such as  $J_{\pm}$  for the total angular momentum or  $I_{\pm}$  for isospin, allow to easily obtain Clebsch-Gordan coefficients in many simple cases.

The operators  $L_i$ , in either of the above choices, form a group which is isomorphic with rotations in three dimensions. A rotation of a vector  $\mathbf{r}$  in 3-d is described by the equation:

$$\mathbf{r}' = \mathbf{M}\mathbf{r}$$

where  $\mathbf{M}$  is an orthogonal and real  $3 \times 3$  matrix. These rotations, and the corresponding matrices, form a group.

1. The product of two rotations, *i.e.* one rotation  $\mathcal{R}_1$  followed by another rotation  $\mathcal{R}_2$  is a rotation  $\mathcal{R}_3$ , given for instance by the matrix  $\mathbf{M}_3 = \mathbf{M}_1 \times \mathbf{M}_2$
2. The unity element exists, in the matrix representation  $\mathbf{M}$  is unity,  $M_{ij} = \delta_{ij}$
3. The inverse rotation,  $\mathcal{R}^{-1}$ , such that  $\mathcal{R}^{-1}\mathcal{R} = \mathbf{1}$  exists.

To understand the meaning of representation and reduction, we begin with the vector  $x_i$ . It belongs to a representation of the group because a rotation transforms it into another vector in  $R_3$ . The components of the new vector are linear combinations of the original ones. Under parity. *i.e.* inversion of the direction of the coordinate axes, the sign of the vector changes. The outer product of two vectors  $x_i$  and  $y_i$  is a set of 9 numbers  $x_i y_j$ , or a  $3 \times 3$  matrix or a tensor  $T_{ij}$ . A rotation mixes the original components and results in a new two index tensor  $\mathbf{T}'$ .  $3 \times 3$  tensors thus constructed form another representation of the rotation group. However we can identify subsets of the  $x_i y_j$  consisting of linear combinations of the components of  $T_{ij}$  which transforms only among themselves. We say that the outer product of  $x_i$  and  $y_i$  is a reducible representation and we proceed to isolate the irreducible representation. The first such is the scalar product  $\mathbf{x} \cdot \mathbf{y} = x_i y_i$ , sum over repeated indices is understood, a one component irreducible representation of the rotation group, called a scalar. The second set is the vector product  $\mathbf{x} \times \mathbf{y}$ , an antisymmetric tensor, with only 3 non zero components. Finally we can build the symmetric  $3 \times 3$  tensor, with zero trace, having 5 non zero components. Since rotations do not change the symmetry of the tensors, the components of symmetric and antisymmetric tensors do not mix and therefore the corresponding representations are irreducible. The scalar, the antisymmetric and the symmetric tensor parts of the tensor constructed do not change under parity, which we will indicate by  $P = +$ .

We now make connections with angular momentum. In quantum mechanics, an  $L = 0$  state is a scalar, with positive parity, which we denote by  $L^P = 0^+$  and has only one component. An  $L = 1$  state transform under rotation as a polar vector  $\mathbf{r}$ . It has three components and negative parity, we denote it by  $L^P = 1^-$ . Remember not to confuse the transformation properties of  $\mathbf{L}$ , an axial vector, with those of the state. An  $L = 2$  state has five components and  $L^P = 2^+$ . We see that the scalar, and symmetric tensor described before, together with the vector  $x_i$  from which we began correspond to the states of orbital angular momentum 0, 1, 2 for a single particle state, having the same dimensions and the same transformation properties, parity included. The reduction of the product of two vectors can be written with an

abbreviation which reminds us of the number of components of the representations:

$$3 \otimes 3 = 1 \oplus 3 \oplus 5.$$

According to the rules for combining angular momenta and parities leads us to writing instead:

$$L_1^{P_1} + L_2^{P_2} = (1^- + 1^-) \Rightarrow \begin{cases} L^P = 0^+ \\ L^P = 1^+ \\ L^P = 2^+ \end{cases}.$$

Thus we see that just from the study of the rotation group we arrive to the rules concerning orbital angular momentum in quantum mechanics. Infact the group of rotations and of transformations under the angular momentum operator are isomorphic. And finally the properties of the group are uniquely consequences of the algebra of the group given by the commutation relations for the operators.

## 21.2 $SU(2)$ and spin

It turns out that the commutation relations derived for the  $L_i$ 's define a more general group than the orthogonal rotations in real space. This group is called  $SU(2)$ , for simple, *i.e.* unimodular or with unit determinant, unitary group in two dimension. Representations of the group can be constructed from the product of the simplest non trivial representation which in this case is a two dimensional representation. The operators acting on the simplest non trivial basis states

$$\begin{pmatrix} 1 \\ 0 \end{pmatrix}, \quad \begin{pmatrix} 0 \\ 1 \end{pmatrix}$$

are unitary, unimodular complex matrices. There are 3  $2 \times 2$  independent matrices ( $n^2 - 1$   $n \times n$  matrices for  $SU(n)$ ), usually taken as the Pauli matrices. The dimensions of the representations of  $SU(2)$  are: 1, 2, 3, 4, ... If we retain the requirement that there be  $2J + 1$  magnetic substates, we can identify the representations of the group with states of total angular momentum  $J=0, 1/2, 1, 3/2, \dots$ . Clearly  $J$  is quantized but can also assume half integer values. The rules for additions of angular momentum follow from the decomposition of the product of representations into irreducible representations:  $|J_1 + J_2| = |J_1 - J_2| \dots J_1 + J_2$

The group  $SU(2)$  appears frequently in particle physics and should become familiar to us. Its connection to angular momentum, as pointed above, does not however prove that it is in fact angular momentum that we are dealing with. It is interesting for that matter to notice that Pauli originally only proposed that electrons should have a two-valued attribute in order to explain the strong doublets in the alkaline

emission lines. Later Uhlenbeck and Goudsmith proposed that the two valued quantity should be angular momentum. The intrinsic angular momentum is a property of many elementary particles and we have many way of measuring it today.

In group theory we define Casimir operators. All members of an irreducible representation are eigenstates of the Casimir operators belonging to the same eigenvalue.  $SU(N)$  has  $N - 1$  Casimir operators, one of which is the so called quadratic Casimir operator, the sum of all the generators of the group. For  $SU(N)$ , the operator is  $J^2 = J_x^2 + J_y^2 + J_z^2$ . The eigenvalues of the Casimir operators completely define the representation. For  $SU(2)$ , representations are uniquely distinguished by the eigenvalue of  $J^2$ , which are  $J(J + 1)$ . We can also refer to a representation by its dimension or number of components,  $2J + 1$ . A simple way to reduce a product of representations is by means of the weight diagram and symmetry arguments. Consider a state  $|ab, J, J_z\rangle$  of two particles  $a, b$  of spin  $1/2$ . Each particle belongs to a representation of dimension 2 and the state of two particles has dimension 4.

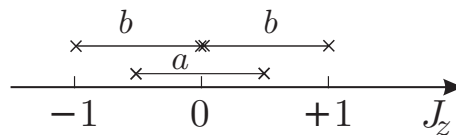


**Fig. 21.3.** The weights,  $J_z$  of particle  $b$  are added to the the two values of particle  $a$ .

The weight in this case is the value of  $J_z, \pm 1/2$  for each particle. The weights of the two particle states are  $-1, 0$  - twice - and  $1$ . The two values of  $0$  for  $J_z=0$  correspond to the states:

$$|ab, 1, 0\rangle = \frac{|a, 1/2, 1/2\rangle|b, 1/2, -1/2\rangle + |b, 1/2, 1/2\rangle|a, 1/2, -1/2\rangle}{\sqrt{2}}$$

$$|ab, 0, 0\rangle = \frac{|a, 1/2, 1/2\rangle|b, 1/2, -1/2\rangle - |b, 1/2, 1/2\rangle|a, 1/2, -1/2\rangle}{\sqrt{2}}$$

where we assign the symmetric state to  $J=1$  and the antisymmetric one to  $J=0$ , because the  $SU(2)$  operations do not change symmetry properties and the states  $|ab, 1, \pm 1\rangle$  are symmetric. We write this decomposition as  $2 \otimes 2 = 1 \oplus 3$ .

### 21.3 $SU(3)$

The simple unitary group in three dimension,  $SU(3)$ , is also of great importance in particle physics. The simplest non trivial state on which the group operates has three componets and the fundamental representation contains 8 indipendent operators. The group has herefore 8 generators  $\lambda_i$  and the matrices are  $U = e^{1/2\lambda_i\omega_i}$ ,

with  $\omega_i$  real. An explicit representation of the  $\lambda_i$  is:

$$\begin{aligned} \lambda_1 &= \begin{pmatrix} 0 & 1 & 0 \\ 1 & 0 & 0 \\ 0 & 0 & 0 \end{pmatrix} & \lambda_4 &= \begin{pmatrix} 0 & 0 & 1 \\ 0 & 0 & 0 \\ 1 & 0 & 0 \end{pmatrix} & \lambda_7 &= \begin{pmatrix} 0 & 0 & 0 \\ 0 & 0 & -i \\ 0 & i & 0 \end{pmatrix} \\ \lambda_2 &= \begin{pmatrix} 0 & -i & 0 \\ -i & 0 & 0 \\ 0 & 0 & 0 \end{pmatrix} & \lambda_5 &= \begin{pmatrix} 0 & 0 & -i \\ 0 & 0 & 0 \\ -i & 0 & 0 \end{pmatrix} & \lambda_8 &= \frac{1}{\sqrt{3}} \begin{pmatrix} 1 & 0 & 0 \\ 0 & 1 & 0 \\ 0 & 0 & -2 \end{pmatrix} \\ \lambda_3 &= \begin{pmatrix} 1 & 0 & 0 \\ 0 & -1 & 0 \\ 0 & 0 & 0 \end{pmatrix} & \lambda_6 &= \begin{pmatrix} 0 & 0 & 0 \\ 0 & 0 & 1 \\ 0 & 1 & 0 \end{pmatrix} \end{aligned}$$

The algebra of the group is defined by:

$$\text{Tr } \lambda_i \lambda_j = \delta_{i,j} \quad [\lambda_i \lambda_j] = 2i f_{ijk} \lambda_k \quad \{\lambda_i \lambda_j\} = 3/4 \delta_{ij} + 2i d_{ijk} \lambda_k$$

where  $\{\dots\}$  is the anticommutator, the group structure constant  $f_{ijk}$  are antisymmetric in any pair of indices while  $d_{ijk}$  are symmetric. In fig. 21.4 we illustrate the weight diagram for the 3 and  $\bar{3}$  representation as well as the decomposition  $3 \otimes \bar{3} = 1 \oplus 8$ .

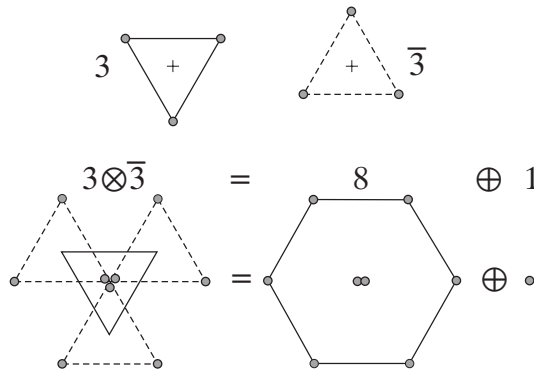


**Fig. 21.4.** The weight diagram for 3,  $\bar{3}$  and the reduction of  $3 \otimes \bar{3}$  to  $1 \oplus 8$ .

In fig. 21.4 we use for weights the eigenvalues of  $\lambda_3$  and  $\lambda_8$  which are diagonal. More precisely we plot on the  $x$ -axis the eigenvalues of  $1/2 \times \lambda_3$  and on the  $y$ -axis those of  $\lambda_8/\sqrt{3}$ . The subdivision of the 9 states from  $3 \otimes \bar{3}$  is obtained from symmetry consideration. Note that the  $(0, 0)$  state appears twice in the octet. If we were to identify the value  $x$  with of  $T_3$ . we would say that the octet of  $SU(3)$  contains an iso-spin singlet and a triplet, both with zero hypercharge.

When we deal with  $SU(3)$  as the gauge group of QCD, it is necessary to compute the scalar product of two color charges, the equivalent of the electric charge squared  $\alpha$  which appears in the potential energy  $V = \alpha/r$ . In other words we want the

expectation values of the scalar product  $\langle C_1 \cdot C_2 \rangle$ , which is the equivalent of the spin $\times$ orbit coupling,  $\langle L \cdot s \rangle$ . The latter is calculated squaring  $L + s = J$ :

$$J^2 = (L + s)^2 = L^2 + s^2 + 2(L \cdot s)$$

from which

$$\langle L \cdot s \rangle = \frac{1}{2}(J(J+1) - L(L+1) - s(s+1)).$$

Let  $C = C_1 + C_2$ , where 1 and 2 stand for two representations of  $SU(3)$ . As for  $SU(2)$ ,  $C^2$  is the quadratic Casimir operator:

$$C^2 = \sum_1^8 \lambda_i^2$$

and

$$\langle C_1 \cdot C_2 \rangle = \frac{1}{2}(\langle C^2 \rangle - \langle C_1^2 \rangle - \langle C_2^2 \rangle).$$

We have to find the eigenvalues of  $C$  for a representation, a slightly boring exercise.

Quadratic Casimir Operator in  $SU(n)$ .

$SU(n)$  is a group of complex matrices  $U$ , which are unitary,  $U^\dagger U = 1$ , and unimodular, simple group,  $\det U \equiv \|U\| = 1$ . The fundamental multiplet is an  $n$ -dimensional spinor:

$$\begin{pmatrix} a_1 \\ a_2 \\ \vdots \\ a_n \end{pmatrix}$$

and the fundamental representation is given by  $n \times n$  matrices. The general form of the matrices is  $U = e^{i\omega_i \frac{\lambda_i}{2}}$  where  $i = 1 \dots n^2 - 1$ , because of unitarity and unimodularity.  $\lambda_i$  are the generators of the group,  $\omega_i$  real constant.

For  $SU(2)$  and  $n = d = 2$ , the dimension of the fundamental representation,  $\lambda_i$  are the Pauli matrices. Setting  $T_i = 1/2\lambda_i$ ,  $\mathbf{T}$  is the angular momentum operator  $\mathbf{J}$  or the isotopic spin operator  $\mathbf{I}$ .  $SU(3)$  has 8 generators  $\lambda_i$  and again we set  $\mathbf{T} = \vec{\lambda}$ . The quadratic Casimir operator  $C = \mathbf{T}^2 = \sum_{i=1}^{2n^2-1} T_i^2$  has the same expectation value for all member of a representation and, in  $SU(N)$ , it is equivalent to average the square of any single operator over the representation or to sum over all generators. Using the former the value of  $\mathbf{T}^2$  is given by:

$$\langle \mathbf{T}^2 \rangle|_d = (n^2 - 1) \sum_{\text{all members of rep.}} T_i^2 / d.$$

For  $SU(2)$  (spin for example), we choose  $J_3$  and verify the well known result  $J^2 = J(J + 1)$  as in the table below, up to  $J=3/2$ .

$d$	$J$	$J_3$	$\sum J_3^2$	$3 \times \Sigma/d$	$J(J + 1)$
2	1/2	1/2 -1/2	1/4 2/4	3/4	3/4
3	1	1 0 -1	1 1 2	2	2
4	3/2	3/2 1/2 -1/2 -3/2	9/4 10/4 19/4 5	15/4	15/4

For  $SU(3)$ , we also chose the equivalent of  $I_3$  and go back to the quark model where we simply look-up all eigenvalue of the third of isospin in 3, 3\*, 6, 8 and 10-dimensional multiplets. The table below gives the expectation value of  $\mathbf{T}^2$  and all that is necessary for the computation.

$d$	$I_3$	$\sum I_3^2$	$8 \times \Sigma/d = T^2$
1	0	0	0
3	1/2, -1/2; 0	2/4	4/3
6	1, 0, 1 1/2, -1/2; 0	2 10/4	10/3
8	1/2, -1/2 1, 0, 1; 0 1/2, -1/2	2/4 10/4 12/4	3
10			6

Next, from  $(\mathbf{T}_a + \mathbf{T}_b)^2 = \mathbf{T}_a^2 + \mathbf{T}_b^2 + 2(\mathbf{T}_a \cdot \mathbf{T}_b)$  we obtain:  $\mathbf{T}_a \cdot \mathbf{T}_b = ((\mathbf{T}_a + \mathbf{T}_b)^2 - \mathbf{T}_a^2 - \mathbf{T}_b^2)/2$ . We can therefore estimate the coulomb interaction potential for a  $q\bar{q}$  pair, taking it proportional to the scalar product of the  $SU(3)$  charges for the 8- and 1-dimensional representation contained in  $3 \times 3^*$ . From the above table:

$$\mathbf{T}^{(3)} \cdot \mathbf{T}^{(3^*)}|_{q\bar{q}, d=1} = (0 - 4/3 - 4/3)/2 = -4/3$$

and likewise for other representations in  $3 \otimes 3^*$  and other combinations. The results are given below, where states with more than two quarks are analyzed assuming that the potential is due to the sum of two body contributions

$$V \propto \sum_{i < j} \langle \mathbf{T}^{(i)} \cdot \mathbf{T}^{(j)} \rangle.$$

Configuration	$\mathbf{T}_a \cdot \mathbf{T}_b$
$q\bar{q} _1$	$-4/3$
$q\bar{q} _8$	$1/6$
$qq _{3^*}$	$-2/3$
$qq _6$	$1/3$
$qqq _1$	$-2$
$qqq _8$	$-1/2$
$qqq _{10}$	$1$
$qqqq _3$	$-2$

References for  $SU(2)$ ,  $SU(3)$ ,  $SU(n)$

L. B. Okun, Leptons and Quarks, North-Holland, Personal library

C. Quigg, Gauge Theories of the Strong, Weak and Electromagnetic Interactions, Benjamin/Cummings, p. 195.

See Quigg. How to get  $\langle C^2 \rangle$  etc.

## 21.4 Magnetic moment

We turn now however to the magnetic moment of a particle, beginning with the magnetic moment associated with the orbital angular momentum of a charged particle. We note that from simplest point of view, the splitting of the strong alkaline lines is understandable in terms of an interaction between the electron magnetic dipole moment and the magnetic field generated by the orbital motion of the electron in the atom. The splitting is due to the fact that the energy of a magnetic dipole  $\vec{\mu}$  in a field  $\mathbf{B}$  is  $-\vec{\mu} \cdot \mathbf{B}$  and if  $\mu_z$  is quantized, assuming only two values, a doublet is observed. Introducing the intrinsic angular momentum, or spin,  $\mathbf{S}$  the magnetic interaction is proportional to  $\mathbf{S} \cdot \mathbf{L}$ . If the electron spin is  $1/2$  and is quantized as the orbital angular momentum, again we obtain the observed doublets. We now do explicitly some calculations.

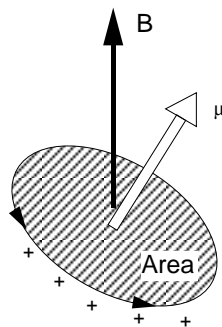


**Fig. 21.5.** A current loop in magnetic field.

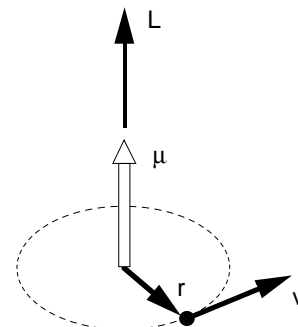


**Fig. 21.6.** A particle in a closed orbit.

Classically a charge moving on a closed orbit is a current loop, which we know is a

magnetic dipole, of magnitude proportional to the loop area and therefore the angular momentum  $\mathbf{L}$ . In gaussian units, the magnetic moment of a current loop is:

$$\mu = \frac{1}{c} \text{current} \times \text{area}.$$

The magnetic moment  $\vec{\mu}$  is perpendicular to the loop and a positive current and the resulting magnetic dipole form a right handed screw. If we consider a particle of charge  $q$ , mass  $m$  and velocity  $v$  moving on a circular path, the current is  $i = q/T = qv/(2\pi r)$  and the magnetic dipole is  $\mu = (1/c) \times qv/(2\pi r) \times \pi r^2 = qvr/2c$ . The angular momentum is  $L = mvr$  and therefore  $\mu = qL/2mc$ , where we still keep  $c$ . The relation is correct also for vectors:

$$\vec{\mu} = \frac{q}{2mc} \mathbf{L}.$$

The main result is that  $\vec{\mu}$  is parallel to  $\mathbf{L}$  and proportional to  $L$ , with  $\mu/L = q/2mc$ . The derivation is of course classical and for a circular orbit, but correct in fact for any central motion.

It is a most amazing fact that the relation is also valid in quantum mechanics, for orbital motion. Let us assume that a similar relation is valid for any angular momentum  $\mathbf{J}=\mathbf{L}+\mathbf{S}$ , which, using the relation derived above, we write, for an electron *i.e.* with  $q = e$ ,  $m = m_e$ , in magnitude:

$$\mu = g \frac{e}{2m_e c} J$$

where  $g$  is an arbitrary constant which is called the Landé factor or more simply the gyromagnetic ratio.  $J$  above is in gaussian units. Multiplying and dividing by  $\hbar$ , the relation becomes:

$$\mu = g \frac{e\hbar}{2m_e c} \frac{J}{\hbar} = g\mu_0 j$$

where  $\mu_0 = \hbar e/2m_e c$  is the so called Bohr magneton and  $j$  the eigen-value of the angular momentum in units of  $\hbar$ . For atomic states, with angular momentum  $l$ ,  $g$  is one, just as for the classical calculation above. For intrinsic angular momentum, *i.e.* for a charged particle with spin, a classical calculation cannot be performed without making untenable assumptions about spinning charge and the likes. One easily finds speeds greater than  $c$  and similar absurdities. Moreover  $g$  is not unity! It is one of the great triumphs of merging quantum mechanics and Lorentz invariance, as Dirac did with his famous equations, that electrons, treated as point particles, have spin 1/2 and for them  $g=2$ , in agreement with experiments, except for corrections of order  $\alpha/2\pi \sim 1/1000$ , which are calculable to great accuracy, another triumph of relativistic quantum mechanics. These corrections have been verified to accuracies of order  $1/10^{10}$  in beautiful experiments.

## 22 App. 3. Symmetries

### 22.1 Constants of Motion

Consider a stationary state  $\Psi$  which satisfies the Schrödinger eq.

$$i \frac{d}{dt} \Psi = H \Psi.$$

Let  $F$  be a physical observable to which corresponds an operator  $F$  and  $\langle F \rangle$  be its expectation value. The question is: when is  $\langle F \rangle$  constant in time, *i.e.* when is  $F$  a conserved quantity? The condition of constancy in time is:

$$\begin{aligned} \frac{d}{dt} \langle F \rangle &= \frac{d}{dt} \int \Psi^* F \Psi d^3x \\ &= \int \left( \frac{d}{dt} \Psi \right)^* F \Psi d^3x + \frac{d}{dt} \int \Psi^* F \left( \frac{d}{dt} \Psi \right) d^3x = 0 \end{aligned}$$

Taking the complex conjugate of the Schr eq.

$$-i \frac{d}{dt} \Psi^* = (H \Psi)^* = \Psi^* H$$

we obtain

$$\begin{aligned} \frac{d}{dt} \langle F \rangle &= i \int \Psi^* (HF - FH) \Psi d^3x = 0 \\ HF - FH &= [H, F] = 0. \end{aligned}$$

Therefore the vanishing of the commutator  $[H, F]$  insures that  $\langle F \rangle$  is a constant of the motion. If  $[H, F] = 0$ ,  $F$  is called a conserved quantity and the states  $\Psi$  can be chosen as simultaneous eigenstates of  $H$  and  $F$ .

$$\begin{aligned} H \Psi &= E \Psi \\ F \Psi &= \mathcal{F} \Psi \end{aligned}$$

### 22.2 Finding Conserved Quantities

In principle, from  $H$  we could extract all ops  $F$  such that  $[H, F]=0$ . However, most often  $H$  is not completely known, but some symmetry properties of  $H$  might be known. If there is some operator  $U$  under which the physical system described by  $H$  is invariant, then there exist a conserved quantity. Let  $U$  be an operator such that under  $U$ :

$$\Psi \xrightarrow{U} \Psi'.$$

In general, the operator  $U$  can be a function of a continuous parameter, the parameter need not even be a scalar. We call the symmetry a continuous symmetry in this case. We begin however with the simple case of a discrete symmetry.

## 22.3 Discrete Symmetries

As a simple example let's consider a discrete symmetry operator  $U$ , such that

$$\Psi \xrightarrow{U} \Psi' \xrightarrow{U} \Psi$$

That is  $U$  on  $\Psi'$  gives back  $\Psi$  or

$$U(U\Psi) = U^2\Psi = U\Psi' = \Psi.$$

This is equivalent to  $U^2 = I$  or  $U = U^{-1}$  and therefore  $U^\dagger = U$ , *i.e.* the operator  $U$  is hermitian and therefore an observable. Let  $U$  be the parity op.  $P$ , defined as the operation which changes the sign of the  $x$ ,  $y$  and  $z$  coordinate axes. Then what are the eigenvalues  $\mathcal{P}$  of  $P$  in  $P\Psi = \mathcal{P}\Psi$ ? The eigenvalues of  $P$  must be  $\pm 1$ , but its not obvious that the eigenstate of  $H$  should be eigenstate of  $P$  since in general  $\Psi(\mathbf{r})$  can be quite different from  $\Psi(-\mathbf{r})$ . But if  $[H, P] = 0$  and  $H\Psi = E\Psi$ , then also  $H\Psi' = E\Psi'$ , *i.e.*, unless  $\Psi$  and  $\Psi'$  are degenerate states belonging to the same eigenvalue  $E$ , than

$$P\Psi = \mathcal{P}\Psi,$$

## 22.4 Other conserved additive Q. N.

If conservation of the numbers  $q_b$ ,  $q_{\ell(e)}$ ,  $q_{\ell(\mu)}$ ,  $q_{\ell(\tau)} \dots$  where to be taken as consequence of a corresponding local gauge symmetry, this requires that the the hamiltonian must be

$$H = H_{kin} + H_{charge-field}$$

with  $H_{charge-field}$  of the form  $q_\zeta A_0^{(\zeta)}$ , where  $A_0^{(\zeta)}$  is the time component of a 4-potential describing a field whose source is the charge  $q_\zeta$ . The quanta of this field are massless photons  $\gamma_\zeta$

Thus there exists the photons  $\gamma_b$ ,  $\gamma_{\ell(e)}$ ,  $\gamma_{\ell(\mu)}$ ,  $\gamma_{\ell(\tau)} \dots$  and  $q_b$ ,  $q_{\ell(e)}$ ,  $q_{\ell(\mu)}$ ,  $q_{\ell(\tau)} \dots$  are charges just like the electric charge, not electric of course, just with all the same properties.

## 22.5 $J^{PC}$ for a fermion anti-fermion pair

Consider a fermion-antifermion pair. The parity of charged particles can only be determined up to a sign, because of charge conservation. However, from the anti-commutation relations for fermions and anti fermion creation and destruction operators, it follows that if  $P|f\rangle = \mathcal{P}_f|f\rangle$  then  $\mathcal{P}_f = -\mathcal{P}_{\bar{f}}$ . Therefore the parity of

a fermion-antifermion pair is given by  $P|f\bar{f}\rangle = -(-1)^L|f\bar{f}\rangle$ , where  $L$  is the pair orbital angular momentum. Because of conservation of charge, electric or of any other kind such as barionic number etc., fermions cannot generally be eigenstate of charge conjugation  $C$ . An  $f\bar{f}$  pair is however neutral in all respects and therefore it can be an eigenstate of  $C$  as well as  $P$ . Fermions obey Fermi-Dirac statistics that is, for two fermions,  $\Psi(f_1, f_2) = -\Psi(f_2, f_1)$ . Remember that two fermions are not distinguishable, by  $f_2, f_1$ , we mean a fermion with coordinates “1” and another with coordinates “2”. We can write the two fermion state as a product of a spin coordinate function and a space function. We can also consider charge, of whatever kind, as an additional coordinate. Then we write

$$\Psi(1, 2) = \Psi(\mathbf{r}_1, \mathbf{r}_2)\Psi(\sigma_1, \sigma_2)\Psi(q_1, q_2).$$

Under the operation  $1\leftrightarrow 2$ , the overall wavefunction changes sign, space and spin parts behave as usual and  $\Psi(q_1, q_2)$  changes or not sign according to the  $C$  eigenvalue of the two fermion state. Then performing a  $1\leftrightarrow 2$  exchange, we can write

$$\begin{aligned} -1 &= (-1)^L \times [ - (-1)^S ] \times C \\ C &= (-1)^S \times (-1)^L \\ P &= -(-1)^L \\ CP &= -(-1)^S \end{aligned}$$

where  $S$  is the spin of the fermion pair, 0 or 1,  $L$  is the orbital angular momentum and  $C$  is the charge conjugation eigenvalue of the fermion pair. Let's consider  $S$ -waves,  $L=0$ . There are two state, singlet and triplet,  ${}^3S_1$  and  ${}^1S_0$ . For the former, from the eq. above we get  $C=-1$  and the latter  $C=1$ . Using further  $\mathcal{P} = -1 \times (-1)^L$  we find  $J^{PC} = 1^{--}$  and  $J^{PC} = 0^{+-}$  for triplet and singlet  $S$ -wave  $f\bar{f}$  states.

We can do the same with the  $P$ -wave states. For singlet  ${}^1P_1$  we find  $C=-1$  and  $\mathcal{P}=1$ , or  $J^{PC} = 0^{+-}$ . For the triplet states  ${}^3P_2, {}^3P_1$  and  ${}^3P_0$  we have  $J^{PC} = 2^{++}, 1^{++}, 0^{++}$ .

This argument is not liked by theorists but it gives the correct answer and can be justified as rigorous. As far as two neutrinos go,  $P$  and  $C$  lead to non physical states and I do not know what to do.

It is said that  $K_L \rightarrow \pi^0 \nu \bar{\nu}$  violates  $CP$  while  $K_S \rightarrow \pi^0 \nu \bar{\nu}$  does not. Since

$$\begin{aligned} CP|\pi^0\rangle &= +|\pi^0\rangle \\ CP|K_1\rangle &= +|K_1\rangle \\ CP|K_2\rangle &= -|K_2\rangle \end{aligned}$$

$K_L \rightarrow \pi^0$  is mostly due to a  $CP$  violating coupling, therefore it is ultimately due to  $\eta$  and  $\Gamma(K_L \rightarrow \pi^0 \nu \bar{\nu}) \propto \eta^2$ . Why however it is said that  $\Gamma(K_S \rightarrow \pi^0 \nu \bar{\nu}) \propto \rho^2 + \eta^2$ ?

## 23 App. 4. CKM Matrix

### 23.1 Definition, representations, examples

$$\mathbf{V} = \begin{pmatrix} V_{ud} & V_{us} & V_{ub} \\ V_{cd} & V_{cs} & V_{cb} \\ V_{td} & V_{ts} & V_{tb} \end{pmatrix}$$

Unitarity is satisfied by the representation:

$$\mathbf{V} = \begin{pmatrix} c_{12}c_{13} & s_{12}c_{13} & s_{13}e^{-i\delta} \\ -s_{12}c_{23} - c_{12}s_{23}s_{13}e^{i\delta} & c_{12}c_{23} - s_{12}s_{23}s_{13}e^{i\delta} & s_{23}c_{13} \\ s_{12}s_{23} - c_{12}c_{23}s_{13}e^{i\delta} & -c_{12}s_{23} - s_{12}c_{23}s_{13}e^{i\delta} & c_{23}c_{13} \end{pmatrix}$$

where  $c_{12} = \cos\theta_{12}$  etc.  $\delta$  is the  $CP$  violating phase. Experiment *plus* unitarity gives, for  $|V_{ij}|$ :

$$\mathbf{V} = \begin{pmatrix} 0.9745 - 0.9760 & 0.217 - 0.224 & 0.0018 - 0.0045 \\ 0.217 - 0.224 & 0.9737 - 0.9753 & 0.036 - 0.042 \\ 0.004 - 0.013 & 0.035 - 0.042 & 0.9991 - 0.0994 \end{pmatrix}$$

Take as an example  $|V_{ud}|=0.975$ ,  $|V_{ub}|=0.003$ ,  $|V_{cb}|=0.04$ . Then we have:

$$\mathbf{V} = \begin{pmatrix} .975 & 0.222184608 & 0.003 e^{-i\delta} \\ \dots & \dots & 0.04 \\ 0.00888746 - 0.00292267 e^{i\delta} & -0.03900035 - 0.00066602 e^{i\delta} & 0.9991956 \end{pmatrix}$$

$$s_{12} = 0.22218561 \quad c_{12} = .97500439$$

$$s_{13} = 0.00030000 \quad c_{13} = .99999550$$

$$s_{23} = 0.04000018 \quad c_{23} = .99919967$$

Check on unitarity

$$\sum_{i=1}^3 V_{ui}V_{ti}^* = [1.1 + .11e^{-i\delta}] \times 10^{-18}$$

## 24 App. 5. Accuracy Estimates

### 24.1 Testing a theory or measuring one of its parameters

Given a theory to be experimentally tested or just the necessity of determining one of its parameters is a fundamental to particle physics. The maximum likelihood method is the general way through which we can do this. We describe in the following the estimations of the number of events required to obtain the desired accuracy in the measurement of a parameter.

### 24.2 A priori estimates

Consider a variable  $x$ , normally distributed around a mean  $\bar{x}$ , with variance  $\sigma^2$ :

$$f(x; \bar{x}) = \frac{1}{\sqrt{2\pi} \sigma} \exp\left(-\frac{(x - \bar{x})^2}{2\sigma^2}\right)$$

The joint probability or likelihood of an observation consisting of a set of  $N$  measurements  $x_i$  is:

$$\mathcal{L} = \prod_1^N \frac{1}{\sqrt{2\pi} \sigma_i} \exp\left(-\frac{(x_i - \bar{x})^2}{2\sigma_i^2}\right).$$

$W = \log \mathcal{L}$  is then  $-1/2 \times$  the  $\chi^2$  function:

$$W = \log \mathcal{L} = -\frac{1}{2} \sum_1^N \frac{(x_i - \bar{x})^2}{\sigma_i^2} = -\frac{1}{2} \chi^2.$$

The best estimate for  $\bar{x}$  is the value which maximizes the likelihood of the observation,  $\mathcal{L}$  or  $W = \log \mathcal{L}$ , obtained by solving

$$2 \frac{\partial W}{\partial \bar{x}} = \sum \frac{x_i - \bar{x}}{\sigma_i^2} = 0$$

which gives the well known result:

$$\bar{x} = \frac{\sum x_i / \sigma_i^2}{\sum 1 / \sigma_i^2}.$$

For large  $N$  the likelihood function approaches a gaussian. If  $\mathcal{L}(x, \bar{x})$  is the likelihood for observing  $x$ ,  $\bar{x}$  being the best estimate, then the *rms* fluctuation of  $x$  is given by:

$$\overline{\delta x^2} = \frac{\int (x - \bar{x})^2 \mathcal{L} dx}{\int \mathcal{L} dx}.$$

For a gaussian likelihood,

$$\mathcal{L}(x; \bar{x}) = \frac{1}{\sqrt{2\pi} \sigma} \exp\left(-\frac{(x - \bar{x})^2}{2\sigma^2}\right)$$

we have  $(\delta x)^2 = \sigma^2$ , where we set  $\overline{\delta x} = \delta x$ . The value of  $\sigma$  can be expressed in terms of the second derivative of  $W$ :

$$\begin{aligned}\frac{\partial W}{\partial \bar{x}} &= \sum \frac{x - \bar{x}}{\sigma^2} \\ \frac{\partial^2 W}{\partial \bar{x}^2} &= -\frac{1}{\sigma^2}\end{aligned}$$

and therefore:

$$\delta x = \sigma = \sqrt{-\frac{1}{\frac{\partial^2 W}{\partial \bar{x}^2}}}\tag{24.12}$$

Consider now a variable  $x$  with a probability density function  $f(x; p)$ , with the usual meaning that  $dP$ , the probability of observing an event at  $x$  in  $dx$ , is  $f(x) dx$ . The function  $f$  is normalized to unit over the whole  $x$ -interval where  $x$  is physical and  $p$  is a (set of) parameter(s) we wish to estimate. From  $\mathcal{L} = \prod f(x, p)$ , for one event, we have  $W = \log \mathcal{L} = \log f$ . If we want the accuracy with which we can determine the parameter  $p$ , we use the result in equation (24.12), relating  $\frac{\partial^2 W}{\partial p^2}$  to  $\delta p$  with:

$$\frac{\partial^2 W}{\partial p^2} = \frac{\partial^2 \log f(x; p)}{\partial p^2}$$

averaged over repeated measurements of one event each:

$$\left\langle \frac{\partial^2 W}{\partial p^2} \right\rangle = \int \frac{\partial^2 \log f(x; p)}{\partial p^2} f(x; p) dx$$

and for  $N$  events

$$\left\langle \frac{\partial^2 W}{\partial p^2} \right\rangle = N \int \frac{\partial^2 \log f(x; p)}{\partial p^2} f(x; p) dx.$$

Computing the derivative in the integral above gives:

$$\int \frac{\partial^2 \log f}{\partial p^2} dx = - \int \frac{1}{f} \left( \frac{\partial f}{\partial p} \right)^2 dx + \int \frac{\partial^2 f}{\partial p^2} dx,$$

where the last term vanishes, exchanging integration and differentiation, since  $\int f dx = 1$ . Thus finally we obtain:

$$\delta p = \frac{1}{\sqrt{N}} \left( \int \frac{1}{f} \left( \frac{\partial f(x; p)}{\partial p} \right)^2 dx \right)^{-\frac{1}{2}}\tag{24.13}$$

### 24.3 Examples

As an application we find the number of events necessary do determine a *slope* parameter  $g$  defined as in  $f(x; g) = (1 + xg)/2$ , with  $x$  in  $\{-1, 1\}$ . The integral in equation (24.13) is:

$$\int_{-1}^1 \frac{x^2}{2(1 + gx)} dx = \frac{1}{2g^3} \left( \log \left( \frac{1 + g}{1 - g} \right) - 2g \right)$$

giving, approximately,  $\delta g = \sqrt{3/N}$ .

For the case of the slope in a Dalitz plot (taken as a circle with center at the origin) population, the probability density is  $f(x; g) = 2/\pi(1 + gx)\sqrt{1 - x^2}$ , with  $x$  in  $\{-1, 1\}$ . The error on  $g$  is given by:

$$(\delta g)^2 = \frac{1}{N} \left( \frac{2}{\pi} \int_{-1}^1 \frac{x^2 \sqrt{1 - x^2}}{1 + gx} dx \right)^{-1} = \frac{k^2}{N}$$

where for  $g = 0.26$ , the value for  $K_{3\pi}^{\pm}$  decays,  $k = 1.9785$  resulting in a fractional accuracy,  $\delta g/g = 7.56/\sqrt{N}$ .

## 24.4 Taking into account the experimental resolution

We assume the resolution function is known, otherwise the case is of course hopeless. There is often the temptation to try to unfold resolution from the data. This procedure is ambiguous and can lead to incorrect results. The correct procedure is very simple. Convolute the resolution with the theory:

$$g'(x; p) = \int g(x - x')r(x') dx',$$

make sure that  $g'$  is correctly normalized and proceed as above.

## 25 App. 6. $\chi$ -squared

### 25.1 Likelihood and $\chi^2$

For variables which are normal-distributed the logarithm of the likelihood function  $\mathcal{L}$  is equal to the negative of the  $\chi^2$  sum. Maximizing the former or its logarithm, since  $\mathcal{L}$  is positive definite, is therefore equivalent to minimizing the  $\chi^2$  sum.

### 25.2 The $\chi^2$ solution

Let  $\mathbf{m}$  be a set of measurements to be matched to a (set) of functions  $\mathbf{f}$ , in the sense of minimizing the sum of the squares of the difference between the functions and the measurements, defined by:

$$\mathbf{m} = \begin{pmatrix} m_1 \\ m_2 \\ \vdots \\ m_N \end{pmatrix}, \quad \mathbf{f} = \begin{pmatrix} f_1 \\ f_2 \\ \vdots \\ f_N \end{pmatrix} \quad (25.14)$$

The elements of the function's vector  $\mathbf{f}$ , are functions of the parameter's vector  $\mathbf{x}$ , to be determined, defined as:

$$\mathbf{x} = \begin{pmatrix} x_1 \\ \vdots \\ x_L \end{pmatrix}, \quad \text{with } L < N. \quad (25.15)$$

Let  $\mathbf{c}$  be the corrections vector to be applied to the measurements, in order to obtain equality with the functions, with the assumption that  $\mathbf{c}$  is unbiased, i.e.  $\langle c_i \rangle = 0$ , defined as:

$$\mathbf{f}(\mathbf{x}) = \mathbf{m} + \mathbf{c}. \quad (25.16)$$

The error matrix of the measurements (the so called covariance matrix) is defined by:

$$(G_m^{-1})_{i,j} = \overline{\delta m_i \delta m_j}. \quad (25.17)$$

In terms of all the above, we define the sum of squares  $SS$  as:

$$SS = \mathbf{c}^T \mathbf{G}_m \mathbf{c} (= \chi^2), \quad (25.18)$$

the general form for  $SS$ , valid also when the measurement errors are correlated and therefore the error matrix is non diagonal. The values of  $\mathbf{x}$  for which  $SS$  is minimum is an unbiased estimate of the parameters  $x_i$  with smallest variance (Gauss–Markov theorem). The matrix  $\mathbf{G}_m$  and its inverse are symmetric, see equation 4. If he

quantities  $\mathbf{m}$  or  $\mathbf{c}$  are normally distributed, the least square sum is the natural logarithm of the likelihood (joint probability) of the observation and is called the  $\chi^2$  function. Its distribution is the well known  $\chi^2$  distribution.

Solving the L simultaneous equations:

$$\frac{\partial(SS)}{\partial \mathbf{x}} = 0 \quad \text{or} \quad \frac{\partial(\chi^2)}{\partial \mathbf{x}} = 0 \quad (25.19)$$

gives the parameter's vector  $\mathbf{x}$ . The solution of the equation above is trivial if  $\mathbf{f}$  is a linear function of  $\mathbf{x}$ . If these is not the case we can solve for  $\mathbf{x}$  by iteration after expanding  $\mathbf{f}$  in Taylor series around a "first guess" for the unknowns,  $\bar{\mathbf{x}}$ :

$$\mathbf{f}(\mathbf{x}) = \mathbf{f}(\bar{\mathbf{x}}) + (\partial \mathbf{f} / \partial \mathbf{x})(\mathbf{x} - \bar{\mathbf{x}}) = \mathbf{f}(\bar{\mathbf{x}}) + \mathbf{A} \Delta \mathbf{x}. \quad (25.20)$$

The last identity defines the matrix  $\mathbf{A}$  ( $A_{ij} = \partial f_i / \partial x_j$ ) and the vector  $\Delta \mathbf{x}$ . In term of the derivative matrix  $\mathbf{A}$ , the vector  $\Delta \mathbf{x}$  and the so called residues,  $\mathbf{r} = \mathbf{f}(\bar{\mathbf{x}}) - \mathbf{m}$ , the correction vector  $\mathbf{c}$  is given by  $\mathbf{c} = \mathbf{r} + \mathbf{A} \Delta \mathbf{x}$  and  $\chi^2$  by:

$$\chi^2 = (\mathbf{r} + \mathbf{A} \Delta \mathbf{x})^T \mathbf{G}_m (\mathbf{r} + \mathbf{A} \Delta \mathbf{x}) \quad (25.21)$$

and ( $\partial \chi^2 / \partial \Delta \mathbf{x} = 0$ ) equation (25.19) becomes

$$2\mathbf{A}^T \mathbf{G}_m (\mathbf{r} + \mathbf{A} \Delta \mathbf{x}) = 0 \quad (25.22)$$

from which one obtains

$$\Delta \mathbf{x} = -(\mathbf{A}^T \mathbf{G}_m \mathbf{A})^{-1} \mathbf{A}^T \mathbf{G}_m \mathbf{r} \quad (25.23)$$

If  $\mathbf{f}$  is linear in  $\bar{\mathbf{x}}$ , this solution is exact, for any  $\mathbf{x}$ , in particular one can choose  $\bar{\mathbf{x}} = 0$  giving  $\mathbf{x} = \Delta \mathbf{x}$ . If  $\mathbf{f}$  is not linear, after a choice of  $\bar{\mathbf{x}}$  and solving for  $\Delta \mathbf{x}$ , one substitutes  $\bar{\mathbf{x}} = \bar{\mathbf{x}} + \Delta \mathbf{x}$  and iterates until  $\chi^2$  is stationary. Next to determining  $\mathbf{x}$  we need the errors for the parameters. The usual propagation of errors

$$\overline{\delta x_i \delta x_j} = \sum_k \sum_l (\partial x_i / \partial m_k) (\partial x_j / \partial m_l) \overline{\delta m_k \delta m_l} \quad (25.24)$$

can be written in our notation as ( $\partial \mathbf{m} = \partial \mathbf{r}$ )

$$\mathbf{G}_x^{-1} = (\partial \Delta \mathbf{x} / \partial \mathbf{r})^T \mathbf{G}_m^{-1} (\partial \Delta \mathbf{x} / \partial \mathbf{r}) \quad (25.25)$$

which, using the solution for  $\Delta \mathbf{x}$ , equation (25.23), gives:

$$\mathbf{G}_x^{-1} = (\mathbf{A}^T \mathbf{G}_m \mathbf{A})^{-1} \mathbf{A}^T \mathbf{G}_m \mathbf{G}_m^{-1} \mathbf{G}_m \mathbf{A} (\mathbf{A}^T \mathbf{G}_m \mathbf{A})^{-1} = (\mathbf{A}^T \mathbf{G}_m \mathbf{A})^{-1}. \quad (25.26)$$

Note that this matrix already appears in equation (25.23) for  $\Delta \mathbf{x}$ .

### 25.3 Matrix dimensions

Sometimes, when writing a program, one can get confused with the matrix dimensions. We explicitly exhibit the dimensions of all matrices. All vectors are taken to have one column, the transposed vectors have one row. The error matrices are by definition, square and symmetric, thus:

$$\mathbf{G}_m^{-1} = \begin{pmatrix} \overline{\delta_1\delta_1} & \overline{\delta_1\delta_2} & \dots & \overline{\delta_1\delta_N} \\ \overline{\delta_2\delta_1} & \overline{\delta_2\delta_2} & \dots & \overline{\delta_2\delta_N} \\ \vdots & \vdots & \ddots & \vdots \\ \overline{\delta_N\delta_1} & \overline{\delta_N\delta_2} & \dots & \overline{\delta_N\delta_N} \end{pmatrix}. \quad (25.27)$$

This is also called the covariance matrix. The complete definition of the matrix elements is:

$$(G_m^{-1})_{i,j} = \overline{\delta m_i \delta m_j} = \overline{(m_i - \bar{m}_i)(m_j - \bar{m}_j)}. \quad (25.28)$$

The diagonal elements of  $\mathbf{G}^{-1}$  are positive definite. If the measurements are uncorrelated, the off-diagonal elements are zero.

The derivative matrix is rectangular, with  $N$  rows, as many as the number of measurements and functions and  $L$  columns, as many as the number of parameters to be determined. Explicitly:

$$\mathbf{A} = \begin{pmatrix} \partial f_1 / \partial x_1 & \dots & \partial f_1 / \partial x_L \\ \vdots & & \vdots \\ \partial f_N / \partial x_1 & \dots & \partial f_N / \partial x_L \end{pmatrix}. \quad (25.29)$$

### 25.4 A Simple Example

Often a series of measurements of a quantity are performed for different discrete values of a single variable, for instance velocity versus time, intensity vs deflection etc. The measurements are expected to be described by some function of the variable, the function containing some arbitrary parameters to be determined. Calling the values of the variable  $v_i$ , the functions of section 1.1 are, in the present case, the values the function to be fitted assumes for the different values of the variable  $v_i$ . We consider the following simple concrete case. Let the functions be given in the form  $f_i = x_1 g(v_i) + x_2 h(v_i)$ . The form of the function  $h$  and  $g$  is known and can be computed for the values of  $v_i$  for which the measurements were performed. The unknowns to be determined are the two parameters  $x_1$  and  $x_2$ .  $\mathbf{A}^T$  is:

$$\mathbf{A}^T = \begin{pmatrix} g(v_1) & g(v_2) & \dots & g(v_N) \\ h(v_1) & h(v_2) & \dots & h(v_N) \end{pmatrix} \equiv \begin{pmatrix} g_1 & g_2 & \dots & g_N \\ h_1 & h_2 & \dots & h_N \end{pmatrix} \quad (25.30)$$

and

$$\mathbf{G}_m = \begin{pmatrix} 1/\delta_1^2 & & & \\ & 1/\delta_2^2 & & \\ & & \ddots & \\ & & & 1/\delta_N^2 \end{pmatrix}, \quad \mathbf{r} = -\mathbf{m}. \quad (25.31)$$

$\mathbf{G}_m$  is a diagonal matrix if the measurements are uncorrelated, as usually counts are. If the measurements consist of counts (i.e. number of events) the a-priori fluctuation on each is the square root of the expected number of counts, i.e.  $\delta_i = \sqrt{f_i}$ . Note that its often stated that the error is given by  $\sqrt{\text{observed count}}$ . This is incorrect and leads to incorrect fits which among other mistakes do not obey simple constraint such as giving the correct area under the curve. Often the least square fit is understood as assigning equal weight to all measurements, i.e. setting

$$\mathbf{G}_m = \begin{pmatrix} 1 & & & \\ & 1 & & \\ & & \ddots & \\ & & & 1 \end{pmatrix} \frac{1}{\sigma^2}.$$

$\mathbf{G}_x$  is given by:

$$\mathbf{G}_x = \mathbf{A}^T \mathbf{G}_m \mathbf{A} = \begin{pmatrix} \sum g_i^2/\delta_i^2 & \sum g_i h_i/\delta_i^2 \\ \sum g_i h_i/\delta_i^2 & \sum h_i^2/\delta_i^2 \end{pmatrix} \quad (25.32)$$

This matrix is trivially inverted, giving

$$\mathbf{G}_x^{-1} = \begin{pmatrix} \sum h_i^2/\delta_i^2 & -\sum g_i h_i/\delta_i^2 \\ -\sum g_i h_i/\delta_i^2 & \sum g_i^2/\delta_i^2 \end{pmatrix} \frac{1}{\det(\mathbf{G}_x)}$$

The solution for  $x_1, x_2$  is:

$$\mathbf{x} = \begin{pmatrix} \sum h_i^2/\delta_i^2 \sum g_i m_i - \sum g_i h_i/\delta_i^2 \sum h_i m_i/\delta_i^2 \\ \sum g_i^2/\delta_i^2 \sum h_i m_i - \sum g_i h_i/\delta_i^2 \sum g_i m_i/\delta_i^2 \end{pmatrix} \frac{1}{\det(\mathbf{G}_x)}$$

For the case of equal errors, we can set them to 1 in the above formula and obtain the least square solution for  $x_1, x_2$ :

$$x_1 = \frac{\sum h_i^2 \sum g_i m_i - \sum g_i h_i \sum h_i m_i}{\sum h_i^2 \sum g_i^2 - (\sum g_i h_i)^2}$$

$$x_2 = \frac{\sum g_i^2 \sum h_i m_i - \sum g_i h_i \sum g_i m_i}{\sum h_i^2 \sum g_i^2 - (\sum g_i h_i)^2}$$

and the errors:  $\delta x_1 = \sqrt{(\mathbf{G}_x)_{2,2}/\det(\mathbf{G}_x)}$ ,  $\delta x_2 = \sqrt{(\mathbf{G}_x)_{1,1}/\det(\mathbf{G}_x)}$ .

While a generalization cannot be given on finite amounts of paper, the solution in matrix form given above allows to write simple programs for solving arbitrarily complicated cases. A  $10 \times 10$  matrix can be inverted in less than a second on a home PC (of 15 years ago!).

## References

1. L. Okun
2. M.E. Peskin
3. Halzen & Martin
4. See for instance: PDG, any year also at [http...](http://pdg.lbl.gov/)
5. L. LePrince-Ringuet and M. Lheritier, *Compt. Rend.* **219** (1944) 618.
6. G.D. Rochester and C.C. Butler, *Nature* **106**, 885 (1947)
7. M. Gell-Mann, *Phys. Rev.* **92** (1953) 833.
8. M. Gell-Man, *Phys. Lett.* **8** (1964) 214; G Zweig, CERN Report 8182/th (1964) 401.
9. M. Gell-Mann and A. Pais, *Phys. Rev.* **97** (1955) 1387.
10. K. Lande *et al.*, *Phys. Rev.* **103** (1956) 1901.
11. J. H. Christenson *et al.*, *Phys. Rev. Lett.* **13** (1964) 138.
12. T. T. Wu and C. N. Yang *Phys. Rev. Lett.* **13** (1964) 380.
13. G. D. Barr *et al.*, *Phys. Lett.* **317** (1993) 233.
14. L. K. Gibbons *et al.*, *Phys. Rev. Lett.* **70** (1993) 1203.
15. R. Adler *et al.*, *NIM* **A379** (1996) 76.
16. R. Adler *et al.*, *Phys. Lett.* **B363** (1995) 237; 243.
17. R. Adler *et al.*, *Phys. Lett.* **B370** (1996) 167.
18. B. Schwingenheuer *et al.*. *Phys. Rev. Lett.* **74** (1995) 4376.
19. J. N. Mathews *et al.*. *Phys. Rev. Lett.* **75** (1995) 2803.
20. R. Adler *et al.*, *Phys. Lett.* **B369** (1996) 367.
21. R. Carosi *et al.*, *Phys. Lett.* **B237** (1990) 303.
22. W. C. Carithers *et al.*, *Phys. Rev. Lett.* **34** (1975) 1244.
23. S. Gjesdal *et al.*, *Phys. Lett.* **B52** (1974) 113.
24. C. Geweniger *et al.*, *Phys. Lett.* **B52** (1974) 108.
25. C. Geweniger *et al.*, *Phys. Lett.* **B48** (1974) 487.
26. M. Cullen *et al.*, *Phys. Lett.* **B32** (1970) 523.
27. L. K. Gibbons *et al.*, *Phys. Rev. Lett.* **70**, (1993) 1199.
28. P. Huet, in *Proc. Workshop on K Physics*, ed. L. Iconomidou-Fayard, (Edition Frontières, 1997) 413; A. Kostelecky, *ibid.*, 407.
29. M. Calvetti, in *Proc. of the 2<sup>nd</sup> Workshop on Physics and Detectors for DAΦNE*, eds. R. Baldini *et al.* (S.I.S., INFN, LNF, Frascati, 1995) 81.
30. B. Winstein, in *Proc. of the 2<sup>nd</sup> Workshop on Physics and Detectors for DAΦNE*, eds. R. Baldini *et al.* (S.I.S., INFN, LNF, Frascati, 1995) 73.
31. J. Lee-Franzini, in *Proc. of the 2<sup>nd</sup> Workshop on Physics and Detectors for DAΦNE*, eds. R. Baldini *et al.* (S.I.S., INFN, LNF, Frascati, 1995) 31.

32. “KLOE, A General Purpose Detector for DAΦNE”, the KLOE Collaboration, Internal Report LNF-019, April 1, 1992.
33. I. Duniez, J. Hauser and J. Rosner, *Phys. Rev. D* **35**, 2166 (1987).
34. P. Franzini, in *Proceedings of the Workshop on Physics and Detectors for DAΦNE*, ed. G. Pancheri (S.I.S., INFN, LNF, Frascati, 1991) 733.
35. M. Kobayashi and T. Maskawa, *Prog. Theor. Phys.* **49**, 652 (1973).
36. N. Cabibbo, *Phys. Rev. Lett.* **10**, 531 (1963).
37. S.L. Glashow, J. Iliopoulos and L. Maiani, *Phys. Rev.* **D2**, 1285 (1970).
38. L. Wolfenstein, *Ann. Rev. Nucl. Part. Sci.*, **36** (1986) 137.
39. A. J. Buras, in *Phenomenology of Unification from Present to Future*, eds. G. Diambri-Palazzi *et al.*, (World Scientific, 1994) 41.
40. For a review of results on  $\Upsilon$  and  $B$  see J. Lee-Franzini, Hidden an Open Beauty in CUSB, in *Proc. of Twenty Beautiful Years of Bottom Physics*, Burnstein *et al.* eds, p. 85, The American Institute of Physics, and references therein.
41.  $B\bar{B}$  Mixing: a Review of Recent Progress, *Phys. Rep* **173**, No 1 (1989).
42. F. Parodi, P. Roudeau and A. Stocchi, preprint hep-ex/9903063.
43. A.D. Sakharov, *Pisma Zh. Eksp. Teor. Fiz.* **5**, 32 (1967).
44. A. Buras *et al.*, *Nucl. Phys.* **B408**, 209 (1993); M. Ciuchini *et al.*, *Z. Phys.* **C68**, 239 (1995), see also Kaon99, Chicago, 1999.
45. S. Bertolini *et al.*, *Nucl. Phys.* **B514**, 93 (1998), see also Kaon99, Chicago, 1999; T. Hambye *et al.*, hep-ph/9906434.
46. C. Jarlskog, *Z. Phys.* **C29**, 491 (1985).
47. G. Isidori, Kaon99, Chicago, 1999.
48. J. Kroll, Kaon99, June 21-26, Chicago, 1999